Czech University of Life Sciences Prague
Faculty of Forestry and Wood Sciences

Stress Detection in Forest Ecosystems Using Advanced Sensor Technologies

Mapování stresu v lesních ekosystémech pomocí pokročilých senzorů DPZ

Dissertation Theses

Author: Tereza Hüttnerová

Supervisor: Assoc. Prof. Peter Surový

Study program: Applied geoinformatics and remote sensing in forestry

Attachment: 0

Prague 2024

Dissertation assignment

CZECH UNIVERSITY OF LIFE SCIENCES PRAGUE

Faculty of Forestry and Wood Sciences

DISSERTATION THESIS TOPIC

Author of thesis:	Ing. Tereza Hüttnerová
Study programme:	Applied geoinformatics and remote sensing in forestry
Thesis supervisor:	doc. Ing. Peter Surový, PhD.
Supervising department:	Department of Forest Management and Remote Sensing
Language of a thesis:	English
Thesis title:	**Mapování stresu v lesních ekosystémech pomocí pokročilých senzorů DPZ**
Objectives of thesis:	The main goal of this thesis is to verify the cut-edge technologies for stress mapping in forest ecosystems. The work has the following sub-goals: • Mapping of microclimatic changes as a result of natural disturbances; • Detection of specific chemicals compounds to identify bark beetle infestation; • Verification of the possibilities of different platforms for remote sensing mapping of natural disturbances.
Methodology:	Forest stands are a more threatened ecosystem, stress manifests in poor health and increased mortality. In the thesis, it is hypothesized that natural disturbances can be identified much earlier than using traditional methods working with changes in spectral reflectance, focusing on non-optical manifestations (chemical mapping, mapping changes in the microclimate). The selection of research areas will take place according to the current situation of natural disturbances, focusing on mature spruce stands and subsequent processes. The data will be collected using modern technologies, concentrating on non-optical mapping. Several techniques and platforms will be tested to obtain data and their subsequent analysis to early detect stress in forest ecosystems (ground collection, UAV platform, satellite platform). The results will be published in scientific journals. The dissertation will be written in English.
The proposed extent of the thesis:	70-80 stran
Keywords:	Remote sensing, non-optical mapping, early detection, electronic noses, natural disturbances, stress mapping

Recommended information sources:

1. Abdullah, H., Skidmore, A. K., Darvishzadeh, R., and Heurich, M. (2019). Sentinel-2 accurately maps green-attack stage of European spruce bark beetle (Ips typographus, L.) compared with Landsat-8. Remote Sens. Ecol. Conserv. 5, 87–106.
2. Anderegg, W. R. L., Kane, J. M., and Anderegg, L. D. L. (2013). Consequences ofwidespread tree mortality triggered by drought and temperature stress. Nat. Clim.Change 3, 30–36.
3. Bowman, D.M.J.S.; Balch, J.K.; Artaxo, P.; Bond, W.J.; Carlson, J.M.; Cochrane, M.A.; D'Antonio, C.M.; DeFries, R.S.; Doyle, J.C.;Harrison, S.P.; et al. Fire in the Earth System. Science 2009, 324, 481–484.
4. Cellini, A.; Blasioli, S.; Biondi, E.; Bertaccini, A.; Braschi, I.; Spinelli, F. Potential Applications and Limitations of Electronic NoseDevices for Plant Disease Diagnosis. Sensors 2017, 17, 2596.
5. Johansson, A., Birgersson, G., and Schlyter, F. (2019). Using synthetic semiochemicalsto train canines to detect bark beetle–infested trees. Ann. For. Sci. 76:58.
6. Kautz, M.; Meddens, A.J.H.; Hall, R.J.; Arneth, A. Biotic Disturbances in Northern Hemisphere Forests—A Synthesis of Recent Data, Uncertainties and Implications for Forest Monitoring and Modelling: Biotic Disturbances in Northern Hemisphere Forests.Glob. Ecol. Biogeogr. 2017, 26, 533–552.
7. Rahman, S.; Alwadie, A.S.; Irfan, M.; Nawaz, R.; Raza, M.; Javed, E.; Awais, M. Wireless E-Nose Sensors to Detect Volatile Organic Gases through Multivariate Analysis. Micromachines 2020, 11, 597.
8. Seidl, R., Thom, D., Kautz, M. et al. Forest disturbances under climate change. Nature Clim Change 7, 395–402 (2017).
9. Senf, C.; Seidl, R.; Hostert, P. Remote Sensing of Forest Insect Disturbances: Current State and Future Directions. Int. J. Appl.Earth Obs. Geoinf. 2017, 60, 49–60.
10. Smigaj, M.; Gaulton, R.; Suárez, J.C.; Barr, S.L. Canopy Temperature from an Unmanned Aerial Vehicle as an Indicator of Tree Stress Associated with Red Band Needle Blight Severity. For. Ecol. Manag. 2019, 433, 699–70.

Expected date:	2024/25 WS - FFWS - State Doctoral Examinations

Anotace

Mapování zdravotního stavu je důležitou součástí lesního hospodářství a jeho včasná identifikace v lesních ekosystémech může minimalizovat šíření přírodních disturbancí. V současné době metody dálkového průzkumu Země pracují s viditelným nebo blízkým infračerveným spektrem pro sledování změn ve spektrální odrazivosti vegetace. V případě napadení kůrovcem jsou příznaky změn místního mikroklimatu a přítomnosti chemické komunikace mnohem dřívějším symptomem než změna spektrální odrazivosti korun. V případě lesních požárů lze rozsah dopadu snadno zmapovat opticky, ale uniklé emise mohou mít mnohem závažnější následky. Tyto neoptické změny lze mapovat speciálními senzorickými přístroji, elektronickými nosy apod. Tato práce ověřuje nejnovější technologie pro sledování přírodních disturbancí v lesních ekosystémech.

Práce je založena na pěti vědeckých článcích; první článek se zabývá mapováním 3D distribuce alfa-pinenu pomocí konvenčních chemických metod (Stríbrská et al., 2023b). Druhý článek (Hüttnerová a Surový, 2024) se zaměřuje na srovnání tří elektronických nosů s cílem včasné identifikace napadení kůrovcem. Třetí článek (Hüttnerová et al., 2023) zkoumá využití komerčního elektronického nosu pro pozemní a bezpilotní sběr dat v napadeném lese. Čtvrtý článek (Hüttnerová a Surovy, v tisku) je zaměřen na validaci satelitních dat Sentinel-5P TROPOMI pro mapování emisí při lesním požáru. Pátý článek (Hüttnerová et al., 2024) se zaměřuje na analýzu potenciálních stresových faktoru mikroreliéfu pro hodnocení přirozené obnovy na holinách vzniklých v důsledku kalamitní těžby.

Práce představuje nový přístup v mapování přírodních disturbancí, a to za využití neoptických senzorů v lesních porostech pro včasnou detekci stresu. V práci bylo možné ověřit využití nejnovějších technologií pro mapování zhoršeného stavu lesních porostů, které se projevuje změnami v chemickém složení, ale i změnou v lokálním mikro-klimatu.

Klíčová slova: Dálkový průzkum Země, neoptické mapování, včasná detekce, elektronický nos, přírodní disturbance, mapování stresu

Annotation

Mapping the health state is an important part of forest management, and early detection of stress in forest ecosystems can minimize the spread of natural disturbances. Currently, remote sensing methods work with the visible or near-infrared spectrum to monitor changes in the spectral reflectance of vegetation. In the case of bark beetle infestation, the symptoms of changes in the local microclimate and the presence of chemical communication are much earlier than change in spectral canopy reflectance. In the case of forest fires, the extent of the impact is easily mapped optically, but escaped emissions can have much more severe consequences. These non-optical changes can be mapped with special sensory devices, electronic noses, etc. This thesis verifies the latest technologies for monitoring natural disturbances in forest ecosystems.

The organization of this thesis is based on five scientific articles; the first article deals with the mapping of the 3D distribution of alpha-pinene using conventional chemical methods (Stříbrská et al., 2023b). The second article (Hüttnerová and Surový, 2024) focus on the comparison of three electronic noses devices with the aim to identify early identification of bark beetle infestation. The third article (Hüttnerová et al., 2023) investigates the use of an commercial electronic nose in an infested forest for ground and unmanned aerial vehicle data collection. The fourth article of the thesis (Hüttnerová and Surovy, in press) is focused on validating Sentinel-5 TROPOMI satellite data for mapping emissions during a forest fire. The fifth article (Hüttnerová et al., 2024) focuses on analyzing potential microrelief stress factors for evaluating natural regeneration in clearings resulting from salvage cutting.

The thesis represents a unique study of a new area: non-optical sensors in forest stands for early stress detection. In the thesis, it was possible to verify the use of the latest technologies for mapping the deteriorated state of forest stands, manifested not only by changes in the chemical cloud but also by different manifestations in the microclimate.

Key words: Remote sensing, non-optical mapping, early detection, electronic noses, natural disturbances, stress mapping

I hereby declare that the thesis entitled *Stress Detection in Forest Ecosystems Using Advanced Sensor Technologies* submitted for the Degree of Philosophy of Applied geoinformatics and remote sensing in forestry is my original work guided by my supervisor. All sources of information, text, illustration, tables, and images have been specifically cited.

……

Tereza Hüttnerová

Acknowledgments

First of all, I would like to express my heartfelt gratitude to my supervisor, Peter Surový, for his invaluable support, inspiration, and patience. Your guidance and willingness to share your expertise motivated me to overcome challenges and deepened my understanding of the topic.

I would also like to thank all co-authors for their cooperation and my colleagues at the Department of Forest Management and Remote Sensing for their help and valuable advice during my studies. Finally, I am deeply grateful to my family for their unwavering support throughout my studies.

The scientific articles included in this thesis was funded by the following research projects:

- **IGA/A_21_18 and IGA/A_26_23**
  Internal Grant Agency of the Faculty of Forestry and Wood Sciences, Czech University of Life Sciences Prague
- **CZ.02.2.69/0.0/0.0/19_073/0016944**
  Improvement in Quality of the Internal Grant Scheme at CZU
- **TH74010001**
  Program CHIST-ERA, Technological Agency of the Czech Republic
- **QK21010435**
  Ministry of Agriculture of the Czech Republic

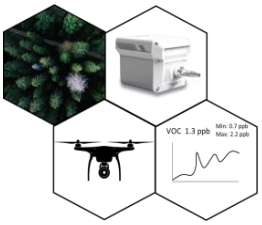

Contents

List of abbreviation

3D	Three-dimensional
AGSs	Amperometric gas sensors
BAGI	Backscatter absorption gas imaging
GC-FID	Gas Chromatography-Flame Ionization Detection
GEDI	Global Ecosystem Dynamics Investigation
GIS	Geographic Information System
GNSS	Global Navigation Satellite System
GPS	Global Positioning System
LiDAR	Light Detection and Ranging
MOXs	Metal oxide semiconductors sensors
NDIRs	Non-dispersive infrared sensors
NDVI	Normalized Difference Vegetation Index
NIR	Near-infrared Radiation
PIDs	Photoionization detectors
PPB	Parts per billion
PPM	Parts per million
RADAR	Radio Detection and Ranging
SDEA	Sensory device for environmental applications
SPME	Solid-phase microextraction
SWIR	Shortwave infrared
TanDEM-X	TerraSAR-X Add-on for Digital Elevation Measurement
TROPOMI	TROPOspheric Monitoring Instrument
UAV	Unmanned aerial vehicle
UV	Ultraviolet light
VOCs	Volatile organic compound

List of the Figures

List of the Tables

Part I

Introduction and Theory

Chapter 1

Thesis Preface

1.1.Foreword

Forests are a very valuable terrestrial ecosystem affecting a whole range of other processes in nature. In recent decades, European forests have faced increased threats from natural disturbances, including insect pests, forest fires, and wind-throw events. Forests have a longer life cycle and cannot respond and adapt quickly enough to sudden changes caused by human operations or climate change. Stressed trees, as a result of climate change, are not as resistant to natural disturbances, which leads to a loss of defenses, the health status of forests deteriorates, and increased mortality is recorded. An important part of forest management and policies is monitoring the health state of forests and early identification of stress can prevent enormous losses. Currently, the detection methods used cannot cover large areas (Field surveys) or cannot detect spectral changes, especially in the early stages of infestation, which are difficult to detect by imaging sensors. However, natural disturbances also bring changes in the form of chemical changes and different manifestations at microclimatic level. The question is how to identify and map these non-optical manifestations. Thus, the presented thesis deals with searching for stress mapping methods in forest ecosystems for early identification to verify the cutting-edge available technologies.

1.2. Research Motivation

Science is like climbing in the dark; you know you are moving upwards, but you don't always see the fastest and easiest way to reach the top. This comparison is even more true for new, unproven methodologies, which may sound like a crazy idea at first but which, after a few years, can take hold as common measurement practice. In my personal life, I like to try new things, overcome my fear, and try to push my boundaries further. That's why I applied for doctoral studies and knew from the beginning that I would like to devote myself to something new and unexplored; that's why I chose the new doctoral program Applied Geoinformatics and Remote Sensing in Forestry.

Forests face many threats that are intensifying due to climate change, and it is thanks technical innovation of modern technologies it is possible to better monitor the changes in the forest and protect forests. However, the methods used are still not fast enough. Therefore, this thesis deals with the possibilities of earlier detection of natural disturbances and innovations in mapping subsequent processes. This thesis uncovers the possibilities of non-optical mapping in the framework of remote sensing in forestry. Not everything important can be seen with the eyes; some processes manifest themselves outside of visual perception yet are key to truly understanding and appreciating the situation.

1.3. Thesis Structure

The thesis consists of four published articles, and one submitted. The thesis is divided into two parts and six chapters. The first part contains a preface and a general introduction to the issue of stress mapping in forest ecosystems using modern methods. The second part of thesis consists of research articles, four articles are published, and one article is submitted.

• **Article I:** Pilot Study of 3D Spatial Distribution of α-Pinene Emitted by Norway Spruce (L.) Karst Recently Infested by *Ips typographus* (L. 1758) (Coleoptera: *Scolytinae*).

• **Article II:** Bark beetle detection method using electronic nose sensors. A possible improvement of early forest disturbance detection?

• **Article III:** Comparison of Individual Sensors in the Electronic Nose for Stress Detection in Forest Stands.

• **Article IV:** Sentinel 5-P TROPOMI sensor analysis for CO temporal and spatial dynamics during fire. Case study Bohemian Switzerland National Park (submitted)

• **Article V:** Drone microrelief analysis to predict the presence of naturally regenerated seedlings.

Chapter 2

Objective of the thesis

In the last decades, scientists have focused on mapping optically visible changes in forests. However, all changes and communication in forest ecosystems are accompanied by non-optical manifestations, which can often be related to manifestation of stress factors. In line with this, the main goal of this thesis has been to verify the cutting-edge technologies for stress mapping in forest ecosystems.

The work has the following sub-goals:

i) Mapping of microclimatic changes as a result of natural disturbances;
ii) Detection of specific chemicals compounds to identify bark beetle infestation;
iii) Verification of the possibilities of different platforms for remote sensing mapping of natural disturbances.

The work deals with the following hypotheses:

Stress in forest stands brings non-optical manifestations that chemical sensors or electronic noses can detect. Identification of these changes can early detect disturbances and thus minimize environmental and economic losses.

Stressed trees produce a several times greater amount of volatile organic compounds and in the event of bark beetle attacks, a unique aggregating pheromone appears as part of communication between individuals.

In these cases, the reduced ability of trees to transpire due to damage brings measurable non-optical manifestations in the change of the local microclimate.

Chapter 3

Theoretical background

3.1. Introduction

People primarily perceive their surroundings visually. At first glance, they can evaluate plants' color, shape, and size and estimate their health status. Similar to the general public, the scientific community focuses mainly on evaluating optical data for the identification of stress in forest ecosystems. However, visual changes are merely the consequences of stress, preceded by several less visible but critical manifestations that can aid in early identification. Thanks to technological progress, it is possible to measure these changes in the non-visible spectrum.

Forests cover roughly a third of the world, representing a unique ecosystem that combines several functions (Forest Europe, 2020). However, in recent decades, they are more exposed to both internal and external stressors. While internal stressors are caused by trees' physiological growth and development, external stressors contain natural disturbances, among which include bark beetles, storms, and forest fires (Seidl et al., 2017). For example, as a result of persistent droughts, forest stands are more susceptible to lose their vitality and health. In addition, natural disturbances interact with other factors such as increasing greenhouse gases (methane, carbon dioxide), thus increasing average temperature, lower annual precipitation, and more extensive drought (Seidl et al., 2014; Fearnside, 2015; Yuan et al., 2021). In Central Europe, the greatest damage is currently caused by bark beetles (biotic natural disturbance); a successful bark beetle attack depends not only on the health of the forest stand but also on the frequency and extent of the attack (Kautz et al., 2017).

Stress mapping in forest ecosystems is integral to forest management; early identification of a deteriorated condition or risk identification can minimize possible ecological, economic, and environmental losses. One method of detecting infestation is field surveys by professional workers who visually inspect each tree to look for first beetle entrance holes, boring dust on the trunk, and resin flows. Field inspection is very accurate but physically and time-consuming, and it is impossible to inspect

larger forest units and less accessible locations in this way (Bárta et al., 2022; Bozzini et al., 2024).

To cover larger areas, remote sensing methods have begun to be used; depending on the required spatial resolution and the extent of the study area, a platform (satellite, aircraft, drone) is considered. The most used sensors on these platforms to identify the deteriorated condition of the forest stands are hyperspectral and multispectral cameras. By combining several channels, vegetation indices can be calculated, which present the health condition of the vegetation based on the differences in spectral reflectance (Zarco-Tejada et al., 2001; Le Maire et al., 2004; Bárta et al., 2022). This method provides an efficient data source for large areas but does not provide information on early infestation (Kautz et al., 2023; Bozzini et al., 2024).

In addition to the spectral changes when a tree is attacked, there are other non-optical symptoms. Bark beetles use an aggregation pheromone to attract females to mate in the host tree. An attacked tree secretes an increased amount of volatile organic substances several times (Ghimire et al., 2016; Jaakkola et al., 2022; Netherer et al., 2024). Other variables that could indicate stress in the forest ecosystem are changes in the local microclimate (Kopáček et al., 2020).

These non-optical manifestations can be recorded by conventional chemical methods, and the analysis can be carried out using a gas chromatograph. This method gives accurate results, but collection and evaluation are time-consuming, and only a few samples can be taken daily. A potential method appears to be using electronic noses, sensing devices composed of several selective sensory units, and recognition software. Electronic noses and similar devices are used in security and industrial site mapping. Evidence that these changes can be detected non-optically after a tree is attacked comes from sniffer dog research, where specially trained dogs can locate infested trees from distances of up to 150 metres (Johansson et al., 2019; Vošvrdová et al., 2023).

3.2. Natural disturbances

Natural disturbances are a fundamental part of ecological processes; they can leave a lasting change and radically affect the structure and functioning of a given ecosystem. Currently, disturbance regimes are changing more frequently, and global changes will bring new spatial patterns and different trajectories of change (Turner, 2010). Disturbance can be described according to the definition of White and Pickett (1985) as "Any relatively discrete event that disrupts the structure of an ecosystem, community, or population, and changes resource availability or the physical environment". Disturbances can be divided according to their origin into abiotic and biotic. Abiotic factors include fires, storms, and hurricanes; and biotic factors include pests and pathogens (Turner, 2010).

In the last twenty years, European forests have been exposed more often to natural disturbances, the most frequent threats being windthrow events (46 %), wild forest fires (24 %), and outbreaks of bark beetles (17 %). As a results, an average of 44 million m^3/year were cut down during the past 70 years due to natural disturbances in the European forests (Patacca et al., 2023). In the Czech Republic, the most serious problem was the Eurasian spruce bark beetle (*Ips typographus* (L.)) calamity, which affected Norway spruce stands [*Picea abies* (L.) Karst.]. All disturbances caused 20 million m^3 of wood harvested out of the total cutting of 25 million m^3 in the Czech Republic. Biotic disturbances (i.e. pests) accounted for roughly 8 million m^3 of harvested timber (Ministerstvo zemědělství, 2023). Forest fires in Czechia occurred only occasionally, having place in 2022 the largest forest fire in the Bohemian Switzerland National Park in modern history. In total, 1,715 ha were affected by fires in 2022, of which 1,600 ha burned in the national park (Ministerstvo zemědělství, 2023).

Regarding Eurasian spruce bark beetle attacks, it is well known that stressed trees secrete far greater amounts of volatile organic substances than in resting conditions (Ghimire et al., 2016; Netherer et al., 2021; Hakola et al., 2023). An overview of the compounds secreted by the host tree (Norway Spruce) is given in **Table 1**, the variability of the representation is most likely caused by the different ages of the tested trees (Borg-Karlson et al., 1993; Baier et al., 2002; Silvestrini et al., 2004).

Tab 1. *Volatile organic compounds secreted by spruce trees as a result of exposure to stress (Netherer et al., 2021).*

VOC	Range
α-pinene	23-39%
β-pinene	25-58%
β-Phellandrene	5 –19%
limonene	1.5–4%
myrcene	1.6–3.4%
Δ-3-carene	0.6–1.1%
camphene	0.2–1 .1%

Another substance that plays an important role in chemical communication is the aggregation pheromone used by individuals of bark beetles to communicate during attacks; it is composed 2-Methyl-3-buten-2-ol, cis-Verbenol, Verbenone, Ipsdienol, and Ipsenol (Birgersson et al., 1984; Netherer et al., 2021; Moliterno et al., 2023). Nevertheless, degrading effects are caused by symbiotic fungi that are associated with the Eurasian spruce bark beetle, which exhaust the tree's resistance and ability to transpire. These fungal compounds are exo- and endo-Brevicomin, 3-Methyl-1-butanol, 2-Methyl-1-butanol, 3-Methyl-1-butyl acetate, 2-Phenylethanol, 2-Phenylethyl acetate (Kandasamy et al., 2019; Netherer et al., 2021, 2024).

In addition to chemical communication and changes in concentrations brought about by stress in forest ecosystems, other non-optical variables, namely changes in the local microclimate, are measurable **(Figure 1)**. A healthy coniferous tree has an average water transpiration of 200 - 300 l/day; if it is damaged, its ability to transpire can be reduced or completely lost. Tree transpiration has a cooling effect on the tree's surroundings; if it is reduced, there is an increase in temperature, a decrease in atmospheric humidity, and pressure can be increased due to these changes (Kopáček et al., 2020).

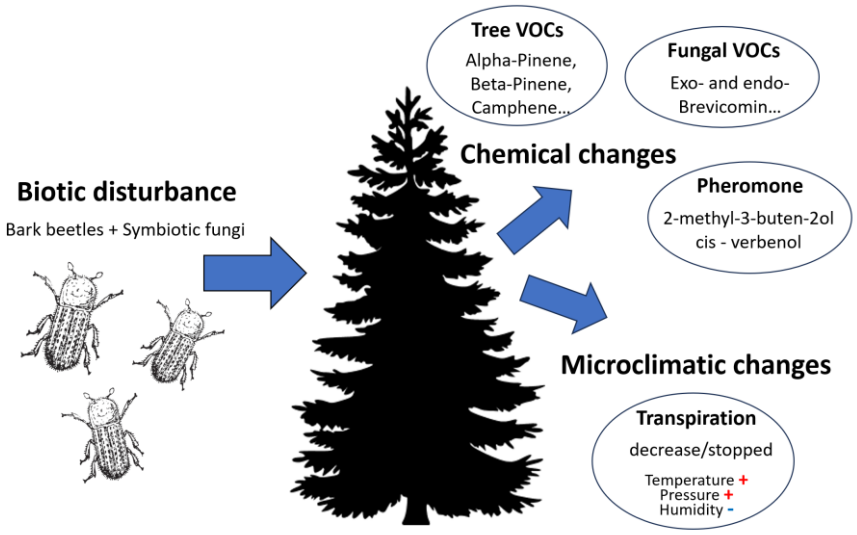

Figure 1. *A simplified scheme of non-optical changes resulting from bark beetle infestation, a specific aggregation pheromone used for communication between individuals, increased volatile organic compounds levels in spruce trees, and changes in microclimate due to reduced tree transpiration.*

3.3.Detection methods of stress in forests

Mapping the health status of forest stands is a part of forest management; precisely, the timely identification of a deteriorated condition can contribute to timely interventions and thus prevent ecological and economic losses. The detection method depends on the desired mapping goals and the size of the territory. For example, to check the condition of a few trees, it is advisable to choose a conventional field survey. In the case of more extensive forests or poorly accessible terrain, it is more appropriate to select remote sensing methods. Another criterion is whether it is sufficient to identify spectral changes in the canopy and dead trees or early detection of the bark beetle stage before emerging from the host tree. Before the individual stress detection methods are described, the attack phases' terminology will be described here. The term "green attack" or "early attack" is the most frequently used in detecting or mapping bark beetle infestation. A more detailed description of the monitored phase is appropriate in study cases because the original use of the term "green attack" was used in North America for a one-year-old attack (USDA Forest Service, 1935).

Considering the life cycle of the bark beetle, which can have up to three generations per year, the time scale of one year is insufficient for mapping the infestation

(Wermelinger, 2004). The bark beetle usually emerges 6 - 10 weeks after infestation, and the canopy is usually still green (Bárta et al., 2022). The term early is not precisely specified and differs for each pest according to the life cycle. Detecting an attack by optical remote sensing after ten weeks is relatively early, but it is already too late to gather information for possible protection of forests (Kautz et al., 2024). Early detection should always be associated with time data regarding the time of infestation (from initial infestation). Also, early detection should be connected with the phase before the emerging beetles from the host tree, when protection is still possible. The detection method comprises the platform, sensor, or several sensors and the statistical evaluation procedure. Furthermore, conventional detection methods and the possibilities of new techniques that bring even earlier identification of attacks will be described.

3.3.1. Conventional techniques

Conventional methods include several techniques such as field survey and chemical analytic methods, which have been proven for years yielding very accurate results. However, they show limitations like the highly time-consuming nature of collection and subsequent processing, unsuitability to map extensive forest stands and inaccessible or poorly accessible locations. But, they are an inherent methodology for validation data.

The traditional method for identifying tree infestations or damage is a field survey by foresters or trained workers. During the field inspection, a visual inspection of each tree occurs, and traces of resin flows, boring dust, and entrance holes are searched for (Birgersson et al., 1984; Christiansen et al., 1987; Bozzini et al., 2024). These tracks, which are easily visually recognizable, are not permanent and may disappear after stronger wind or rain (CABI, 2022). Field surveys are not affordable for detecting infestation in large areas or poorly accessible terrain due to the time requirement.

Conventional chemical methods use sampling cartridges and solid-phase microextraction fibers (SPME) to identify the presence of aggregation pheromone or volatile organic compounds (Jaakkola et al., 2022; Stříbrská et al., 2023b). An indisputable advantage is the high sensitivity and the ability to accurately determine the concentrations of the substances under investigation, thanks to gas

chromatography methods. However, its main disadvantage is that it is very time-consuming (approx. 1 hour per sample), and the subsequent analysis is done on a gas chromatograph. In addition, samples must be kept cold when transported from the field and analyzed immediately.

3.3.2. Odor-based mapping

A new stress detection method in forest stands is non-optical mapping, which deals with monitoring groups of volatile organic substances, aggregation pheromones, or changes in microclimate manifestations. Sensors containing microchips and electronic noses can convert chemical concentrations or microclimate values (temperature, air humidity, talc) into an electrical signal and then a digital number (Hüttnerová et al., 2023). Next, the four basic types of chemical sensing devices that can be used for environmental studies are briefly presented (Single-gas sensors, High-tech optical analytic sensors, Multi-gas detector, and Electronic nose).

1. Single-gas sensors

A miniature device containing one sensor is usually small, lightweight, and has low energy consumption. As part of the measurement, it usually provides data on the measured concentration, and it is possible to set the parameters during the measurement, the measured values are recorded on the memory card. They are used for security applications, environmental monitoring and food inspection (Fine et al., 2010; Loutfi et al., 2015a; Baron and Saffell, 2017). Popular types within these low-cost, miniature ones are metal oxide semiconductors sensors (MOXs), photoionization detectors (PIDs), amperometric gas sensors (AGSs), and non-dispersive infrared sensors (NDIRs) (Burgués and Marco, 2020).

MOX is a conductometric electrochemical sensor designed to detect volatile organic compound (VOCs) in parts per million (ppm) resolution. These sensors work based on changes in electrical resistance when exposed to gases at high temperatures (150 – 500 °C). MOX sensors are small in size with a long life of over 10 years and a quick response to changes in concentrations in about 10 seconds; the measurement of the sensor is very sensitive to changes in humidity (so it can be used as a sensitive sensor to monitor changes in humidity (Chen and Lu, 2005). The sensitivity of MOX sensors

is not precisely specified but can be improved by subsequent data processing techniques (Wang et al., 2010; Korotcenkov and Cho, 2013; Burgués and Marco, 2018).

PID sensors are universal wide-spectrum devices with the detectability of inorganic gases and VOCs with a sensitivity from 10 parts per billion (ppb) to 10,000 ppm and a response time of a few seconds. The measurement principle consists in the number of excited ions of ionized gas molecules based on the shining of UV light, the gas concentration output is obtained by measuring the intensity of the ionized gas current. They are conventionally used for toxic mapping in industrial areas (Licen et al., 2020). PID sensors archives high detection precision, but its disadvantages are that it is expensive and cannot map gases with high ionization energy, such as CO, CO_2, O_3, and SO_2 (Burgués and Marco, 2020).

AGSs represent a very promising amperometric detection method for measuring inorganic gases in units of ppb and ppm (CO, SO_2, NO, NO_2, H_2S); the sensors work based on an electrochemical reaction monitored within electrochemical cells. Three electrodes (working, reference, and counter) are placed in the liquid electrolyte solution with a catalyst (Stetter and Li, 2008). The detected gas enters the sensor through a porous membrane, which regulates the amount entering and controls diffusion; the output signal is learned based on the flow of current between the working and counter electrodes. This method minimizes the influence of temperature on the measurement and correlates with the concentration of the detectable gas. The advantage is the possibility of linear measurement of one gas concentration; the sensor is also suitable for battery power – low consumption (<1mW). On the other hand, sensors provide a slow response and are very sensitive to temperature changes (Burgués and Marco, 2020; Hunter et al., 2020).

NDIR sensors are composed of an infrared lamp, a chamber, an optical filter to filter out unwanted wavelengths that do not relate to the target gas and an infrared detector. NDIR sensor is based on measuring the attenuation of infrared radiation in the air; light from the source of infrared radiation passes through the light-conducting chamber, is absorbed by the gas in the chamber, and then the remaining part falls on the infrared detector. The measurement output is the difference between emitted and received light by the detector. The technology works based on the physical properties

of gases and is suitable for CO_2 mapping. The accuracy of NDIR depends on changes in ambient temperature and light absorption pressure; for the most portable measurement, you need to have stable conditions (Hodgkinson and Tatam, 2013; Dinh et al., 2016; Martin et al., 2017).

2. High-tech optical analytic sensor

Optical analytical methods measure the physical characteristics of gases. They use the absorption of gases during excitation by Infrared Radiation (IR) and Ultraviolet light (UV), suitable for these analyses are gases that do not have overlapping properties with others (CO_2, CH_4, O_3) (Andersen et al., 2010; Popa and Udrea, 2019). Optical analytical sensors achieve a higher detection accuracy than sensors that measure chemical-physical properties. A miniature laser spectrometer is a suitable technique for measuring CH_4 concentrations using an unmanned aerial vehicle (UAV) (Smith et al., 2017). For large-scale measurement (determining the cumulative concentration in the cloud), there is a stand-off laser emitter method and detectors located at one end; it works on the principle of emitting a beam towards the mapped objects, and a photodiode captures the backscattered light (Yang et al., 2018).

The optical imaging of gas concentrations includes the backscatter absorption gas imaging (BAGI) technique using thermal imaging or infrared cameras measuring the thermal differences between the gas under investigation and its surroundings up to approx. 10m (McRae and Kulp, 1993). For the changes on the video stream to be noticeable, there must be a temperature difference of at least two Celsius degrees (2 °C) and suitable climatic conditions (warm weather, no wind or weak wind, clear sky) (Ravikumar et al., 2017; Burgués and Marco, 2020).

3. Multi-gas detector

A multi-gas detector is a device that holds several sensors in one detection unit and provides measurements for multiple gases. The multi-gas detector is often equipped with from 5 to 10 sensors of the type AGS, PID, NDIR, and MOX. In addition to individual sensors, it contains the necessary electronics, charging system, and measurement data logging within the unified detector. The sensors are inserted into the chamber, where a fan or a pump supplies air. The detector can work independently of another device (UAV); that is, it has its Global Navigation Satellite System (GNSS), battery system, and data transmission, and the second type is integrated, which uses

the mentioned components from an unmanned vehicle (such a detector has a lower weight but does not work independently) (Carrozzo et al., 2018; Zifarelli et al., 2022).

4. Electronic nose

The electronic nose is currently the most high-tech system for detecting and analyzing chemical data; it is composed of a hardware part, individual sensors for gas detection, and software for analyzing and exporting measured data. The principle of the electronic nose is based on the human sense of smell; based on several selective sensors, the electronic nose can estimate the concentration and recognize the given gas, just like the human nose, which can, for example, identify the "smell of the forest" from the "smell of the city" (Gardner and Bartlett, 1999). Electronic noses cover many areas: medicine, the food industry, security, and environmental studies (Loutfi et al., 2015b; Wojnowski et al., 2019; Bax et al., 2020) and can bring the possibility of a more extensive view of the given issue thanks to the collection of data by a more significant number of sensors and faster analysis and evaluation of the given phenomenon thanks to software that enables real-time results display. However, electronic noses are burdened by limitations as their basic type, and depending on the types of sensors used, some can be sensitive to temperature, humidity, and pressure changes. Furthermore, individual sensors need to be regularly calibrated and replaced (Romain and Nicolas, 2010).

Conventional use of chemical sensors and electronic noses is in industry and air quality monitoring; sensors are also used in agriculture, specifically to detect pests that are manifested by the excretion of specific chemical compounds (Fuentes et al., 2021; Marković et al., 2021; Khorramifar et al., 2023; Alfieri et al., 2024; Wang and Chen, 2024). Evidence that it is possible to map chemical changes in forestry is research testing the abilities of specially trained dogs. Sniffer dogs can detect infested trees up to a distance of 150 m and are up to four times faster compared to field workers. Especially dogs that are trained to detect semiochemicals, substances similar to the aggregation pheromone. The sniffer dog method can help with the early detection of infestations (Johansson et al., 2019; Vošvrdová et al., 2023).

For odor mapping it is important to take into account the life cycle of the bark beetle and the weather, as the bark beetle is capable of flight at a minimum temperature of 16.5 °C; the optimal temperature for flight and, therefore, attack is 22 – 26 °C

(Wermelinger, 2004). Changes in the microclimate due to reduced ability or complete transpiration loss will not be measurable in cloudy conditions. Ground collection is a suitable means to test the usability of chemical sensors and electronic noses; for more extensive collection, interaction with UAVs would be more appropriate.

UAVs appear suitable for mapping more extensive study areas or inaccessible parts in several fields such as forest inventory, health monitoring, mapping of regeneration, etc. (Puliti et al., 2017, 2018; Slavík et al., 2020; Dainelli et al., 2021; Buchelt et al., 2024). The choice of a suitable UAV depends on several factors: the weight of the payload (chemical sensor), the size of the study area, the type of landscape, and the required resolution of the outputs. Fixed wing type can map a large area very efficiently; the limitation is a lower payload; a suitable application of chemical mapping is, for example, the inspection of pipelines (Burgués and Marco, 2020).

There is usually limited space for maneuvering for forestry mapping; UAVs with a vertical take-off and landing system are suitable. A multi-rotor type is often used, where another advantage is a higher payload (it can be equipped with several sensors or a heavy electronic nose system), which brings energy requirements and, thus, leads to a shorter flight time. When using a multirotor for chemical mapping, it is necessary to consider the influence of the vertical flow of air based on the movement of the rotors ("downwash"); this phenomenon can be minimized by using a sampling tube and sampling the air in front of the drone (Burgués and Marco, 2020; Zhan et al., 2022).

3.3.3. Remote sensing

Remote sensing is a popular method for mapping forest ecosystems and assessing their health status nowadays, mainly focusing on natural disturbances in the latter (Klouček et al., 2019; Götz et al., 2020; Honkavaara et al., 2020; Bárta et al., 2021; Minařík et al., 2021; Dalponte et al., 2022; Zakrzewska and Kopeć, 2022). According to their distance from the earth's surface, these devices can be classified as spaceborne (e.g. satellites), airborne (e.g. aircraft) and close-range (e.g. UAV). And different targets will require different devices. For example, satellite data can provide information for larger areas and with greater temporal frequency of acquisition (high-temporal-resolution data). But, their spatial resolution is insufficient for individual trees early detection of bark beetle infestation and in the case of passive

data, images are limited by cloud cover (Immitzer and Atzberger, 2014; Latifi et al., 2018; Abdullah et al., 2019a; Huo et al., 2022). The aerial platform enables a better spatial resolution of the images, the possibility of choosing sensors according to the study's objectives, and data collection dates. The disadvantage is the cost of getting high-temporal-resolution data (Bárta et al., 2022; Zakrzewska and Kopeć, 2022). The optical images obtained by the UAV platform overcome the limitation of insufficient resolution quality; a great advantage is the time flexibility in data collection and the choice of sensors. The limiting factor is the flight time of the UAV given by the battery capacity (approx. 30 min/one battery) and the impossibility of evaluating the deteriorated state of health for larger forest areas. The most frequently used platform and sensor for biotic natural disturbance (mainly bark beetle) detection was a combination of satellite platform and multispectral sensor in last twenty years (Kautz et al., 2024).

The health status of forest stands can be mapped using changes in the spectral reflectance by calculating vegetation indices. Based on the spectral changes in the canopy, remote sensing methods usually divide stage of attack into three stages according to foliage color: green-attack, red-attack, gray-attack (Wulder et al., 2006). The first stage is described as successful colonization by the bark beetle, but the visual appearance of the tree is unchanged; the needles are still green. The tree dies during the second and third stages, and their spectral expression changes significantly (from red to gray) (Bárta et al., 2022). For the possible rescue and minimization of damage due to the spread of the bark beetle to surrounding trees, it is important to detect attacked trees in the "green-attack" phase (Fahse and Heurich, 2011; Abdullah et al., 2019b).

The vegetation index combines several bands, usually from the visible or near-visible spectrum, to identify degraded vegetation quality. The most widely used is the Normalized Difference Vegetation Index (NDVI) GREEN/NIR, Piecewise index PI B($\rho_{710 + 738-522}$), Greenness GI, and Normalized difference photochemical reflectance index (PRI) are also used to evaluate the state of health in connection with bark beetle infestation (Gitelson and Merzlyak, 1997; Zarco-Tejada et al., 2001; Le Maire et al., 2004; Zhang et al., 2018; Bárta et al., 2022). In the case of a bark beetle attack, methods working with changes in the spectral reflectance of the canopy cannot detect early attack because changes in the canopy occur in only 40% of attacked

individuals, and the first changes after infestation are only visible after 6-10 weeks (Kautz et al., 2023; Bozzini et al., 2024). However, methods based on changes in the spectral reflectance of objects are suitable for identifying dead trees to evaluate the extent of calamity and for a safety evaluation of the fall of dead trees in the tourist area, for example (Matejčíková et al., 2024).

Satellite data is also used for mapping non-biotic natural disturbances, mainly determining the extent and burn severity of fires (Hantson et al., 2013; Parks et al., 2014; Teodoro and Amaral, 2019). Vegetation indices are conventionally used to determine changes in the state of health, the differenced normalized burn ratio is used to compare the phases before and after the fire and identify biomass loss (Mathews and Kinoshita, 2020). The Sentinel-5 Precursor satellite was launched with the European Space Agency's TROPOMI (TROPOspheric Monitoring Instrument) sensor to map climate change and emissions (Schneising et al., 2019). This satellite has channels in ultraviolet-visible (270–500 nm), near-infrared (675–775 nm), and shortwave infrared (SWIR) (2305–2385 nm) and is focused on air quality mapping through several products: methane, carbon monoxide, sulfur dioxide, nitrogen dioxide, formaldehyde, and UV Aerosol Index (Veefkind et al., 2012). Data products are used for mapping mainly fires, changes in environment and air pollution (Schneising et al., 2019; Ghasempour et al., 2021; Xulu et al., 2021).

Part II

Research

Chapter 4

Materials and methods

This chapter describes the study areas, the sensors used, the data collection methodology, and subsequent data processing and analysis. Considering the novelty of the topic and the focus on technology verification, this section will describe the procedures within the research part. The presented methodologies were tested mainly on the territory of Czechia, but the methods are potentially applicable anywhere. In the case of applying the presented methodology in a different climate, it would be necessary to recalibrate the models for local conditions. However, based on the results obtained, we already know and can predict which variables will be significant for specific phenomena.

The material used, data collection, and analysis were based on long-term testing, the search for new approaches, and getting knowledge from other research areas. For example, using electronic noses in industry and monitoring forest fires in Australia. Research attempts often failed, data were lost during collection, or the analyses did not yield meaningful results. At the time of writing this thesis and related scientific articles, there were only a few studies on similar topics. The author of this thesis approached the solution with the utmost integrity.

4.1.Study area

The study areas included forest stands affected by biotic, abiotic natural disturbances and subsequent processes. The study area of non-biotic research is the Bohemian Switzerland National Park on the border with Germany, which falling into the protective forest category. It is where the largest fire in the modern history of Czechia was recorded and the most affected place regarding abiotic disturbance. Biotic disturbances occur more often in Czechia, and therefore, the selection of sites for testing the methodology was more comprehensive; the study areas were selected based on several criteria: the study area was mainly formed by commercial forests or Forests with aiming forestry research and forestry education, where monoculture of Norway spruce [*Picea abies* (L.) Karst] was the most common system. Study area represented

a mature spruce stand that was heavily attacked by *Ips typographus* in the early phase (within 1-2 weeks of age). Surroundings of the infested part of the forest belonged to healthy forest conditions as a requirement for possible comparison of sensor reactions. The stress of forest stands due to bark beetle infestation was also mapped in the Harz National Park (the eastern part of Sachsen-Anhalt in Germany) and in the Ore Mountains, where coniferous trees were stressed due to drought and bark beetle infestation. Subsequent processes (mapping the natural regeneration process) were tested on clearing areas due to salvage cutting. The plots were 0.74 ha -1.32 ha in size, dominated by Norway spruce. Bark beetles attacked the forest, which was harvested at the beginning of 2021. The areas were monitored for natural development without manual planting.

4.2. Materials

Several materials were used for stress mapping in forest stands, as specified below, along with their selection justification. These were conventional chemical methods, electronic noses, the TROPOMI sensor, and unmanned aerial vehicles.

Conventional analytical chemical methods such as Solid-Phase Microextraction (PDMS/CAR/DVB, Supelco, PA, USA) and sampling sorbent cartridges HayeSep-Q® (30 mg, Sigma-Aldrich, St. Louis, MO, USA) were used to accurately verify chemical compounds and their amounts. The used sampling cartridges were commercially produced 6 x 70 mm glass tube cartridges with 80-100 grit Tenax TA and 20-40 grit Anasorb CSC sorbent material. The sampling cartridges are of the passive type and must be used with a sampling pump (Pocket Pump Touch series 220 – 100, SKC company). These methods enable an exact determination of the substances in the sample, including their quantity. The sampling and processing method by gas chromatography is time-consuming and it is not possible to create an extensive measurement point network, it is a suitable method for validating the measurement and verifying whether the investigated stress substances are present in the stand.

Electronic noses were used for a more extensive collection and faster analysis of the measured samples, and the main goal was to verify their applicability for early stress identification in forest ecosystems. Three electronic noses are commercially available; one was specifically built in close cooperation with the Czech Technical University

in Prague for environmental applications. As part of the thesis, the following electronic noses were tested:

1) Sniffer 4D V2 sensor ©2022 SZ Soarability Technologies Co., Ltd.: Shenzhen, China ("Sniffer4D")

Electronic nose Sniffer **(Figure 2)** is a commercial electronic nose used for a wide range of mapping applications; it is a complex system consisting of multi-gas hardware and analysis software. The electronic nose can be used for ground measurements and interaction with DJI drones for more extensive mapping analyses. The Sniffer comprises a 1 GHz ARM processing chip with a memory capacity of 512 MB. The essential equipment of the sensor includes units for measuring temperature in the range of −40 - 85 °C with a resolution of 0.1 °C, humidity in the range of 0 – 100% with a resolution of 0.1%, and pressure in the range of 30 kPa - 110 kPa with a resolution of 0.01 kPa. It is also possible to equip the variable electronic nose with chemical sensors VOC_S, SO_2, CO, O_3 + NO_2, $PM_{1.0}$, $PM_{2.5}$, PM_{10}, CxHy, H_2S, and HCl.

***Figure 2**. Electronic nose Sniffer as a payload on the DJI Matrice 600 Pro drone with 1 m long Teflon tube for data collection (Hüttnerová et al., 2023).*

2) Miniature Bosch sensor device © Bosch Sensortec GmbH 2023 ("Bosch")

The Bosch BME688 sensor with built-in AI (**Figure 3**) is a very miniature device suitable for environmental mapping applications. It can measure volatile organic compounds, volatile sulfur compounds, hydrogen, carbon monoxide, and other similar

gases. For environmental applications, the microclimate is a very desirable indicator. The Bosch sensor includes a temperature sensor in the range of -40 - 85°C (sensitivity ±1°C), a humidity sensor measuring in the range of 0 - 100% with an accuracy of ±3%, a sensor pressure measurement in the range 300 – 1 100 hPa (sensitivity ±1 hPa) and also a chemical unit of the Metal-Oxide Semiconductor type (the exact sensitivity is not given by the manufacturer, but the sensor can map VOCs in tens ppb).

Figure 3. *On the left side is Handheld VOCs Detector Tiger (is described below in section 4) Handheld VOC Detector Tiger), in the upper right in the red rectangle is Miniature Bosch sensor device (Hüttnerová and Surový, 2024).*

3) Sensory device for environmental applications ("SDEA")

SDEA was constructed based on close cooperation with Associate Professor Jirovský from the Czech Technical University in Prague as an output of a University Grant Competition, where the author of this thesis was the principal researcher. The SDEA is designed as a mobile accumulator-powered unit and consists of two main components: 1) a source battery unit located in the lower part of the carrier and 2) a sensor unit located approximately 60 cm from the operator's head on the support rod **(Figure 4).**

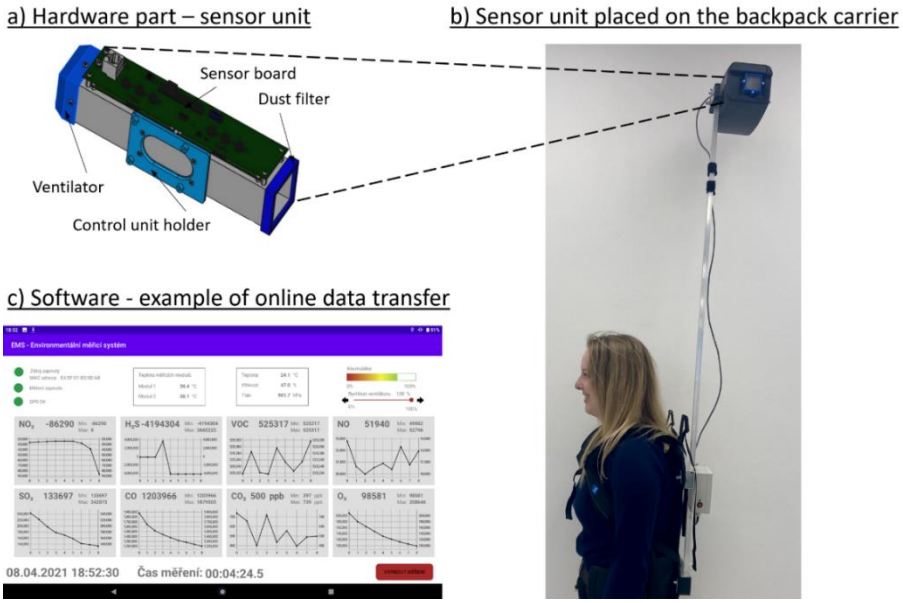

Figure 4. *Comprehensive overview of the Sensory device for environmental applications: (a) sensor unit assembly consisting of the ventilator, control unitholder, dust filter, and sensor board; B) the main sensory part is located 60 cm above the operator's head; (C) software part: layout of data on the notepad screen. The notepad screen is divided into four parts: an informative part at the top left (three items marked with status—source, measurement, and Global Navigation Satellite System), measured values at the top of the screen + fan speed, a part containing eight graphs for estimated quantities, and a status line at the bottom of the screen (Hüttnerová and Surový, 2024).*

Both components (source battery and sensor unit) are connected to each other by a cable that enables the charging of the electronic nose and the communication of the individual parts. The central part of the source battery unit is the accumulator, followed by circuits for charging and circuits for monitoring the status of the accumulator. The entire sensor unit is under a protective removable cover, and the tunnel is made of an aluminum profile. Air enters the sensor unit through a dust filter and is extracted by a fan on the opposite side of the aluminum profile. Inside, there are individual sensor units and electronics on the sensor board **(Table 2)**. The temperature, humidity, and pressure sensors are opposite the control unit holder.

Tab 2. *The sensor unit includes several cross-sensitive chemical sensors (Hüttnerová and Surový, 2024).*

	Type of sensor	Range	Sensitivity
NO_2	MOX	20 ppm	in the order of ppb
H_2S	MOX	400 ppm	in the order of ppb
VOC	PID	40 ppm	in the order of ppb
NO	MOX	20 ppm	in the order of ppb
SO_2	MOX	50 ppm	in the order of ppb
CO	MOX	500 ppm	in the order of ppb
CO_2	NDIR/thermopile	5,000 ppm	1 ppm
O_3	MOX	20 ppm	in the order of ppb

The entire sensor unit is controlled using a Raspberry microcomputer, which manages the work of individual sensor units, switches some sensors on and off to save battery, and controls time delays between individual records for others. The Raspberry microcomputer converts analog values from individual sensors into numerical values, which, based on specified conversion coefficients, convert into data in measurable units (ppb or ppm). The classic notepad communicates with the Raspberry microcomputer via Bluetooth and controls the sensor units, display, and storage of measured values. Information about individual processes is displayed in the upper left part of the informative section. If it is switched off or the actual measurement is not started, the communication via Bluetooth is not switched on either, and the status is displayed in red - it is impossible to measure and save values. As soon as communication via Bluetooth is established, the status wheel changes to green, and the measurement can be started. The measurement record includes location information, and the correct GNSS function is indicated separately. The upper part displays data on the temperature, humidity, pressure, and temperature states of individual measuring modules. The indicators on the right side are the battery status and an editable item for the set-up airflow through the sensor part. There is one more green button on the display, which can be used to switch between three states: from the measurement status off is the stage Measurement initialization, from the measurement initialization state is the stage Turn on the measurement, from the measurement status on is the Turn off the measurement.

The control unit processes the measured outputs in the following format:

<Date and Time>; <GNSS: number of satellites>; <GNSS: accuracy [m]>; <Latitude [°]>; <Longitude [°]>; <Fan speed [%]>; <NO_2 [ppb]>; <H_2S [ppb]>; <VOC [ppb]>; <NO [ppb]>; <SO_2 [ppb]>; <CO [ppb]>; <CO_2 [ppb]>; <O_3 [ppb]>; <Temperature of module 1 [°]>; <Temperature of module 2 [°]>; <Battery status [%]>; <Outside temperature [°]>; <Pressure [hPa]>; <Relative Humidity [%]>.

4) Handheld VOC Detector Tiger © 2024 Ion Science UK. Ion Science is registered trademark on Ion Science Ltd. (“Tiger”)

The Handheld Tiger sensor aims to detect volatile organic compounds; the sensor unit is photoionization technology (PID) type, ranges from 0-20,000 ppm with a sensitivity of 1 ppb (achieved during isobutylene calibrations at 20 °C) and can quickly display the measured concentration in about two seconds. The Handheld Tiger sensor

has a library of approximately 750 volatile organic substances. Before starting data collection, the user selects a chemical substance of interest from the library. Then, it can be measured at a maximum of one concentration of selected VOCs at a time. The data is displayed in real-time on the device's display and saved in text format for subsequent data processing. Tiger is without a GNSS unit and temperature-humidity-pressure unit.

As part of the electronic nose tests, a field worker was chosen as the carrier for ground level and data collection above the forest canopy; it was the multi-copter DJI Matric 600 Pro (©2022 SZ DJI Technology Co., Ltd.: Shenzhen, China) due to its higher carrying capacity and the possibility of interactive payload suspension. The multirotor DJI Phantom 4 Pro (©2022 SZ DJI Technology Co., Ltd., Shenzhen, China) was used to monitor subsequent processes, i.e., mapping the restoration of forests, which are inherently linked to consequences of natural disturbances like salvage cutting. The DJI Phantom 4 Pro has a built-in 20-megapixel RGB camera. Electronic noses were used for early detection of stress due to biotic disturbance. For non-biotic natural disturbance (forest fire) were used Sentinel-5 Precursor satellite data. Because during the fires, it was not possible to visit the affected area, thus it was impossible to collect data in situ using drones or electronic noses.

Sentinel-5 satellite has a TROPOspheric Monitoring Instrument sensor (TROPOMI) and provides daily air quality monitoring and climate mapping. It was launched in October 2017 as part of the EU Copernicus program for sun-synchronous polar orbiting. It is a nadir-viewing spectrometer measuring the ultraviolet, visible, near-infrared, and shortwave infrared wavelengths. The first dataset was published in June 2018, and currently, all datasets are freely available. Sentinel-5 provides data products on Aerosol Index, Aerosol Layer Height, Carbon Monoxide, Cloud Properties, Formaldehyde, Methane, Nitrogen Dioxide, Ozone Profile, Ozone Total Column, and Sulfur Dioxide.

4.3. Laboratory tests

Before the field investigation, the methods were verified in laboratory conditions using conventional chemical methods. The primary goal of the laboratory testing was to determine the mixture and amount of volatile organic substances secreted by spruce trees, as well as the aggregation pheromone produced by bark beetles for

communication and test the sampling conventional chemical methods for open space collection. For laboratory tests, artificial evaporators were made of 1) volatile organic compounds, simulating the exhalation of stressed spruce trees spruces, most often caused by bark beetle calamity, and 2) substances (aggregation pheromone) exhaled by bark beetles that they used for communication (2-methyl-3-buten-2-ol). Their formation (composition, size, evaporation) was based on Ghimire et al. (2016). The evaporators were first subjected to a gravimetric analysis where each type of evaporator was weighed for two weeks to determine the actual evaporation.

Next, conventional chemical methods were optimized for collecting data in open space and determining the spread of a cloud of chemical substances under set measurable abiotic conditions in an Ecophysiological laboratory, wind tunnel, and glass bell by using SPME fibres and sampling sorbent cartridges. Conventional analytic chemical methods do not offer the possibility of online display of results in real-time during measurement. Conventional chemical methods were analyzed by Gas Chromatography-Flame Ionization Detection (GC-FID) Agilent 8890 (Agilent, CA, USA) and the results displayed on the chromatograph. According to the standards, specific substances identifying stress in the forest were specified. The gas chromatography process consists of dividing the components between the mobile phase and the stationary phase. The mobile phase is the carrier gas, and the stationary phase is located in the chromatographic column, the separation principle works so that the stationary phase passes through the carrier gas through the column.

First, the sample is introduced into the injection column and evaporates there, then it is carried in the form of vapors by the carrier gas into the column. The components of the given sample are sorbed at the beginning of the column and then desorbed by the newly arriving carrier gas. The sample components pass through the column at their specific speed, as given by the distribution constant. The carrier gas brings the uniform components to the column and the separation process is constantly repeated, in the final phase the substances leave the columns in order of increasing values of the distribution constants and enter the detector, where the immediate concentration of the separated substances is determined.

The output of the sample analysis based on the principle of gas chromatography is a graphic record expressing the dependence of the recorded signal of the detector on

time (chromatograph, **Figure 5**). Identifying the substances displayed on the chromatograph is based on the agreement of the investigated unknown substance and the standard, measured under the same experimental conditions (Krofta, n.d.).

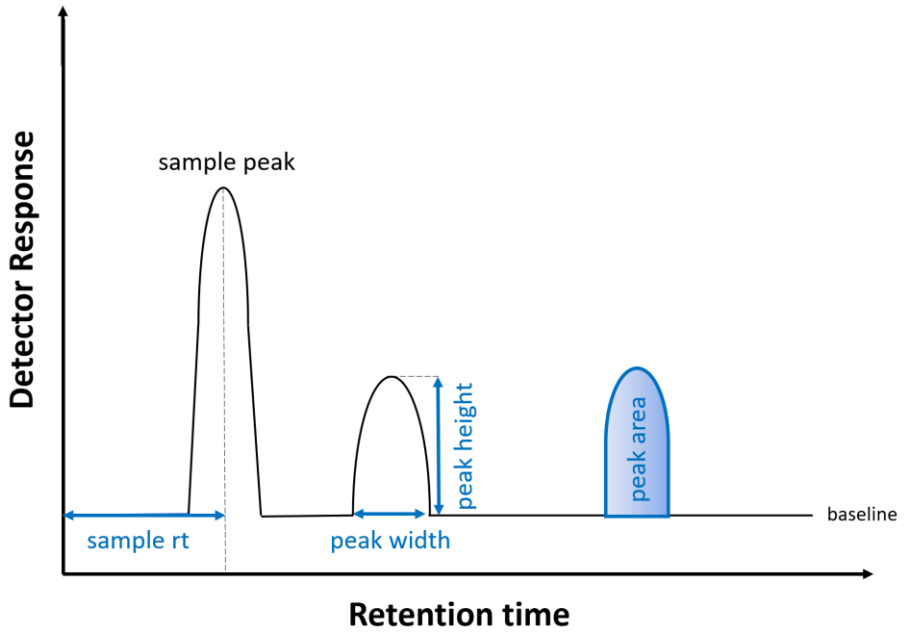

Figure 5. *A simplified demonstration of the chromatograph, where components of the sample are divided and displayed in peaks, based on the position of the peak (retention time), the given compound can be identified, and the area of the peak (and its height) is proportional to the amount of the substance in the given sample. Gas chromatography assumes that peaks have the shape of a Gaussian distribution, and each of them is described by three indicators: retention time, peak height, and peak width.*

Laboratory tests made it possible to find a suitable method for the subsequent data collection in the field and, therefore, to verify whether these specific stress-identifying substances are located near the attacked trees during field collection. At the same time, the response of electronic noses in the laboratory to artificially created vaporizers was verified.

4.4. Field data collection

The field collection technique was developed according to the type of disturbance. In the case of biotic disturbances, they could be observed at several locations and access was not restricted. Therefore, a more extensive survey could take place here, and several techniques could be tested. Abiotic disturbances are less frequent in Czechia, to the point that only one large-scale forest fire has been recorded in modern history. In addition, while mapping during a fire is very limited, it is an important part

of non-optical monitoring due to large-scale emissions. All this made necessary to use satellite images to monitor the abiotic disturbances considered in this thesis. Further in the thesis, field non-optical data collection is described based on the division into biotic disturbance, abiotic disturbance, and related subsequent processes.

4.4.1. Biotic disturbances

At each measurement, the condition of every single tree in the study area was carefully examined. A first control of the infestation was carried out by conducting a field survey, focusing on the boring dust on the trunk, resin flows, and the first bark beetle entrance holes. The second control method was the collection of UAV data with an RGB camera for a possible visual assessment of the condition of the canopy. The flight plan was prepared in the DJI Ground Station Pro application (©2022 SZ DJI Technology Co., Ltd.: Shenzhen, China) with a Front Overlap Ratio and Side Overlap Ration: 85% at a height of 80 m.

The presence of specific chemical substances indicators of stress in the forest was verified using conventional chemical methods SPME fibers and cartridges with HayeSep-Q® sorbent. A heavily infected early-stage spruce was selected in the test area, around which a special structure was attached as holders for SPME fibers and cartridges. The data collection schema (**Figure 6**) around the tree was set to three heights (130 cm, 260 cm, and 400 cm) and in four directions according to the cardinal (north, south, west, east) and in two distances from tree (5 cm, 100 cm). The structure prepared in this way served as safe sampling and ensured the possibility of comparing concentrations according to the sampling position. Data collection on SPME fibers and cartridges lasted 60 min each time, all samples were transported in dry ice.

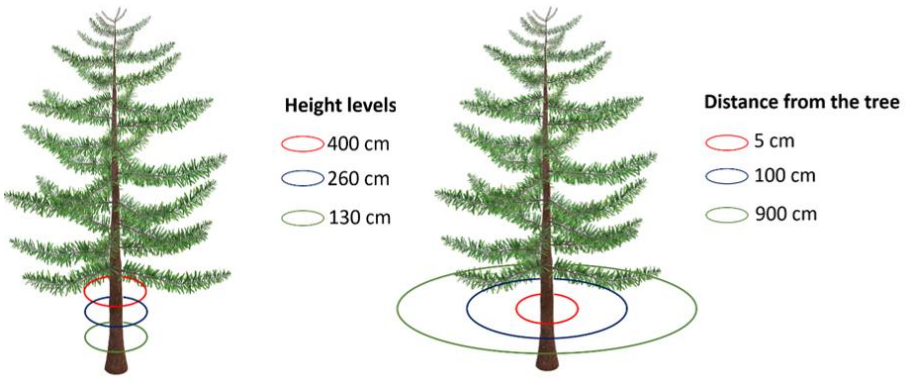

Figure 6. *A data collection scheme was used for alpha-pinene sampling using conventional chemical methods near a spruce tree infested by the bark beetle, focusing on comparing sampling heights, distances from the tree, and orientation (Stříbrská et al., 2023).*

Before the odor mapping, the electronic noses were stabilized to the ambient temperature, humidity, and pressure, and the actual measurement started after 30 minutes. During each measurement, temperature and humidity were monitored on-site. External data loggers were used if the electronic sensor was not equipped with these sensor units. In addition to information about the microclimate, it was necessary to obtain positional data, data flight logs from the drone were used to determine the measurement position in the case of data collection above the canopy. In the case of ground collection, information on positions was obtained from electronic noses with a GNSS; the Sniffer electronic nose has a satellite positioning module that supports the Global Positioning System, BeiDou Navigation Satellite System, and GLObalnaya NAvigatsionnaya Sputnikovaya Sistema. The SDEA electronic nose has a GNSS unit as part of the notebook, and for each measured record, it gives information about the number of satellites and the average accuracy; in the framework of the own measurements under the forest canopy, the average number of satellites was 13 with an average accuracy of 5.28 m. The Tiger detector and neither Bosch contain a GNSS module; the positional information was derived from the SDEA electronic nose during simultaneous acquisition based on synchronization according to time stamp.

Data collection using electronic noses was carried out in two different ways: 1) A figure-eight trajectory was used to verify the ability of electronic noses to detect changes due to stress in forest ecosystems. Data collection was carried out by an operator at ground level. The operator walked through the infested part of the forest to a part of the healthy forest, where the operator turned in a semi-circle and returned through the infested part. This procedure was repeated several times during the day to

allow for statistical evaluation of the reactions of the electronic noses to the presumed non-optical changes in the infested forest **(Figure 7)**.

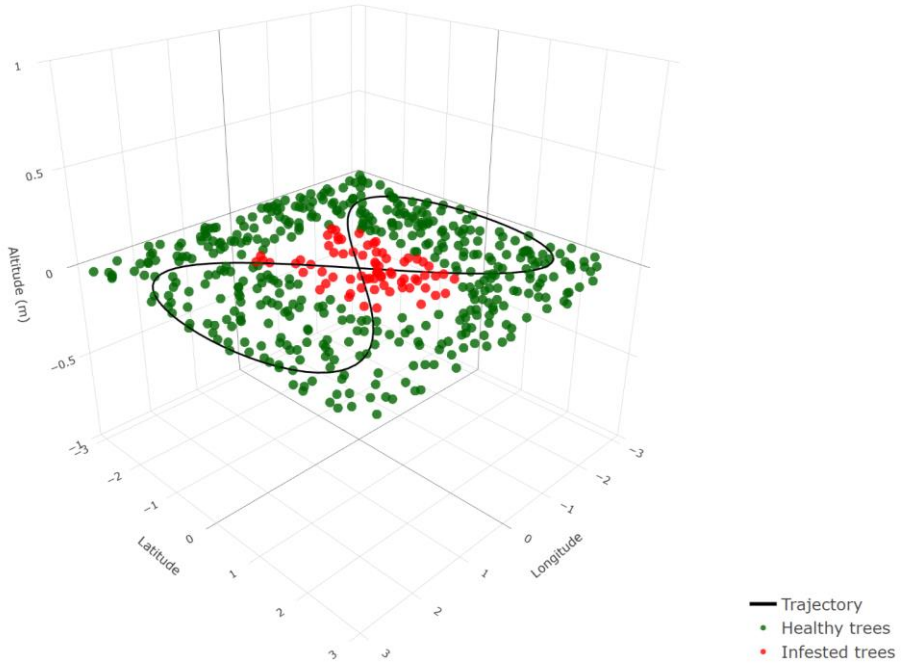

Figure 7. *The trajectory for ground data collection by an electronic nose for verification of detection capability.*

2) the trajectory was maintained in the so-called zig zag pattern in order to maintain the largest possible gaps between individual measurements and the air was as little disturbed as possible by the drone's flight or the walking of the operator **(Figure 8)**.

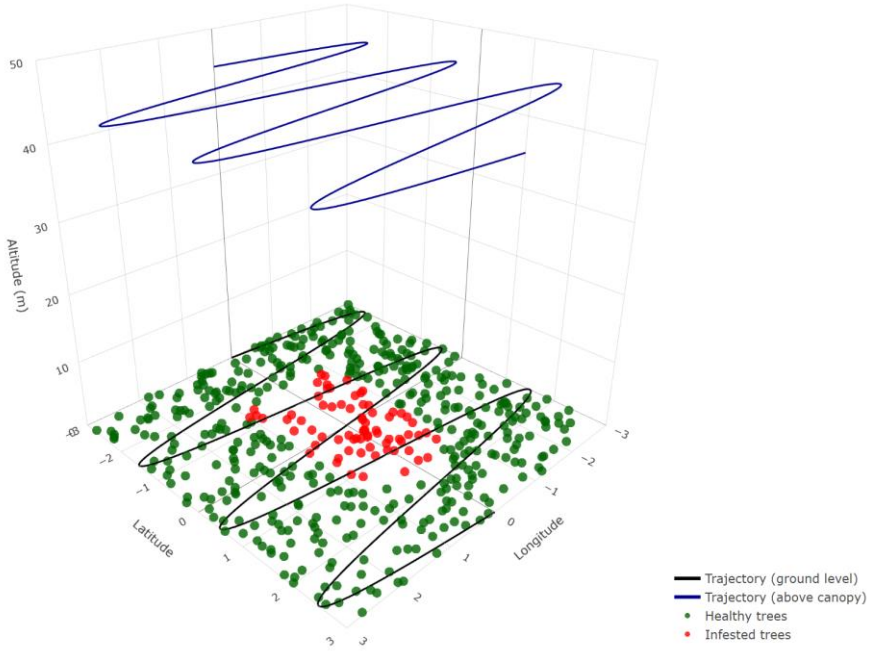

Figure 8. *The trajectory used for data collection by the electronic nose to verify sensor response in different heights: ground collection and UAV collection above the forest canopy.*

4.4.2. Abiotic disturbances

For abiotic disturbance (forest fire), a satellite platform Sentinel 5P was used with data product COPERNICUS/S5P/OFFL/. The data was obtained through the Google Earth Engine portal as a georeferenced raster format (GeoTIFF type) (Gorelick et al., 2017). To verify satellite non-optical technology and the possibility of mathematical modeling a useful time series of the emissions spread, the following periods were chosen: 1) ten periods before the fire were monitored from 3.6. 2022 to 22.7. 2022, 2) seven periods during the fire from 23.7. 2022 to 12.8. 2022, and 3) ten periods after the end of the fire from 13.8. 2022 to 1.10. 2022.

Two satellite analyses were performed in the thesis. The first focused on evaluating changes in individual buffer areas from the fire epicenter (1-30 km with kilometer intervals). The goal was to find the maximum distance where the difference in emissions caused by the fire was still evident. We also used this analysis (changepoint package R) to evaluate all Sentinel 5 data products that could record increased emissions (NO_2, SO_2, CO, HCHO, CH_4, and UV Aerosol Index). In the second analysis, a multidimensional raster was created that connects individual raster images of the same area (national park). Next, we created a space-time cube to visualize and

analyze spatiotemporal emissions data. To evaluate the size of the affected area and the duration of the emission cloud, the Change Point Detection function (**Figure 9**) was used, which divides the time series into individual segments according to changes in statistical properties (Mean shift, Standard deviation, Slope, and Count).

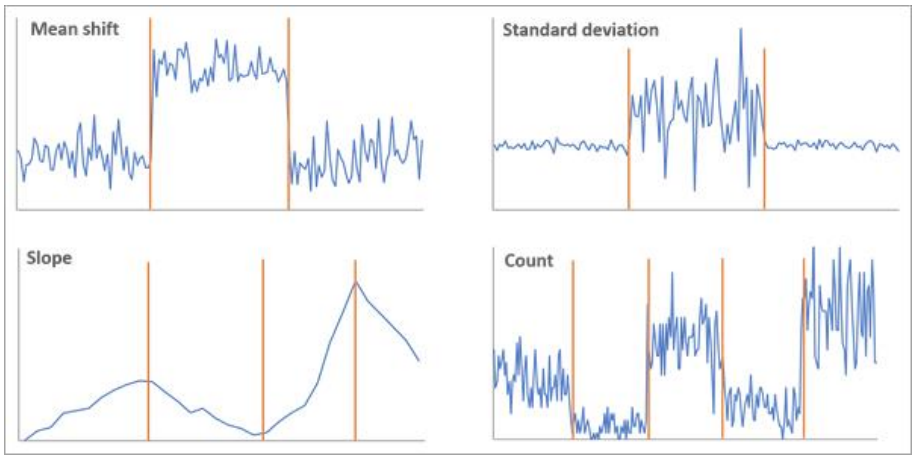

Figure 9. *A simplified blue line chart shows change point detection methods using mean shift, standard deviation, slope, and count. Vertical orange lines present the change points. (ArcGIS Pro 3.4., 2024).*

4.4.3. Subsequent processes

Clearing areas were created due to a bark beetle infestation in beginning of 2021. To minimize the edge effect, a special sub-plot was made in center of each plot to monitor the impact of ungulate browsing and the effect of different types of soil preparations on natural regeneration. The subplot is divided into two equal parts with a free strip marked as "D" of width two meters: the unfenced part is marked "A," "B," and "C," and the fenced part is marked "E," "F," and "G". Furthermore, parts "A" and "E" were prepared by clearing the branches, and the soil was prepared with single-disk soil cutters; from parts "B" and "F," only large branches were removed, and no mechanical or manual soil treatment was applied, parts "C" and "G" were cleared of branches and the soil prepared with a plow (**Figure 10**). The surrounding area was cleared of branches without special soil preparation.

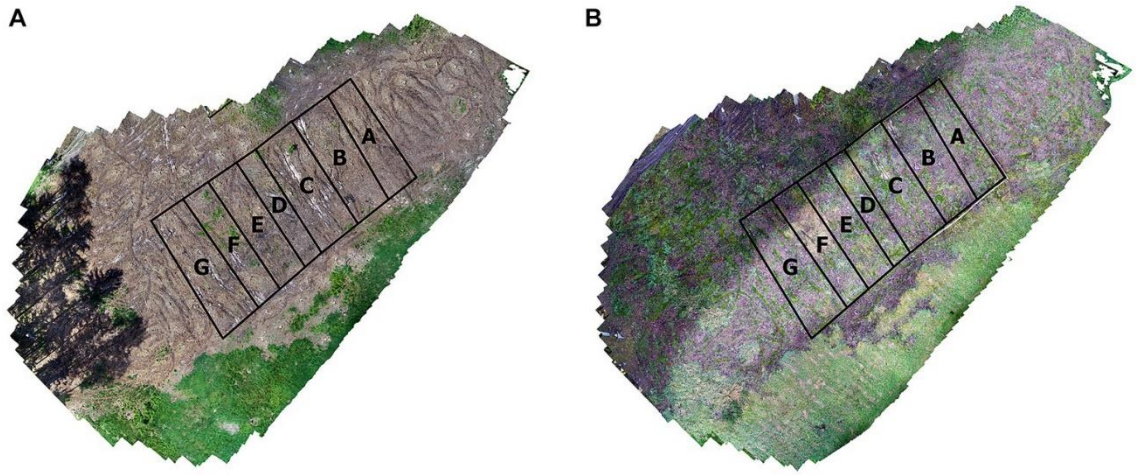

Figure 10. *Scheme of preparation of the sub-area with individual parts marked on the orthophoto from A) spring 2021, B) spring 2022 (Hüttnerová et al., 2024).*

The methodology for evaluating the suitability of areas for natural regeneration aims at effectively obtaining data, which is why the DJI Phantom 4 Pro multicopter with an RGB camera was chosen (good maneuverability, lower acquisition costs, fast data processing using the photogrammetric method). Data was acquired according to a pre-created mission in the DJI Ground Station application (©2022 SZ DJI Technology Co., Ltd.: Shenzhen, China) for each plot in two resolution details:

1) Capturing information (Hover and Capture Mode) about microrelief in very high resolution 0.4 cm/pix with the following parameters of flight mission: Height above the ground: 15 m, Front Overlap Ratio and Side Overlap Ratio: 85 %, and Flight Speed: 5 m/s.

2) Capturing (without hovering mode) information about plots and their surroundings with the following parameters of flight mission: Height above the ground: 110 m, Front Overlap Ratio and Side Overlap Ratio: 85 %, and Flight Speed: 8.8 m/s.

Chapter 5

Results

The detailed research results are presented in individual articles; in this part, the most important findings are summarized, and the research questions of the thesis are answered. The main goal of the thesis was to verify the cutting-edge technologies for stress mapping in forest ecosystems. As part of the research, several sensors and data processing techniques were verified. The study itself was experimental, and the field of non-optical remote sensing is new in forestry. Bark infestation, forest fire, and mortality stress resulting from natural forest regeneration were mapped. The tested methods proved very promising for early stress detection. Electronic noses were able to map early bark beetle infestations during ground data collection. Close-range data collection with UAVs has not yet demonstrated the ability to detect changes above the tree canopy, but they were verified for mapping mortality stress in terms of modelling relief variables. With satellite data from the TROPOMI sensor, we were able to map the spread of emissions from forest fires.

The first article deals with conventional chemical methods and their possible use in open space for three-dimensional (3D) mapping of chemical substances. The second article focuses on the early detection (within one week of the first attack) of bark beetle infestation using electronic noses. The third article focuses on mapping chemical changes in an attacked forest and compares ground collection with UAV collection. The fourth article validates a satellite TROPOMI sensor for mapping the emission of carbon monoxide. The fifth article deals with the analysis of microrelief after a natural disturbance and maps subsequent regeneration processes based on spatial analysis.

5.1. Pilot Study of 3D Spatial Distribution of α-Pinene Emitted by Norway Spruce (L.) Karst Recently Infested by Ips typographus (L. 1758) (Coleoptera: Scolytinae)

Barbora Stříbrská, Antonioni Acacio Campos Moliterno, **Tereza Hüttnerová**, Martin Leiner, Peter Surový, Anna Jirošová

Faculty of Forestry and Wood Science, Czech University of Life Sciences (CZU Prague), Kamýcká 129,165 21 Prague, Czech Republic

Forests 2024, 15(1), 10; https://doi.org/10.3390/f15010010

Author´s contribution: 15 %

Summary of the article

An article focusing on findings from conventional chemical methods and their application for measurements in open space. This publication was preceded by extensive laboratory tests during which artificial evaporators were created to simulate volatile organic substances and bark beetle pheromones. Then, we collected data in the field to map the 3D alpha-pinene cloud around the infected spruce. The presented methodology provides the possibility to determine the increased amount of alpha-pinene in the field, which is the primary substance secreted by spruce trees in the event of stress in several times higher concentrations than during rest. The method is limited to a smaller number of samplings due to the time-consuming nature of sampling and subsequent analysis of the samples by analytical chemistry. Therefore, this methodology is a suitable validation method for electronic nose mapping, which can provide measurements with a very high temporal resolution and bring the possibility of effective mapping of entire forest stands.

Full article

forests

MDPI

Article

Pilot Study of 3D Spatial Distribution of α-Pinene Emitted by Norway Spruce (L.) Karst Recently Infested by *Ips typographus (L. 1758) (Coleoptera: Scolytinae)*

Barbora Stříbrská, Antonioni Acacio Campos Moliterno, Tereza Hüttnerová, Martin Leiner, Peter Surový and Anna Jirošová *

Faculty of Forestry and Wood Sciences, Czech University of Life Sciences Prague, 16500 Prague, Czech Republic; stribrska@fld.czu.cz (B.S.); moliterno@fld.czu.cz (A.A.C.M.); huttnerovat@fld.czu.cz (T.H.); leiner@fld.czu.cz (M.L.); surovy@fld.czu.cz (P.S.)
* Correspondence: jirosovaa@fld.czu.cz

Abstract: The Eurasian Spruce Bark Beetle (*Ips typographus*) (L. 1758) (Coleoptera: Scolytinae) poses a significant threat to Eurasia's Norway spruce (*Picea abies*) (L.) Karst, forests. Early detection of infested trees is crucial to control beetle outbreaks and allow salvage logging before the next generation emerges. Besides traditional methods, new approaches focus on monitoring volatile organic compounds, mainly monoterpenes, emitted by infested trees. Using analytical chemistry, we studied the distribution of these compounds, particularly α-pinene, around infested trees. In lab trials, we optimized α-pinene detection using dynamic absorption and solid-phase microextraction (SPME), analyzed by gas chromatography with flame ionization detection (GC-FID). We conducted forest trials, revealing varying α-pinene abundance due to changing conditions. However, consistent trends emerged: levels were highest near the infested tree stem and 1.3 m above ground in the first trial and at a 1 m distance from the infested stem in the second. We generated a three-dimensional cloud depicting the distribution of α-pinene around infested trees in their natural habitat. These findings open avenues for detecting bark beetles on a large scale by mapping elevated concentrations of volatile organic compounds emitted by infested trees, potentially leading to alternative pest management methods. Scanning methods, such as electronic sensors combined with remote sensing, hold promise for this application.

Keywords: early attack detection; bark beetle; VOC; α-pinene; *Picea abies*; SPME; Eurasian Spruce Bark Beetle

check for updates

Citation: Stříbrská, B.; Moliterno, A.A.C.; Hüttnerová, T.; Leiner, M.; Surový, P.; Jirošová, A. Pilot Study of 3D Spatial Distribution of α-Pinene Emitted by Norway Spruce (L.) Karst Recently Infested by *Ips typographus (L. 1758) (Coleoptera: Scolytinae). Forests* **2024**, *15*, 10. https://doi.org/10.3390/f15010010

Academic Editor: Qing-He Zhang

Received: 14 November 2023
Revised: 14 December 2023
Accepted: 17 December 2023
Published: 20 December 2023

Copyright: © 2023 by the authors. Licensee MDPI, Basel, Switzerland. This article is an open access article distributed under the terms and conditions of the Creative Commons Attribution (CC BY) license (https://creativecommons.org/licenses/by/4.0/).

1. Introduction

The Eurasian Spruce Bark Beetle *Ips typographus* (L. 1758) (Coleoptera: Scolytinae) is the main pest of Norway spruce, *Picea abies* (L.) Karst. forests in the Central European region. Over the past decade, the combination of ongoing climate change, economically driven silvicultural practices, and the presence of spruce stands in areas beyond their natural range have weakened the natural defense mechanisms of trees and resulted in the occurrence of severe bark beetle spreading [1]. In the Czech Republic, outbreaks started after severe drought events in 2015 and 2018 [2] and led to an exponential increase in salvage logging volume from 2017 to 2020, with the volume rising from approximately 5.9 million m^3 in 2017 to 26.2 million m^3 in 2020 [3,4] (Figure S1).

The initial step in managing a bark beetle outbreak is early detection of newly infested trees to enable timely salvage before the emergence of offspring [4]. Forest keepers typically rely on traditional methods, which involve personally observing the boring dust produced by infesting beetles [5]. However, during bark beetle outbreaks in large, forested areas, this approach has severe limitations, often resulting in the exponential spread of the beetles.

Hence, an alternative method for early detection on a large scale is needed. Remote sensing techniques have been extensively investigated, using the detection of different indicators from spectral features to temperature [6] and recently also involving chemical substances (Sentinel SP) [7].

Recent research by [8] has proposed measuring the emission of volatile organic compounds (VOCs) from infested spruce as an indicator of bark beetle attacks. Furthermore, various methods for detecting these VOCs at different developmental stages have been introduced. Current research is investigating the utilization of an electronic nose equipped with nonspecific sensors for VOC detection [9]. Likewise, nonspecific metal oxide sensors have been mounted on UAVs to assess the concentration of α-pinene in forest environments [10]. Notably, natural olfaction systems of dogs trained to detect bark beetle pheromones have proven more effective in finding infested trees in cooperation with their dog handler compared to human experts only [11,12].

The VOC emitted by conifer mainly consists of hemi- and monoterpenes, which are produced as defense secondary metabolites. The conifer's immediate defense mechanism against wood-boring insects is the exudation of constitutive resin, which has a toxic and immobilizing effect on beetles [13]. In the later stages of a bark beetle attack, the production of resin is induced in the newly formed resin ducts in the phloem, xylem, and bark [14]. The resin is a mixture of terpenic compounds. The monoterpenes are volatile and form the main content of VOCs emitted by conifers. In spruce, α-pinene, β-pinene, Δ-carene, limonene, β-phellandrene, camphene, and myrcene dominate [15] but resin also contains sesquiterpenes and a high content of highly viscous diterpenes [16,17]. Oxidized forms of all terpenes are also present.

In addition to resin emissions from the stem, volatile terpenes are also emitted from the needles in the canopy of conifers [18,19]. The emission rate of volatile terpenes from healthy trees is influenced by various macro- and microclimatic conditions, such as temperature and humidity [17,20]. Different temperatures, and consequently varying VOC emissions, are observed in clearings and forest edges within fragmented forests [17,21]. Furthermore, VOC emissions in conifer forests exhibit vertical variations [22] and follow a diurnal rhythm dependent on tree physiological processes [19]. The terpenes emissions from conifer forests are widely discussed in the context of terpenes as a free radical source in the atmosphere [23–25], because hemi and monoterpenes are photochemically reactive compounds that affect ozone and carbon monoxide concentrations and their oxidation products can participate in the formation of secondary organic aerosol and cloud condensation nuclei [26].

When Norway spruces are attacked by bark beetles, the content of emitted terpenes from the stem significantly increases during the first two weeks of infestation. This growth is primarily attributed to the opening of constitutive resin storage and is quantified in the close vicinity of the stem. Different methods used for quantification have yielded a wide range of results, ranging from a 10 to 100-fold upturn [8,27,28]. The dominant compound in emissions was always α-pinene, representing the time and spatial distribution of the other main monoterpenes [8]. The bouquet of infested trees also includes the aggregation pheromone produced by bark beetles. Beetles use this scent for navigation to aggregate, allowing them to overcome the tree's defense during the infestation [29]. The content of bark beetle pheromones is several orders of magnitude lower than that of α-pinene in forests [30]. However, beetles are capable of discerning this signal from the background of host odors thanks to specialized receptors on their antennae, the organs responsible for perceiving smells [31]. Furthermore, beetles may orient themselves by detecting host compounds, primarily terpenes, when choosing a suitable host tree or habitat [32]. They also have specialized receptors for host compounds [33].

Numerous studies have investigated monoterpenes emitted by conifers in both laboratory and natural conditions. In the laboratory, collection systems can be readily optimized, as detailed in a comprehensive review [34]. In field conditions, VOC collection is more complex, and various techniques have been employed to address specific research questions [35].

The most common approach involves dynamic headspace sampling with compound collection onto sorbents, followed by extraction into solvents or thermal desorption. Additionally, solid-phase microextraction methods have been utilized (as shown in Table 1) [36,37].

Table 1. Methods of VOC collection from conifers in forests.

Tree Species/ Stress Occasions	Sampling Specification	Compound (Unit)	Technical Parameters (Sorbent; Amount; Flow Rate)	Time of Sorption	Analytical Method	Source
Picea abies/ intact forest	Stem (not specify) 5 m above the ground; stainless steel TD tubes	Individual monoterpenes α-pinene 3.07 ± 0.25 ppbv	Tenax TA, (35/60) 200 mg; 200 mL/min	30 min	GC-MS	[38]
Picea abies/ attacked trees	Stem 1.3 m above the ground; surrounded PET (25 × 38 cm) encloser	Individual monoterpenes α-pinene 62.8 ± 23.6 μg h^{-1} m^{-2} bark area	Tenax-TA a Carbopack-B, (60/80) 100/100 mg; 200 mL/min	60 min	GC-MS	[28]
Picea engelmannii/ attacked trees	Stem 0.5 to 1.5 m above the ground; the trunk by dynamic sampling <1 cm from stem (sorbent trap)	Individual monoterpenes α-pinene 8.5 ± 2.1 ng L^{-1}	Porapak Q 110 mg; 400 mL/min	120 min	GC-MS	[39]
Picea abies/ attacked trees on forest edge	Stem 3 h 1–2 m above the ground; sanitized T gllas tube	Verbenone (ng/3 h): α-pinene (μg/3 h) 0.6 (ng/3 h): (μg/3 h)	Porapak Q, (80/100) 70 mg; 20 mL/min	180 min	GC-MS	[40]
Pseudotsuga menziesii/ attacked trees	Branch 1.5 m above the ground; Teflon bag (50 × 75 cm)	Individual VOCs α-pinene 813.9 ± 482.29 ng h^{-1} g^{-1} fresh weight	HayeSep-Q 30 mg; 500 mL/min	30 min	GC-MS	[41]
Pinus rigida and *Pinus koraiensis*/intact forest	Branch 20 L Tedlar bag	Total monoterpenes emission (μgC gdw^{-1} h^{-1}) *Pinus rigida* 0.9 μgC gdw^{-1} h^{-1} *Pinus koraiensis* 0.4 μgC gdw^{-1} h^{-1}	Tenax TA, (60/80) and Carbotrap, (20/40) 200 mg; 100–200 mL/min	15–60 min	GC-MS GC-FID	[42]
Pinus sylvestris/ intact forest	Branch canopy height; (FEP) copolymer foil (50 μm thickness) mounted in cylindrical frames	Individual monoterpenes α-pinene 917 ± 58 ng h^{-1} g^{-1} (April) α-pinene 75 ± 12 ng h^{-1} g^{-1} (July)	Tenax TA, (60/80) and Carbotrap, (20/40) 50–100 mg; 100 mL/min	60 min	GC-MS GC-FID	[43]
Pinus sylvestris and *Picea abies*/intact forest	Branch 18 L all-Teflon chamber made of 0.05 mm transparent FEP-Teflon film enclosing a 20–30 cm branch segment	Acetone and α-pinene (ng gdw^{-1} h^{-1}) α-pinene 80 ng gdw^{-1} h^{-1} Monoterpene emission 900 ± 640 ng C gdw^{-1} h^{-1}	Tenax TA 200 mg; 100 mL/min	12–40 min	GC-MS GC-FID	[44]
Picea abies/ attacked trees	Stem 1.3 m above the ground; tree trunk chamber connected with PTFE tubing	Individual VOCs (μg m^{-2} h^{-1}) α-pinene 911.14 μg m^{-2} h^{-1}	Tenax TA and Carbograph 1TD 200 mL/min	30 min	GC-MS	[27]
Picea abies/stress from sun irradiation	Stem 3.5 m above the ground; aluminum chamber	Individual monoterpenes sum of eight main MT 8.5 log10 VOC	SPME	60 min (from 1 to 2 p.m.)	GC-MS	[17]
Picea abies/attacked trees	Stem 3.5 m above the ground; aluminum chamber	Individual monoterpenes α-pinene 9.5 $\log_{10}$ sum peak area	SPME	60 min (from 1 to 2 p.m.)	GC-MS	[8]
Lerosa NP forest/conifer forest; 6 different plots	open air	Individual VOCs 894 abundance relative to hexanal (%)	SPME	300 min (from 10 a.m. to 3 p.m.)	GC-MS	[45]

To study emissions on an ecosystem scale, researchers have employed various instrumental techniques, such as proton-transfer-reaction-time-of-flight (PTR-TOF) [46–48] mass spectrometry for quantifying monoterpene fluxes [19] or specialized gas chromatographs installed in situ at collection sites. However, these instruments can be expensive and lack portability, restricting data collection to a limited number of sites [49].

Hypothesis and objectives: This study is founded on a previously proposed concept suggesting that the number of volatile organic compounds emitted by trees, particularly monoterpenes, significantly increases within two weeks of bark beetle infestation [8]. This increase can serve as a measurable characteristic upon which the foundation of a newly developed alternative early bark beetle detection method may be based.

Our objectives were to optimize the collection of α-pinene emissions from spruce logs subjected to a controlled simulative bark beetle infestation in the laboratory and consequently detect the outdoor 3D dispersion of monoterpenes, represented by α-pinene, in the surroundings of freshly infested spruce trees at horizontal and vertical distances. We employed analytical chemistry methods for collecting VOCs, which are not typically used for VOC collection in open environments.

Particular objectives were:

1. Assess the distribution of α-pinene at different distances from and heights within a simulatively infested log pile in the laboratory, considering specific temperature conditions.
2. Validate the feasibility of measuring the distribution of α-pinene under actual field conditions, specifically focusing on naturally *Ips typographus*-infested trees within a forest environment.
3. Consider other influencing factors, such as temperature, wind speed, and the immediate surroundings of the forest.
4. Compare the effectiveness of the Solid-Phase Microextraction (SPME) method with HayeSep-Q® sorbent cartridges, which involve drawing air through them using air pumps.

2. Materials and Methods

2.1. Optimization of VOC Collection from Simulatively Infested Spruce Logs in a Laboratory

The experiments were conducted under laboratory conditions (25 ± 1 °C, humidity 60% ± 10%) using three fresh-cut logs (height of 40, diameter of 25 cm) of *Picea abies* previously stored in a cold room (−5 °C). The experiment was repeated three times at one-week intervals. Prior of all repetitions, logs were acclimated for 24 h before volatile collection in the conditions described above. Logs were arranged vertically in piles from the floor: The lowest log represented level 1—L1 (20 cm), the middle log level 2—L2 (60 cm), and the upper log level 3—L3 (100 cm) (Figure 1a). To prevent unwanted VOC emissions from fresh-cut logs, the upper and lower exposed surfaces were covered with PE plastic film.

The bark beetle attack was simulated by drilling holes (Ø 2 mm × 0.3 cm deep) into the bark and phloem on the surface of the logs (100 holes per log, spaced in 5 cm spin) to mimic the production of VOC emissions during bark beetle infestation.

VOCs were collected from each of the three levels (L1, L2, and L3) at two distances, 5 cm and 30 cm from the bark surface, using Solid-Phase Microextraction (SPME) fibers (PDMS/CAR/DVB, Supelco, PA, USA) as shown in Figure 1b. The SPME fibers were fixed in protective hard plastic cylindrical chambers hung in an open space (7.2 cm high, Ø 5.2 cm, material PP, Merci, CZE), with an open bottom and a hole covered by septa in the upper lid to hold the fiber. To follow the distance and cardinal directions described above, the chambers in the experimental apparatus were fixed by metal wires.

SPME collection was conducted for 15 min, beginning 2 h after drilling, under controlled conditions (25 ± 1 °C, humidity 60% ± 10%). A total of 24 samples were taken, with 8 samples per level (n = 24).

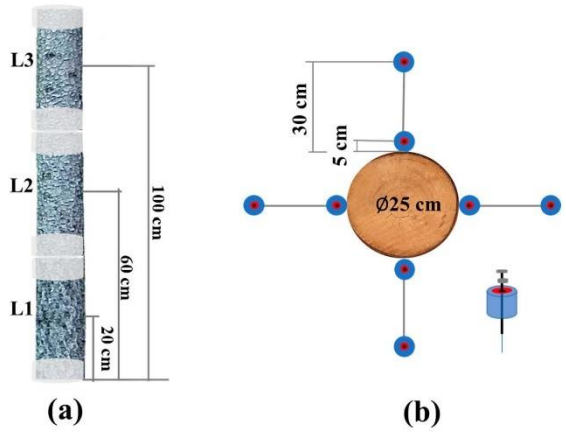

Figure 1. Volatile collection of α-pinene under laboratory conditions from fresh drilled logs of *Picea abies*. (**a**) The collection of α-pinene occurred across three height levels, namely L1, L2, and L3. (**b**) Top view of the log pile; black dots indicate distances between the bark surface and the point of collection of α-pinene for each level.

2.2. Field Collection of Distributed VOCs Emitted by the Ips typographus Naturally Infested Picea abies

We conducted two collections of VOCs from naturally infested trees in the field at different locations and during different periods of the 2022 growing season. In this study, we did not measure VOCs from non-infested trees as controls. This decision stems from the continuation of our prior study [8] and existing literature reports (Table 1), which have consistently demonstrated several-fold increases in emissions from infested trees using similar techniques. Both collections took place on the Forests ČZU property near Kostelec nad Černými lesy, the Czech Republic. The area is characterized by a mature forest primarily composed of a 90-year-old Norway spruce (*P. abies*) plantation, situated at an altitude of 400–450 m above sea level (Figures 2 and 3).

The distributed VOCs were collected within 900 m around the freshly *Ips typographus*-infested individual Norway spruces. The infestation status was found by the occurrence of fresh frass at the stem's base, and infestation stadia were specified by assessing the beetle attack density exhibited by the sampled tree. Both sampled trees were in the nuptial chamber building attack stadia, approximately two weeks from the beginning of the mass attack.

The VOCs were collected from infested trees at three different height levels from the ground (1.3 m, 2.6 m, and 4 m). Collection chambers were placed at three different distances from the tree trunk (5 cm, 100 cm, and 900 cm away from the tree) (Figure 3). The row of collection chambers was oriented in four cardinal directions: north (N), east (E), south (S), and west (W) (see Figures 2–4 for reference). Dataloggers were used throughout the experiment to measure the temperature and humidity (Tables S1 and S2), and an anemometer was used to measure the wind speed (Figures 2 and 3).

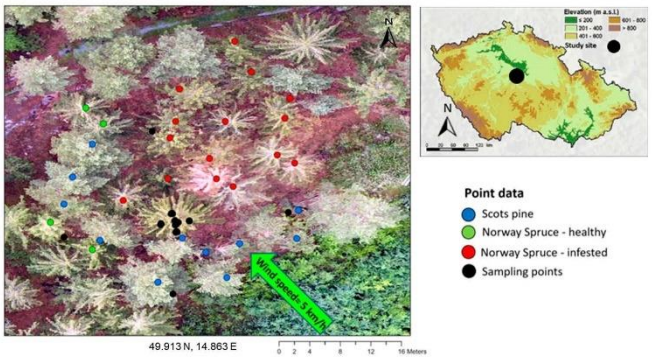

Figure 2. Study site for the first forest spatial VOC measurement around the infested tree (30 June 2022). Locality Forests ČZU close to Stříbrná Skalice, the Czech Republic (49.913 N, 14.863 E). Black points—sampling points around the sampled bark beetle-infested tree, in nuptial chamber infestation stadia; red points—Norway spruce infested trees in later stadia of infestation or dead; green—healthy Norway Spruce trees; blue points—Scot pines.

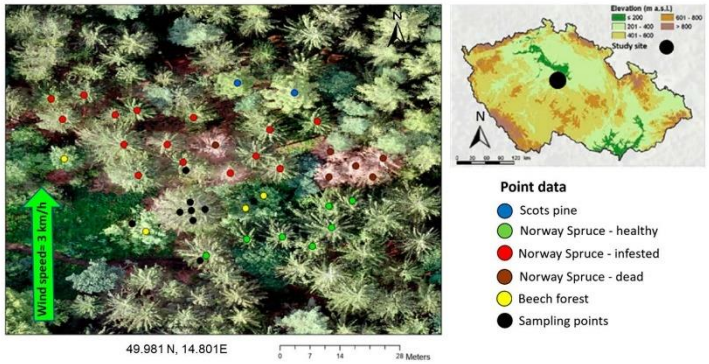

Figure 3. Study site for the second forest spatial VOC measurement around the infested tree (24 August 2022) for data in the ČZU Forests close to Vyžlovka, the Czech Republic (49.981 N, 14.801 E). Black points—sampling points; red points—Norway spruce infested trees; green—healthy Norway Spruce trees; brown points—dead Norway Spruce trees; blue points—Scot pines; yellow points—beech trees.

Two analytical approaches were employed to collect VOCs from infested trees in natural forest conditions [27,28,45]:

Sorption onto SPME fibers (PDMS/CAR/DVB, Supelco, PA, USA): Eight SPMEs fixed in protective chambers were positioned at three height levels: L1 (130 cm), L2 (240 cm), and L3 (400 cm). They were placed at two distances from the tree (5 cm and 100 cm) in the immediate proximity of the tree in four cardinal directions: north, south, west, and east. Additionally, four fibers were positioned 900 cm away from the tree in the same direction. These SPMEs were exposed for 60 min to collect volatile organic compounds (VOCs) from the forest air. After collection, the fibers were sealed in vials with septa in the same manner as in the laboratory. They were then placed on dry ice and subsequently stored in a freezer at −18 °C before undergoing measurement using Gas Chromatography-Flame Ionization Detection GC-FID, Agilent 8890 (Agilent, CA, USA).

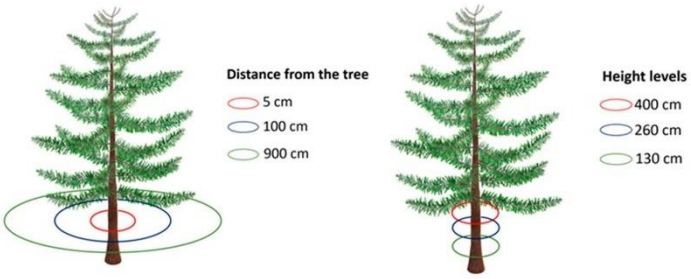

Figure 4. Established collection directions for VOCs around trees newly infested by bark beetles.

Sorption using cartridges (inner Ø 3 mm) filled with HayeSep-Q® sorbent (30 mg, Sigma-Aldrich, St. Louis, MO, USA,): This approach involved filtering the surrounding air through sorbent in cartridges sucked by sampling pumps (Pocket Pump Touch; Serie 220–1000, Eighty Four, PA, USA). The pumps were calibrated to operate at a flow rate of 100 mL/min for 60 min. Of the 12 air pumps, the chosen measurements were established along the first height level (130 cm from the ground) in all cardinal directions and different distance levels, and two cartridges were set up at the second height level in north and south directions at a 5 cm distance from the bark surface.

2.3. Chemical Analyses of SMPE Fiber and Cartridges via Gas Chromatography-Flame Ionization Detection (GC-FID)

Cartridges were washed with 1 mL of GC-grade hexane (GC-capillary grade; Avantor, PA, USA) and stored at −18 °C for further chemical analysis.

The SPME and cartridge analyses were carried out via Gas Chromatography-Flame Ionization Detection (GC-FID) Agilent 8890 (Agilent, CA, USA). The GC-FID was equipped with a DB-WAX capillary column (30 m × 320 µm × 0.25 µm film thickness; Agilent, CA, USA). The GC oven program followed a temperature profile of the initial temperature at 40 °C for 2 min, followed by a ramping rate of 10 °C per minute to reach 230 °C, where it was held for 2 min. The carrier gas He flow was 1.5 mL·min^{-1}. The inlet operated in spitless mode and the inlet temperature was 220 °C. For the desorption of SPME fibers, an SPME liner was used (n°5190-4048, 78.5 × 0.75 mm id, Agilent, CA, USA). The extracts in hexane (1 µL) from the cartridge collection were analyzed in spitless mode.

2.4. Determination of Relative Quantities of α-Pinene via SPME and Absolute Quantities Sorbed to Cartridges

On the chromatogram, peaks of the main spruce monoterpenes and other volatile organic compounds (VOCs) from the forest air near *P. abies* were observed. However, to describe their 3D distribution, only the most abundant α-pinene was chosen, as it adequately represents the trend of the other main monoterpenes [8].

In both collection methods, α-pinene's peak identity was confirmed by comparing its retention time with the commercial standard (α-pinene, Sigma-Aldrich, St. Louis, MO, USA).

The abundance of α-pinene collected via SPME fiber was determined by measuring the peak area of α-pinene divided by the sum of areas of the peaks of the five main monoterpenes chosen (α-pinene, β-pinene, Δ-carene, limonene, camphene, and myrcene, 1.8 cineole) comparing it across individual samples. The quantification of α-pinene in the cartridge extracts was based on a calibration curve (Figure S2) constructed using the commercial standard of α-pinene diluted in hexane at 0.1, 0.5, 1, 10, 25, 50, and 100 µg/mL. The amount of α-pinene in one cartridge, expressed here as µg/mL, means µg/(6 L of air) in the vicinity of an infested tree.

2.5. Statistical Analyses

Statistical analyses were performed using Statistica (version 14.0.0.15). The normality assumption was tested using the Shapiro–Wilk test, and in each case, the null hypothesis (H0) was rejected, indicating the need for nonparametric testing. The Kruskal–Wallis test was used to compare individual levels, distances, and cardinal directions. When the test showed statistical differences, post hoc tests were conducted to examine differences between repetitions.

For SPME analysis, the dependent variable was the relative peak area of α-pinene collected. For cartridges, the amount of α-pinene quantified by the calibration curve was the dependent variable. In both analyses, the independent variables were the distance and height measurements.

3. Results

3.1. Optimization of VOC Collection to SPME in a Laboratory

The three VOC collections in the laboratory, taken at different times, were considered three repetitions since they were kept under the same experimental conditions (temperature and method of log drilling). Statistical analysis was conducted on all of them together ($n = 72$).

The abundance of α-pinene, the main monoterpene representing trends of other MT, was statistically highest at a 5 cm distance from the drilled stems compared to a 30 cm distance from the drilled stems ($p = 0.0362$) (Figure 5a).

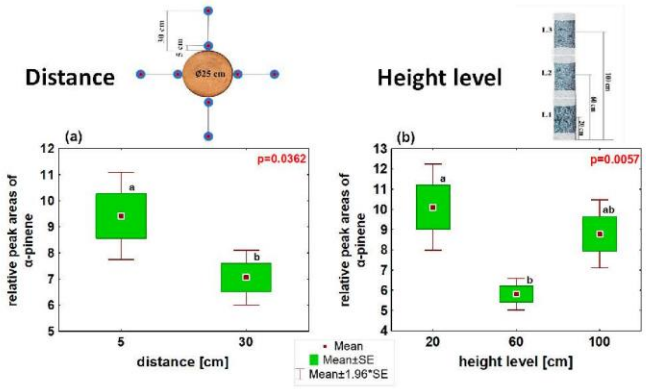

Figure 5. SPME laboratory data collections of α-pinene, three replications. (**a**) Abundance of α-pinene for lab experiment at different distances from drilled stem (5 cm and 30 cm); (**b**) abundance of α-pinene for lab experiment at different height levels from the ground (L1—20 cm; L2—60 cm; L3—100 cm). Small red squares—Means; green boxes—Means ± SE; Whiskers—Means ±1.96*SE. Lowercase letters above columns indicate significant differences between different distance or different height level. The *p*-values result from Kruskal–Wallis test; $n = 72$.

In the vertical direction, the distribution of α-pinene was statistically different ($p = 0.006$). The lowest abundance was observed at the medium level L2 (60 cm from the ground), and it was significantly different from the abundance at the bottom level L1 (20 cm from the ground) (post-hoc; $p = 0.007$) (Figure 5b).

3.2. α-Pinene Spatial Distribution around Norway Spruce Infested by Ips typographus for Two Weeks

The conditions in the first forest spatial VOC measurement conducted on 30 June 2022 on two-week naturally infested trees were an average temperature of 25.1 °C, average humidity of 72.6%, wind speed of 5 km/h, wind direction from the SE, and sunshine. The abundance of α-pinene emitted from the naturally infested tree was upregulated at a 5 cm distance from the stem. This upregulation was detected by both collection methods, with a significant increase observed using SPME ($p = 0.036$), where 5 cm and 100 cm distances significantly differed ($p = 0.036$ post hoc) (Figure 6a) and a non-significant increase was observed using sorption to cartridges ($p = 0.0585$). A trend of a decreasing α-pinene concentration at a 900 cm distance from the infested tree was observed in the collection involving cartridges (Figure 6d), but not in the collection using SPME (Figure 6a).

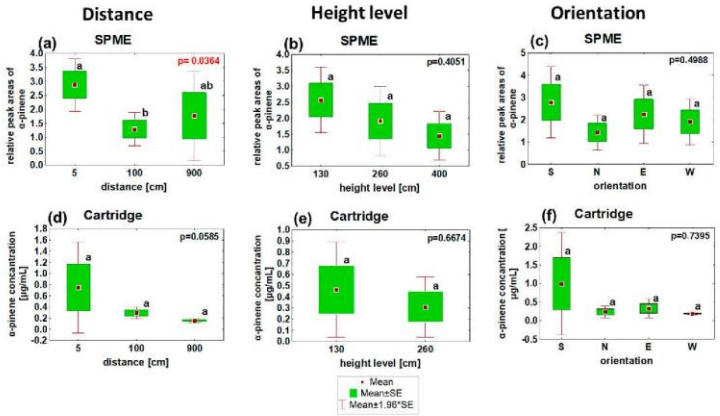

Figure 6. First field detection of α-pinene distribution around *Ips typographus*-infested spruce (30 June 2022). (**a**) Abundance of α-pinene collected by SPME in different distances from stem (5 cm; 100 cm; 900 cm); (**b**) abundance of α-pinene collected by SPME at different height levels from ground (130 cm; 260 cm; 400 cm); (**c**) abundance of α-pinene collected by SPME in cardinal directions (S—south; N—north; E—east; W—west); (**d**) abundance of α-pinene collected by HayeSep-Q® cartridges in different distances from stem (5 cm; 100 cm; 900 cm); (**e**) abundance of α-pinene collected by HayeSep-Q® cartridges at different height levels from ground (130 cm; 260 cm); (**f**) abundance of α-pinene collected by HayeSep-Q® cartridges in cardinal directions (S—south; N—north; E—east; W—west). Small red squares—Means; green boxes—Means ± SE; Whiskers—Means ±1.96*SE. Lowercase letters above columns indicate significant differences between different distance different height level, and different orientation. The *p*-values result from Kruskal–Wallis test. ($n = 27$ SPME samples) (cartridges $n = 12$).

In the vertical direction, a weak, non-significant trend was observed in the accumulation of α-pinene in the bottom level of the stem at 130 cm above the ground, decreasing with altitude up to 400 cm above the ground. This trend was consistent across both collection methods (Figure 6b,e).

Regarding cardinal orientation, there was no significant accumulation of α-pinene on any of the measured sides. However, considering the high variability of the data, there was a trend of increased α-pinene abundance on the south side of the infested stem, as observed with both SPME fiber and cartridge collection methods (Figure 6c,f).

A 3D depiction of the α-pinene collection using SPME fiber on 30 June 2022 is shown in Figure 7. Increased color saturation in the visualization corresponds to higher accumulated

α-pinene levels. The accumulation aligns with Figure 6, indicating elevated concentrations at the first level (130 cm). In terms of distance, there is a notable increase at 5 cm from the stem. Beyond 900 cm, there is considerable variation in α-pinene amounts, making it difficult to observe a clear trend. Regarding the orientation, slightly higher concentrations are observed on the south and east sides, though are not significantly dominant.

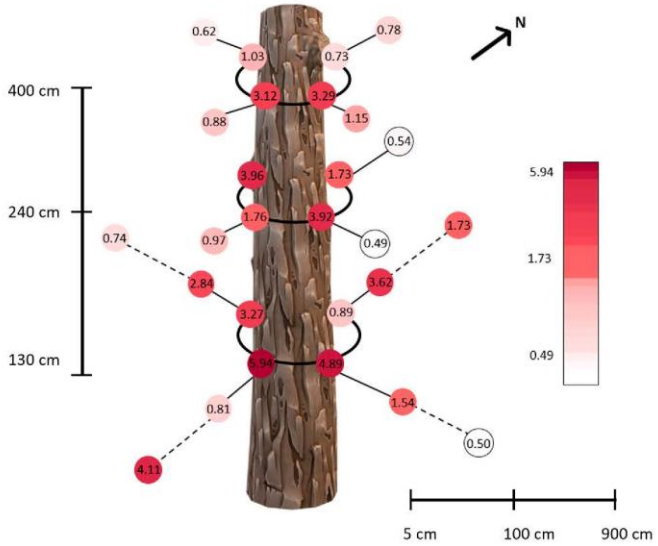

Figure 7. 3D distribution of α-pinene collected by SPME in first field data collection (30 June 2022). More saturated color means a higher abundance of α-pinene. The numbers in circles are relative peak areas of α-pinene.

The conditions for the second VOC measurement in the forest open space around a naturally infested tree, conducted on 24 August 2022, differed from the first collection in terms of location and environmental factors (average temperature of 20.7 °C, average humidity of 78.8%, wind speed of 3 km/h, wind direction from S, and sunshine).

α-pinene abundance significantly increased at a 100 cm distance from the stem, as detected by SPME ($p = 0.0037$) (Figure 8a) and sorption to cartridges ($p = 0.0244$) (Figure 8d), compared to both the 5 cm and 900 cm distances considered as controls.

A non-significant, very weak trend was observed for the accumulation of α-pinene at a height of 260 cm from the ground measured by SPME (Figure 8b). No significant differences were found in α-pinene accumulation in any cardinal direction (Figure 8c,e).

The 3D depiction of α-pinene collection using SPME fiber during the second field collection on 24 August 2022 is shown in Figure 9. Notably, there is an increase 100 cm from the stem in terms of distance and higher accumulation at the second level, 260 cm from the ground. This aligns with Figure 8.

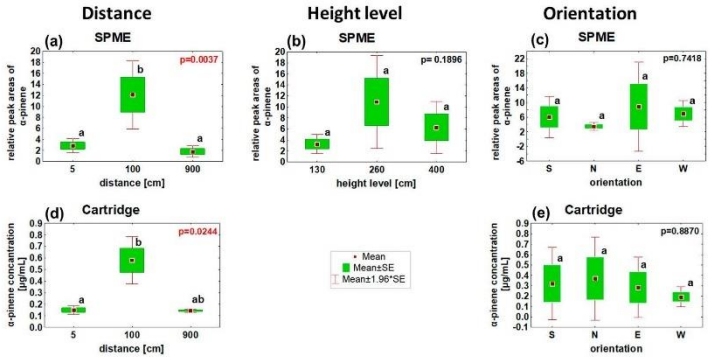

Figure 8. The second field detection of α-pinene distribution around *Ips typographus*-infested spruce (24 August 2022). (**a**) Abundance of α-pinene collected by SPME at different distances from stem (5 cm; 100 cm; 900 cm); (**b**) abundance of α-pinene collected by SPME at different height levels from ground (130 cm; 260 cm; 400 cm); (**c**) abundance of α-pinene collected by SPME in cardinal directions (S—south; N—north; E—east; W—west); (**d**) abundance of α-pinene collected by HayeSep-Q® cartridges at different distances from stem (5 cm; 100 cm; 900 cm); (**e**) abundance of α-pinene collected by HayeSep-Q® cartridges at different height levels from ground (130 cm; 260 cm), abundance of α-pinene collected by HayeSep-Q® cartridges in cardinal directions (S—south; N—north; E—east; W—west). Small red squares—Means; green boxes—Means ± SE; Whiskers—Means ±1.96*SE. Lowercase letters above columns indicate significant differences between different distance, different height level, and different orientation. The *p*-values result from Kruskal–Wallis test. (n = 22 SPME samples) (cartridges n = 12).

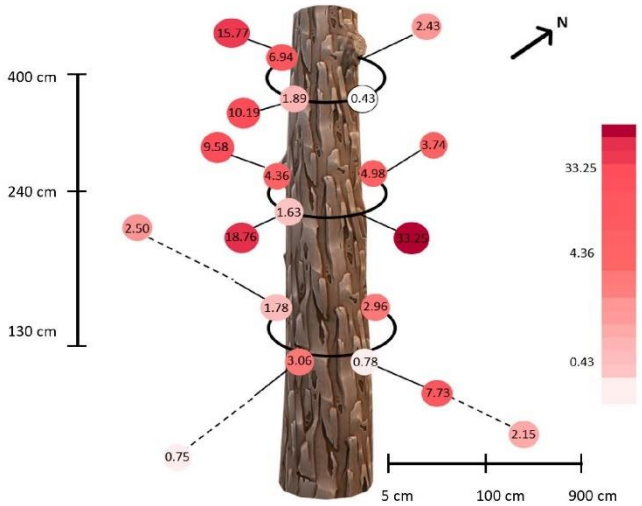

Figure 9. 3D distribution of α-pinene collected by SPME in second field data collection (24 August 2022). More saturated color means a higher amount of collected α-pinene. The numbers in circles are relative peak areas of α-pinene.

4. Discussion

The volatile compounds emitted by infested trees have been studied in two main contexts: atmospheric chemistry processes, with a focus on reactive particle formation [50], and ecological roles related to bark beetles and their predators [27,28,32,51]. Most reports in atmospheric chemistry measured volatiles at the canopy or twig level [52]. Emission measurements of biogenic volatile organic compounds (BVOC) from infested trees appeared in only a few studies investigating the potential use of these emissions as early attack detection markers [9,10,39]. Our study is unique as it examines emissions within a distance of 10 m of the infested tree, specifically at ground level and up to 5 m, where α-pinene accumulates at an average infestation season temperature of 20 to 25 °C in central European forests [53]. This novel approach contributes new insights to our understanding of volatiles emitted by bark beetle-infested trees.

Primarily, in our study, we employed laboratory optimization techniques to collect volatiles from freshly infested trees. The main emitted compound, α-pinene, was selected as a representative of the primary monoterpenes. It reflects the trends observed in other monoterpenes emitted by spruce trees infested by bark beetles [54].

In the laboratory, where the temperature was 25 °C, we observed a higher abundance of α-pinene in the open space in the closest proximity to logs, particularly in the lowest and highest positions. This increase was likely caused by the proximity of open log cuts and exposed bark edges, despite our attempts to prevent them by covering them with PE foil.

The first detection of α-pinene in the surroundings of a naturally infested tree in the field was conducted approximately two weeks after the beginning of a mass attack on the tree, corresponding with the time the monoterpene emission peaks [8,50]. This detection also took place at a temperature of 25 °C, when, expectedly, α-pinene vapors are heavier than air (with a vapor pressure of 4.9 mm Hg at 27 °C) [55].

Similar to our laboratory findings and reports from the literature [27,28], we observed the highest abundance of α-pinene in the immediate vicinity of the infested tree. Vertically, α-pinene accumulated at the lowest level, approximately 1.3 m above the ground, which was confirmed by two different collection methods:

The lower-level accumulation of the monoterpenes under similar conditions was previously observed as the output of the continual measuring campaign of BVOC in the forest. It has been reported that monoterpenes are emitted by healthy trees during the daytime, but they are also more susceptible to degradation in the atmosphere during the same period [53]. Monoterpenes are known to be unstable in the atmosphere, with a relatively short lifetime, often lasting only hours or even minutes, forming atmospheric secondary organic aerosol particles, followed by reactions with ozone and radicals like NO, OH, and NO_3 [56]. As a result of their decomposition, methanol and acetone, both of which are highly abundant in the forest atmosphere, are produced, alongside other products. Additionally, at higher elevations in the forest, strong air streams are present, resulting in monoterpenes having a higher 'mixing ratio,' which implies a lower concentration. The monoterpenes accumulate at lower altitudes in the forest, particularly during the nighttime [57].

The abundance of α-pinene in the controls placed at a further distance from the tree (9 m) exhibited greater variability [10].

This variability was most likely influenced by the surrounding trees. There were spruces, some of them in more progressed infestation stadia, or even dead and intact pines. In naturally infested trees, we also assessed an α-pinene orientation related to the infested stem's cardinal direction. During the first field collection, we noticed a non-significant trend of higher α-pinene levels on the south side of the stem, despite the prevailing wind coming from the opposite direction. This was attributed to the tree's location near the forest edge, allowing for direct afternoon sunlight exposure during collection [17,21].

The second collection, conducted later in the season, took place at a lower temperature of 22 °C. Interestingly, the highest abundance of monoterpenes was not observed at the lowest position, but rather at a height of 2.6 m, Additionally, it was not closest to the tree

stem, but rather 1 m away. Results were confirmed again by two collection methods, Solid-Phase Microextraction (SPME) and HayeSep-Q® Cartridge sampling, conducted at two different time intervals. This sampled tree, despite being in a similar stage of infestation as the first tree, was fully surrounded by other trees, including some broadleaf varieties in the vicinity, resulting in no direct irradiation of the stem.

During this collection, we did not observe any significant influence of sunlight exposure or wind speed on the orientation of increased α-pinene abundance.

The temperature and humidity differences in altitude were recorded on the same experimental plot [9]. The highest temperatures were observed approximately 1 m above the ground with an upward gradient. This temperature variation may impact the higher abundance of α-pinene at an altitude of 2.6 m compared to ground level due to the physical properties of pinene vapors.

The variation in outcomes between the first and second field collections was attributed to differences in the surroundings of the measured trees, distinct parts of the season, and, primarily, variations in temperature and humidity conditions [36,37].

In forest practices, our 3D distribution data of α-pinene emitted by freshly infested spruces may serve as a foundation for scanning techniques, demonstrating promising potential for managing bark beetle populations by facilitating early attack detection.

The most advanced technique for volatile scanning in situ can be based on field and portable Gas Chromatography-Mass Spectrometry (GC-MS) instruments, which are possible to mount on UAV. These instruments have the capability to separate, identify, and quantify VOC compounds in situ and collect data at short intervals. Existing instruments on the market have been tested for various analytes, primarily for military applications [58]. However, reliable devices for detecting terpenes and other infestation marker VOCs are still lacking.

To specifically select markers of infestation by *Ips typographus* and exclude infestations of different herbivores (as relevant bark species or defoliators) from the complex odor environment of a natural forest, such as bark beetle pheromones and spruce host compounds, an olfactory perception system of the bark beetles, antennae can be used as a specific detector working via electroantennography principles [59,60]. Ongoing research is exploring the application of this method in insect pest detection, with future directions aiming to target insect protein odorant receptors for specific compounds indicative of infestation [31].

However, the most potentially promising novel device is a non-specific electronic nose, designed for real-time chemical substance detection (e.g., detecting dangerous gas leaks or measuring concentrations near landfills, monitoring volcanic activity, etc.). We previously conducted tests to explore the feasibility of early-stage stress detection in forest stands using an electronic nose, specifically the Sniffer4D [9].

Due to limitations in measuring VOCs with non-specific sensors in forests, especially in areas with higher concentrations of compounds from fresh clearings, debris, and broken trees, an ideal approach would involve integrating environmental VOC scanning with other data collected through different scanning methods. This integration could be achieved, ideally using UAV vehicles equipped with various sensors for high-resolution data collection [61]. The map of VOC abundance can be automatically overlaid with aerial maps of the area, changes in reflectance, dedicated vegetation indices [6], or temperature fluctuations [62].

Limitation of the Study

The reported study is considered a pilot trial investigating the distribution of monoterpenes around infested trees at ground level and up to 5 m. To enhance the study, future research employing classical collection and analytical techniques should result in confirmation of the quantitative monoterpene distribution. The expanded study will involve a large-scale tree group, multiple replications for robust statistical analyses, and a focus on genetically relevant trees. To ensure control, infested and non-infested trees will be monitored simultaneously, maintaining consistent bark beetle infestation density. Standardized

environmental conditions will be implemented to minimize variability, with the potential to explore environmental conditions as a variable.

5. Conclusions

In summary of this pilot study, VOCs, represented here by α-pinene, emitted by freshly attacked trees may act as detectable markers for timely infestation. The spatial distribution of their concentration in an open space follows a gradient pattern that can be analyzed using various collection techniques. However, this distribution is notably influenced by environmental factors. With further optimization and integration with other scanning methods, these VOCs emitted by freshly infested trees can be used to develop effective "early detection methods" for bark beetles. Real-time data distribution provides a strong foundation for implementing crucial scanning techniques in early attack detection strategies.

Supplementary Materials: The following supporting information can be downloaded at: https://www.mdpi.com/article/10.3390/f15010010/s1, Table S1. The averages of the temperature and humidity in the first data collection 30 June 2022 in two periods of collections (SPME and cartridge collection). Table S2. The averages of the temperature and humidity in the second data collection 24 August 2022 in two periods of collections (SPME and cartridge collection). Figure S1. The map of development of Norway spruce logging due to bark beetle infestation in the Czech Republic in the period 9/2021–7/2022. Figure S2. Calibration curve of α-pinene. Constructed using commercial standard of α-pinene diluted in hexane to 0.1; 0.5; 1; 10; 25; 50 and 100 µg/mL.

Author Contributions: B.S.: experimental work, data curation, statistical data processing, and writing draft. A.A.C.M.: experimental work, GC-FID analysis, and writing draft and editing. T.H.: experimental work, figures processing. M.L.: experimental work and attack expertise. P.S.: editing manuscript and supervision. A.J.: conceptualization, data sampling, formal analysis, writing, editing, and supervision. All authors contributed to the article and approved the submitted version. All authors have read and agreed to the published version of the manuscript.

Funding: The project was funded by "EXTEMIT-K", No. CZ.02.1.01/0.0/0.0/15_003/0000433, Ministry of Education, Youth and Sport, Operational Programme Research, Development and Education, Internal Grant Commission BS [IGA A_21_01] at the Faculty of Forestry and Wood Sciences, Czech University of Life sciences, Prague, Czech Republic, and Internal Grant Commission ML [IGA A_23_17] at the Faculty of Forestry and Wood Sciences, Czech University of Life sciences, Prague, Czech Republic and EU project "UGC", No. CZ.02.2.69/0.0/0.0/19_073/0016944 project number 75/2021 financed by OP RDE at the Czech University of Life Sciences, Prague, Czech Republic, and AJ and AACM were funded by the National Agency for Agricultural Research NAZV QK1910480.

Data Availability Statement: Data are available in the article and in the Supplementary Materials.

Acknowledgments: We thank Forests ČZU for providing the experimental plots and Karel Kuželka for the pointing of coordinates of the experimental plots, and to Jiří Trombík for assistance with graphical abstract.

Conflicts of Interest: The authors declare that the research was conducted in the absence of any commercial or financial relationships that could be construed as a potential conflict of interest.

References

1. Biedermann, P.H.W.; Müller, J.; Grégoire, J.C.; Gruppe, A.; Hagge, J.; Hammerbacher, A.; Hofstetter, R.W.; Kandasamy, D.; Kolarik, M.; Kostovcik, M.; et al. Bark Beetle Population Dynamics in the Anthropocene: Challenges and Solutions. *Trends Ecol. Evol.* **2019**, *34*, 914–924. [CrossRef]
2. Hlásny, T.; König, L.; Krokene, P.; Lindner, M.; Montagné-Huck, C.; Müller, J.; Qin, H.; Raffa, K.F.; Schelhaas, M.J.; Svoboda, M.; et al. Bark Beetle Outbreaks in Europe: State of Knowledge and Ways Forward for Management. *Curr. For. Rep.* **2021**, *7*, 138–165. [CrossRef]
3. Hlásny, T.; Zimová, S.; Merganičová, K.; Štěpánek, P.; Modlinger, R.; Turčáni, M. Devastating Outbreak of Bark Beetles in the Czech Republic: Drivers, Impacts, and Management Implications. *For. Ecol. Manag.* **2021**, *490*, 119075. [CrossRef]
4. Hlásny, T.; Barka, I.; Merganičová, K.; Křístek, Š.; Modlinger, R.; Turčáni, M.; Marušák, R. A New Framework for Prognosing Forest Resources under Intensified Disturbance Impacts: Case of the Czech Republic. *For. Ecol. Manag.* **2022**, *523*, 120483. [CrossRef]

5. Kautz, M.; Schopf, R.; Ohser, J. The "Sun-Effect": Microclimatic Alterations Predispose Forest Edges to Bark Beetle Infestations. *Eur. J. For. Res.* **2013**, *132*, 453–465. [CrossRef]
6. Huo, L.; Persson, H.J.; Lindberg, E. Remote Sensing of Environment Early Detection of Forest Stress from European Spruce Bark Beetle Attack, and a New Vegetation Index: Normalized Distance Red & SWIR (NDRS). *Remote Sens. Environ.* **2021**, *255*, 112240. [CrossRef]
7. Van Der Velde, I.R.; Van Der Werf, G.R.; Houweling, S.; Maasakkers, J.D.; Borsdorff, T.; Landgraf, J.; Tol, P.; Van Kempen, T.A.; Van Hees, R.; Hoogeveen, R.; et al. Vast CO2 Release from Australian Fires in 2019–2020 Constrained by Satellite. *Nature* **2021**, *597*, 366–369. [CrossRef]
8. Stříbrská, B.; Hradecký, J.; Čepl, J.; Modlinger, R.; Tomášková, I.; Jirošová, A. Physiological and Biochemical Indicators in Norway Spruces Freshly Infested by *Ips typographus*: Potential for Early Detection Methods. *Front. For. Glob. Chang.* **2023**, *6*, 1197229. [CrossRef]
9. Hüttnerová, T.; Paczkowski, S.; Neubert, T.; Jirošová, A.; Surový, P. Comparison of Individual Sensors in the Electronic Nose for Stress Detection in Forest Stands. *Sensors* **2023**, *23*, 2001. [CrossRef]
10. Paczkowski, S.; Datta, P.; Irion, H.; Paczkowska, M.; Habert, T.; Pelz, S.; Jaeger, D. Evaluation of Early Bark Beetle Infestation Localization by Drone-Based Monoterpene Detection. *Forests* **2021**, *12*, 228. [CrossRef]
11. Vošvrdová, N.; Johansson, A.; Turčáni, M.; Jakuš, R.; Tyšer, D.; Schlyter, F.; Modlinger, R. Dogs Trained to Recognise a Bark Beetle Pheromone Locate Recently Attacked Spruces Better than Human Experts. *For. Ecol. Manag.* **2023**, *528*, 120626. [CrossRef]
12. Johansson, A.; Birgersson, G.; Schlyter, F. Using Synthetic Semiochemicals to Train Canines to Detect Bark Beetle–Infested Trees. *Ann. For. Sci.* **2019**, *76*, 1–10. [CrossRef]
13. Boone, C.K.; Aukema, B.H.; Bohlmann, J.; Carroll, A.L.; Raffa, K.F. Efficacy of Tree Defense Physiology Varies with Bark Beetle Population Density: A Basis for Positive Feedback in Eruptive Species. *Can. J. For. Res.* **2011**, *41*, 1174–1188. [CrossRef]
14. Franceschi, V.R.; Krokene, P.; Christiansen, E.; Krekling, T. Anatomical and Chemical Defenses of Conifer Bark against Bark Beetles and Other Pests. *New Phytol.* **2005**, *167*, 353–376. [CrossRef] [PubMed]
15. Borg-Karlson, A.K.; Lindström, M.; Norin, T.; Persson, M.; Valterová, I. Enantiomeric Composition of Monoterpene Hydrocarbons in Different Tissues of Norway Spruce, Picea Ab/Es (L) Karst. A Multi-Dimensional Gas Chromatography Study. *Acta Chem. Scand.* **1993**, *47*, 138–144. [CrossRef]
16. Netherer, S.; Kandasamy, D.; Jirosová, A.; Kalinová, B.; Schebeck, M.; Schlyter, F. Interactions among Norway Spruce, the Bark Beetle *Ips typographus* and Its Fungal Symbionts in Times of Drought. *J. Pest Sci.* **2021**, *94*, 591–614. [CrossRef] [PubMed]
17. Stříbrská, B.; Hradecký, J.; Čepl, J.; Tomášková, I.; Jakuš, R.; Modlinger, R.; Netherer, S.; Jirošová, A. Forest Margins Provide Favourable Microclimatic Niches to Swarming Bark Beetles, but Norway Spruce Trees Were Not Attacked by *Ips typographus* Shortly after Edge Creation in a Field Experiment. *For. Ecol. Manag.* **2022**, *506*, 119950. [CrossRef]
18. Lerdau, M.; Litvak, M.; Palmer, P.; Monson, R. Controls over Monoterpene Emissions from Boreal Forest Conifers. *Tree Physiol.* **1997**, *17*, 563–569. [CrossRef]
19. Juráň, S.; Pallozzi, E.; Guidolotti, G.; Fares, S.; Šigut, L.; Calfapietra, C.; Alivernini, A.; Savi, F.; Večeřová, K.; Křůmal, K.; et al. Fluxes of Biogenic Volatile Organic Compounds above Temperate Norway Spruce Forest of the Czech Republic. *Agric. For. Meteorol.* **2017**, *232*, 500–513. [CrossRef]
20. Baier, P.; Bader, R.; Rosner, S. Monoterpene Content and Monoterpene Emission of Norway Spruce (*Pices abies* L. Karst.) Bark in Relation to Primary Attraction of Bark Beetles (Col. Scolytidae). In *Physiology and Genetics of Tree-Phytophage Interactions*; Lieutier, F., Mattson, W.J., Wagner, M.R., Eds.; Les Colloques de l'INRA: Gujan, France, 1999; Volume 90, pp. 249–259.
21. Marešová, J.; Majdák, A.; Jakuš, R.; Hradecký, J.; Kalinová, B.; Blaženec, M. The Short-Term Effect of Sudden Gap Creation on Tree Temperature and Volatile Composition Profiles in a Norway Spruce Stand. *Trees* **2020**, *34*, 1397–1409. [CrossRef]
22. Amin, H.; Atkins, P.T.; Russo, R.S.; Brown, A.W.; Sive, B.; Hallar, A.G.; Hu, K.E. Effect of Bark Beetle Infestation on Secondary Organic Aerosol Precursor Emissions. *Environ. Sci. Technol.* **2012**, *46*, 5696–5703. [CrossRef] [PubMed]
23. Joensuu, J.; Altimir, N.; Hakola, H.; Rostás, M.; Raivonen, M.; Vestenius, M. Role of Needle Surface Waxes in Dynamic Exchange of Mono- and Sesquiterpenes. *Atmos. Chem. Phys.* **2016**, *16*, 7813–7823. [CrossRef]
24. Kivimäenpää, M.; Magsarjav, N.; Ghimire, R.; Markkanen, J.; Heijari, J.; Vuorinen, M.; Holopainen, J.K. Influence of Tree Provenance on Biogenic VOC Emissions of Scots Pine (*Pinus sylvestris*) Stumps. *Atmos. Environ.* **2012**, *60*, 477–485. [CrossRef]
25. Cataldo, F.; Ursini, O.; Lilla, E.; Angelini, G.; Cataldo, F.; Ursini, O.; Lilla, E.; Angelini, G. Ozone: Science & Engineering Turpentine Oil Studied by Chirooptical Methods; Some Ozonolysis of α-Pinene, β-Pinene, d-and l-Turpentine Oil Studied by Chirooptical Methods; Some Implications on the Atmospheric Chemistry of Biogenic Volatile Organic Compo. *Ozone Sci. Eng.* **2010**, *9512*, 274–285. [CrossRef]
26. Yu, H.; Holopainen, J.K.; Kivimäenpää, M.; Virtanen, A.; Blande, J.D. Potential of Climate Change and Herbivory to Affect the Release and Atmospheric Reactions of BVOCs from Boreal and Subarctic Forests. *Molecules* **2021**, *26*, 2283. [CrossRef] [PubMed]
27. Jaakkola, E.; Gärtner, A.; Jönsson, A.M.; Olsson, K.L.P.; Holst, T. Spruce Bark Beetle (*Ips typographus*) Infestation Cause up to 700 Times Higher Bark BVOC Emission Rates from Norway Spruce (*Picea abies*). *Biogeosci. Discuss* **2022**, *3*, 1–32. [CrossRef]
28. Ghimire, R.P.; Kivimäenpää, M.; Blomqvist, M.; Holopainen, T.; Lyytikäinen-Saarenmaa, P.; Holopainen, J.K. Effect of Bark Beetle (*Ips typographus* L.) Attack on Bark VOC Emissions of Norway Spruce (*Picea abies* Karst.) Trees. *Atmos. Environ.* **2016**, *126*, 145–152. [CrossRef]

29. Raffa, K.F.; Andersson, M.N.; Schlyter, F. Host Selection by Bark Beetles: Playing the Odds in a High-Stakes Game. In *Advances in Insect Physiology*; Tittiger, C., Blomquist, G.J., Eds.; Academic Press: London, UK, 2016; Volume 50, pp. 1–74, ISBN 9780128027233.
30. Erbilgin, N.; Powell, J.S.; Raffa, K.F. Effect of Varying Monoterpene Concentrations on the Response of *Ips Pini* (Coleoptera: Scolytidae) to Its Aggregation Pheromone: Implications for Pest Management and Ecology of Bark Beetles. *Agric. For. Entomol.* **2003**, *5*, 269–274. [CrossRef]
31. Bohbot, J.D.; Vernick, S. He Emergence of Insect Odorant Receptor-Based Biosensors. *Biosensors* **2020**, *10*, 26. [CrossRef]
32. Lehmanski, L.M.; Kandasamy, D.; Andersson, M.N.; Netherer, S.; Alves, E.G.; Huang, J.; Hartmann, H. Viewpoints Addressing a Century-Old Hypothesis – Do Pioneer Beetles of *Ips typographus* Use Volatile Cues to Find Suitable Host Trees? *New Phytol.* **2023**, *238*, 1762–1770. [CrossRef]
33. Andersson, M.N.; Larsson, M.C.; Schlyter, F. Specificity and Redundancy in the Olfactory System of the Bark Beetle *Ips typographus*: Single-Cell Responses to Ecologically Relevant Odors. *J. Insect Physiol.* **2009**, *55*, 556–567. [CrossRef] [PubMed]
34. Tholl, D.; Boland, W.; Hansel, A.; Loreto, F.; Ro, U.S.R. Practical Approaches to Plant Volatile Analysis. *Plant J.* **2006**, *45*, 540–560. [CrossRef] [PubMed]
35. Tholl, D.; Weinhold, A.; Röse, U.S.R. Practical Approaches to Plant Volatile Collection and Analysis. In *Biology of Plant Volatiles*; CRC Press: Boca Raton, FL, USA, 2020; p. 24.
36. Malik, T.G.; Sahu, L.K.; Gupta, M.; Mir, B.A.; Gajbhiye, T.; Dubey, R.; McCormick, A.C.; Pandey, S.K. Environmental Factors Affecting Monoterpene Emissions from Terrestrial Vegetation. *Plants* **2023**, *12*, 3146. [CrossRef] [PubMed]
37. Perreca, E.; Gershenzon, J.; Eberl, F. Tree Volatiles. In *Biology of Plant Volatiles*; CRC Press: Boca Raton, FL, USA, 2020; p. 15, ISBN 9780429455612.
38. Křůmal, K.; Mikuška, P.; Večeřová, K.; Urban, O.; Pallozzi, E.; Večeřa, Z. Wet Effluent Diffusion Denuder: The Tool for Determination of Monoterpenes in Forest. *Talanta* **2016**, *153*, 260–267. [CrossRef] [PubMed]
39. Amin, H.S.; Russo, R.S.; Sive, B.; Hoebeke, E.R.; Dodson, C.; Mccubbin, I.B.; Hallar, A.G.; Huff, K.E. Monoterpene Emissions from Bark Beetle Infested Engelmann Spruce Trees. *Atmos. Environ.* **2013**, *72*, 130–133. [CrossRef]
40. Birgersson, G.; Bergström, G. Volatiles Released from Individual Spruce Bark Beetle Entrance Holes Quantitative Variations during the First Week of Attack. *J. Chem. Ecol.* **1989**, *15*, 2465–2483. [CrossRef] [PubMed]
41. Giunta, A.D.; Runyon, J.B.; Jenkins, M.J.; Teich, M. Volatile and Within-Needle Terpene Changes to Douglas-Fir Trees Associated with Douglas-Fir Beetle (Coleoptera: Curculionidae) Attack. *Environ. Entomol.* **2016**, *45*, 920–929. [CrossRef] [PubMed]
42. Son, Y.; Kim, K.; Jung, I.; Lee, S.; Kim, J. Seasonal Variations and Emission Fluxes of Monoterpene Emitted from Coniferous Trees in East Asia: Focused on *Pinus Rigida* and *Pinus Koraiensis*. *J. Atmos. Chem.* **2015**, *72*, 27–41. [CrossRef]
43. Komenda, M.; Koppmann, R.; Wald, H. Monoterpene Emissions from Scots Pine (*Pinus sylvestris*): Field Studies of Emission Rate Variabilities. *J. Geophys. Res. Atmos.* **2002**, *107*, ACH-1. [CrossRef]
44. Janson, R.; Serves, C. De Acetone and Monoterpene Emissions from the Boreal Forest in Northern Europe. *Atmos. Environ.* **2001**, *35*, 4629–4637. [CrossRef]
45. Raveane, L.; Tisato, F.; Isak, I.; Traldi, P. Analyses of BioVOCs Variation Related to Vegetation Predominance in the Natural Park of Ampezzo Dolomites, UNESCO World Heritage Area of Dolomites. *J. For. Res.* **2013**, *24*, 439–448. [CrossRef]
46. Graus, M.; Hansel, A.; Wisthaler, A.; Lindinger, C.; Forkel, R.; Hauff, K.; Steinbrecher, R. A Relaxed-Eddy-Accumulation Method for the Measurement of Isoprenoid Canopy-Fluxes Using an Online Gas-Chromatographic Technique and PTR-MS Simultaneously. *Atmos. Environ.* **2006**, *40*, 43–54. [CrossRef]
47. Pallozzi, E.; Guidolotti, G.; Ciccioli, P.; Brilli, F.; Feil, S.; Calfapietra, C. Does the Novel Fast-GC Coupled with PTR-TOF-MS Allow a Significant Advancement in Detecting VOC Emissions from Plants? *Agric. For. Meteorol.* **2016**, *216*, 232–240. [CrossRef]
48. Ruuskanen, T.M.; Kolari, P.; Bäck, J.; Kulmala, M.; Rinne, J.; Hakola, H.; Taipale, R.; Raivonen, M.; Altimir, N.; Hari, P. On-Line Field Measurements of Monoterpene Emissions from Scots Pine by Proton-Transfer-Reaction Mass Spectrometry. *Boreal. Environ. Res.* **2005**, *10*, 553–567.
49. Bouvier-Brown, N.C.; Goldstein, A.H.; Gilman, J.B.; Kuster, W.C.; De Gouw, J.A. In-Situ Ambient Quantification of Monoterpenes, Sesquiterpenes, and Related Oxygenated Compounds during BEARPEX 2007: Implications for Gas-and Particle-Phase Chemistry. *Atmos. Chem. Phys.* **2009**, *9*, 5505–5518. [CrossRef]
50. Faiola, C.; Taipale, D. Impact of Insect Herbivory on Plant Stress Volatile Emissions from Trees: A Synthesis of Quantitative Measurements and Recommendations for Future Research. *Atmos. Environ. X* **2020**, *5*, 100060. [CrossRef]
51. Sousa, M.; Birgersson, G.; Karlsson Green, K.; Pollet, M.; Becher, P.G. Odors Attracting the Long-Legged Predator Medetera Signaticornis Loew to *Ips typographus* L. Infested Norway Spruce Trees. *J. Chem. Ecol.* **2023**, *49*, 451–464. [CrossRef]
52. Bergström, R.; Hallquist, M.; Simpson, D.; Wildt, J.; Mentel, T.F. Biotic Stress: A Significant Contributor to Organic Aerosol in Europe? *Atmos. Chem. Phys.* **2014**, *14*, 13643–13660. [CrossRef]
53. Park, J.H.; Goldstein, A.H.; Timkovsky, J.; Fares, S.; Weber, R.; Karlik, J.; Holzinger, R. Eddy Covariance Emission and Deposition Flux Measurements Using Proton Transfer Reaction–Time of Flight–Mass Spectrometry (PTR-TOF-MS): Comparison with PTR-MS Measured Vertical Gradients and Fluxes. *Atmos. Chem. Phys.* **2013**, *13*, 1439–1456. [CrossRef]
54. Hakola, H.; Taipale, D.; Praplan, A.; Schallhart, S.; Thomas, S.; Tykkä, T.; Helin, A.; Bäck, J.; Hellén, H. Emissions of Volatile Organic Compounds from Norway Spruce and Potential Atmospheric Impacts. *Front. For. Glob. Chang.* **2023**, *6*, 1116414. [CrossRef]

55. NJ Health Alpha-PINENE. Available online: https://nj.gov/health/eoh/rtkweb/documents/fs/0052.pdf (accessed on 11 December 2023).
56. Baker, J.; Arey, J.; Atkinson, R. Kinetics of the Gas-Phase Reactions of OH Radicals, NO_3 Radicals and O_3 with Three C 7-Carbonyls Formed from the Atmospheric Reactions of Myrcene, Ocimene and Terpinolene. *J. Atmos. Chem.* **2004**, *48*, 241–260. [CrossRef]
57. Guenther, A. Biological and Chemical Diversity of Biogenic Volatile Organic Emissions into the Atmosphere. *Int. Sch. Res. Not.* **2013**, 786290. [CrossRef]
58. Duan, C.; Li, J.; Zhang, Y.; Ding, K.; Geng, X. Portable Instruments for On-Site Analysis of Environmental Samples. *Trends Anal. Chem.* **2022**, *154*, 116653. [CrossRef]
59. Hummel, H.E.; Miller, T.A. *Techniques in Pheromone Research*; Springer Science & Business Media: New York, NY, USA, 2012; ISBN 978-1-4612-9743-7.
60. McQuate, S. The Smellicopter Is an Obstacle-Avoiding Drone That Uses a Live Moth Antenna to Seek out Smells. Available online: https://www.washington.edu/news/2020/12/07/smellicopter-avoids-obstacles-uses-live-moth-antenna-to-smell/ (accessed on 11 December 2023).
61. Pajares, G. Overview and Current Status of Remote Sensing Applications Based on Unmanned Aerial Vehicles (UAVs). *Photogramm. Eng. Remote. Sens.* **2015**, *81*, 281–330. [CrossRef]
62. Smigaj, M.; Gaulton, R.; Suárez, J.C.; Barr, S.L. Forest Ecology and Management Canopy Temperature from an Unmanned Aerial Vehicle as an Indicator of Tree Stress Associated with Red Band Needle Blight Severity. *For. Ecol. Manag.* **2019**, *433*, 699–708. [CrossRef]

Disclaimer/Publisher's Note: The statements, opinions and data contained in all publications are solely those of the individual author(s) and contributor(s) and not of MDPI and/or the editor(s). MDPI and/or the editor(s) disclaim responsibility for any injury to people or property resulting from any ideas, methods, instructions or products referred to in the content.

5.2. Bark beetle detection method using electronic nose sensors. A possible improvement of early forest disturbance detection?

Tereza Hüttnerová, Peter Surový

Faculty of Forestry and Wood Science, Czech University of Life Sciences (CZU Prague), Kamýcká 129,165 21 Prague, Czech Republic

Front. For. Glob. Change, 30 August 2024, Sec. Forest Disturbance, Volume 7 - 2024 | https://doi.org/10.3389/ffgc.2024.1445094

Author´s contribution: 60 %

Summary of the article

In addition to the chemical changes present during biotic disturbance, it is possible to measure other non-optical manifestations. These changes relate to tree transpiration, each healthy coniferous tree transpires approximately 200-300 liters of water per day. In the case of bark beetle damage, the ability to transpire is reduced or completely suspended. Changes in transpiration will be reflected in the local microclimate. This article comprehensively maps non-optical changes, including chemical manifestations and microclimate changes. We verified three electronic noses in the attacked spruce stand for early detection. To verify the ability of electronic noses to distinguish between an infested and a healthy forest, the ground collection was used in a total of six repetitions in the same trajectory. A very high ability to identify infestation was demonstrated for the two tested electronic noses. The Miniature Bosch sensor device achieved an accuracy of 95%, and Sensory device for environmental applications had an accuracy of 89%. The most significant influence on the model had variables related to the changes in the local microclimate.

Full article

frontiers | Frontiers in Forests and Global Change

TYPE Original Research
PUBLISHED 30 August 2024
DOI 10.3389/ffgc.2024.1445094

Check for updates

OPEN ACCESS

EDITED BY
Milica Zlatkovic,
University of Novi Sad, Serbia

REVIEWED BY
Fredrik Schlyter,
Czech University of Life Sciences Prague, Czechia
Manuela Branco,
University of Lisbon, Portugal

*CORRESPONDENCE
Tereza Hüttnerová
huttnerovat@afld.czu.cz

RECEIVED 06 June 2024
ACCEPTED 20 August 2024
PUBLISHED 30 August 2024

CITATION
Hüttnerová T and Surový P (2024) Bark beetle detection method using electronic nose sensors. A possible improvement of early forest disturbance detection?
Front. For. Glob. Change 7:1445094.
doi: 10.3389/ffgc.2024.1445094

COPYRIGHT
© 2024 Hüttnerová and Surový. This is an open-access article distributed under the terms of the Creative Commons Attribution License (CC BY). The use, distribution or reproduction in other forums is permitted, provided the original author(s) and the copyright owner(s) are credited and that the original publication in this journal is cited, in accordance with accepted academic practice. No use, distribution or reproduction is permitted which does not comply with these terms.

Bark beetle detection method using electronic nose sensors. A possible improvement of early forest disturbance detection?

Tereza Hüttnerová* and Peter Surový

Faculty of Forestry and Wood Sciences, Czech University of Life Sciences Prague, Prague, Czechia

Forest ecosystems are long-term exposed to dry periods in Europe, which leads to a significant loss of vitality and higher mortality, especially in coniferous forests. Identifying stress in the early stages when measures can be taken to protect the forest and living trees is crucial. Current detection methods are based on field surveys by forest workers or remote sensing methods to cover larger areas, which use changes in spectral reflectance of the forest canopy. In some cases, the attacked trees do not change their appearance, and based on calculations of vegetation indices from remote sensing data, the attack cannot be mapped. We present an innovative methodology based on non-optical analysis, namely identifying a group of volatile compounds and microclimate signs in forest stands that indicate stress factors in forest stands. An attacked tree by a bark beetle produces increased amounts of biogenic volatile organic compounds associated with defense, and the microclimate changes due to interrupted transpiration. In addition, the bark beetle uses the aggregation pheromone to attract more individuals and to attack the tree massively. In this study, we tested three electronic noses (Miniature Bosch sensor device with 25,419 samples, Sensory device for environmental applications with 193 samples, Handheld VOC Detector Tiger with 170 samples) in a freshly infested spruce stand. The measurement was conducted at ground level with the help of a human operator and was repeated six times to verify the detection capability of the electronic noses. To verify the capability of electronic noses to predict tree infestation, we used machine learning Random Forest. The results demonstrated that electronic noses can detect bark beetle infestation start (within 1 week of the first attack). The Miniature Bosch sensor device achieved the highest accuracy with a value of 95%, in distinguishing forest sections that are healthy and infested; the second most accurate electronic nose is the Sensory device for environmental applications, with an accuracy of 89%. Our proposed methodology could be used to detect bark beetle presence.

KEYWORDS

electronic noses, forest disturbances, odor mapping, stress detection, bark beetle, early detection

1 Introduction

Coniferous forest stands have been grappling with intense stress recently, including fires, drought, windstorms, and insect pests. The leading causes of damage are biotic disturbances, especially insect infestation. The resistance of the forest stand to stress is directly related to its vitality and the level of insect attack. Among the most significant pests are insects that feed on

the bast fibers of living trees, such as the Eurasian spruce bark beetle (*Ips typographus* (L.)) (Hais et al., 2016; Fernandez-Carrillo et al., 2020; Bárta et al., 2021). The emergence of bark beetles is often associated with increased temperature and drought, and the intensity of infestation depends on the complex interaction between the bark beetle, climatic conditions, forest conditions, and extreme natural events such as storms and fires (Schelhaas et al., 2003; Jönsson et al., 2012; Marini et al., 2017; Hlásny et al., 2019; Patacca et al., 2023; Netherer et al., 2024).

Stressed trees under bark beetle attack secrete several times more biogenic volatile organic substances (mostly α-pinene, camphene, myrcene) than under resting conditions (Ghimire et al., 2016; Jaakkola et al., 2022; Hakola et al., 2023; Lehmanski et al., 2023; Netherer et al., 2024). In the event of an attack by the Eurasian spruce bark beetle, as part of the chemical communication between these individuals, an aggregation pheromone is secreted, composed of 2-methyl-3-buten-2-ol and cis-verbenol (Birgersson et al., 1984; Netherer et al., 2021; Moliterno et al., 2023). In addition to chemical changes, tree damage by bark beetles brings other non-optical symptoms, such as a change in the microclimate. Forest understories locally influence the microclimate, and compared to open areas, provide lower average temperatures and higher air humidity (Geiger et al., 1995; Morecroft et al., 1998; Aussenac, 2000; Kašpar et al., 2021). A healthy tree has transpiration 200–300 liters of water per day; in case of damage, the ability to transpire is impaired or completely stopped. In the case of reduced transpiration capacity of damaged trees, the temperature buffering decreases, and thus, leads to a higher temperature and lower air humidity (Kopáček et al., 2020).

Monitoring natural disturbances in a forest ecosystem is a key element for forest management and in forest-protected areas like national parks for taking precautionary measures (tourism safety, fire, etc.). Early identification of stress conditions of forest stands can prevent significant economic and ecological damage. A very accurate but time-consuming method is a field inspection by forest experts; during a field visit, each tree can be carefully mapped, and it is also possible to record the initial state of infestation based on observing the first beetle entrance holes, boring dust on the trunk, and resin flows (Birgersson et al., 1984; Abdullah et al., 2019a; Bárta et al., 2022; Bozzini et al., 2024). This technique cannot be used to check extensive forest stands or hard-to-reach locations and requires a very close visual examination of each tree to identify symptoms of infestation. For larger areas, remote sensing methods are used, and a suitable carrier (satellite, aircraft, drone) is chosen according to the required resolution and characteristics of the study area. Health status can be observed based on the different spectral reflectance of vegetation, for example, Piecewise index PI B(710 + 738–522), Greenness GI, NDVI GREEN/NIR, Normalized difference photochemical reflectance index PRI, and ANCB index (Gitelson and Merzlyak, 1997; Zarco-Tejada et al., 2001; Le Maire et al., 2004; Zhang et al., 2018; Bárta et al., 2022). Canopy change methods monitoring deviations in spectral reflectance cannot identify early attacks; approximately only 40% of attacked trees change their spectral expression in the crown, and if a change occurs after 6–10 weeks, the red or gray attack is not timely enough (Kautz et al., 2023; Bozzini et al., 2024). True early methods deal with bark beetle pheromone detection based on a specially trained dog, which can upwind orientation to the pheromone plume from single trees under attack up to 150 m (Johansson et al., 2019) and, compared to visual human detection, achieves significantly better results in identifying an early attack (Vošvrdová et al., 2023).

Non-optical mapping, namely the monitoring of a group of volatile compounds and microclimate cues, appears to be a promising method. New sensors utilizing microchip architecture and electronic nose technology have recently emerged. These sensors can convert the concentration of chemical substances into electrical signals, which are then transformed into digital numbers. Over the past decade, there has been a significant increase of interest for using electronic sensors across various applications (food product quality control, air quality monitoring, disease diagnosis, and environmental monitoring). This trend reflects the growing awareness of the possibilities electronic sensors offer in ensuring accurate, reliable, and efficient data collection, which significantly benefits research, industry, and public health (Pobkrut et al., 2016; Cellini et al., 2017; Xing et al., 2019; Tiele et al., 2020; Fuentes et al., 2021). Due to continuous technological advances, weight reduction, and better integration with other devices, electronic sensors are becoming capable of greater detection accuracy. Electronic sensors are evaluated based on sensitivity given in units of ppb (parts per billion). These criteria are key in assessing the ability of sensors to provide reliable and accurate measurements in various environments and applications (Deshmukh et al., 2015; Ye et al., 2021).

In this research, we followed up on our previous study (Hüttnerová et al., 2023), where we demonstrated the detectability of a substance indicating the presence or proximity of infested and dead trees with an electronic nose Sniffer4D. Data collection occurred on three different height levels (ground, 60 m, 80 m); the best results were achieved by a wide-range Hydrogen Chloride (HCL) Sensing Module at ground level. No correlation between stress compounds and distance from infested trees was recorded above the forest canopy, which can be caused by higher airflow divergence in the area above the forest canopy. The study by Vošvrdová et al. (2023), which focuses on identifying synthetic semiochemicals in the forest by a specially trained dog, confirms the possibility of ground detectability. In this study, we focus on ground-taken data for benchmarking several sensor responses to the presence of attacked trees.

We hypothesized that specific chemical compounds present in the forest stand during a stress event (bark beetle attack) would be detectable by electronic nose. We assumed that trees that are infested by bark beetles would produce more volatile organic compounds, and the stress of trees would lead to a change in their temperature and humidity profile. At the same time, aggregation pheromones, which bark beetles use to communicate, will be present in the forest. In the case of the ability of electronic noses to detect an increased amount of volatile organic substances or the presence of an aggregation pheromone or changes in the temperature or humidity profile, we will be able to identify an attack in the early stage of infestation and thus prevent enormous economic and ecological losses. The main goals of this research were (1) to evaluate the ability of electronic sensors to detect bark beetle infestation (2) to determine which factors influenced the most often measured increased values near attacked trees. We assessed the measured values with electronic noses in a spruce stand attacked by the Eurasian spruce bark beetle and in a healthy stand using a machine learning algorithm.

Following our previous study and the ever-expanding insect pests destroying valuable forest ecosystems, we asked the following specific research questions:

1 Can the tested electronic sensors capture specific substances that identify stress in the forest ecosystem?
2 Which electronic nose achieved the most accurate results based on the machine learning evaluation?
3 What model variables were the most significant predictors for stress detection in the forest stand?

2 Materials and methods

2.1 Study area

The study area of 1.42 ha was located 35 km south-east of Prague; the forest stands to fall into category 32d – Forests with aiming forestry research and forestry education; the area was represented by monoculture Norway spruce [*Picea abies* (L.) Karst.] in age class 5 (81–100 years). Data collection took place on September 4th, 2023 (11:10 a.m. – 1:10 p.m.); the outside temperature was around 19°C, and humidity 46%. The mean annual temperature of the study area in 2023 was 10.4°C; the long-term average temperatures in the Central Bohemian Region and Prague is 9.3°C. The maximum temperature, 19.0°C, was recorded in July, and the minimum temperature, −0.6°C, was recorded in January. The mean annual precipitation in 2023 was 607 mm, whereas the long-term average in the region is 583 mm (Czech Hydrometeorological Institute, 2023).

Data collection was performed six times, and the measurement trajectory was kept identical for a possible evaluation of the sensitivity of the sensors (Figure 1). The trajectory was chosen in the shape of figure eight to evaluate the sensors' response to the occurrence of stress factors in the forest ecosystem. The research area was one with a size of 1.42 ha; the invaded area was approximately 80 × 50 m. Each collection took approximately 15–20 min (6 repetitions) when the operator slowly walked through the study area and simultaneously collected data by all electronic sensors at ground level. Our approach is not based on detecting individual trees but on detecting an area (area-based method).

2.2 Materials

Three electronic noses were used as part of data collection to verify their suitability for stress mapping in forest ecosystems. Two sensors are commercially available on the regular market, and one sensor was specifically designed for environmental measurements. Therefore, it is described in detail below.

2.2.1 Miniature Bosch sensor device © Bosch Sensortec GmbH 2023 (Bosch)

This sensor was the BME688 AI miniature environmental sensing device, which can detect volatile organic compounds, volatile sulfur compounds and other gases like carbon monoxide and hydrogen in the ppb resolution. The sensor includes a unit for measuring temperature in the range of −40-85°C with sensitivity ±1°C, a humidity sensor in the range of 0–100% with sensitivity ±3%, a unit for measuring pressure in the range of 300–1,100 hPa with sensitivity ±1 hPa, and a Metal-Oxide Semiconductor (MOX) gas sensor. The manufacturer does not directly state the range and sensitivity of the MOX sensor unit but based on the general characteristics of MOX sensors and the focus on the Air Quality Index (AQI), which Bosch company describes in the datasheet, it can be estimated that the sensor can detect VOCs in the tens of ppb.

2.2.2 Sensory device for environmental applications (SDEA)

The next device for monitoring the bark beetle is designed as a mobile unit powered by an accumulator and containing two basic parts—a source part that is fixed in the lower part of the carrier and a sensor part located on a support rod at a height of about 60 cm above the head of the experimenter (Figure 2).

The source unit and the sensor part are connected to each other by a cable, enabling both power supply to the sensor part and communication between the two units. The source unit contains the accumulator, the circuits for charging the accumulator, and the circuits for monitoring the status of the source unit. The sensor unit is in a removable cover and contains sensors in a tunnel formed by an aluminum profile. Air enters the tunnel through a dust filter and is extracted by a fan on the opposite side of the aluminum profile. Holes are made in the profile, in which sensors for individual types of gas are stored, and their outputs are processed by the control unit located on the handle on the side of the profile.

Individual sensors include:

- NO_2 electrochemical sensor, range 20 ppm, sensitivity in the order of ppb
- H_2S electrochemical sensor, range 400 ppm, sensitivity in the order of ppb
- VOC photoionization sensor, range 40 ppm, sensitivity in the order of ppb (isobutylene)
- NO electrochemical sensor, range 20 ppm, sensitivity in the order of ppb
- SO_2 electrochemical sensor, range 50 ppm, sensitivity in the order of ppb
- CO electrochemical sensor, range 500 ppm, sensitivity in the order of ppb
- CO_2 IR/thermopile sensor, range 5,000 ppm, sensitivity 1 ppm
- O_3 electrochemical sensor, range 20 ppm, sensitivity in the order of ppb

The sensors, together with the electronics, are placed on the sensor board and their measuring part extends into the space of the measuring tunnel. The exception is the temperature and humidity sensor, which is located on the side (against the control unit holder, not visible in the picture). The entire sensor unit is controlled by a Raspberry microcomputer, which takes analog values from individual sensors, converts them into numerical data, and converts these data according to set conversion coefficients and data in measurable units, namely ppb or ppm. At the same time, it controls the work of the sensors, because some sensors have time delays between individual measurements, or it is necessary to turn them on and off to save batteries.

The last part of the system is a regular notepad, which communicates with the Raspberry control unit using the Bluetooth interface and is used to control the sensor unit, display, and save the measured values. The statuses of the individual processes are displayed in the informative section at the top left. As long as the source is

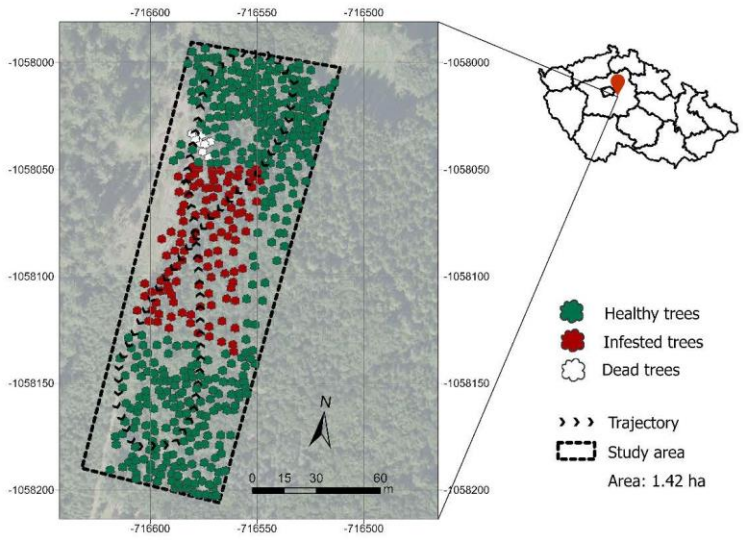

FIGURE 1
The study area 35 km away from Prague (Prague West district, Czechia) displays a forest stand, which was heavily infested by bark beetles (infested trees are marked red, healthy ones in green, and dead trees in white). Black arrows mark the trajectory of data collection.

turned off or the measuring application is not running, which means that Bluetooth communication is not turned on, the status of the source is red and cannot be measured. After establishing a connection with the measuring device, the status wheel turns green, which means measuring is possible. The correct GPS function is indicated separately, as the location data is part of the recording.

Furthermore, the upper part contains environmental data on the state of the air in the measured location (temperature, humidity, and pressure) and the state of the measuring device, especially the temperature of the individual measuring modules. These are important for correcting the measured values of electrochemical sensors, as they are highly temperature dependent. Battery status and airflow rate in the measuring unit are on the far right of the display.

The last icon on the display is a green button that sets one of three values:

- Measurement initialization (from the measurement status off),
- Turn on the measurement (from the measurement initialization state),
- Turn off the measurement (from the measurement status on).

Simultaneously with online measurement, a set of measured data is written at regular intervals, which has the following structure (in .csv format separated by semi-colons):

> <Date and Time>; <GPS: number of satellites>; <GPS: accuracy [m]>; <Latitude [°]>; <Longitude [°]>; <Fan speed [%]>; <NO_2 [ppb]>; <H_2S [ppb]>; <VOC [ppb]>; <NO [ppb]>; <SO_2 [ppb]>; <CO [ppb]>; <CO_2 [ppb]>; <O_3 [ppb]>; <Temperature of module 1 [°]>; <Temperature of module 2 [°]>; <Battery status [%]>; <Outside temperature [°]>; <Pressure [hPa]>; <Relative Humidity [%]>.

2.2.3 Handheld VOC Detector Tiger © 2024 Ion Science UK. Ion Science is registered trademark on Ion Science Ltd. (Tiger)

Detector Tiger has photoionization technology (PID) for detecting volatile organic compounds. The detector can display measured values very quickly and accurately. It is suitable for screening and locating, for example, leaking dangerous gases. The sensor system has a response time of 2 s and can detect up to 750 volatile organic substances. The range of the sensor is 0–20,000 ppm with sensitivity 1 ppb. Figure 3 shows the Miniature Bosch sensor device and Handheld VOC Detector Tiger.

2.3 Data processing

First, we evaluated the health status of the trees in the study area; the trees were classified into three categories (dead, infested, and healthy). The assessment was carried out in two ways; first, based on a field investigation, the bark of the trees was inspected with a focus on locating the bark beetle entrance holes, boring dust on the trunk, and resin flows. Natural infestation (without chemical baiting) of coniferous trees was within a week of the first attack by the bark beetle,

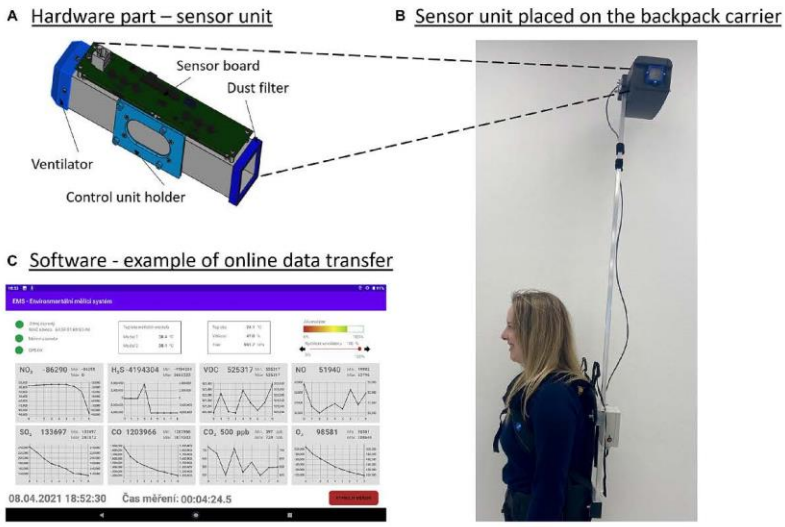

FIGURE 2
Comprehensive overview of the Sensory device for environmental applications: **(A)** sensor unit assembly consisting of the ventilator, control unit holder, dust filter, and sensor board; **(B)** the main sensory part is located 60 cm above the operator's head; **(C)** software part: layout of data on the notepad screen. The notepad screen is divided into four parts: an informative part at the top left (three items marked with status—source, measurement, and GPS), measured values at the top of the screen + fan speed, a part containing eight graphs for estimated quantities, and a status line at the bottom of the screen.

and the study area was selected based on consultation with Field technician, who performs regular checks of the status of trees. The second method for determining the state of health was based on optical data obtained from a UAV; the area was captured with a DJI Phantom4 Pro multirotor with an RGB camera at the height of 90 m, and the images were processed using the Structure from Motion method. We visually evaluated the spectral characteristics of the tree canopy from the orthophoto mosaic (Figure 4). Spruce trees in the study area were categorized [healthy, attacked, dead] and stored as a point layer.

The measurement results from the sensors were exported in .csv format, we used the R Studio and ArcGIS Pro software's for all data analysis. Each electronic nose measurement dataset was annotated by two labels (infested forest, healthy forest). These labels were assigned based on the position of the measurement within the forest. Using the *Select by Location* functionality, measurement positions in the attacked stand were selected and assigned the "Infested" attribute. The procedure was repeated for measurement positions in the healthy part of the forest, and the "Healthy" attribute was assigned. Due to the low number of dead trees, they were not considered in the machine learning models.

We train machine learning algorithm Random Forest (Breiman, 2001), which is widely used for classification tasks in environmental studies. The input data for the model does not have to be standardized, which ensures a more straightforward interpretation of the results (Müller et al., 2022). We used the R package *randomForest* (Liaw and Wiener, 2002), *caret* (Kuhn, 2008), *kernlab* (Karatzoglou et al., 2004), and *boot* (Davison and Hinkley, 1997) to create three binary classifications for each dataset measured by the electronic nose (Sensory device for environmental applications, Handheld VOC Detector Tiger, Miniature Bosch sensor device). The dataset was split 80:20 into training and validation sets. We used the resampling method *repeatedcv.*, which is used to set K-fold cross-validation, and for the *repeats* argument, we chose the value three, and this argument controls the number of repetitions; the K parameter is regulated by the *number* argument, which we chose 20 (Kuhn, 2008). The goal was to find out which electronic nose has the most sensitive predictive ability and what variables affect the values of electronic nose sensors. We selected the explanatory variables based on the technical equipment of the sensor. The machine learning model was based on 25,419 samples for the Miniature Bosch sensor device, 193 samples for the Sensory device for environmental applications, and 170 samples for the Handheld VOC Detector Tiger. The number of samples varied depending on the time resolution of the electronic nose for recording values; data collection was carried out simultaneously by all three electronic sensors along the same trajectory.

2.3.1 Miniature Bosch sensor device

We used input explanatory variables of outside temperature (*Temperature*), pressure (*Pressure*), relative humidity (*Humidity*), and

data collection number (*Data_col*). The Bosch device provides one information about chemical measurement, and that is Resistance. Gassenzor (*Gas*), which we used for the dependent variable in the model. We used the following model formula:

$$rf\_classifier <- train\begin{pmatrix} Location \sim Temperature + Pressure \\ +Humidity + Gas + Data\_col, data \\ = trainData, method = "rf," trControl \\ = train.control \end{pmatrix}$$

FIGURE 3
On the left side is Handheld VOC Detector Tiger, in the upper right in the red rectangle is Miniature Bosch sensor device.

2.3.2 Sensory device for environmental applications

For Sensory devices for environmental applications, we used input explanatory variables such as outside temperature (*Outside_tem*), temperature of module 1 (*TEM_mod1*), temperature of module 2 (*TEM_mod2*), pressure (*Pressure*), relative humidity (*Humidity*), and data collection number (*Data_col*). This electronic nose is equipped with several cross-sensitive sensors which can record values for all sensors simultaneously, so the explanatory variables of the gases were NO_2, H_2S, VOC, NO, SO_2, CO, CO_2, O_3. We used the following model formula:

$$rf\_classifier <- train\begin{pmatrix} Location \sim NO_2 + H_2S + VOC + NO \\ +SO_2 + CO + CO_2 + O_3 + TEM\_mod1 \\ +TEM\_mod2 + Outside\_tem + Pressure \\ +Humidity + Data\_col, data = trainData, \\ method = "rf," trControl = train.control \end{pmatrix}$$

2.3.3 Handheld VOC Detector Tiger

This sensor device is not equipped with a temperature, humidity, and pressure monitoring unit. The Tiger detector contains a gas library primarily focused on safety monitoring; within the software settings, measuring and recording information on one compound at a time is possible. We collected data for pinene in the first and second

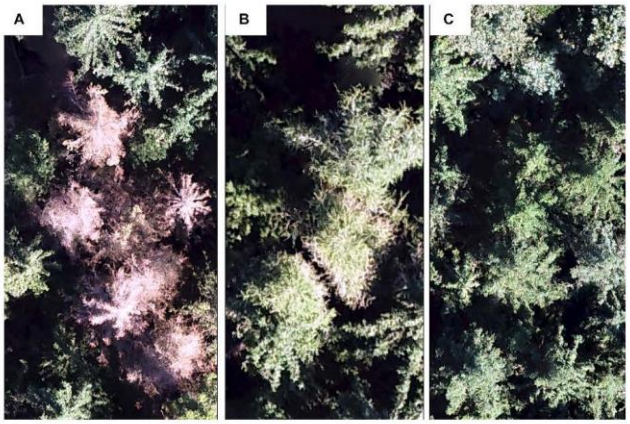

FIGURE 4
An example of the health status of the trees on the orthomosaic. **(A)** dead trees, **(B)** infested trees, **(C)** healthy trees.

measurements, methyl-butanol in the third, camphene in the fourth measurement, carene in the fifth, and pinene again in the sixth measurement. For evaluation we used explanatory variables of gas response (*Gas*), and data collection number (*Data_col*). We used the following model formula:

$$rf\_classifier <- train\left(\begin{matrix} Location \sim Gas, data = trainData, \\ method = "rf", trControl = train.control \end{matrix}\right).$$

3 Results

First, the results achieved for individual electronic noses will be described from the highest predictive ability of the models to the lowest. Then, the importance of the variables will be presented.

3.1 Miniature Bosch sensor device

The best model is selected automatically by the random forest algorithm, based on the highest accuracy, the outputs also provide set of best solutions based on the amount of variables included in the model (mtry), and kappa accuracy which is another way of measuring the performance especially in imbalanced datasets (Cohen, 1960). The results show the same accuracy for all the combinations of variables, mean the simpler model (the one with two variables) might be easier for future practical applicability (Table 1).

The Confusion Matrix is used to evaluate the performance of the classification model; it shows how often the actual classes were confused with the predicted ones. In the prediction part of the testing, accuracy 0.95 was achieved with a Kappa value 0.89. The sensitivity (true positive rate) was 0.97, and the specificity (true negative rate) was 0.91. The Confusion Matrix is used to evaluate the performance of the classification model; it shows how often the actual classes were confused with the predicted ones (Table 2).

3.2 Sensory device for environmental applications

The best model is selected automatically by the random forest algorithm, based on the highest accuracy. The results in Table 3 show the highest accuracy (0.89) for the combination with eight variables (mtry).

In the prediction part of the testing, accuracy 0.93 was achieved with a Kappa value 0.84. The sensitivity (true positive rate) was 1.00, and the specificity (true negative rate) was 0.81. Detailed confusion matrix values for the Sensory device for environmental applications are shown in Table 4.

3.3 Handheld VOC Detector Tiger

The tuning parameter "mtry" was held constant at a value of 2 (Table 5). The third of the sensors Handheld VOC Detector Tiger, received Kappa 0.16, and its predictive ability for forest stress detection was the lowest.

In the prediction part of the testing, accuracy 0.65 was achieved with a Kappa value 0.21. The sensitivity (true positive rate) was 0.85, and the specificity (true negative rate) was 0.35. Detailed confusion matrix values for the Handheld VOC Detector Tiger are shown in Table 6.

The importance of the variables for all tested electronic noses is shown in Figure 5. It was determined by the varImp function from the R software caret package, which provides information about the importance of variables for machine learning algorithms. The importance score of 100 indicates that the variable affects the model predictions most, while the variable with an importance score of 0 is irrelevant to the model's predictive ability, i.e., the least.

For the Miniature Bosch sensor device, the relative humidity sensor (100.00) had the most important influence on the predictive ability to detect infestation or healthy forest, followed by the pressure sensor (98.12) and temperature sensor (57.97). In the case of infested trees, it reduces the transpiration flow in the tree; with less water capacity, the trees cannot regulate the temperature profile and thus can lead to overheats. The reduction of transpiration close to the tree affects the air humidity and the pressure in the environment (slight increase); dry air is denser than humid air. A sensor unit measuring gases had a moderate effect on the model, and by 22.86. The variable "Data collection" did not affect the model (0.00), which means that the model performed very well for all data collections. The SDEA, which also achieved a very high predictive ability, had the most significant variable, the pressure-sensitive sensor (100.00), followed by the chemical sensor cross-sensitive to NO_2 gas (11.17). The cross-sensitive sensor to CO_2 gas had an effect of 9.92 on the model, and the sensor sensitive to H_2S (5.34). The outdoor temperature slightly affected the predictive ability, namely 3.73 and the humidity sensor (1.75). Measurement time (Data Collection variable) also did not affect the model, and predictive ability was achieved for the entire measurement. The Handheld VOC Detector

TABLE 2 Confusion matrix values for the Miniature Bosch sensor device.

Prediction	Healthy	Infested
Healthy	4,017	194
Infested	121	2034

TABLE 1 Results for different amount of random variables for the Miniature Bosch sensor device.

mtry	Accuracy	Kappa
2	0.95	0.88
3	0.95	0.89
5	0.95	0.88

TABLE 3 Results for different amount of random variables for the Sensory device for environmental applications.

mtry	Accuracy	Kappa
2	0.84	0.67
8	0.89	0.77
14	0.88	0.75

TABLE 4 Confusion matrix values for the Sensory device for environmental applications.

Prediction	Healthy	Infested
Healthy	27	3
Infested	0	13

TABLE 5 Results for the Handheld VOC Detector Tiger.

mtry	Accuracy	Kappa
2	0.60	0.16

TABLE 6 Confusion matrix values for the Handheld VOC Detector Tiger.

Prediction	Healthy	Infested
Healthy	22	11
Infested	4	6

Tiger did not achieve a good prediction ability for identifying stress in the forest ecosystem; based on the comparison of the importance of the variables, the gas sensor achieved 100.00, and the variable "Data collection" was also 0.00. The complete variable importance results for all three electronic noses are shown in Appendix.

4 Discussion

Based on our research findings, we can answer the scientific questions posed. We conclude that electronic noses can detect changes in volatile compounds and microclimate cues after bark beetle infestation. The Miniature Bosch sensor device achieved the highest accuracy in distinguishing forest sections that are healthy and infested (more addressed in Section 4.2 Electronic noses), and a more significant indicator of infestation was relative humidity, temperature, and pressure sensors (more discussed in Section 4.3 Influence of variables from statistical evaluation).

The presented methodology is a potential solution for the early identification of stress in forest stands, focusing on fresh attacks till 1 week old caused by bark beetle infestation. Early detection is essential for minimizing the spread of bark beetles to surrounding trees and thus reducing ecological and economic loss. In the case of late detection of the infestation, the bark beetle will spread to other trees, and from the point of view of safety and preventing further spread, the best solution is to cut down the trees and take them safely away from the forest stands. The financial costs must be allocated to the cutting and restoring forest stands. On small-scale clearings created because of natural disturbances, it is possible to reforest by natural regeneration if there are mature forest stands in the surrounding stands; in the case of large-scale sites, the natural distribution of sowing may be insufficient, and it is necessary to use artificial afforestation.

4.1 Detection methods

Conventional methods of infestation detection are field visits by forest experts and marking infested trees based on visual inspection; this method is very time and physically demanding (Stadelmann et al., 2013; Leverkus et al., 2021; Bárta et al., 2022). Remote Sensing methods can detect the deteriorated condition of the stand based on the change in the spectral reflectance of tree needles. Still, it is not possible to detect early infestation with this method. In the case of an attacked tree, the spectral reflectance of the canopy will be changed after 6–10 weeks, and only approximately 40% of the attacked trees show crown degradation; these findings do not confirm the potential of satellite or aerial detection systems (Kautz et al., 2023). Stress detection based on the analysis of crowns from a remote sensing image is challenging; the most accurate results are achieved at the end of the growing season (Latifi et al., 2018; Bárta et al., 2021; Huo et al., 2021). When using single spectral channels, the quality is insufficient; better results are achieved when using several spectral channels and calculating the vegetation index (Kautz et al., 2024). The authors of several studies argue about the importance of using the red-edge and NIR band (Abdullah et al., 2019a,b; Minařík et al., 2020; Hellwig et al., 2021; Trubin et al., 2023).

The scientific community has been mainly concerned with mapping and analyzing the healthy status of forests in the optical and near-infrared bands in the last decade. Analysis of chemical substances can bring new information about natural disturbances and help with early detection. In the case of monitoring bark beetle infestation of spruce stands, it is possible to focus on odor mapping; on the one hand, the bark beetle uses an aggregation pheromone to communicate with its individuals; still, the presence of pheromones in the forest is below the mark of the sensitivity and selectivity of electronic sensors; on the other hand it is possible to map biogenic volatile organic substances, which are secreted from the bark of trees; in the case of stress events, these substances are secreted in several times larger quantities. Therefore, chemical mapping could provide a very effective source of information about the attack, even at an early stage. We proved the detection ability of early infestation by electronic noses up to 1 week from the first attack. Early attack can be detected using specially trained snifferdogs, which can detect synthetic semiochemicals (identical to the species-specific major pheromone components of Eurasian spruce bark beetle) (Johansson et al., 2019; Vošvrdová et al., 2023). Chemical mapping is already conventionally used in security and industry, e.g., for detecting the leakage of dangerous gases or mapping air quality in cities, and several studies have already appeared in agriculture that intend to detect crop pests (Zhou and Wang, 2011; Abdullah et al., 2018; Arroyo et al., 2020; Rahman et al., 2020; Fuentes et al., 2021; Sudama et al., 2022).

4.2 Electronic noses

Of the tested electronic noses, the Miniature Bosch sensor device achieved the best capabilities, followed by a Sensory device for environmental applications. The Miniature Bosch sensor device, with a very favorable price, could be used to create a more comprehensive network of stationary measurements in spruce stands for early identification of stress factors. So, it would perform a function like the detection sensors for triggering the smoke detection alarm. The sensors could send the values to the cloud in real-time and display them on the map portal. We recommend and will further use a Sensory device for environmental applications to map local areas with a risk of a bark beetle outbreak due to its software equipment, which

can show measurement results in real-time and has GPS. A possible interaction here for both mentioned electronic noses is with a drone platform, where a larger area of the forest ecosystem could be explored; the detection capability above the forest canopy has not yet been proven, and a potential solution appears to be collecting data under the forest canopy with manual flight mode.

Paczkowski et al. (2021) research focused on testing the applicability of sensors GGS1330, GGS2330, and GGS5330 to detect aggregation pheromone and biogenic volatile organic compounds; the results show the potential use of this device to verify the detectability of alpha-pinene, which is the main component of biogenic volatile organic compounds from spruce stands when their sensor was able to capture different concentrations. The detection capability of elevated concentrations has not been demonstrated by UAV data collection above canopies. Similar results were also obtained by Hüttnerová et al. (2023), where the electronic nose Sniffer4D with DJI Matrice 600 Pro was verified for early detection of bark beetles; the ability of the electronic nose to detect increased concentrations of chemical substances was also not confirmed, but the

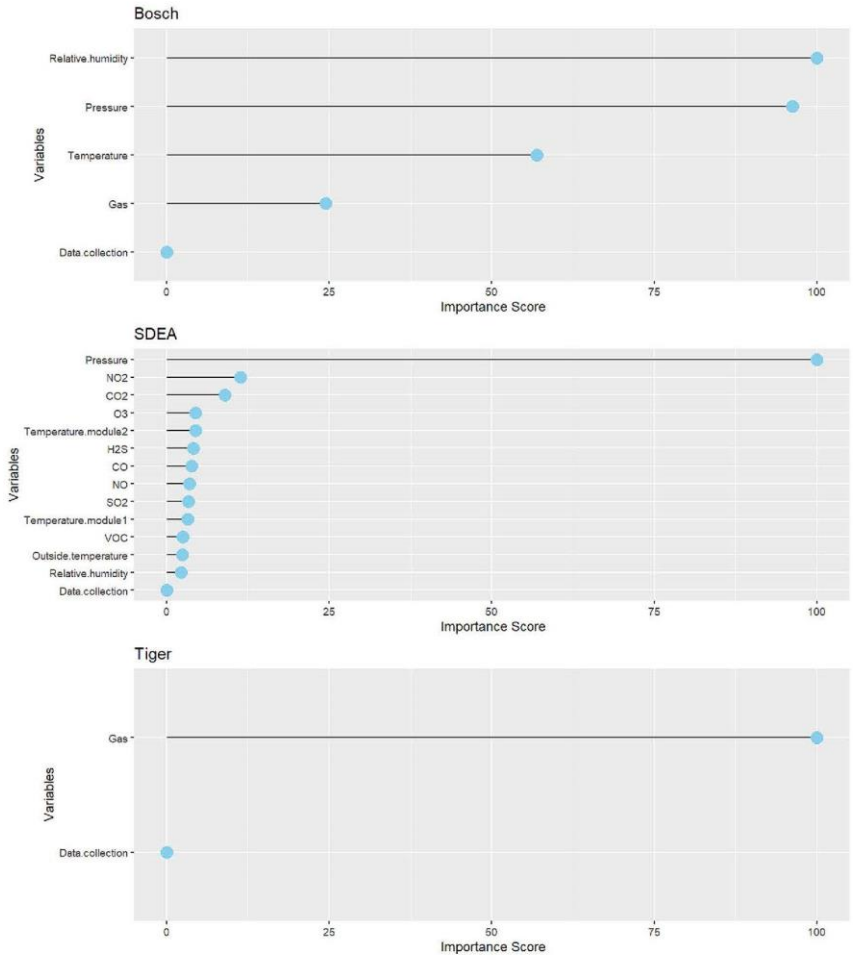

FIGURE 5
Overview of the importance of variables for sensor the Miniature Bosch sensor device, the Sensory device for environmental applications, the Handheld VOC Detector Tiger. The importance score of 100 indicates that the variable affects the model predictions most, while the variable with an importance score of 0 is irrelevant to the model's predictive ability, i.e., the least.

detection ability of the electronic nose was demonstrated under the crowns when they were data collected on the ground and the research find out that wide-range Hydrogen Chloride (HCL) sensor performed most reliably. The results of this study and the conclusions published by Paczkowski et al. (2021) and Hüttnerová et al. (2023) demonstrate the ability of electronic noses to detect specific substances present in forest stands when attacked by bark beetles.

4.3 Influence of variables from statistical evaluation

Our research proved the influence of variables that represented non-optical measurement. The relative humidity, temperature, and pressure sensors were a more significant indicator of infestation. Bark beetle is associated with symbiotic ophiostomatoid fungi that degrade spruce toxins, help to exhaust tree defenses, and thus lead to impaired conductive tissues and reduce transpiration (Netherer et al., 2021, 2024). Transpiration has a cooling effect on trees and an effect on air humidity; reduced transpiration leads to changes in local humidity, and this can increase air pressure. Differences in humidity are logical, but identifying differences between infected and healthy forests on rainy or cold cloudy days will not work because healthy trees do not transpire under these conditions.

In the case of infested trees, the transpiration flow is reduced in the tree; with less water capacity, the trees cannot regulate the temperature profile and thus can lead to overheats. The reduction of transpiration close to the tree affects the air humidity and the pressure in the environment (slight increase); dry air is denser than humid air. Another factor that can cause an increase in air temperature is canopy loss due to bark degradation (Anderegg et al., 2013; Wehner and Stednick, 2017).

Long-term microclimate changes were demonstrated in study Kopáček et al. (2020), and the changes were attributed to reducing or stopping tree transpiration of trees; there was an increase in daily mean air temperature (2 m above ground) of 1.6 and 0.5°C per year, and relative humidity was on the disturbed plots of land on average 4% lower. In our research, we noted much faster changes in microclimate clues, which suggests that the changes will manifest themselves significantly faster.

4.4 Limitations and future challenges

The presented methodology offers the possibility of early detection of bark beetle infestation based on identifying volatile compounds and microclimate cues found in the forest environment during bark beetle attack. With this methodology, it is not necessary to rely only on the spectral changes of the tree canopy to identify infestations. The limitation of this methodology is currently the size range of the area we can analyze. A time-efficient innovative method is the use of snifferdogs, which are twice as fast in detecting bark beetle infestation as human experts; the searching abilities of a dog are four times higher than human experts in the case of randomized plots because the dog can smell the pheromone at a greater distance (Vošvrdová et al., 2023).

For the possibilities of a large-scale detection system, it would be advisable to use the UAV platform and first try to verify the detection above the tree canopy, which has not been confirmed for the time being, or to test the possibilities of flying under the tree canopy. The battery capacity limits the data collection by the drone; the average flight time is about 30 min, depending on its load. A potential solution would also be creating a warning mapping system, where each electronic nose would be connected to a cloud system and send the currently measured values from the forest area in real-time. The system could serve as a suitable screening method of a preventive nature; for this purpose, the use of the Miniature Bosch sensor device would be appropriate in terms of its dimensions and financial availability.

In the case of global use, it would be necessary to recalibrate our model to local conditions; for example, a different climate can be predicted in Northern Europe than in the tested conditions in Czechia. However, we know from research which variables are significant for tested electronic noses and identify early bark beetle infestation.

5 Conclusion

In this study, we focused on evaluating three electronic noses for stress detection in forest stands, which were heavily attacked by bark beetles. This research aims at early detection of bark beetle infestation by novel technology of odor mapping as a more viable alternative to optical detection, which may be unreliable if the trees do not demonstrate signs of beetle attack. The possibility of detecting beetles by odor signals was clearly proven to be possible using dogs (Johansson et al., 2019; Vošvrdová et al., 2023). The predictive ability of electronic noses was evaluated based on machine learning model with two classes ("Healthy", "Infested"), we found that electronic noses can obtain sensitive information about stressors in forest ecosystems and thus help detect problematic areas for further analysis or action. The Miniature Bosch sensor device achieved the highest values for the ability to predict the infested trees, followed by Sensory devices for environmental applications. The presented methodology provides a very effective and fast solution for stress monitoring in forest stands, mainly for detecting bark beetle outbreaks. This monitoring could contribute to more effective mapping and prediction of the spread of infestations in forest ecosystems, thus radically minimizing the ecological and economic damages caused by insect pests.

Data availability statement

The raw data supporting the conclusions of this article will be made available by the authors, without undue reservation.

Ethics statement

Written informed consent was obtained from the individual(s) for the publication of any identifiable images or data included in this article.

Author contributions

TH: Conceptualization, Data curation, Formal analysis, Funding acquisition, Investigation, Methodology, Project

administration, Resources, Software, Visualization, Writing – original draft. PS: Conceptualization, Formal analysis, Investigation, Methodology, Software, Supervision, Writing – review & editing, Funding acquisition.

Funding

The author(s) declare financial support was received for the research, authorship, and/or publication of this article. This research was funded by Czech University of Life Sciences, Faculty of Forestry and Wood Sciences IGA/A_26_23 and by the Technological Agency of the Czech Republic through program CHIST-ERA, grant number TH74010001.

Conflict of interest

The authors declare that the research was conducted in the absence of any commercial or financial relationships that could be construed as a potential conflict of interest.

Publisher's note

All claims expressed in this article are solely those of the authors and do not necessarily represent those of their affiliated organizations, or those of the publisher, the editors and the reviewers. Any product that may be evaluated in this article, or claim that may be made by its manufacturer, is not guaranteed or endorsed by the publisher.

References

Abdullah, H., Skidmore, A. K., Darvishzadeh, R., and Heurich, M. (2019a). Sentinel-2 accurately maps green-attack stage of European spruce bark beetle (Ips typographus, L.) compared with Landsat-8. *Remote Sens. Ecol. Conserv.* 5, 87–106. doi: 10.1002/rse2.93

Abdullah, H., Skidmore, A. K., Darvishzadeh, R., and Heurich, M. (2019b). Timing of red-edge and shortwave infrared reflectance critical for early stress detection induced by bark beetle (Ips typographus, L.) attack. *Int. J. Appl. Earth Obs. Geoinf.* 82:101900. doi: 10.1016/j.jag.2019.101900

Abdullah, A. H., Sudin, S., Mat Ajit, M. I., Ahmad Saad, F. S., Kamaruddin, K., Ghazali, F., et al. (2018). Development of ESP32-based Wi-Fi electronic nose system for monitoring LPG leakage at gas cylinder refurbish plant. In 2018 International Conference on Computational Approach in Smart Systems Design and Applications (ICASSDA), Kuching: IEEE, 1–5. doi: 10.1109/ICASSDA.2018.8477594

Anderegg, W. R. L., Kane, J. M., and Anderegg, L. D. L. (2013). Consequences of widespread tree mortality triggered by drought and temperature stress. *Nat. Clim. Change* 3, 30–36. doi: 10.1038/nclimate1635

Arroyo, P., Meléndez, F., Suárez, J. I., Herrero, J. L., Rodríguez, S., and Lozano, J. (2020). Electronic nose with digital gas sensors connected via Bluetooth to a smartphone for air quality measurements. *Sensors* 20:786. doi: 10.3390/s20030786

Aussenac, G. (2000). Interactions between forest stands and microclimate: ecophysiological aspects and consequences for silviculture. *Ann. For. Sci.* 57, 287–301. doi: 10.1051/forest:2000119

Bárta, V., Hanuš, J., Dobrovolný, L., and Homolová, L. (2022). Comparison of field survey and remote sensing techniques for detection of bark beetle-infested trees. *For. Ecol. Manag.* 506:119984. doi: 10.1016/j.foreco.2021.119984

Bárta, V., Lukeš, P., and Homolová, L. (2021). Early detection of bark beetle infestation in Norway spruce forests of Central Europe using Sentinel-2. *Int. J. Appl. Earth Obs. Geoinf.* 100:102335. doi: 10.1016/j.jag.2021.102335

Birgersson, G., Schlyter, F., Löfqvist, J., and Bergström, G. (1984). Quantitative variation of pheromone components in the spruce bark beetleIps typographus from different attack phases. *J. Chem. Ecol.* 10, 1029–1055. doi: 10.1007/BF00987511

Bozzini, A., Brugnaro, S., Morgante, G., Santoiemma, G., Deganutti, L., Finozzi, V., et al. (2024). Drone-based early detection of bark beetle infested spruce trees differs in endemic and epidemic populations. *Front. For. Glob. Change* 7:1385687. doi: 10.3389/ffgc.2024.1385687

Breiman, L. (2001). Random forests. *Mach. Learn.* 45, 5–32. doi: 10.1023/A:1010933404324

Cellini, A., Blasioli, S., Biondi, E., Bertaccini, A., Braschi, I., and Spinelli, F. (2017). Potential applications and limitations of electronic nose devices for plant disease diagnosis. *Sensors* 17:2596. doi: 10.3390/s17112596

Cohen, J. (1960). A coefficient of agreement for nominal scales. *Educ. Psychol. Meas.* 20, 37–46. doi: 10.1177/001316446002000104

Czech Hydrometeorological Institute (2023). Historical data: weather: maps of climate characteristics. Czech Hydrometeorological Institute. Available at: https://www.chmi.cz/historicka-data/pocasi/uzemni-teploty (accessed May 16, 2024).

Davison, A. C., and Hinkley, D. V. (1997). Bootstrap methods and their application. *1st* Edn. Cambridge: Cambridge University Press.

Deshmukh, S., Bandyopadhyay, R., Bhattacharyya, N., Pandey, R. A., and Jana, A. (2015). Application of electronic nose for industrial odors and gaseous emissions measurement and monitoring – an overview. *Talanta* 144, 329–340. doi: 10.1016/j.talanta.2015.06.050

Fernandez-Carrillo, A., Patočka, Z., Dobrovolný, L., Franco-Nieto, A., and Revilla-Romero, B. (2020). Monitoring bark beetle Forest damage in Central Europe. A remote sensing approach validated with field data. *Remote Sens.* 12:3634. doi: 10.3390/rs12213634

Fuentes, S., Tongson, E., Unnithan, R. R., and Gonzalez Viejo, C. (2021). Early detection of aphid infestation and insect-plant interaction assessment in wheat using a low-cost electronic nose (E-nose), near-infrared spectroscopy and machine learning modeling. *Sensors* 21:5948. doi: 10.3390/s21175948

Geiger, R., Aron, R. H., and Todhunter, P. (1995). The climate near the ground. Wiesbaden: Vieweg+Teubner Verlag.

Ghimire, R. P., Kivimäenpää, M., Blomqvist, M., Holopainen, T., Lyytikäinen-Saarenmaa, P., and Holopainen, J. K. (2016). Effect of bark beetle (Ips typographus L.) attack on bark VOC emissions of Norway spruce (*Picea abies* karst.) trees. *Atmos. Environ.* 126, 145–152. doi: 10.1016/j.atmosenv.2015.11.049

Gitelson, A. A., and Merzlyak, M. N. (1997). Remote estimation of chlorophyll content in higher plant leaves. *Int. J. Remote Sens.* 18, 2691–2697. doi: 10.1080/014311697217558

Hais, M., Wild, J., Berec, L., Brůna, J., Kennedy, R., Braaten, J., et al. (2016). Landsat imagery spectral trajectories—important variables for spatially predicting the risks of bark beetle disturbance. *Remote Sens.* 8:687. doi: 10.3390/rs8080687

Hakola, H., Taipale, D., Praplan, A., Schallhart, S., Thomas, S., Tykkä, T., et al. (2023). Emissions of volatile organic compounds from Norway spruce and potential atmospheric impacts. *Front. For. Glob. Change* 6:1116414. doi: 10.3389/ffgc.2023.1116414

Helbwig, F. M., Stelmaszczuk-Górska, M. A., Dubois, C., Wolsza, M., Truckenbrodt, S. C., Sagichewski, H., et al. (2021). Mapping European spruce bark beetle infestation at its early phase using gyrocopter-mounted hyperspectral data and field measurements. *Remote Sens.* 13:4659. doi: 10.3390/rs13224659

Hlásny, T., Krokene, P., Liebhold, A., Montagné-Huck, C., Müller, J., Qin, H., et al. (2019). Living with bark beetles: impacts, outlook and management options. European Forest Institute. Available at: https://doi.org/10.36333/fs08

Huo, L., Persson, H. J., and Lindberg, E. (2021). Early detection of forest stress from European spruce bark beetle attack, and a new vegetation index: normalized distance red & SWIR (NDRS). *Remote Sens. Environ.* 255:112240. doi: 10.1016/j.rse.2020.112240

Hüttnerová, T., Paczkowski, S., Neubert, T., Jirošová, A., and Surový, P. (2023). Comparison of individual sensors in the electronic nose for stress detection in Forest stands. *Sensors* 23:2001. doi: 10.3390/s23042001

Jaakkola, E., Gärtner, A., Jönsson, A. M., Ljung, K., Olsson, P.-O., and Holst, T. (2022). Spruce bark beetle (Ips typographus) infestation cause up to 700 times higher bark BVOC emission rates from Norway spruce (*Picea abies*). *Biogeosciences* 20, 803–826. doi: 10.5194/bg-2022-125

Johansson, A., Birgersson, G., and Schlyter, F. (2019). Using synthetic semiochemicals to train canines to detect bark beetle–infested trees. *Ann. For. Sci.* 76:58. doi: 10.1007/s13595-019-0841-z

Jönsson, A. M., Schroeder, L. M., Lagergren, F., Anderbrant, O., and Smith, B. (2012). Guess the impact of Ips typographus—an ecosystem modelling approach for simulating spruce bark beetle outbreaks. *Agric. For. Meteorol.* 166–167, 188–200. doi: 10.1016/j.agrformet.2012.07.012

Karatzoglou, A., Smola, A., Hornik, K., and Zeileis, A. (2004). Kernlab – an S4 package for kernel methods in R. *J. Stat. Soft.* 11, 1–20. doi: 10.18637/jss.v011.i09

Kašpar, V., Hederová, L., Macek, M., Müllerová, J., Prošek, J., Surový, P., et al. (2021). Temperature buffering in temperate forests: comparing microclimate models based on ground measurements with active and passive remote sensing. *Remote Sens. Environ.* 263:112522. doi: 10.1016/j.rse.2021.112522

Kautz, M., Feurer, J., and Adler, P. (2024). Early detection of bark beetle (Ips typographus) infestations by remote sensing – a critical review of recent research. *For. Ecol. Manag.* 556:121595. doi: 10.1016/j.foreco.2023.121595

Kautz, M., Peter, F. J., Harms, L., Kammen, S., and Delb, H. (2023). Patterns, drivers and detectability of infestation symptoms following attacks by the European spruce bark beetle. *J. Pest. Sci.* 96, 403–414. doi: 10.1007/s10340-022-01490-8

Kopáček, J., Bače, R., Hejzlar, J., Kaňa, J., Kučera, T., Matějka, K., et al. (2020). Changes in microclimate and hydrology in an unmanaged mountain forest catchment after insect-induced tree dieback. *Sci. Total Environ.* 720:137518. doi: 10.1016/j.scitotenv.2020.137518

Kuhn, M. (2008). Building predictive models in R using the caret package. *J. Stat. Soft.* 28, 1–26. doi: 10.18637/jss.v028.i05

Latifi, H., Dahms, T., Beudert, B., Heurich, M., Kübert, C., and Dech, S. (2018). Synthetic RapidEye data used for the detection of area-based spruce tree mortality induced by bark beetles. *Gisci. Remote Sens.* 55, 839–859. doi: 10.1080/15481603.2018.1458463

Le Maire, G., François, C., and Dufrêne, E. (2004). Towards universal broad leaf chlorophyll indices using PROSPECT simulated database and hyperspectral reflectance measurements. *Remote Sens. Environ.* 89, 1–28. doi: 10.1016/j.rse.2003.09.004

Lehmanski, L. M. A., Kandasamy, D., Andersson, M. N., Netherer, S., Alves, E. G., Huang, J., et al. (2023). Addressing a century-old hypothesis – do pioneer beetles of Ips typographus use volatile cues to find suitable host trees? *New Phytol.* 238, 1762–1770. doi: 10.1111/nph.18865

Leverkus, A. B., Buma, B., Wagenbrenner, J., Burton, P. J., Lingua, E., Marzano, R., et al. (2021). Tamm review: does salvage logging mitigate subsequent forest disturbances? *For. Ecol. Manag.* 481:118721. doi: 10.1016/j.foreco.2020.118721

Liaw, A., and Wiener, M. (2002). Classification and regression by randomForest. Available at: https://cran.r-project.org/doc/Rnews/ (Accessed April 10, 2024).

Marini, L., Økland, B., Jönsson, A. M., Bentz, B., Carroll, A., Forster, B., et al. (2017). Climate drivers of bark beetle outbreak dynamics in Norway spruce forests. *Ecography* 40, 1426–1435. doi: 10.1111/ecog.02769

Minařík, R., Langhammer, J., and Lendzioch, T. (2020). Automatic tree crown extraction from UAS multispectral imagery for the detection of bark beetle disturbance in mixed forests. *Remote Sens.* 12:4081. doi: 10.3390/rs12244081

Moliterno, A. A. C., Jakuš, R., Modlinger, R., Unelius, C. R., Schlyter, F., and Jirošová, A. (2023). Field effects of oxygenated monoterpenes and estragole combined with pheromone on attraction of Ips typographus and its natural enemies. *Front. For. Glob. Change* 6:1292581. doi: 10.3389/ffgc.2023.1292581

Morecroft, M. D., Taylor, M. E., and Oliver, H. R. (1998). Air and soil microclimates of deciduous woodland compared to an open site. *Agric. For. Meteorol.* 90, 141–156. doi: 10.1016/S0168-1923(97)00070-1

Müller, M., Olsson, P.-O., Eklundh, L., Jamali, S., and Ardö, J. (2022). Features predisposing forest to bark beetle outbreaks and their dynamics during drought. *For. Ecol. Manag.* 523:120480. doi: 10.1016/j.foreco.2022.120480

Netherer, S., Kandasamy, D., Jirosová, A., Kalinová, B., Schebeck, M., and Schlyter, F. (2021). Interactions among Norway spruce, the bark beetle Ips typographus and its fungal symbionts in times of drought. *J. Pest. Sci.* 94, 591–614. doi: 10.1007/s10340-021-01341-y

Netherer, S., Lehmanski, L., Bachlehner, A., Rosner, S., Savi, T., Schmidt, A., et al. (2024). Drought increases Norway spruce susceptibility to the Eurasian spruce bark beetle and its associated fungi. *New Phytol.* 242, 1000–1017. doi: 10.1111/nph.19635

Paczkowski, S., Datta, P., Irion, H., Paczkowska, M., Habert, T., Pelz, S., et al. (2021). Evaluation of early bark beetle infestation localization by drone-based monoterpene detection. *Forests* 12:228. doi: 10.3390/f12020228

Patacca, M., Lindner, M., Lucas-Borja, M. E., Cordonnier, T., Fidej, G., Gardiner, B., et al. (2023). Significant increase in natural disturbance impacts on European forests since 1950. *Glob. Chang. Biol.* 29, 1359–1376. doi: 10.1111/gcb.16531

Pobkrut, T., Eamsa-ard, T., and Kerdcharoen, T. (2016). Sensor drone for aerial odor mapping for agriculture and security services. In 2016 13th International Conference on Electrical Engineering/Electronics, Computer, Telecommunications and Information Technology (ECTI-CON), Chiang Mai, Thailand: IEEE, 1–5. doi: 10.1109/ECTICon.2016.7561340

Rahman, S., Alwadie, A. S., Irfan, M., Nawaz, R., Raza, M., Javed, E., et al. (2020). Wireless E-nose sensors to detect volatile organic gases through multivariate analysis. *Micromachines* 11:597. doi: 10.3390/mi11060597

Schelhaas, M., Nabuurs, G., and Schuck, A. (2003). Natural disturbances in the European forests in the 19th and 20th centuries. *Glob. Chang. Biol.* 9, 1620–1633. doi: 10.1046/j.1365-2486.2003.00684.x

Stadelmann, G., Bugmann, H., Meier, F., Wermelinger, B., and Bigler, C. (2013). Effects of salvage logging and sanitation felling on bark beetle (Ips typographus L.) infestations. *For. Ecol. Manag.* 305, 273–281. doi: 10.1016/j.foreco.2013.06.003

Sudama, K. A., Rivai, M., Aulia, D., and Mujiono, T. (2022). Electronic nose based on gas sensor Array and neural network for indoor hydrogen gas control system. In 2022 1st International Conference on Information System & Information Technology (ICISIT), Yogyakarta, Indonesia: IEEE, 187–192. doi: 10.1109/ICISIT54091.2022.9872796

Tiele, A., Wicaksono, A., Ayyala, S. K., and Covington, J. A. (2020). Development of a compact, IoT-enabled electronic nose for breath analysis. *Electronics* 9:84. doi: 10.3390/electronics9010084

Trubin, A., Kozhoridze, G., Zabihi, K., Modlinger, R., Singh, V. V., Surový, P., et al. (2023). Detection of susceptible Norway spruce to bark beetle attack using planet scope multispectral imagery. *Front. For. Glob. Change* 6:1130721. doi: 10.3389/ffgc.2023.1130721

Vošvrdová, N., Johansson, A., Turčáni, M., Jakuš, R., Tyšer, D., Schlyter, F., et al. (2023). Dogs trained to recognise a bark beetle pheromone locate recently attacked spruces better than human experts. *For. Ecol. Manag.* 528:120626. doi: 10.1016/j.foreco.2022.120626

Wehner, C. E., and Stednick, J. D. (2017). Effects of mountain pine beetle-killed forests on source water contributions to streamflow in headwater streams of the Colorado Rocky Mountains. *Front. Earth Sci.* 11, 496–504. doi: 10.1007/s11707-017-0660-1

Xing, Y., Vincent, T., Cole, M., and Gardner, J. (2019). Real-time thermal modulation of high bandwidth MOX gas sensors for mobile robot applications. *Sensors* 19:1180. doi: 10.3390/s19051180

Ye, Z., Liu, Y., and Li, Q. (2021). Recent progress in smart electronic nose technologies enabled with machine learning methods. *Sensors* 21:7620. doi: 10.3390/s21227620

Zarco-Tejada, P. J., Miller, J. R., Noland, T. L., Mohammed, G. H., and Sampson, P. H. (2001). Scaling-up and model inversion methods with narrowband optical indices for chlorophyll content estimation in closed forest canopies with hyperspectral data. *IEEE Trans. Geosci. Remote Sens.* 39, 1491–1507. doi: 10.1109/36.934080

Zhang, N., Zhang, X., Yang, G., Zhu, C., Huo, L., and Feng, H. (2018). Assessment of defoliation during the Dendrolimus tabulaeformis Tsai et Liu disaster outbreak using UAV-based hyperspectral images. *Remote Sens. Environ.* 217, 323–339. doi: 10.1016/j.rse.2018.08.024

Zhou, B., and Wang, J. (2011). Use of electronic nose technology for identifying rice infestation by *Nilaparvata lugens*. *Sensors Actuators B Chem.* 160, 15–21. doi: 10.1016/j.snb.2011.07.002

Appendix

TABLE A1 Output data from the Random Forest machine learning model used for evaluation of variables importance.

Variable importance	Bosch	SDEA	Tiger
Relative humidity	100.00	1.75	X
Pressure	98.12	100	X
Temperature	57.97	3.73	X
Gas	22.86	X	100
Data collection	0.00	0.00	0.00
NO_2	X	11.64	X
CO_2	X	9.92	X
H_2S	X	5.34	X
O_3	X	4.06	X
CO	X	4.89	X
NO	X	3.42	X
SO2	X	3.82	X
VOC	X	2.62	X
Temperature module 1	X	5.11	X
Temperature module 2	X	5.05	X

5.3. Comparison of Individual Sensors in the Electronic Nose for Stress Detection in Forest Stands

Tereza Hüttnerová[1], Sebastian Paczkowski[2], Tarek Neubert[2], Anna Jirošová[1], Peter Surový[1]

[1] Faculty of Forestry and Wood Science, Czech University of Life Sciences (CZU Prague), Kamýcká 129,165 21 Prague, Czech Republic

[2] Department of Forest Work Science and Engineering, Georg August University Göttingen, Büsgenweg 4,37077 Göttingen, Germany

Sensors 2023, 23(4), 2001; https://doi.org/10.3390/s23042001

Author´s contribution: 50 %

Summary of the article

The article compares individual sensors of a commercial electronic nose for early identification of stress caused by bark beetle infestation. The individual sensors of the electronic nose are cross-sensitive, so even though they are designed to detect a specific compound. Sensor units can also react to other compounds, which the manufacturer has not tested. In the study case, it is a group of volatile organic substances and an aggregation pheromone. In addition to comparing the detection ability of individual sensors, two heights are compared in the data collection framework: ground and UAV collection. The results showed that the highest correlation between the values recorded by the sensors and the distance from the attacked trees for the HCl, SO_2, and H_2S sensor units during the ground measurement. Data collection by UAV above canopy did not show detection capability. It could be caused by the more significant influence of wind speed and direction or specific behavior of chemical substances that can accumulate more near the ground.

Full article

sensors

MDPI

Brief Report

Comparison of Individual Sensors in the Electronic Nose for Stress Detection in Forest Stands

Tereza Hüttnerová [1], Sebastian Paczkowski [2], Tarek Neubert [2], Anna Jirošová [1] and Peter Surový [1,*]

[1] Faculty of Forestry and Wood Science, Czech University of Life Sciences (CZU Prague), Kamýcká 129, 165 21 Prague, Czech Republic
[2] Department of Forest Work Science and Engineering, Georg August University Göttingen, Büsgenweg 4, 37077 Göttingen, Germany
* Correspondence: surovy@fld.czu.cz

Abstract: Forests are increasingly exposed to natural disturbances, including drought, wildfires, pest outbreaks, and windthrow events. Due to prolonged droughts in the last years in Europe, European forest stands significantly lost vitality, and their health condition deteriorated, leading to high mortality rates, especially, but not limited to, Norway spruce. This phenomenon is growing, and new regions are being affected; thus, it is necessary to identify stress in the early stages when actions can be taken to protect the forest and living trees. Current detection methods are based on field walks by forest workers or deploying remote sensing methods for coverage of the larger territory. These methods are based on changes in spectral reflectance that can detect attacks only at an advanced stage after the significant changes in the canopy. An innovative approach appears to be a method based on odor mapping, specifically detecting chemical substances which are present in the forest stands and indicate triggering of constitutive defense of stressed trees. The bark beetle attacking a tree, for example, produces a several times higher amount of defense-related volatile organic compounds. At the same time, the bark beetle has an aggregation pheromone to attract conspecifics to overcome the tree defense by mass attack. These substances can be detected using conventional chemical methods (solid-phase microextraction fibers and cartridges), and it is proven that they are detectable by dogs. The disadvantage of classic chemical analysis methods is the long sampling time in the forest, and at the same time, the results must be analyzed in the laboratory using a gas chromatograph. A potential alternative novel device appears to be an electronic nose, which is designed to detect chemical substances online (for example, dangerous gas leaks or measure concentrations above landfills, volcanic activity, etc.). We tested the possibility of early-stage stress detection in the forest stands using an electronic nose Sniffer4D and compared the individual sensors in it for detecting the presence of attacked and dead trees. Our results indicate the promising applicability of the electronic nose for stress mapping in the forest ecosystem, and more data collection could prove this approach.

Keywords: unmanned aerial vehicles; electronic nose; 3D odor mapping; natural disturbance; early detection

check for updates

Citation: Hüttnerová, T.; Paczkowski, S.; Neubert, T.; Jirošová, A.; Surový, P. Comparison of Individual Sensors in the Electronic Nose for Stress Detection in Forest Stands. *Sensors* **2023**, *23*, 2001. https://doi.org/10.3390/s23042001

Academic Editors: Sindhuja Sankaran and Chongyuan Zhang

Received: 30 December 2022
Revised: 5 February 2023
Accepted: 9 February 2023
Published: 10 February 2023

Copyright: © 2023 by the authors. Licensee MDPI, Basel, Switzerland. This article is an open access article distributed under the terms and conditions of the Creative Commons Attribution (CC BY) license (https://creativecommons.org/licenses/by/4.0/).

1. Introduction

Monitoring stress in a forest is an important component of forest management, and the early detection of stress conditions in forest stands can prevent significant economic and environmental losses. Forest stands are exposed as all living systems to stress factors, which can be of two origins: (1) internal (by physiological growth and development) and (2) external (by natural disturbances) [1]. The natural disturbance disorders interact both with each other (biotic x abiotic) but also with other factors such as increasing carbon dioxide in the atmosphere and climate change—increased temperature and drought [2–5]. The most vulnerable losses are brought mainly by biotic disturbances, mainly outbreaks of insects. The resistance to stress of a forest stand depends on its vitality and the degree

and frequency of attack by insects [6]. The biggest damage is caused by insects feeding on the bast fibers of living trees, such as bark beetles [7]. The more extensive spread of bark beetles is mainly due to increasing temperature and drought [8,9]. The intensity and extent of the attack depend on direct and indirect interactions of the bark beetle with climate, susceptibility of forest, windthrow, and fires [10]. Increased temperature over the winter reduces bark beetle mortality and thus contributes to more generations per year [6].

To avoid economic and ecological losses, timely identification of forest stand stress is essential. Detection of stress in the forest is usually performed by a ground walk by trained specialists who can identify signs of stress. For the larger areas usually, remote sensing images are used to study the change in reflectance or values of some dedicated vegetation indices. The limiting factors of images obtained from a satellite are their temporal and spatial resolution; when mapping the spread of wildfire or insect outbreaks, these data are insufficiently accurate [11]. The solution might be the use of unmanned aerial vehicles (UAV), which can capture a local area with high spatial accuracy (in cm) [12]. UAV mapping is an important component in effective data collection, accurate terrain mapping, and measurement of toxic substances in the air. The UAV can be equipped with different types of sensors [13,14].

In the visible spectrum and near the near-infrared channel, the deteriorated state of forest stands can be monitored through vegetation indices (NDVI, Greenness Index). The accuracy of these indices is usually linearly correlated with the increasing length of the attack and intensity of the attack [15]. However, in some cases, an attacked tree does not show a change in spectral reflectance and is not marked as attacked/damaged in this approach [16]. A thermal camera was also used to capture the degraded state of forest stands. The appropriate timing of data collection is important. No significant disease-dependent correlation has yet been captured with morning collection, while the strongest relationship was obtained at the time of highest solar radiation, which coincides with the time of maximum photosynthetic activities near the trees, i.e., at noon [17].

Current rapid technological development brought into question studies related to chemical ecology, the studies which are focused on chemical processes such as the use of pheromones for beetle communication, the plant-beetle-based communication by attractants, and anti-attractants. Finally, it was proved that not only beetles can detect chemical substances, but dogs can be trained to do so [18]. This work ultimately proves it is possible to detect stressed trees by chemical substances.

Relatively new sensors have appeared on the market based on microchip architecture and electronic noses that can convert the concentration of chemical substances into a voltage and then to a digital number. This sensor is used in the field of security and the military. In agriculture, these sensors have been used to detect odors from livestock, hazardous chemical, biological compounds, and for early detection and prediction of pest insects (for example: Aphid Infestation, Lepidoptera) [19,20]. In forestry, it is possible with these sensors to detect VOCs and other chemical components, which can identify stress factors [12,21]. Other sensors include H_2S, HCL, nitrogen, and next SO_2, CO, O_3, NO_2, and, for example, sensors for measuring the content of dust particles in the air ($PM_{1.0}$, $PM_{2.5}$, PM_{10}). Remote sensing methods currently seek to obtain chemical data, and the electronic nose could be potentially suitable for calibration ground measurement [22].

During the attack, the pioneer beetles who search for appropriate habitats are the freshly emerged males. Once they land on the target host tree and successfully start to bore in the bark, they start producing aggregation pheromone (2-methyl-3-buten-2-ol and cis-verbenol) to attract conspecifics for a mass attack (Figure 1) [23,24]. Eco-friendly strategies to monitor pest insects have received huge attention due to reducing pesticide usage. The pheromones and VOCs act as powerful tools against pest insects [25,26]. Plants may respond to an insect attack with the emission of VOCs, and these odors may be correlated with the early attack [25,26]. Interestingly, plants may differentiate in their response between mechanical and herbivore damages, such as those caused by pest insects [27,28].

Elevated levels of VOCs can be detected by conventional chemical methods, cartridges, or solid-phase microextraction fibers (SPME) [29,30]. The increased emissions from infested trees were 6–20 times higher than healthy individuals [30,31]. Measurements using cartridges and solid-phase microextraction fibers provide only single-point measurements; neither fibers nor cartridges can be used repeatedly in the field. Proven chemical methods yield accurate measurements, but the data must first be analyzed on a gas chromatograph. During SPME data collection, fibers are exposed to air, typically for one hour. In open space, this time could increase even more. Gas chromatography analysis of one SPME or cartridge takes about 10–30 min, depending on the method used [31,32]. These steps delay the final statistical evaluation and eventual remediation of the attacked trees.

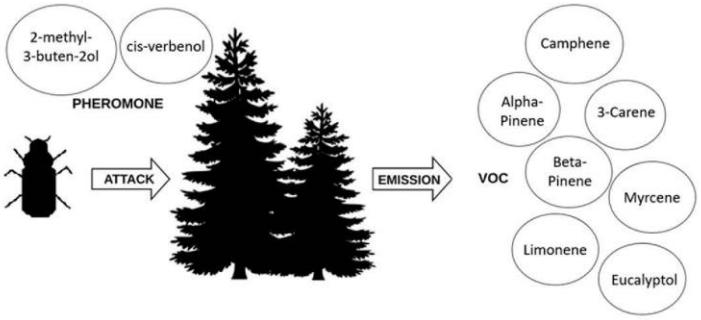

Figure 1. A simplified scheme—when a bark beetle attacks, trees secrete an increased amount of volatile organic substances; on the other hand, the male nesting in the tree starts to produce an aggregation pheromone from his body to attract females to mate.

In this research, we hypothesized that there is a substance detectable by the electronic nose which indicates the presence or near distance of attacked and/or dead trees. We hypothesized that from the set of sensors included in the electronic nose, some or all would react as the distance to the dead and attacked tree becomes smaller, indicating the higher concentration of the substance present in the stressed tree. Our research aims to verify the applicability of the electronic nose for stress mapping in the forest environment. Our goal is to find suitable sensors that will respond to the presence of a substance identifying infested trees [33,34].

The electronic nose appears as an important tool to detect VOCs in different scenarios, including the emission of VOCs caused by herbivory-induced species of pest insects. This research could be a valuable part of new strategies against an outbreak of pest insects such as bark beetles. The benefit of this study is the comparison of individual sensors of the electronic nose for detecting stress in the forest ecosystem. Thus, we bring pilot research for scientists to determine which sensors are more appropriate to choose for analyzing the occurrence of bark beetle attacks in the following season. Timely identification would reduce environmental and economic damage.

In light of the bark beetle outbreaks and the current detection method, which can detect stress in forests in the late stage of infestation, the present brief report sets out to examine the following:

1. Is the specific substance that identifies stressed trees detectable by the Sniffer4D electronic nose?
2. What sensors will correlate with distance from stressed trees?
3. Can stress be detected by these sensors even above treetops using UAVs where the concentration is hypothetically lower?

2. Materials and Methods

2.1. Study Site

The study was conducted at the property of the University Forest Enterprise near Vyžlovka, southeast of Prague (Figure 2). The forest is used for forestry research and teaching, and the particular forest stand is a single-story with a density of stocking 0.8. Field experiments were established in a mixed stand, where the dominant stand is 80–100-year-old allochthonous Norway spruce with accessory species beech, oak, and maple [35]. The terrain is relatively flat, and the type of soil is brown soil, strongly acidic podzolized. The primary rock in the area is slightly (to medium) grained two-mica granite [36]. The study region is a slightly warm area characterized by an average yearly temperature of 8 °C and an average precipitation of 600 mm [37].

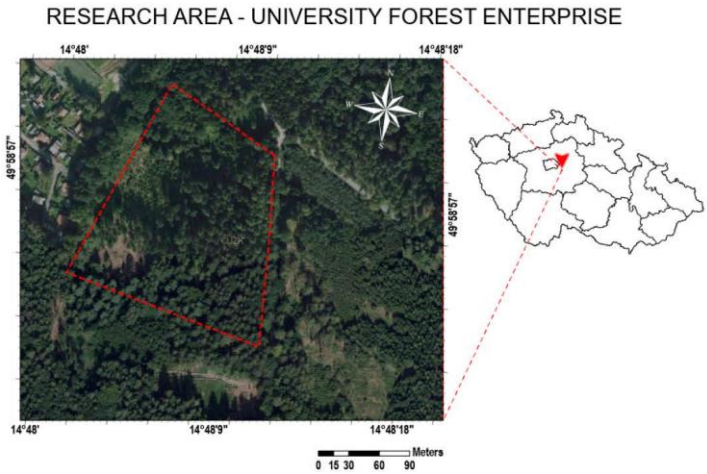

Figure 2. Location of study plot in Vyžlovka, Czech Republic, in a coordinate system S-JTSK Krovak East North, data source: ČÚZK.

2.2. Data Collection

We collected data on 24 August 2022; ground collection took place from 12:10 to 12:25 and 16:00 to 16:15, and collection using UAV took place between 15:40 and 15:55. On the ground level, we recorded during data collection a temperature of 20–23 °C and a humidity of 38.8–52.0%; during flight, we recorded 19–20 °C and a humidity of 45–50%. Data collection took place at two heights, ground measurement and above the canopy. The primary statistical description of the collected data is in Table 1, and the kernel density figures of individual sensors are given in Appendix A. Before the actual measurement, the stand was visually evaluated, and each tree's health status and degree of infestation were examined (Figure 3). The state of the infestation was evaluated by a field survey, during which we evaluated the visual condition of the bark and needles and the development phase of the bark beetle. A tree that had not yet spawned the next generation was identified as the early stage of infestation. Trees that already had visible outcomes, holes, and needles that changed spectral expression were identified as dead trees. This is a classic forestry management tool for the identification of an infested tree in the Czech Republic.

Table 1. Description of collected data, first ground collection, second ground collection, and UAV data collection.

Data Collection	Sample Number	Sample Category	Mean	Standard Deviation
First ground measurement	1148	VOCs	0.372	0.001
		SO_2	20.007	7.486
		CO	0.235	0.032
		$O_3 + NO_2$	741.040	227.101
		$PM_{1.0}$	16.541	1.102
		$PM_{2.5}$	22.951	1.740
		PM_{10}	25.614	1.774
		CxHy	0.079	0.003
		H_2S	217.614	53.369
		HCL	1.263	1.693
Second ground measurement	811	VOCs	0.376	0.001
		SO_2	30.709	8.624
		CO	0.253	0.035
		$O_3 + NO_2$	135.970	23.466
		$PM_{1.0}$	15.260	0.769
		$PM_{2.5}$	20.059	1.363
		PM_{10}	22.520	1.513
		CxHy	0.085	0.003
		H_2S	269.391	54.577
		HCL	1.912	1.832
UAV measurement	815	VOCs	0.376	0.002
		SO_2	23.378	5.061
		CO	0.211	0.026
		$O_3 + NO_2$	171.156	25.642
		$PM_{1.0}$	15.781	0.890
		$PM_{2.5}$	21.509	1.247
		PM_{10}	23.927	1.320
		CxHy	0.085	0.001
		H_2S	217.501	11.957
		HCL	0	0

Figure 3. The orthomosaic was created from images taken from the UAV DJI Mavic with a visible spectrum in channel R, G, B. The image shows a point layer of trees; black points represent snags, red points indicate an early-stage infestation of trees, on the left is a clearing area; the other trees were not attacked.

Data were collected under the canopy by carrying the sensor and above the tree canopy by flying the DJI Matric 600 Pro multi-copter (©2022 SZ DJI Technology Co., Ltd.: Shenzhen, China). The electronic nose was placed on the drone, and air collection took place through a sampling tube, which was placed one meter in front of the drone to minimize the multi-

copter's downwash effect (Figure 4). The flight was carried out manually due to numerous obstacles during the flight, mainly under the crowns of trees. Large horizontal and vertical gaps were kept in flight (Figure 5). The first flight was carried out as low as possible above the crowns (60 m), and then we flew 20 m higher to verify the captured VOC substances at a greater distance from the attacked trees.

Figure 4. Electronic nose Sniffer 4D placed on multi-copter DJI Matrice 600; Teflon meter tube was used for sampling air.

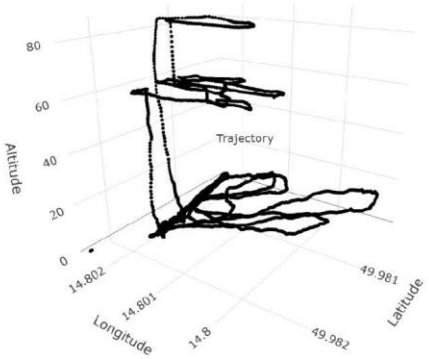

Figure 5. The trajectory of the sensor's measurements. The measurement was first carried out on the ground level and then by an unmanned aerial vehicle—first; we descended just above the treetops (approx. 60 m), then we made a short flight at the height of 80 m.

2.3. Electronic Nose

The Sniffer 4D V2 sensor (©2022 SZ Soarability Technologies Co., Ltd.: Shenzhen, China) is a multi-gas and mapping device used in drone and ground measurement applications. The sensor is composed of multi-gas detection hardware and analysis software. This system is capable of measuring and, at the same time, visually presenting the detected concentrations of gases of interest in real-time. The sensor is constructed from a 1 GHz ARM main processing unit (processing chip) and 512 MB memory. The sensor can measure temperature, humidity, and pressure (range −40~85 °C, 0~100% RH, 30 kPa~110 kPa;

theoretical resolution: 0.1 °C, 0.1% RH, 0.01 kPa; time resolution: 1 s. The sensor was equipped with components for measuring VOCs, SO_2, CO, O_3 + NO_2, $PM_{1.0}$, $PM_{2.5}$, PM_{10}, CxHy, H_2S, and HCL [38]. As part of the measurement, the response of all the sensor components was evaluated, aiming to find the specific sensor or sensors that would be the most sensitive to the chemical substances released during a bark beetle attack.

2.4. Analysis of Sensors Data

The measurement values for individual sensors were evaluated using Pearson's correlation coefficient to determine the correlation between the distance from the trees and the value measured by the sensor. The assumption is that these values depend on each other; the closer we are to early-stage infestation trees/dead trees, the higher the values are measured by the sensors, thus representing a negative correlation coefficient. The weather affects the bark beetles' activity, so measuring temperature and humidity is also important. The ideal temperature is around 25 °C without rain occurrence on data collection day. The 3D models represent humidity (Figure 6a) and temperature (Figure 6b) measurements during the entire data collection. Temperature and humidity significantly affect the spread of bark beetles; for example, the bark beetle is active at a temperature of 16 to 32 °C, and the optimum flight temperature is 22–26 °C (for searching for suitable host trees). In laboratory conditions, a relative humidity of 70% is used for growing bark beetles [39,40].

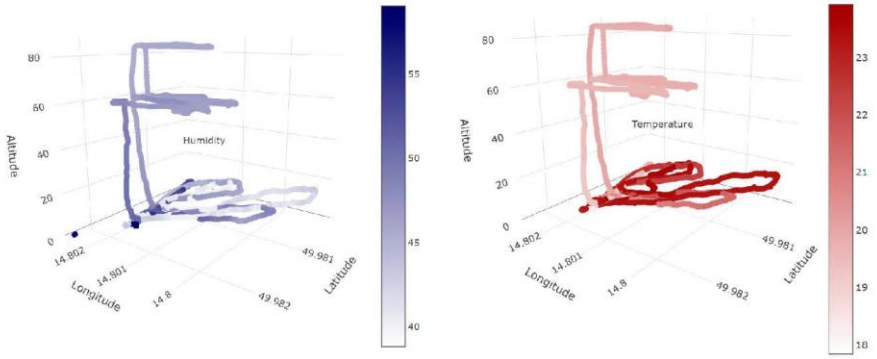

(**a**) (**b**)

Figure 6. 3D models present the humidity (**a**) and temperature (**b**) measured by the sensor during the entire field experiment.

3. Results

The individual sensors of the electronic nose are cross-sensitive, i.e., a sensor primarily created for CO_2 detection may be sensitive to specific compounds of VOCs or pheromones. Therefore, in our study, we verified several sensors of the electronic nose, intending to find the most responsive ones to the presence of dead trees and trees attacked by the bark beetle. Such an application is in the initiation phase, and more experiments are needed. In this work, we evaluated the responsiveness of the individual sensors for indicating the distance of dead trees and trees attacked by a bark beetle. According to the study questions, we find out the following: (1) the results point to the potential use of the electronic nose for stress monitoring in forest stands and (2) individual sensors can detect specific compounds that identify stress. The highest sensor values were recorded near the most attacked trees. The highest correlation was recorded with the HCL, SO_2, and H_2S sensors during ground measurements. The ability to detect stress above the canopy using a UAV has not been proven. A more detailed explanation of the results and their causes is below.

Table 2 presents the Pearson correlation coefficient results for the ground first and second measurements for dead trees. At the first measurement, the highest correlation was recorded for the HCL (−0.456) sensor, followed by SO_2 (−0.209) and H_2S (−0.132). During the second ground measurement, the most accurate measurement coefficient values were for the H_2S (−0.432) sensor, next for HCL (−0.378) and SO_2 (−0.360). We successfully managed to detect a chemical substance that identified the presence of dead trees, both during the first ground measurement and during the second one.

Table 2. Pearson's correlation coefficient results of data first and second ground collection for dead trees.

Data Collection	Condition of Trees	Sensor	Pearson's Correlation Coefficient
First ground measurement	Dead trees	VOCs	0.322
		SO_2	**−0.209**
		CO	0.071
		$O_3 + NO_2$	0.629
		$PM_{1.0}$	0.300
		$PM_{2.5}$	0.284
		PM_{10}	0.237
		CxHy	−0.071
		H_2S	**−0.132**
		HCL	**−0.456**
Second ground measurement	Dead trees	VOCs	−0.036
		SO_2	**−0.360**
		CO	0.394
		$O_3 + NO_2$	0.108
		$PM_{1.0}$	0.189
		$PM_{2.5}$	0.000
		PM_{10}	−0.052
		CxHy	−0.146
		H_2S	**−0.432**
		HCL	**−0.378**

Table 3 presents Pearson correlation coefficients for the first and second ground measurements for early-stage infestation trees. This data collection also fulfilled the assumption that any of the sensors would react to substances that identify the presence or appear near the location of the early-stage infestation trees. At the first measurement, the highest accuracy was recorded for the HCL (−0.427) sensor, followed by SO_2 (−0.164) and H_2S (−0.100). During the second ground measurement, the most accurate measurement coefficient values were for the H_2S (−0.486) sensor, next for SO_2 (−0.480), and C_xH_y (−0.339).

Table 3. Pearson's correlation coefficient results of data first and second ground collection for early-stage infestation trees.

Data Collection	Condition of Trees	Sensor	Pearson's Correlation Coefficient
First ground measurement	Early stage of infestation	VOCs	0.230
		SO_2	**−0.164**
		CO	0.062
		$O_3 + NO_2$	0.648
		$PM_{1.0}$	0.274
		$PM_{2.5}$	0.285
		PM_{10}	0.219
		CxHy	−0.076
		H_2S	**−0.100**
		HCL	**−0.427**

Table 3. *Cont.*

Data Collection	Condition of Trees	Sensor	Pearson's Correlation Coefficient
Second ground measurement	Early stage of infestation	VOCs	0.165
		SO_2	**−0.480**
		CO	0.337
		$O_3 + NO_2$	−0.150
		$PM_{1.0}$	0.231
		$PM_{2.5}$	−0.048
		PM_{10}	−0.068
		CxHy	**−0.339**
		H_2S	**−0.486**
		HCL	−0.118

Table 4 presents the Pearson correlation coefficient results for the UAV measurements for early-stage infestation and dead trees. No higher correlation coefficient values were achieved with UAV data collection. The reason for these results may lie in the lower concentrations above the forest canopy of the substances released during the attack. Another hypothetic cause could have been weather conditions (e.g., the wind taking the substances away, though no significant wind was registered on the day); in the future, it would be advisable to equip the electronic nose with an anemometer for the next measurements. As part of measurements with an anemometer, we will be able better interpret and record the spread of chemical compounds in the forest environment.

Table 4. Pearson's correlation coefficient results of UAV collection for early-stage infestation and dead trees.

Data Collection	Condition of Trees	Sensor	Pearson's Correlation Coefficient
UAV measurement	Early stage of infestation	VOCs	0.445
		SO_2	0.415
		CO	0.464
		$O_3 + NO_2$	0.501
		$PM_{1.0}$	−0.020
		$PM_{2.5}$	−0.033
		PM_{10}	0.021
		CxHy	0.065
		H_2S	0.250
		HCL	NA
UAV measurement	Dead trees	VOCs	0.346
		SO_2	0.294
		CO	0.377
		$O_3 + NO_2$	0.357
		$PM_{1.0}$	−0.006
		$PM_{2.5}$	−0.101
		PM_{10}	−0.056
		CxHy	0.140
		H_2S	0.140
		HCL	NA

The results are promising for further research in this area. Mostly HCL but followed by SO_2, and H_2S sensors proved to be the most suitable for chemical substances released when attacked by bark beetles (Figure 7a,b). The other sensors reacted for increased concentrations in the clearing area.

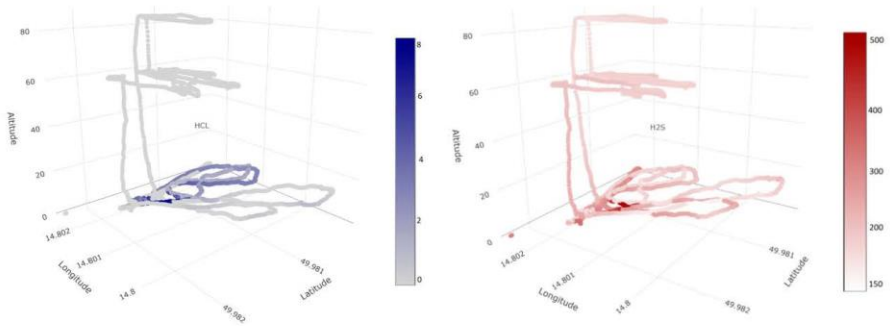

(a) (b)

Figure 7. 3D models present the most sensitive sensors during data collection: (**a**) HCL sensor and (**b**) H_2S sensor measured by electronic nose.

4. Discussion

Measuring chemical substances using electronic noses is a promising methodology in forestry [12,21]. This system is already verified for monitoring odors from agricultural farms and dangerous gas leaks from industrial sites [41–44]. This research provides information on suitable electronic nose sensors for stress detection in the forest ecosystem. Measuring VOCs in the air is challenging in terms of the impossibility of repeatability of measurements under the same conditions. Constantly changing climatic and weather conditions change concentrations and direction of spread [2–4].

Our research demonstrated the detectability of a specific substance, which is released during stress in spruce trees, by specific electronic nose sensors. The HCL, H_2S, and SO_2 sensor during ground measurements (first and second ground data collection) was the most sensitive for our purposes. Some sensors responded to the presence of another substance, so they showed the opposite trend. At this moment, we are not aware of any work that would clearly and undoubtedly prove which substances are released and in which quantities, and, in particular, which sensors react to them. This study is not globally conclusive, and that further study is needed. The research team of Paczkowski et al. [21] achieved similar results in the detection of bark beetle infestation, where they compared the sensitivity of GGS2330 SnO_3, GGS1330 SnO_2, and GGS5330 WO_3; they recorded the highest reaction with the GGS2330 sensor with a SnO_3 surface suitable for detecting easily thermally oxidized VOCs.

Early detection of infestation is desirable not only in forestry but also in agriculture. The research methodology remains similar, and the aim of the assessment is the interaction between the insect and the plant. An accuracy of 94.2–99.2% was achieved when monitoring wheat aphid infestation; data collected were obtained by a cheap electronic nose [19]. The signal from the electronic nose was used to distinguish rice infested and not infested by the Nilaparvata lugens pest; the correlation coefficient reached a value of 0.78 between the predicted pests and the actual ones recorded using machine learning models [33].

Ground data collection provides important information, but for forestry applications, it would be better to have comprehensive data from several measurement heights, and thus also above the tree canopy. In this brief report, we have not proven a correlation between the distance from the attacked trees and the values measured by the sensors during UAV data collection. First, we flew at a height of 60 m; then, we climbed vertically to a height of 80 m. This procedure was chosen to minimize the influence of the downwash effect [45]. We used a sampling tube for data collection; the Teflon tube was 1 m long and was used to collect air in front of the UAV. A meter distance is sufficient to minimize disturbances during data collection [46]. Despite these measures, the same results were not achieved as

with ground data collection. It is possible that the mixing of wind above the tree canopy caused this. Another factor may be the substance values were below the detection limit of the tested sensors, and measuring with a drone disturbs the air with the movement of the rotors (downwash effect). Therefore, paying attention to this aspect before data measurement is crucial. The effect of the height above the canopy was investigated by a Winsen ME4-C_2H_4 electrochemical sensor in a research study focused on the ideal harvest time of apples. The results show that the ethylene concentration decreased by 95% at 4 m and 90% at 2 m above the trees [47].

The potential solution may be creating a canopy height model. Based on the data on tree heights, it would be possible to move closer to the forest crowns and, thus, more accurately capture VOCs from the upper part of the crowns. If even this maximum approach to the trees' canopy would not help, there is the option of manual flight below the tree canopy.

Several factors, including increased drought and insect pests, can cause stress. So, direct detection of the bark beetle is very complicated; the aggregation pheromone, which is produced by representatives of the bark beetle, is in very low concentrations in the forest stand. Therefore, it might be easier to detect just-released VOCs, which signify an increased stress level in trees [31]. In recent years, stress has mainly been caused by bark beetle overgrowth in coniferous forests in the Czech Republic.

Our research points to the suitability of the HCL, H_2S, and SO_2 sensors for stress detection. However, further data collection in diverse areas is desirable. For further research, we recommend verifying UAV data collection in close proximity to tree canopies. It would be appropriate to repeat the experiment over a longer time horizon and monitor temporal changes both in the daily regime and in terms of the rate and development of infestation in the forest stand. For global conclusions, more extensive data collection will be necessary, as other factors (e.g., humidity, temperature, air pressure) may influence the results, and it is in no way possible to catch all in one experiment.

5. Conclusions

The presented research describes a potential methodology for the early detection of bark-beetle-caused stress in the early stages of infestation (green attack) and dead trees, which are usually the result of the previous attack. Using electronic noses and similar sensors has been a proven methodology for faster data evaluation in the industry for years. Therefore, applying electronic sensing noses in forestry represents such a potential. The main advantage of this method is fast data processing; primary measurement data can be checked in real-time using the software. Early identification of attacked trees would bring enormous ecological and financial savings. We tested several sensors from an electronic nose to detect dead and infested trees, and the HCL sensor performed most reliably, providing accurate and higher correlation values with the distance to the target. The highest accuracy was achieved during the first and second ground measurements. We confirmed our hypotheses, and as part of the research, we managed to detect with specific sensors the increased presence of a substance that identifies bark beetle infestation (i.e., stressed trees). The results from the data obtained by the UAV do not indicate decreasing trends from the targets, which could be caused by a lower concentration of substances above the tree canopy or an influence of higher wind movement. The results presented here are very promising, but the research needs to be followed up with further experiments to verify the use of other sensors, and in different situations.

Author Contributions: Conceptualization, S.P. and P.S.; methodology, S.P.; data curation, P.S. and T.N.; writing—original draft preparation, T.H.; writing—review and editing, T.N. and A.J.; visualization, T.H. and T.N.; supervision, P.S. and A.J.; funding acquisition, T.H. and S.P. All authors have read and agreed to the published version of the manuscript.

Funding: This research was funded by Improvement in Quality of the Internal Grant Scheme at CZU, reg. no. CZ.02.2.69/0.0/0.0/19_073/0016944.

Institutional Review Board Statement: Not applicable.

Informed Consent Statement: Not applicable.

Data Availability Statement: Data are available upon request by the authors.

Conflicts of Interest: The authors declare no conflict of interest. The funders had no role in the design of the study; in the collection, analyses, or interpretation of data; in the writing of the manuscript; or in the decision to publish the results.

Appendix A

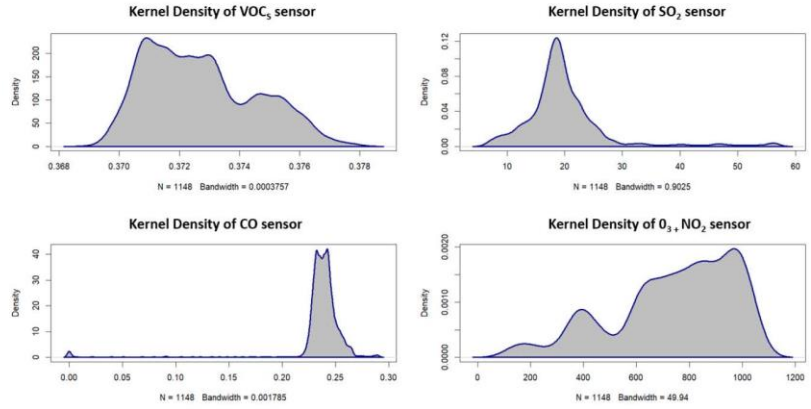

Figure A1. Kernel density for first ground measurement (VOCs sensor, SO_2 sensor, CO sensor, $O_3 + NO_2$ sensor).

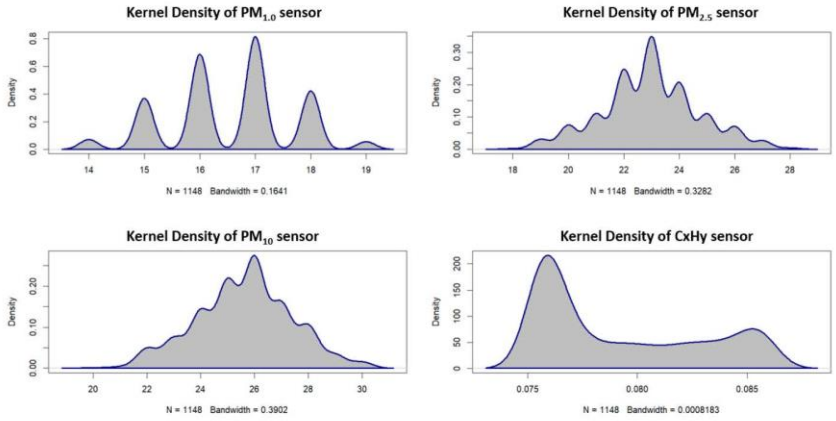

Figure A2. Kernel density for first ground measurement ($PM_{1.0}$ sensor, $PM_{2.5}$ sensor, PM_{10} sensor, C_XH_Y sensor).

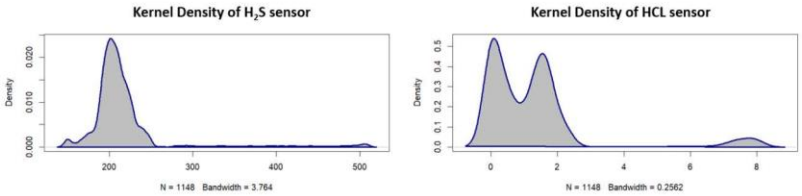

Figure A3. Kernel density for first ground measurement (H_2S sensor, HCL sensor).

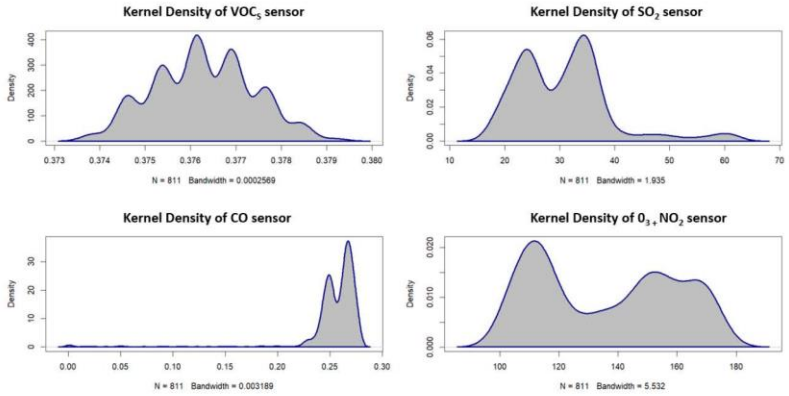

Figure A4. Kernel density for second ground measurement (VOCs sensor, SO_2 sensor, CO sensor, O_3 + NO_2 sensor).

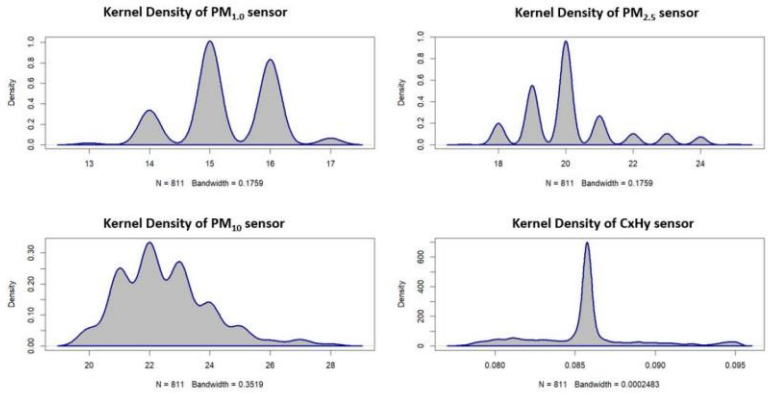

Figure A5. Kernel density for first second measurement ($PM_{1.0}$ sensor, $PM_{2.5}$ sensor, PM_{10} sensor, C_XH_Y sensor).

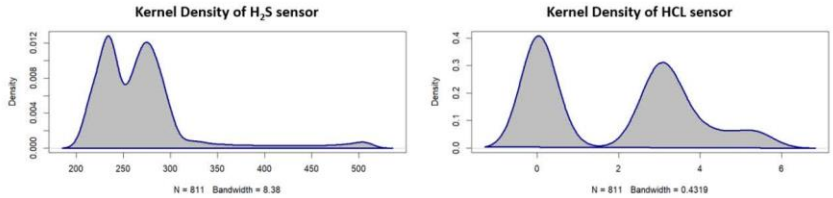

Figure A6. Kernel density for second ground measurement (H_2S sensor, HCL sensor).

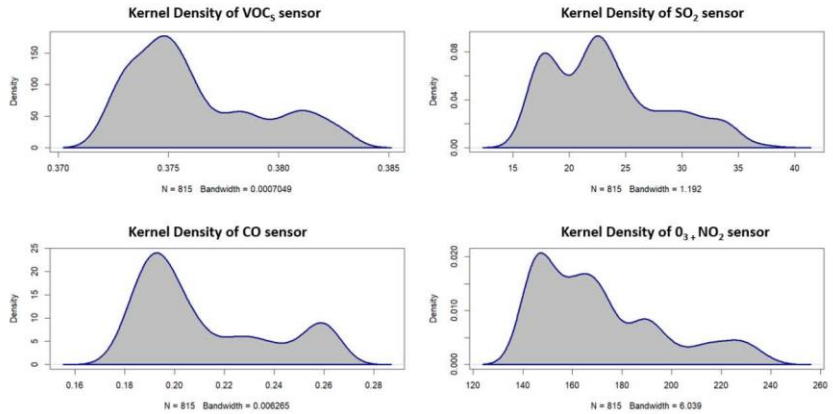

Figure A7. Kernel density for UAV measurement (VOCs sensor, SO_2 sensor, CO sensor, O_3 + NO_2 sensor).

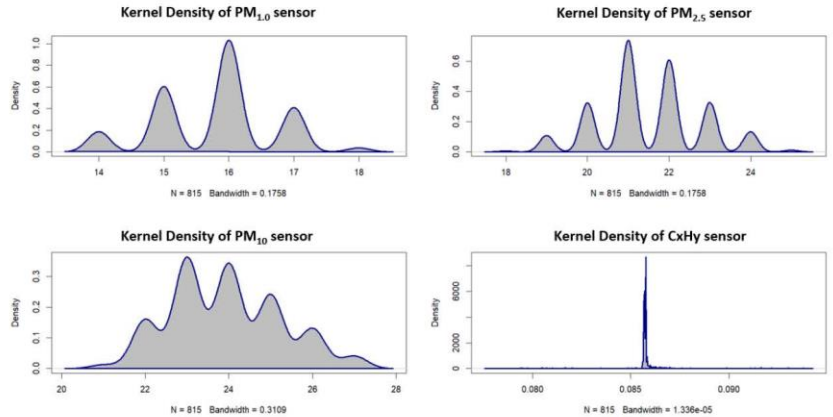

Figure A8. Kernel density for UAV measurement ($PM_{1.0}$ sensor, $PM_{2.5}$ sensor, PM_{10} sensor, C_XH_Y sensor).

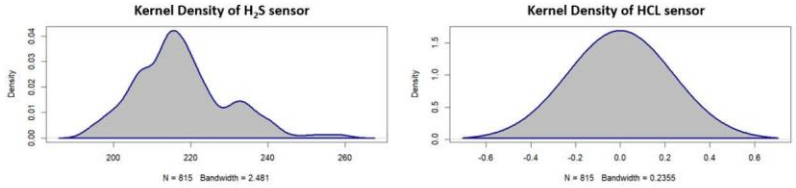

Figure A9. Kernel density for UAV measurement (H_2S sensor, HCL sensor).

References

1. Seidl, R.; Thom, D.; Kautz, M.; Martin-Benito, D.; Peltoniemi, M.; Vacchiano, G.; Wild, J.; Ascoli, D.; Petr, M.; Honkaniemi, J.; et al. Forest Disturbances under Climate Change. *Nat. Clim. Chang.* **2017**, *7*, 395–402. [CrossRef]
2. Fearnside, P.M. Deforestation Soars in the Amazon. *Nature* **2015**, *521*, 423. [CrossRef]
3. Yuan, K.; Zhu, Q.; Zheng, S.; Zhao, L.; Chen, M.; Riley, W.J.; Cai, X.; Ma, H.; Li, F.; Wu, H.; et al. Deforestation Reshapes Land-Surface Energy-Flux Partitioning. *Environ. Res. Lett.* **2021**, *16*, 024014. [CrossRef]
4. Bowman, D.M.J.S.; Balch, J.K.; Artaxo, P.; Bond, W.J.; Carlson, J.M.; Cochrane, M.A.; D'Antonio, C.M.; DeFries, R.S.; Doyle, J.C.; Harrison, S.P.; et al. Fire in the Earth System. *Science* **2009**, *324*, 481–484. [CrossRef] [PubMed]
5. Zhu, Q.; Li, F.; Riley, W.J.; Xu, L.; Zhao, L.; Yuan, K.; Wu, H.; Gong, J.; Randerson, J. Building a Machine Learning Surrogate Model for Wildfire Activities within a Global Earth System Model. *Geosci. Model Dev.* **2022**, *15*, 1899–1911. [CrossRef]
6. Kautz, M.; Meddens, A.J.H.; Hall, R.J.; Arneth, A. Biotic Disturbances in Northern Hemisphere Forests—A Synthesis of Recent Data, Uncertainties and Implications for Forest Monitoring and Modelling: Biotic Disturbances in Northern Hemisphere Forests. *Glob. Ecol. Biogeogr.* **2017**, *26*, 533–552. [CrossRef]
7. Seidl, R.; Donato, D.C.; Raffa, K.F.; Turner, M.G. Spatial Variability in Tree Regeneration after Wildfire Delays and Dampens Future Bark Beetle Outbreaks. *Proc. Natl. Acad. Sci. USA* **2016**, *113*, 13075–13080. [CrossRef]
8. Stadelmann, G.; Bugmann, H.; Wermelinger, B.; Bigler, C. Spatial Interactions between Storm Damage and Subsequent Infestations by the European Spruce Bark Beetle. *For. Ecol. Manag.* **2014**, *318*, 167–174. [CrossRef]
9. Chinellato, F.; Faccoli, M.; Marini, L.; Battisti, A. Distribution of Norway Spruce Bark and Wood-Boring Beetles along Alpine Elevational Gradients: Norway Spruce Bark and Wood Beetles along Altitude. *Agric. For. Entomol.* **2014**, *16*, 111–118. [CrossRef]
10. Senf, C.; Seidl, R.; Hostert, P. Remote Sensing of Forest Insect Disturbances: Current State and Future Directions. *Int. J. Appl. Earth Obs. Geoinf.* **2017**, *60*, 49–60. [CrossRef] [PubMed]
11. Meigs, G.W.; Kennedy, R.E.; Cohen, W.B. A Landsat Time Series Approach to Characterize Bark Beetle and Defoliator Impacts on Tree Mortality and Surface Fuels in Conifer Forests. *Remote Sens. Environ.* **2011**, *115*, 3707–3718. [CrossRef]
12. Pajares, G. Overview and Current Status of Remote Sensing Applications Based on Unmanned Aerial Vehicles (UAVs). *Photogramm. Eng. Remote Sens.* **2015**, *81*, 281–330. [CrossRef]
13. Burgués, J.; Marco, S. Environmental Chemical Sensing Using Small Drones: A Review. *Sci. Total Environ.* **2020**, *748*, 141172. [CrossRef] [PubMed]
14. Hall, R.J.; Castilla, G.; White, J.C.; Cooke, B.J.; Skakun, R.S. Remote Sensing of Forest Pest Damage: A Review and Lessons Learned from a Canadian Perspective. *Can. Entomol.* **2016**, *148*, S296–S356. [CrossRef]
15. Klouček, T.; Komárek, J.; Surový, P.; Hrach, K.; Janata, P.; Vašíček, B. The Use of UAV Mounted Sensors for Precise Detection of Bark Beetle Infestation. *Remote Sens.* **2019**, *11*, 1561. [CrossRef]
16. Huo, L.; Persson, H.J.; Lindberg, E. Early Detection of Forest Stress from European Spruce Bark Beetle Attack, and a New Vegetation Index: Normalized Distance Red & SWIR (NDRS). *Remote Sens. Environ.* **2021**, *255*, 112240. [CrossRef]
17. Smigaj, M.; Gaulton, R.; Suárez, J.C.; Barr, S.L. Canopy Temperature from an Unmanned Aerial Vehicle as an Indicator of Tree Stress Associated with Red Band Needle Blight Severity. *For. Ecol. Manag.* **2019**, *433*, 699–708. [CrossRef]
18. Vošvrdová, N.; Johansson, A.; Turčáni, M.; Jakuš, R.; Tyšer, D.; Schlyter, F.; Modlinger, R. Dogs Trained to Recognise a Bark Beetle Pheromone Locate Recently Attacked Spruces Better than Human Experts. *For. Ecol. Manag.* **2023**, *528*, 120626. [CrossRef]
19. Fuentes, S.; Tongson, E.; Unnithan, R.R.; Gonzalez Viejo, C. Early Detection of Aphid Infestation and Insect-Plant Interaction Assessment in Wheat Using a Low-Cost Electronic Nose (E-Nose), Near-Infrared Spectroscopy and Machine Learning Modeling. *Sensors* **2021**, *21*, 5948. [CrossRef]
20. Marković, D.; Vujičić, D.; Tanasković, S.; Đorđević, B.; Randić, S.; Stamenković, Z. Prediction of Pest Insect Appearance Using Sensors and Machine Learning. *Sensors* **2021**, *21*, 4846. [CrossRef]
21. Paczkowski, S.; Datta, P.; Irion, H.; Paczkowska, M.; Habert, T.; Pelz, S.; Jaeger, D. Evaluation of Early Bark Beetle Infestation Localization by Drone-Based Monoterpene Detection. *Forests* **2021**, *12*, 228. [CrossRef]
22. Kuhlmann, G.; Henne, S.; Meijer, Y.; Brunner, D. Quantifying CO2 Emissions of Power Plants With CO2 and NO2 Imaging Satellites. *Front. Remote Sens.* **2021**, *2*, 689838. [CrossRef]
23. Schlyter, F.; Birgersson, G. Individual Variation in Bark Beetle and Moth Pheromones—A Comparison and an Evolutionary Background. *Ecography* **1989**, *12*, 457–465. [CrossRef]

24. Ramakrishnan, R.; Hradecký, J.; Roy, A.; Kalinová, B.; Mendezes, R.C.; Synek, J.; Bláha, J.; Svatoš, A.; Jirošová, A. Metabolomics and Transcriptomics of Pheromone Biosynthesis in an Aggressive Forest Pest Ips Typographus. *Insect Biochem. Mol. Biol.* **2022**, *140*, 103680. [CrossRef]
25. Pickett, J.A.; Wadhams, L.J.; Woodcock, C.M. Developing Sustainable Pest Control from Chemical Ecology. *Agric. Ecosyst. Environ.* **1997**, *64*, 149–156. [CrossRef]
26. Martins, C.B.C.; Zarbin, P.H.G. Volatile Organic Compounds of Conspecific-Damaged Eucalyptus Benthamii Influence Responses of Mated Females of Thaumastocoris Peregrinus. *J. Chem. Ecol.* **2013**, *39*, 602–611. [CrossRef]
27. Paré, P.W.; Tumlinson, J.H. Plant Volatiles as a Defense against Insect Herbivores. *Plant Physiol.* **1999**, *121*, 325–332. [CrossRef]
28. Martins, C.; Vidal, D.; Gomes, S.; Zarbin, P. Volatile Organic Compounds (VOCs) Emitted by Ilex Paraguariensis Plants Are Affected by the Herbivory of the Lepidopteran Thelosia Camina and the Coleopteran Hedypathes Betulinus. *J. Braz. Chem. Soc.* **2017**, *28*, 1204–1211. [CrossRef]
29. Valencia-Ortiz, M.; Marzougui, A.; Zhang, C.; Bali, S.; Odubiyi, S.; Sathuvalli, V.; Bosque-Pérez, N.A.; Pumphrey, M.O.; Sankaran, S. Biogenic VOCs Emission Profiles Associated with Plant-Pest Interaction for Phenotyping Applications. *Sensors* **2022**, *22*, 4870. [CrossRef]
30. Jaakkola, E.; Gärtner, A.; Jönsson, A.M.; Ljung, K.; Olsson, P.-O.; Holst, T. Spruce Bark Beetle (*Ips typographus*) Infestation Cause up to 700 Times Higher Bark BVOC Emission Rates from Norway Spruce (*Picea abies*). *Biogeosci. Discuss.* **2022**. *in review*. [CrossRef]
31. Ghimire, R.P.; Kivimäenpää, M.; Blomqvist, M.; Holopainen, T.; Lyytikäinen-Saarenmaa, P.; Holopainen, J.K. Effect of Bark Beetle (*Ips typographus* L.) Attack on Bark VOC Emissions of Norway Spruce (*Picea abies* Karst.) Trees. *Atmos. Environ.* **2016**, *126*, 145–152. [CrossRef]
32. Rahmani, R.; Hedenström, E.; Schroeder, M. SPME Collection and GC-MS Analysis of Volatiles Emitted during the Attack of Male *Polygraphus Poligraphus* (Coleoptera, Curculionidae) on Norway Spruce. *Z. Nat. C* **2015**, *70*, 265–273. [CrossRef] [PubMed]
33. Zhou, B.; Wang, J. Use of Electronic Nose Technology for Identifying Rice Infestation by Nilaparvata Lugens. *Sens. Actuators B Chem.* **2011**, *160*, 15–21. [CrossRef]
34. Cellini, A.; Blasioli, S.; Biondi, E.; Bertaccini, A.; Braschi, I.; Spinelli, F. Potential Applications and Limitations of Electronic Nose Devices for Plant Disease Diagnosis. *Sensors* **2017**, *17*, 2596. [CrossRef] [PubMed]
35. ÚHÚL: Informace o Lesním Hospodářství. Available online: https://geoportal.uhul.cz/mapy/mapylhpovyst.html (accessed on 18 November 2022).
36. Půdní Mapa 1:50,000. Available online: https://mapy.geology.cz/pudy/# (accessed on 18 November 2022).
37. Portál ČHMÚ: Historická Data: Počasí: Mapy Charakteristik Klimatu. Available online: https://www.chmi.cz/historicka-data/pocasi/mapy-charakteristik-klimatu (accessed on 18 November 2022).
38. Sniffer4D–Mobile Air Poluttant Mapping System–Drone-Based Air Pollutant Mapping System. Available online: http://sniffer4d.eu/ (accessed on 18 November 2022).
39. Ogris, N.; Ferlan, M.; Hauptman, T.; Pavlin, R.; Kavčič, A.; Jurc, M.; de Groot, M. RITY–A Phenology Model of Ips Typographus as a Tool for Optimization of Its Monitoring. *Ecol. Model.* **2019**, *410*, 108775. [CrossRef]
40. Wermelinger, B. Ecology and Management of the Spruce Bark Beetle Ips Typographus—A Review of Recent Research. *For. Ecol. Manag.* **2004**, *202*, 67–82. [CrossRef]
41. Abdullah, A.H.; Sudin, S.; Mat Ajit, M.I.; Ahmad Saad, F.S.; Kamaruddin, K.; Ghazali, F.; Ahmad, Z.A.; Abu Bakar, M.A. Development of ESP32-Based Wi-Fi Electronic Nose System for Monitoring LPG Leakage at Gas Cylinder Refurbish Plant. In Proceedings of the 2018 International Conference on Computational Approach in Smart Systems Design and Applications (ICASSDA), Kuching, Malaysia, 15–17 August 2018; pp. 1–5. [CrossRef]
42. Sudama, K.A.; Rivai, M.; Aulia, D.; Mujiono, T. Electronic Nose Based on Gas Sensor Array and Neural Network for Indoor Hydrogen Gas Control System. In Proceedings of the 2022 1st International Conference on Information System & Information Technology (ICISIT), Yogyakarta, Indonesia, 26–27 July 2022; pp. 187–192. [CrossRef]
43. Arroyo, P.; Meléndez, F.; Suárez, J.I.; Herrero, J.L.; Rodríguez, S.; Lozano, J. Electronic Nose with Digital Gas Sensors Connected via Bluetooth to a Smartphone for Air Quality Measurements. *Sensors* **2020**, *20*, 786. [CrossRef]
44. Rahman, S.; Alwadie, A.S.; Irfan, M.; Nawaz, R.; Raza, M.; Javed, E.; Awais, M. Wireless E-Nose Sensors to Detect Volatile Organic Gases through Multivariate Analysis. *Micromachines* **2020**, *11*, 597. [CrossRef]
45. Hedworth, H.; Page, J.; Sohl, J.; Saad, T. Investigating Errors Observed during UAV-Based Vertical Measurements Using Computational Fluid Dynamics. *Drones* **2022**, *6*, 253. [CrossRef]
46. Wang, T.; Han, W.; Zhang, M.; Yao, X.; Zhang, L.; Peng, X.; Li, C.; Dan, X. Unmanned Aerial Vehicle-Borne Sensor System for Atmosphere-Particulate-Matter Measurements: Design and Experiments. *Sensors* **2019**, *20*, 57. [CrossRef]
47. Valente, J.; Almeida, R.; Kooistra, L. A Comprehensive Study of the Potential Application of Flying Ethylene-Sensitive Sensors for Ripeness Detection in Apple Orchards. *Sensors* **2019**, *19*, 372. [CrossRef] [PubMed]

Disclaimer/Publisher's Note: The statements, opinions and data contained in all publications are solely those of the individual author(s) and contributor(s) and not of MDPI and/or the editor(s). MDPI and/or the editor(s) disclaim responsibility for any injury to people or property resulting from any ideas, methods, instructions or products referred to in the content.

5.4. Sentinel 5-P TROPOMI sensor analysis for CO temporal and spatial dynamics during fire. Case study Bohemian Switzerland National Park

Tereza Hüttnerová, Peter Surový

Faculty of Forestry and Wood Science, Czech University of Life Sciences (CZU Prague), Kamýcká 129,165 21 Prague, Czech Republic

Formath (This article is submitted, and the final version after the revision process could be different)

Author´s contribution: 60 %

Summary of the article

European forests stressed by drought are subsequently more sensitive to natural disturbances. In recent years, it has been map the increased occurrence of bark beetle, forest fire, and wind through events. Sentinel5-P satellite data provide global coverage with fine time scales and can be used to map non-optical changes in inaccessible areas. It is impossible to map emissions by ground or UAV collection during forest fires from a safety perspective. Bohemian Switzerland National Park. First, an enormous bark beetle calamity was noticed in the national park, followed by long-term drought and the largest fire in the modern history of Czechia. The fire affected the local fauna and flora, and the leaking emissions from large-scale forest fires can significantly impact global warming. The article validates the Sentinel 5-P TROPOMI sensor for mapping the emission cloud due to a forest fire. The methods used were space-time cube and change point analysis. We recorded the most reliable results for the carbon monoxide data product. The emission plume affected an area of 27,000 ha, with a 37.6% increase in emissions recorded during the first three days compared to the unaffected area.

Full article

Title: Sentinel 5-P TROPOMI sensor analysis for CO temporal and spatial dynamics during fire. Case study Bohemian Switzerland National Park

Tereza HÜTTNEROVÁ*, Peter SUROVÝ

Faculty of Forestry and Wood Science, Czech University of Life Sciences (CZU Prague), Kamýcká 129, 165 21 Prague, Czech Republic; huttnerovat@fld.czu.cz (T.H.); surovy@fld.czu.cz (P.S.)

* Correspondence: huttnerovat@fld.czu.cz

Abstract

As a result of climate change, forest fires are beginning increasingly threaten Europe's forest ecosystems especially in the areas where they are not common (central and northern Europe). Remote sensing technology nowadays offers novel breakthrough methods for analysis and data gathering of such information and provides valuable insights for researchers and practitioners to learn more about fire activity and its interaction with forest ecosystems. This research focuses on analysis of novel Sentinel5-P TROPOMI satellite data to monitor chemical emission in the Czech Switzerland National Park during the largest fire in modern history in the Czech Republic. We have verified the responses of individual data products using the changepoint package in R and a space-time cube with change-point analysis in ArcGIS Pro. The CO data product provided significant differences in the emission plume during the fire compared to the unaffected areas. This mapping technique determined the size of the affected area at 27,000 ha, and the infestation lasted 6 days from the fire outbreak. Based on satellite observations, a 37.6% increase in CO emissions appeared during the first three days of the fire, and an 18.5% increase in CO during the fourth to sixth days of the fire compared to background data. This mapping technique can serve as an entry point for strategic planning of post-disturbances interventions and analysis.

Keywords: remote sensing, chemical mapping, Sentinel 5-P, forest fire, natural disturbances

1. INTRODUCTION

Forest ecosystems in Europe cover roughly a third of the territory, and in the last decade, they have been significantly degraded (Forest Europe, 2020). Climate change has a negative effect on the health state, which increases average temperatures and reduces precipitation or change the precipitation distribution over year, leading to significant stress in vegetation which was historically adapted to different conditions. Increased drought during the summer is considered one of the causes of more extreme fire weather (Jolly et al., 2019; Huang et al., 2020; Jain et al., 2022; Grünig et al., 2023); forest fires threaten local fauna and flora but also negatively affect the functions of forest ecosystems, reduce carbon storage (Bowman et al., 2021; Case et al., 2021), and increase risks to infrastructure and human health (Keeley et al., 2011; Ganteaume et al., 2021).

European forests stressed by drought are consequently more susceptible to natural disturbances; in the last twenty years, the most significant damages have been caused by windthrow events (46 %), forest fires (24 %), and bark beetles (17 %) (Patacca et al., 2023). On average, 43.8 million m^3/year are cut down in European forests due to natural disturbances in the last 70 years (Patacca et al., 2023). Forest health has been monitored regularly in Czechia since 1986 based on the international program of the European Economic Commission (ICP Forests). Defoliation of forests in Czechia is the highest in Europe and is a severe and persistent problem. It was created due to high emissions in the past; the condition is gradually improving. The current issue is the receding bark beetle outbreak, which has affected majority of spruce forests. Total cutting in 2022 amounted to 25.1 million m^3; salvage cutting due to natural disturbances accounted for 79 % (19.8 million m^3), and of this cutting due to bark beetle infestation represented 8.3 million m^3. In many areas forests are more susceptible to forest fires. In Czech Republic, most of the fires so far did not reach large extent, despite the fact that the frequency of the fires is growing alarmingly. Exception in this trend is forest fire from year 2022, where in inaccessible areas of national park in combination with strong wind the forest fire extended to more than 1000 hectares, making it so the largest ever fire in Czech modern history. The total area of forest stands affected by fire in 2022 was approximately 1 715 ha (in 2021: 410 ha) (Ministerstvo zemědělství, 2023).

Forest fires are a source of greenhouse gases (carbon dioxide (CO_2), methane (CH_4), nitrous oxide (N_2O)) and photochemically reactive compounds (carbon monoxide (CO), non-methane volatile organic carbon (NMVOC), nitrogen oxides (NOx) and others). Forest fires affect the climate directly through greenhouse gases and aerosols but also indirectly through a secondary

impact on the atmosphere, for example, the formation of ozone O_3 (Urbanski et al., 2008). CO is an atmospheric pollutant that is colorless, odorless, and tasteless, and in high concentrations, can be dangerous for the human body. CO is an indirect influencer of climate change directly affects the concentration of primary greenhouse gases (Schneising et al., 2019). Remote sensing allows the efficient mapping of more extensive areas affected by natural disturbances. The extent of the covered study area and the quality of the images depends on the platform used. Satellite data are used for predictive analysis of fire occurrence, spread mapping, and ecological research on the effects of fire on ecosystems (Xiao-rui et al., 2005; Ross et al., 2013). Changes in the spectral reflectance of individual bands are used to evaluate health status. The indices used for fire mapping are: Normalized Burn Ratio (dNBR), Burned Area Index (BAI), and normalized difference vegetation index (NDVI) (Chuvieco et al., 2002; Miller and Thode, 2007; Soverel et al., 2010). In addition to the spectral changes during forest fires, there are non-optical manifestations, namely the increased emissions production. These non-optical changes can be measured locally using hand-held detectors to assess a small area rapidly. However, for global mapping, these methods are ineffective, and some locations are not accessible for inspection due to rugged terrain or property rights. These shortcomings are eliminated by the possibility of using satellite data.

Analysis of the forest fire by remote sensing data in Czech was performed by Berdych (2024) and it was shown that optical remote sensing products like optical aerial imagery including the NIR information and Lidar data acquired periodically before the fire and on purpose after the fire. The remote sensing data were compared to the fire inventory for individual components like standing tree severity, lying tree severity, crown severity and litter severity. Most significantly were values for NDVI after which was in correlation with standing tree severity and lying tree severity. These two values were also clearly correlated with Lidar difference (e.g. metrics obtained from the before and after Lidar scans, mostly mean and standard deviation).

Berdych (2024) also constructed various machine learning algorithms for analysis of variable importance to estimate fire severity, namely random forest and support vector machine models with various kernels. Among the most significant variables obtained from remote sensing materials the lidar height difference, standard deviation of the difference and combination of before and after NDVI values proved to have significant impact on severity assessment.

The modern remote sensing data include and provide possibilities for direct assessment of severity in larger scale for estimating the emissions to the atmosphere. The Greenhouse Gases Observing Satellite (GOSAT) is the first satellite to detect CO_2 and CH_4 emissions since 2009.

It carries two instruments, the Thermal and Near Infrared Sensor for Carbon Observation Fourier-Transform Spectrometer and the TANSO Cloud and Aerosol Imager (Hamazaki et al., 2007; Ross et al., 2013; Lunt et al., 2019; Maasakkers et al., 2019). Recent scientific studies have addressed the validation of the TROPOMI sensor for emissions mapping in various tasks (Figure 1). TROPOMI NO_2 and CO data products were used to characterize biomass combustion efficiency and analyze pollutants from the burning process (Van Der Velde et al., 2021a), forest fires were monitored in Portugal with TROPOMI´s data product CO and CH_4 (Magro et al., 2021).

Figure 1. Sentinel-5 satellite with TROPOMI sensor focused on environmental monitoring operations (Photo: ©ESA; ESA - Sentinel-5P and Tropomi)

Information about the emission can be used to estimate the emissions to the atmosphere caused by the fire. Such example was demonstrated in (Van Der Velde et al., 2021b). The authors utilized CO estimates measured by TROPOMI, developed analytical Bayesian inversion, and observed ratios between emitted carbon dioxide and carbon monoxide and estimated the total carbon release to the atmosphere. They concluded that from November 2019 to January 2020 715 teragrams of carbon dioxide were released to the atmosphere approximately double the estimates from previous inventories. Similar study conducted by Wan et al. (2022), focused on estimation of CO and NO_2 emissions. They combined data from TROPOMI with fire counts and fire radiative power (FRP) from MODIS and estimated temporal and spatial variation of NO_2 and CO.

In this paper we focus on analysis of TROPOMI CO data, and the goal is mathematical modeling and analysis of the spread of emissions from a forest fire and to verify capability of the Sentinel-5 satellite products for mapping emissions from forest fires for possible input in other mathematical spatial models as shown in (Yoshimoto et al., 2017).

2. METHODS

2.1 Study area

The study area is one of four national parks in the Czech Republic (Figure 2), located in the Děčín district and adjacent to the border with Germany. The main objects of protection are sandstone formations and biotopes directly linked to them. Forest stands covered most of the land (95 %), and the initially dominant forest beech was displaced by spruce. The species composition in the forest is not natural; it was influenced by past forest management activity; the park's current representation is 60% Norway spruce, 20% forest pine, and 10% forest beech. The area of the national park is 7,933 ha. In 2018, extreme windthrow events took place in the park, followed by extensive outbreaks of bark beetles on the spruce stands. Standing dead spruce trees remained in the park; the trees were not cut down. The largest fire in the Czech Republic in modern history took place in Bohemian Switzerland National Park. It started on July 23 and spread to the German side on July 25, 2022. Forest fires burned approximately 1,200 ha. The fire was extinguished on August 12, 2022.

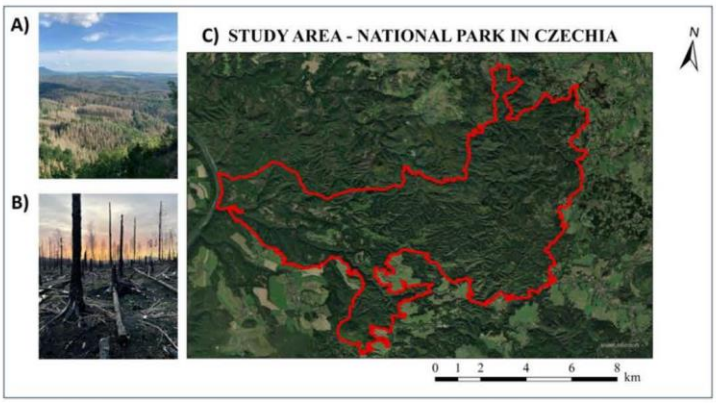

Figure 2. The study area of the national park, A) forest cover affected by bark beetles in 2020 - the gray crowns of dead trees are visible, B) the area of the park affected by fire in 2022, C) the extent of the national park - a very high forest-type land cover.

2.2 Data

For the chemical analysis of the fire in the national park, we used images from the European Space Agency's Sentinel-5 Precursor satellite, a low Earth orbit polar whose primary mission is to map air quality and monitor climate change. The satellite carries the sensor TROPOspheric Monitoring Instrument (TROPOMI), which has ultraviolet-visible (270–500 nm), near-infrared (675–775 nm), and shortwave infrared (SWIR) (2305–2385 nm) spectral bands and can map fundamental atmospheric indicators nitrogen dioxide (NO_2), sulfur dioxide (SO_2), carbon monoxide (CO), formaldehyde (HCHO), Methane (CH_4), and UV Aerosol Index with spatial resolution approximately 7 x 7 km^2 (Bowman et al., 2021). After examining the characteristics of the data products and their response to forest fires, the CO product was used for data analysis. Another possibility was data product CH_4, which lacked data for the monitored periods (NA). The images were downloaded from the Google Earth Engine portal (data collection of COPERNICUS/S5P/OFFL/) as a georeferenced raster format (GeoTIFF type) as average values od data products for the specified time period (Gorelick et al., 2017).

The forest fire was monitored over approximately four months, focusing on the before, during, and after the fires. Ten periods before the fire were monitored from 3.6. 2022 to 22.7. 2022, then seven periods during the fire from 23.7. 2022 to 12.8. 2022 and ten periods after the end of the fire from 13.8. 2022 to 1.10. 2022. The exact time definition of the individual periods is given in Appendix 1.

Example of the code to get an image showing CO before a fire:

```
var dataset = ee.ImageCollection("COPERNICUS/S5P/OFFL/L3_CO")
var image = dataset.filterBounds(roi)
        .filterDate('2022-06-01T00:00:01', '2022-07-22T23:59:00')
        .select('CO_column_number_density')
        .mean()
        .clip(roi)
var band_viz = {
  min: 0,
  max: 0.05,
  palette: ['black', 'blue', 'purple', 'cyan', 'green', 'yellow', 'red']};
Map.addLayer(image, band_viz)
```

```
print(image)
// Export the image, specifying scale and region.
Export.image.toDrive({
  image: image,
  description: 'CO_pred',
  scale: 1113.2,
  region: roi});
```

2.3 Data analysis

The data analysis was divided into two steps. In the first step we analyzed buffers around the fire center in order to estimate the importance of individual variables. We used the R Studio 2024.04.0 (©2009-2024 Posit Software, PBC) and ArcGIS Pro 3.3.0 (©2023 ESRI Inc., Redlands, CA, United States) software's for all data analysis.

2.3.1 Analysis 1 – Buffering

First, we created multiple buffers in kilometer intervals (1-30 km, Figure 3) from the input polygon of the fire area (i.e., the territory of the national park affected by a forest fire and defined based on optical images and ground survey).

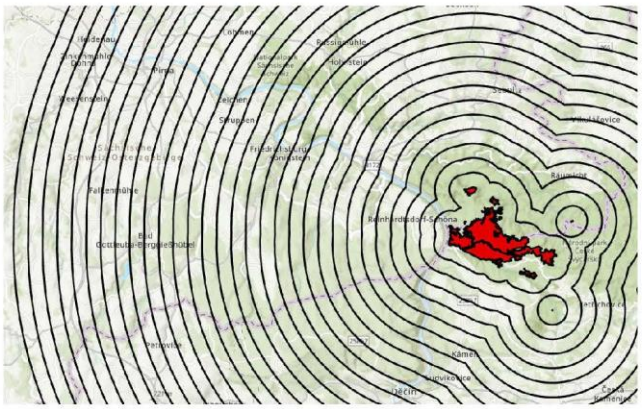

Figure 3. The area affected by the fire (red polygon) and individual polygon segments show multi buffers at kilometer intervals.

This analysis was also performed to evaluate all data products that could capture differences in forest fire cases: NO_2, SO_2, CO, HCHO, CH_4, and UV Aerosol Index. The aim was to find the maximum distance where there was still a change in emissions and in what periods the changes occurred. However, from the preliminary results, changes during the fire were only recorded for the carbon monoxide product, so we continued to work only with this data set. For all time periods and individual buffers, we summarized the values using the *Zonal Statistics as Table* (Spatial Analyst) tool and we searched for change points for individual distances from the fire epicenter using the *changepoints* package (Killick, 2011) with the settings:

cpt_result <- cpt.var(concentration_data, penalty = "AIC", Q = 3)

2.3.2 Analysis 2. Point based analysis of Multidimensional raster data

A multidimensional raster was created, representing the same area captured multiple times, in our study case, a forest fire in a national park. Individual satellite carbon monoxide images were combined into a multidimensional raster in .crf format, designed for working with large-scale data; in this format, the data is divided into individual tiles to facilitate working with the data. To preserve metadata information, the *Build Multidimensional Info* (Data Management) function was used, and the names of variables (individual raster images of study time periods) were stored with their numerical values of recorded carbon monoxide concentration along with the dimension (date of acquisition).

Subsequently, the *Create Space Time Cube From Multidimensional Raster Layer* (Space Time Pattern Mining, Figure 4) function was applied to create a spatiotemporal representation from a multidimensional raster to visualize and analyze spatiotemporal data mapping forest fire emissions. The individual rasters have the same cell size (x and y are the same), and the created space-time cube consists of grids. The trends of values over time are analyzed using the Mann-Kendall statistical method. The individual periods of the examined Sentinel-5 data product were specified in the *Time Step Interval* parameter (the used periods are precisely described in section 2.2 Data)

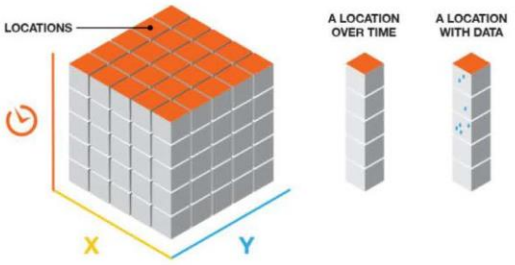

Figure 4. A sample spatial cube consists of a grid; its dimensions are rows, columns, and time steps. The rows and columns describe the spatial extent, and the time steps describe the temporal extent (ArcGIS Pro 3.4., 2024)

In the created Space Time Cube, all-time steps where the statistic property changed significantly were identified, and individual change points divided the time series into segments, with the values in each segment having a similar statistic property. Change points are then defined as the first step in each new segment, ending with the beginning of the next segment. Shifts in the concentration of the analysis variable carbon monoxide concentration were detected, statistical properties of the carbon monoxide concentration are constant in each segment, and at each change point, they change to a new value. The total number of change points is one less than the number of segments. Four methods of *Change Point Detection* (Space Time Pattern Mining) were tested: Mean shift, Standard deviation, Slope (Linear trend), and Count.

The Mean shift method (Figure 5) focuses on detecting points where changes occur in the mean value of the analyzed variable. It assumes that the data values are distributed according to a normal distribution, which means that the probability behavior of the data is symmetrical. Most values are concentrated around the mean. An important assumption is that all periods share the same standard deviation, which means that the dispersion of the data is constant over time. The data is divided into segments during the analysis, with each segment's mean value constant. If a change point is detected, the mean value changes. This approach is particularly suitable for examining time series, where sudden changes may occur due to various factors, such as environmental changes, events, or other external influences (ArcGIS Pro 3.4., 2024).

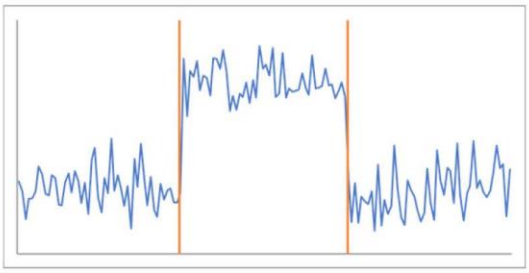

*Figure 5. Simplified blue line chart showing change point detection methods using **mean shift**, vertical orange lines which presents the change points (ArcGIS Pro 3.4., 2024)*

The Standard deviation method (Figure 6) focuses on detecting changes in the standard deviation of the variable being analyzed, which means that it tracks how the variance or variability of the data changes over time. It assumes that the data values are distributed according to a normal distribution, which means that the probability distribution of the data has a symmetrical shape. The critical assumption of the method is that the mean value of the data remains constant over all periods, regardless of the changes in variability detected. The data are divided into segments, with the standard deviation being constant in each segment. If a change point is detected, it means that the variability of the data has changed dramatically. This method can be crucial for forecasting, planning, or ensuring safety in a study area (ArcGIS Pro 3.4., 2024).

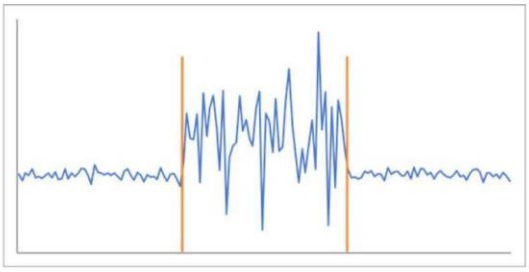

*Figure 6. Simplified blue line chart showing change point detection methods using **standard deviation**, vertical orange lines which presents the change points (ArcGIS Pro 3.4., 2024)*

The Slope (Linear trend) method (Figure 7) is designed to detect changes in the linear trend of the analyzed variable. This method monitors whether and when the slope or direction of data development changes over time. It is assumed that the data values are normally distributed, meaning they are symmetrical, and most values are concentrated around the mean. The average

value in each segment is defined by a straight line with a certain slope and intercept. In each segment, the slope and intercept of the line are constant, changing when detecting a change point. The standard deviation, which describes the variability of the data around this line, remains the same in all periods. The method provides valuable information about the long-term development of a process or system, which is invaluable for decision-making and planning (ArcGIS Pro 3.4., 2024).

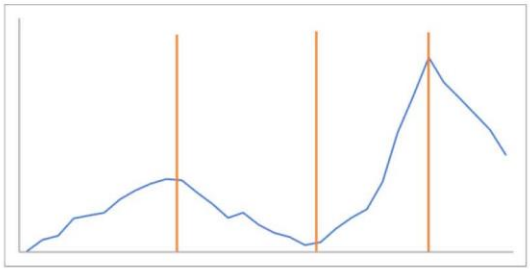

*Figure 7. Simplified blue line chart showing change point detection methods using **slope (Linear trend)**, vertical orange lines which presents the change points (ArcGIS Pro 3.4., 2024)*

The Count method (Figure 8) focuses on detecting changes in the mean value of the analyzed variable, which represents the number of events. This method assumes that the data follows a Poisson distribution. The mean value is constant within each time segment but can change once a change point is detected. If a change point is detected, there has been a change in the frequency of the analyzed event. The method can be used, for example, for areas where there is a need to monitor and respond to changes in criminality, and healthcare (ArcGIS Pro 3.4., 2024).

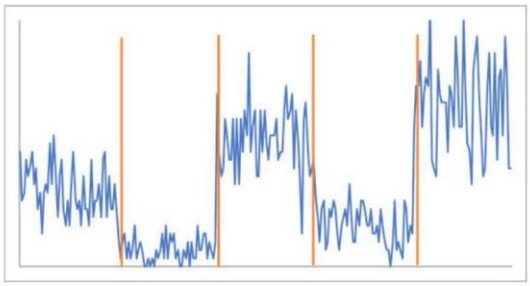

*Figure 8. Simplified blue line chart showing change point detection methods using **Count**, vertical orange lines which presents the change points (ArcGIS Pro 3.4., 2024)*

The main output of Change Point detection methods is a feature class, which contains one feature for each location in the input space-time cube. This feature class has records in the table of contents about the number of change points detected, the date of the first change point, and the date of the last change point detected in a study area (ArcGIS Pro 3.4., 2024).

3. RESULTS

Below, the results obtained from Analysis 1 – Buffering will be described first, followed by the results from 2. Point-based analysis of Multidimensional raster data.

In the first step, we searched for change points in R using the changepoint function. We verified all data products from Sentinel-5 that could be related to forest fire emissions or their secondary effects, specifically using datasets for NO_2, SO_2, CO, HCHO, and UV Aerosol. The changepoint calculations assumed three changes (the start of the fire, the highest emissions achieved, and the end of the fire). The only dataset in which we got the change points corresponding to the forest fire timeline was CO. Based on our assumption of three changes, the first change after the start of the fire was recorded in period 12, which is a dataset for period 26.7. till 28.7.2022, this change indicates a period of highest concentrations (Figure 9). Subsequent changes were detected only at the end of the monitored periods 26 and 27, representing the dataset for periods 24.9. – 28.9. 2022 and 29.9 – 3.10.2022. Of the three expected changes, only two were recorded, and when the fire broke out, we recorded the changes within 8 km of the fire epicenter. This data evaluation does not include the spatial dimension in the calculation, and the results do not fully reflect the mapped phenomenon of forest fire. Therefore, we used the second data analysis approach: change point detection based on the spatiotemporal cube.

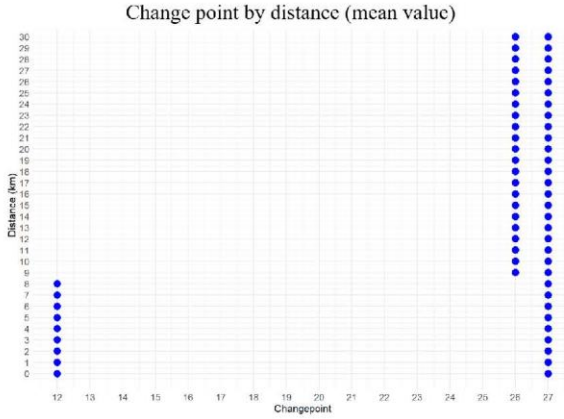

Figure 9. Change points for carbon monoxide, on the x-axis, are the periods when the changes occurred (1st - 10th is the period before the fire, 11th - 17th is the period during the fire, and 18th - 27th is the period after the fire.

We used a multidimensional raster and a space-time cube for a more detailed spatial mapping analysis to identify increased carbon monoxide levels during the forest fire. The emissions were most severe in the central to eastern part of the national park, with subsequent spread to the east (Germany), where the forest fire was also partially extended. Figure 10 shows a space-time cube of CO for possible mapping of concentration changes in both spatial and temporal scales, which overcomes the limitation noted in Analysis 1.

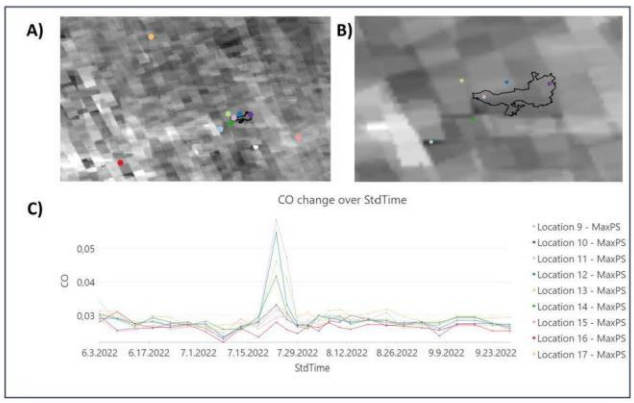

Figure 10. Space time cube of carbon monoxide concentrations, A) a more comprehensive view of the national park area (black-bordered polygon), B) a more detailed view of the national park, C) a graph showing the course of concentrations for specific locations defined by points throughout the monitored timeline (the fire started on 7.23.2022)

We achieved the best results using the Mean shift method of point detection and we obtained information about the pixels where the changes occurred and not; we divided pixels into two groups according to the recorded changes (Figure 11). For group "*At least one change*", red pixels), we involved all pixels where we achieved at least one change from the beginning of the fire; in total, it was 346 pixels. For group "*No change*" (blue pixels) we selected the same number of pixels in the surroundings of the affected area, where we didn't map any changes. Each group covers an area of approximately 27,000 ha.

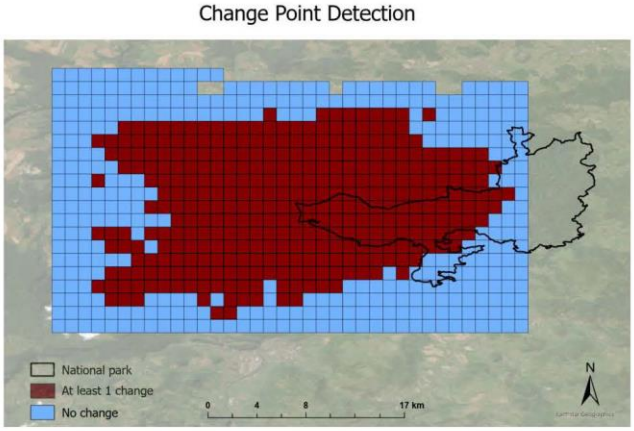

Figure 11. Red pixels are areas where there has been at least one change in carbon monoxide concentration since the start of the fire. Blue pixels are areas without changes where no increased concentration was recorded.

Then, we summed up the CO values for the "*At least one change*" and "*No change*" groups. The "*No change*" group served as background data, i.e., for establishing the current average CO concentration without a stress event caused by a natural disturbance. From the background values, we determined the increase in concentration for the affected area (the group marked "*At least one change*"). We monitored differences in CO emissions in three daily periods, i.e. period 11 (23.7. - 25.7.), period 12 (26.7. - 28.7.), period 13 (29.7. - 31.7.), period 14 (1.8. - 3.8. 2022), period 15 (4.8. - 6.8. 2022), period 16 (7.8. - 9.8. 2022), period 17 (10.8. - 12.8. 2022).

In Figure 12, we graphically display the mapped differences in CO emissions during the fire for affected vs. unaffected areas. The forest fire started on 23.7.2020; period 11 is for dataset 23.7. – 25.7.2022, and here we recorded a 37.6% increase in CO compared to the background value; we also recorded an 18.5% increase in CO for period 12 (26.7. – 28.7.2022). Increased

CO emissions were observed in the first six days of the fire for an area affected by the chemical plume of 27,000 ha. In the remaining periods of the fire (i.e., 29.7. – 12.8.2022), we did not record increased CO emissions.

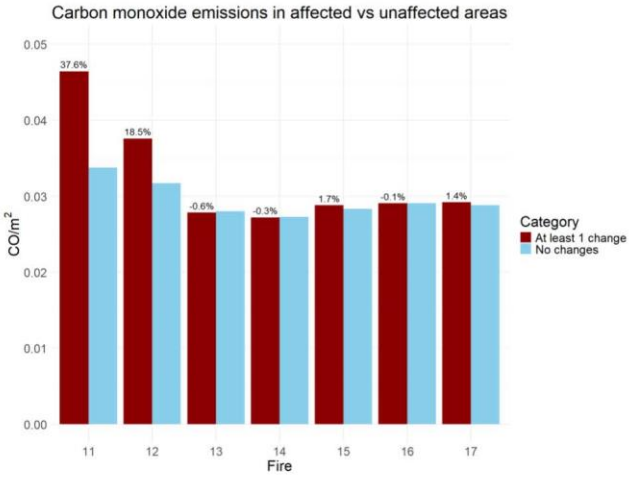

Figure 12. CO amounts for categories "At least 1 change" and "No changes" for the monitored forest fire, differences in CO emissions were monitored in three daily periods, i.e. period 11 (23.7. - 25.7.), period 12 (26.7. - 28.7.), period 13 (29.7. - 31.7.), period 14 (1.8. - 3.8. 2022), period 15 (4.8. - 6.8. 2022), period 16 (7.8. - 9.8. 2022), period 17 (10.8. - 12.8. 2022).

4. DISCUSSION

In this study, we validated the potential of Sentinel5P TROPOMI data for non-optical mapping of natural disturbances, focusing on a case study of a forest fire in a national park in Czechia. First, relevant data products were searched for those mapped changes concerning the forest fire behavior. Of the potential data products (CH_4, NO_2, SO_2, CO, HCHO, and UV Aerosol) that could record emissions, the most promising results were obtained for the CO data product. CH_4 was unavailable for the area of interest from June to September 2022. Similar results were observed by Magro et al. (2021) when mapping fires in Portugal, where CO provided a clear trend, and the results were evident with the fire behavior; CH_4 measurements did not show the same clear trend; elevated values could only be identified at the beginning of the fire, not to estimate its direction. CH_4 is a lighter gas than CO, so it can cause errors in the measurement because this gas is better carried by the wind gust (Magro et al., 2021).

Forest fires are not as common in Central and Northern Europe, but due to global changes, they can be predicted to become more common. The importance of monitoring emissions from forest fires is confirmed by studies from areas where forest fires are a severe natural disturbance. Extensive forest fires were recorded in Australia in 2019 and 2020; Wan et al. (2022) used TROPOMI products NO_2 and CO to analyze temporal and spatial emission variations based on determining emission factors and ratios. The TROPOMI instrument was able to characterize changes on a regional scale during biomass burning; boreal forest fires produce a 3x to 6x greater increase in NO_2 and CO emissions than in the case of savannas or tropical forests (Van Der Velde et al., 2021a).

In addition to the TROPOMI sensor tested in our research, there are other remote sensing techniques for mapping forest ecosystems, such as increased concentrations of CO_2 and CH_4, which were investigated in simulations, and the spectrometer of the GOSAT satellite demonstrated the ability to map increased values of atmospheric gases during boreal, tropical and savanna forest fires (Ross et al., 2013). The Nechita-Banda et al. (2018) study used data from the IASI (Infrared Atmospheric Sounding Interferometer) and MOPITT (Measurements of Pollution in the Troposphere) satellites to analyze carbon monoxide emissions during peatland fires in Indonesia in 2015. They used infrared spectroscopy and inverse modeling. Their results showed a significant increase in CO emissions during the fires, with the total carbon released into the atmosphere estimated at 0.35–0.60 Pg.

Satellite data for mapping natural disturbances brings frequent data obtaining and extensive coverage of the study area, which can be at the expense of spatial resolution. Nechita-Banda et al. (2018) report that the sensitivity of their model based on satellite observations indicates that it can separate emission regions that are 300 km away, and in their study, they mention the availability of finer temporal and spatial scales thanks to the Sentinel-5P TROPOMI data products. One of the first studies using TROPOMI data (Borsdorff et al., 2018) emphasizes global coverage with frequent data acquisitions. In their study compared TROPOMI with measurements from the European Centre for Medium-Range Weather Forecasts, finding very good agreement between the two datasets with an average difference of +3.2% and a correlation coefficient of 0.97. The scientific findings highlight the ability of TROPOMI for emissions mapping; from our results, we determined the first and last day of contamination from the CO data product. We were also able to determine the size of the affected area (27,000 ha) through mapping analyses.

The problematic part remains to determine the total emissions released during the entire duration of the forest fire. Satellite measurements are obtained during a short interval of about 5 minutes; however, emissions can vary greatly during the day depending on intensity, type of burned biomass, etc. Based on our results, a rough estimate can be made based on the affected area of 27,000 ha, where changes were recorded within the first six days of the fire. A difference of 0.013 mol/m^2 was recorded for the first three days of the fire, and from the fourth to the sixth day, the difference was 0.006 mol/m^2. Based on the molar mass of CO, which is 28.01, the concentration can be converted from mol/m^2 to g/m^2. The total CO released from the forest fire could be determined at 421 tons at the moment of the Sentinel snapshot. Conversion to the total release could be calculated using the gas dynamics within the column of the raster, but that would be in this case very speculative and, therefore, not included in the results.

5. CONLUSION

In this research, we focused on validating the data product of the Sentinel-5 TROPOMI satellite for mapping forest fire emissions. The case study focused on a national park where an extensive bark beetle calamity was first recorded, followed by standing dead trees and long-term drought. Subsequently, on July 23, 2022, the largest forest fire in the modern history of the Czech Republic broke out there. The research found that the CO product data provided the most relevant information. The area affected by the emissions was 27,000 ha, and the infestation was mappable within the first six days of the fires. In the affected area, the initial increase in CO was 37.6% compared to the unaffected part. This research provides an entry point for chemical mapping of forest fire plume spread. It provides a methodology for obtaining data for modeling intervention operations to optimize them. Using non-optical satellite data, we can determine the duration of the emission cloud, its first and last day. It is also possible to map the extent of the affected area and determine the difference in emission concentration in the affected area against the background. The challenge remains in determining total emissions from remote sensing methods, specifically in taking the time perspective into snapshot images.

AKNOWLEDGEMENT

This research was funded by Czech University of Life Sciences, Faculty of Forestry and Wood Sciences IGA/A_26_23

REFERENCES

ArcGIS Pro 3.4. (2024). *How change point detection works*. How Change Point Detection works-ArcGIS Pro | Documentation. https://pro.arcgis.com/en/pro-app/latest/tool-reference/space-time-pattern-mining/how-change-point-detection-works.htm

Berdych, M. (2024). Analýza materiálů DPZ pro hodnocení intenzity lesního požáru v NP České Švýcarsko 2022. Prague: CZU Prague.

Borsdorff, T., Aan de Brugh, J., Hu, H., Aben, I., Hasekamp, O., and Landgraf, J. (2018). Measuring Carbon Monoxide With TROPOMI: First Results and a Comparison With ECMWF-IFS Analysis Data. *Geophysical Research Letters* 45, 2826–2832. doi: 10.1002/2018GL077045

Bowman, D. M. J. S., Williamson, G. J., Price, O. F., Ndalila, M. N., and Bradstock, R. A. (2021). Australian forests, megafires and the risk of dwindling carbon stocks. *Plant Cell & Environment* 44, 347–355. doi: 10.1111/pce.13916

Case, M. J., Johnson, B. G., Bartowitz, K. J., and Hudiburg, T. W. (2021). Forests of the future: Climate change impacts and implications for carbon storage in the Pacific Northwest, USA. *Forest Ecology and Management* 482, 118886. doi: 10.1016/j.foreco.2020.118886

Chuvieco, E., Martín, M. P., and Palacios, A. (2002). Assessment of different spectral indices in the red-near-infrared spectral domain for burned land discrimination. *International Journal of Remote Sensing* 23, 5103–5110. doi: 10.1080/01431160210153129

Forest Europe (2020). State of Europe's Forests 2020 Report. *Bonn, Germany*.

Ganteaume, A., Barbero, R., Jappiot, M., and Maillé, E. (2021). Understanding future changes to fires in southern Europe and their impacts on the wildland-urban interface. *Journal of Safety Science and Resilience* 2, 20–29. doi: 10.1016/j.jnlssr.2021.01.001

Gorelick, N., Hancher, M., Dixon, M., Ilyushchenko, S., Thau, D., and Moore, R. (2017). Google Earth Engine: Planetary-scale geospatial analysis for everyone. *Remote Sensing of Environment* 202, 18–27. doi: 10.1016/j.rse.2017.06.031

Grünig, M., Seidl, R., and Senf, C. (2023). Increasing aridity causes larger and more severe forest fires across Europe. *Global Change Biology* 29, 1648–1659. doi: 10.1111/gcb.16547

Hamazaki, T., Kaneko, Y., Kuze, A., and Suto, H. (2007). Greenhouse Gases Observation from Space with TANSO-FTS on GOSAT., in *Fourier Transform Spectroscopy/ Hyperspectral Imaging and Sounding of the Environment*, (Santa Fe, New Mexico: OSA), FWB1. doi: 10.1364/FTS.2007.FWB1

Huang, Y., Jin, Y., Schwartz, M. W., and Thorne, J. H. (2020). Intensified burn severity in California's northern coastal mountains by drier climatic condition. *Environ. Res. Lett.* 15, 104033. doi: 10.1088/1748-9326/aba6af

Jain, P., Castellanos-Acuna, D., Coogan, S. C. P., Abatzoglou, J. T., and Flannigan, M. D. (2022). Observed increases in extreme fire weather driven by atmospheric humidity and temperature. *Nat. Clim. Chang.* 12, 63–70. doi: 10.1038/s41558-021-01224-1

Jolly, W., Freeborn, P., Page, W., and Butler, B. (2019). Severe Fire Danger Index: A Forecastable Metric to Inform Firefighter and Community Wildfire Risk Management. *Fire* 2, 47. doi: 10.3390/fire2030047

Keeley, J. E., Bond, W. J., Bradstock, R. A., Pausas, J. G., and Rundel, P. W. (2011). *Fire in Mediterranean Ecosystems: Ecology, Evolution and Management.*, 1st Edn. Cambridge University Press. doi: 10.1017/CBO9781139033091

Killick, R. (2011). changepoint: Methods for Changepoint Detection. 2.3. doi: 10.32614/CRAN.package.changepoint

Lunt, M. F., Palmer, P. I., Feng, L., Taylor, C. M., Boesch, H., and Parker, R. J. (2019). An increase in methane emissions from tropical Africa between 2010 and 2016 inferred from satellite data. *Atmos. Chem. Phys.* 19, 14721–14740. doi: 10.5194/acp-19-14721-2019

Maasakkers, J. D., Jacob, D. J., Sulprizio, M. P., Scarpelli, T. R., Nesser, H., Sheng, J.-X., et al. (2019). Global distribution of methane emissions, emission trends, and OH concentrations and trends inferred from an inversion of GOSAT satellite data for 2010–2015. *Atmos. Chem. Phys.* 19, 7859–7881. doi: 10.5194/acp-19-7859-2019

Magro, C., Nunes, L., Gonçalves, O., Neng, N., Nogueira, J., Rego, F., et al. (2021). Atmospheric Trends of CO and CH4 from Extreme Wildfires in Portugal Using Sentinel-5P TROPOMI Level-2 Data. *Fire* 4, 25. doi: 10.3390/fire4020025

Miller, J. D., and Thode, A. E. (2007). Quantifying burn severity in a heterogeneous landscape with a relative version of the delta Normalized Burn Ratio (dNBR). *Remote Sensing of Environment* 109, 66–80. doi: 10.1016/j.rse.2006.12.006

Ministerstvo zemědělství (2023). Zpráva o stavu lesa a lesního hospodářství 2022. Available at: www.eagri.cz

Nechita-Banda, N., Krol, M., Van Der Werf, G. R., Kaiser, J. W., Pandey, S., Huijnen, V., et al. (2018). Monitoring emissions from the 2015 Indonesian fires using CO satellite data. *Phil. Trans. R. Soc. B* 373, 20170307. doi: 10.1098/rstb.2017.0307

Patacca, M., Lindner, M., Lucas-Borja, M. E., Cordonnier, T., Fidej, G., Gardiner, B., et al. (2023). Significant increase in natural disturbance impacts on European forests since 1950. *Global Change Biology* 29, 1359–1376. doi: 10.1111/gcb.16531

Ross, A. N., Wooster, M. J., Boesch, H., and Parker, R. (2013). First satellite measurements of carbon dioxide and methane emission ratios in wildfire plumes. *Geophysical Research Letters* 40, 4098–4102. doi: 10.1002/grl.50733

Schneising, O., Buchwitz, M., Reuter, M., Bovensmann, H., Burrows, J. P., Borsdorff, T., et al. (2019). A scientific algorithm to simultaneously retrieve carbon monoxide and methane from TROPOMI onboard Sentinel-5 Precursor. *Atmos. Meas. Tech.* 12, 6771–6802. doi: 10.5194/amt-12-6771-2019

Soverel, N. O., Perrakis, D. D. B., and Coops, N. C. (2010). Estimating burn severity from Landsat dNBR and RdNBR indices across western Canada. *Remote Sensing of Environment* 114, 1896–1909. doi: 10.1016/j.rse.2010.03.013

Urbanski, S. P., Hao, W. M., and Baker, S. (2008). "Chapter 4 Chemical Composition of Wildland Fire Emissions," in *Developments in Environmental Science*, (Elsevier), 79–107. doi: 10.1016/S1474-8177(08)00004-1

Van Der Velde, I. R., Van Der Werf, G. R., Houweling, S., Eskes, H. J., Veefkind, J. P., Borsdorff, T., et al. (2021a). Biomass burning combustion efficiency observed from space using measurements of CO and NO₂ by the TROPOspheric Monitoring Instrument (TROPOMI). *Atmos. Chem. Phys.* 21, 597–616. doi: 10.5194/acp-21-597-2021

Van Der Velde, I. R., Van Der Werf, G. R., Houweling, S., Maasakkers, J. D., Borsdorff, T., Landgraf, J., et al. (2021b). Vast CO2 release from Australian fires in 2019–2020 constrained by satellite. *Nature* 597, 366–369. doi: 10.1038/s41586-021-03712-y

Wan, N., Xiong, X., Kluitenberg, G. J., Hutchinson, J. M. S., Aiken, R., Zhao, H., et al. (2022). Estimation of Biomass Burning Emission of NO_2 and CO from 2019–2020 Australia Fires Based on Satellite Observations. doi: 10.5194/acp-2022-447

Xiao-rui, T., Mcrae, D. J., Li-fu, S., Ming-yu, W., and Hong, L. (2005). Satellite remote-sensing technologies used in forest fire management. *Journal of Forestry Research* 16, 73–78. doi: 10.1007/BF02856861

Yoshimoto, A., Asante, P., Konoshima, M., and Surový, P. (2017). INTEGER PROGRAMMING APPROACH TO CONTROL INVASIVE SPECIES SPREAD BASED ON CELLULAR AUTOMATON MODEL. *Natural Resource Modeling* 30, nrm.12101. doi: 10.1111/nrm.12101

APPENDIX 1

The period examined was:

1) before the fire:

1. '2022-06-03T00:00:01', '2022-06-07T23:59:00', *"before_fire1"*
2. '2022-06-08T00:00:01', '2022-06-12T23:59:00', *"before_fire2"*
3. '2022-06-13T00:00:01', '2022-06-17T23:59:00', *"before_fire3"*
4. '2022-06-18T00:00:01', '2022-06-22T23:59:00', *"before_fire4"*
5. '2022-06-23T00:00:01', '2022-06-27T23:59:00', *"before_fire5"*
6. '2022-06-28T00:00:01', '2022-07-02T23:59:00', *"before_fire6"*
7. '2022-07-03T00:00:01', '2022-07-07T23:59:00' *"before_fire7"*
8. '2022-07-08T00:00:01', '2022-07-12T23:59:00', *"before_fire8"*
9. '2022-07-13T00:00:01', '2022-07-17T23:59:00', *"before_fire9"*
10. '2022-07-18T00:00:01', '2022-07-22T23:59:00', *"before_fire10"*

2) during the fire:

11. '2022-07-23T00:00:01', '2022-07-25T23:59:00', *"fire1"*
12. '2022-07-26T00:00:01', '2022-07-28T23:59:00', *"fire2"*
13. '2022-07-29T00:00:01', '2022-07-31T23:59:00', *"fire3"*
14. '2022-08-01T00:00:01', '2022-08-03T23:59:00', *"fire4"*
15. '2022-08-04T00:00:01', '2022-08-06T23:59:00', *"fire5"*
16. '2022-08-07T00:00:01', '2022-08-09T23:59:00', *"fire6"*
17. '2022-08-10T00:00:01', '2022-08-12T23:59:00', *"fire7"*

3) after the fire:

18. '2022-08-13T00:00:01', '2022-08-17T23:59:00', *"after_fire1"*
19. '2022-08-18T00:00:01', '2022-08-22T23:59:00', *"after_fire2"*
20. '2022-08-23T00:00:01', '2022-08-27T23:59:00', *"after_fire3"*
21. '2022-08-28T00:00:01', '2022-09-01T23:59:00', *"after_fire4"*
22. '2022-09-02T00:00:01', '2022-09-06T23:59:00', *"after_fire5"*
23. '2022-09-07T00:00:01', '2022-09-11T23:59:00', *"after_fire6"*
24. '2022-09-12T00:00:01', '2022-09-16T23:59:00', *"after_fire7"*
25. '2022-09-17T00:00:01', '2022-09-21T23:59:00', *"after_fire8"*
26. '2022-09-22T00:00:01', '2022-09-26T23:59:00', *"after_fire9"*
27. '2022-09-27T00:00:01', '2022-10-01T23:59:00', *"after_fire10"*

5.5. Drone microrelief analysis to predict the presence of naturally regenerated seedlings

Tereza Hüttnerová[1], Robert Muscarella[2], Peter Surový[1]

[1] Faculty of Forestry and Wood Science, Czech University of Life Sciences (CZU Prague), Kamýcká 129,165 21 Prague, Czech Republic

[2] Department of Plant Ecology and Evolution, Evolutionary Biology Center, Uppsala University, Uppsala, Sweden

Front. For. Glob. Change, 11 January 2024, Sec. Forest Management, Volume 6 - 2023 | https://doi.org/10.3389/ffgc.2023.1329675

IF: 2.7 (2023), AIS value: 1.040 (2023)

Author´s contribution: 60 %

Summary of the article

As a result of large-scale natural disturbances, which are increasingly common even in European conditions, more intensive harvesting occurs due to stress, damage, and subsequent death of stands. Deforested areas are at risk of soil erosion, and according to the law, the owner is obliged to ensure restoration. The article focuses on evaluating natural regeneration in clearings after salvage cutting due bark beetle infestation. For each study area and the surrounding forest, a detailed terrain model was obtained from UAV collection, individual variables (topographic wetness index, solar area radiation, fencing, type of soil preparation, and distance to the nearest mature forest edge) were obtained through spatial analysis and 3D models, and subsequently, the influence of the variables on the newly naturally restored elements of the vegetation was verified. The presented methodology is an appropriate solution for assessing the suitability of areas for regeneration and for decision management in the framework of strategic planning for regeneration.

Full article

frontiers | Frontiers in Forests and Global Change

TYPE Original Research
PUBLISHED 11 January 2024
DOI 10.3389/ffgc.2023.1329675

Check for updates

OPEN ACCESS

EDITED BY
Yashwant Singh Rawat,
Federal Technical and Vocational Education and Training Institute (FTVETI), Ethiopia

REVIEWED BY
Maciej Pach,
University of Agriculture in Krakow, Poland
Sergio Espinoza,
Catholic University of the Maule, Chile

*CORRESPONDENCE
Tereza Hüttnerová
huttnerovat@fld.czu.cz

RECEIVED 29 October 2023
ACCEPTED 26 December 2023
PUBLISHED 11 January 2024

CITATION
Hüttnerová T, Muscarella R and Surový P (2024) Drone microrelief analysis to predict the presence of naturally regenerated seedlings.
Front. For. Glob. Change 6:1329675.
doi: 10.3389/ffgc.2023.1329675

COPYRIGHT
© 2024 Hüttnerová, Muscarella and Surový. This is an open-access article distributed under the terms of the Creative Commons Attribution License (CC BY). The use, distribution or reproduction in other forums is permitted, provided the original author(s) and the copyright owner(s) are credited and that the original publication in this journal is cited, in accordance with accepted academic practice. No use, distribution or reproduction is permitted which does not comply with these terms.

Drone microrelief analysis to predict the presence of naturally regenerated seedlings

Tereza Hüttnerová[1]*, Robert Muscarella[2] and Peter Surový[1]

[1]Faculty of Forestry and Wood Sciences, Czech University of Life Sciences Prague, Prague, Czechia, [2]Department of Plant Ecology and Evolution, Evolutionary Biology Center, Uppsala University, Uppsala, Sweden

Three-dimensional (3D) mapping and unmanned aerial vehicles (UAVs) are essential components of the future development of forestry technology. Regeneration of forest stands must be ensured according to the law in the required quality and species composition. Forest management focuses on the optimization of economic costs and quality-assured seedlings. Predicting the suitability of the plots' environment for natural forest regeneration can contribute to better strategic planning and save time and money by reducing manual work. Although the savings may be considered negligible on small forested plots, they are significant for large cleared areas, such as those harvested after large beetle infestations or strong windstorms, which are increasingly common in European forests. We present a methodology based on spatial analysis and 3D mapping to study the microrelief and surrounding of recently cleared areas. We collected data on four plots in the spring and autumn of a single year after the harvest of four Norway spruce [*Picea abies* (L.) Karst.] stands near Radlice, Czechia using a multirotor Phantom 4 Pro UAV with a red, green, blue (RGB) camera. We used RGB imagery to compute microrelief data at a very high spatial resolution and the surrounding forest stands after harvesting. We used the microrelief data to estimate the amount of water accumulation and incoming solar radiation across the sites. Based on presence data of newly-established seedlings, we used linear mixed effects models to create a suitability map for each site. Model variables included topographic wetness index, solar area radiation, fencing, type of soil preparation, and distance to the nearest mature forest edge. The topographic wetness index and fencing had strong positive influence on seedling establishment, while solar radiation had a negative influence. Our proposed methodology could be used to predict spontaneous regeneration on cleared harvest areas, or it can estimate how much area is suitable for regeneration, which can lead to important investment decisions.

KEYWORDS

unmanned aerial vehicle, clearing cut, 3D maps, spatial analysis, natural regeneration, forest monitoring, soil moisture

1 Introduction

Forests are among the most valuable terrestrial ecosystems, but they are also highly susceptible to potential threats and damage. For example, the long lifespan of trees means that they are unable to quickly adapt to damaging human practices and natural disturbances related to climate change. It is predicted that Europe's forests will experience an increase in the

occurrence of storms, fires, and insect pests (Seidl et al., 2014; European Commission and Joint Research Centre, 2020; Huo et al., 2021). The primary consequences may include the reduced resistance of forest ecosystems and associated communities and processes, and also a depleted and less predictable wood supply. Predicting natural responses to these changes and responding in a timely manner will be critical to help sustain the many benefits provided by forest ecosystems. Therefore, it is essential to restore quality forest habitats in a timely and efficient manner. To maximize regeneration efforts, it is advisable to minimize seedling death or failure during the early establishment phases of reforestation. Typically, manual treatment of entire areas is conducted to re-establish trees, but this is physical, time-consuming, and financially costly.

The forest regeneration plan must follow the binding decrees and reflect the prescribed standards. The minimum number of trees must be preserved in individual areas, which Decree No. 456/2021 Coll determines. In the framework of regeneration, forest management is guided by a target management set of stands, in which are determined by different forest stands with similar or the same climatic and soil conditions (Sequens, 2007). Natural regeneration of forest stands can be an effective, cost-efficient means to reforest disturbed stands, but it is highly variable and dependent on several factors, including seed availability, browsing pressure, and other site-specific factors, such as soil type, aspect, and slope, which affect microsite quality (Hanssen, 2003; Březina and Dobrovolný, 2011; Çalışkan et al., 2014; Vacek et al., 2014). The identification of potential areas of natural regeneration through environmental suitability analysis can improve the efficiency of site preparation and afforestation needs, and reduce associated costs.

The cost effectiveness of unmanned aerial vehicles (UAVs) for mapping forest stand characteristics allows for an innovative approach to quickly evaluate relatively small areas (100 s of sq. km) with high spatial resolution. Multirotor UAVs can carry various types of sensors weighing several kilograms, and they have excellent maneuverability, including the benefit of a vertical take-off and landing, which is important in a forest environment. A limiting factor with the multirotor UAVs can be that increased sensor weights reduce operating time, thus leading to a smaller mapping area.

The light detection and ranging (LiDAR) sensor can accurately map vertical forest canopy structure, including the tree canopy, the ground below the trees, and the space between canopy and ground (Brede et al., 2017; Wieser et al., 2017). A hyperspectral camera is used for species classification (Hycza et al., 2018; Tusa et al., 2019). Multispectral cameras can help evaluate the health status of forest stands through vegetation indices (Klouček et al., 2019; Junttila et al., 2022). A financially inexpensive option is cameras with RGB channels that can monitor the area in the visible spectrum. Using the structure-from-motion (SfM) metric, a very accurate 3D terrain model can be created. Information on topographic variables (digital elevation model, slope, and aspect) and other metrics, such as solar radiation and topographic wetness index, can be obtained from high resolution 3D models, all of which can be compiled to provide valuable information for species distribution models (SDMs).

Species distribution models evaluate the relationship between environmental variables and presence data on occurrence (or occurrence and absence data; Franklin and Miller, 2009; Franklin, 2010). Algorithms for SDMs are diverse and depend on the types of occurrence data, the range and quality of environmental variables, and study objectives. Algorithms are based on the extrapolation of values from environment variables in the places where the species occurs. These models have been used for predicting species distributions and richness, evaluating the correlation of environmental variables and occurrence data, and the dispersal of species to other areas (Wollan et al., 2008; Elith et al., 2011; Falk and Mellert, 2011). To predict the occurrence of a species or determine the suitability of a habitat for any given species, it is necessary to know terrain variables and predictors that affect growth, which are primarily influenced by water and solar radiation.

Solar radiation has a significant impact on site water balance through heating water, soil medium, evapotranspiration, melting snow, and ice, and, thus, it also has a strong influence on the establishment and presence of vegetation (Guisan and Zimmermann, 2000; Meentemeyer et al., 2001; Brang et al., 2005; Lebourgeois, 2007; Piedallu and Gégout, 2007). Solar radiation can be measured using ground meteorological stations and then the data can be interpolated for the given data area (Thornton et al., 2000; Piedallu and Gégout, 2007), although the limited number of point measurements cannot sufficiently characterize the terrain variability, and there is a significant distortion of solar radiation maps (Fu and Rich, 2002). Geographic information system (GIS) tools can more accurately map incident solar radiation because they work with the detailed morphology of the terrain, and they can also include the degree of cloud cover in the calculation (Zhu, 2016).

We hypothesized that features of the terrain relief, soil treatment, and fencing would influence the presence of naturally occurring seedlings. We assumed that areas with appropriate levels of soil moisture and sunlight would increase the probability of occurrence, and that fencing would have a positive effect on survival due to the protection of vegetation from browsing by deer. However, areas of excessive moisture can reduce the number of seedlings. The main objectives of this research were (1) to create terrain models based on the Structure from motion metric and to perform raster analyses of water accumulation and solar potential, and (2) to evaluate which factors influence the presence of naturally regenerated seedlings based on data obtained from a UAV. We assessed the correlation between vegetation establishment and microsite conditions to identify areas that would require limited intervention (e.g., no site preparation) to reforest.

We asked the following specific research questions:

1. Can a drone with an RGB camera provide accurate enough micro-relief information based on Structure from Motion metrics?
2. Is it possible to evaluate the importance of predictors for evaluating naturally regenerated trees based on a generalized linear mixed-effects model?

2 Materials and methods

2.1 Study area

The study area, Kamenný vrch (456 m above sea level), is located near Radlice, Kolín district, Czech Republic (Figure 1); the forested area is used for forestry research and education. Four plots with a size of 0.74–1.32 ha were selected for treatment and their overstories, dominated by Norway spruce [*Picea abies* (L.) Karst.], were felled in

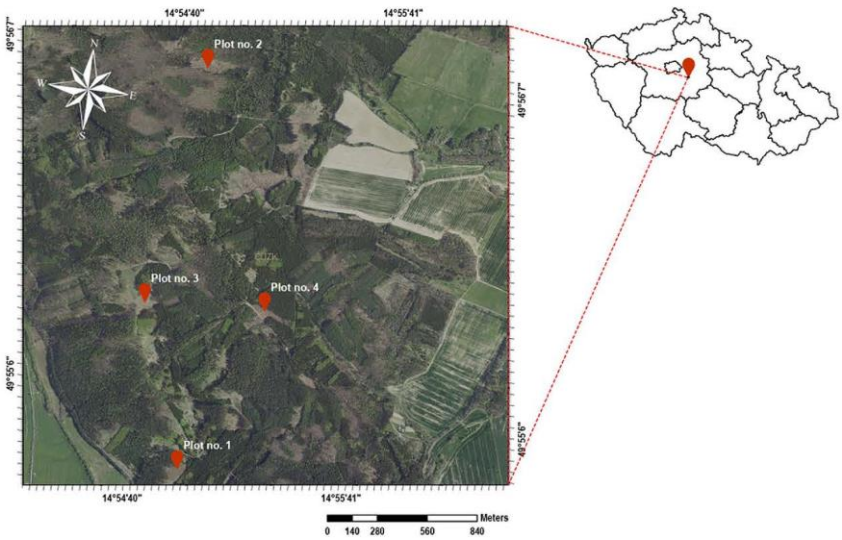

FIGURE 1
Study area near Radlice, Kolín district, Czech Republic displaying felled plots were left to regenerate naturally; Data source: Czech Office for Surveying, Mapping, and Cadastre.

early 2021. Natural regeneration of the forest without planting was monitored in these plots (Figure 2). Plots no. 1 and no. 4 have a target management set of stands of 43—Acid habitats of medium positions, and plots no. 2 and no. 3 have a target management set of stands of 45—Nutritional habitats of medium positions.

Based on the target management set of stands, the planned restoration for plot no. 1 was as follows: Norway spruce 50%, European beech [*Fagus sylvatica* (L.)] 35%, European larch [*Larix decidua* (Mill.)] 10%, and largeleaf linden [*Tilia platyphyllos* (Scop.)] 5%; for plot no. 2: Norway spruce 65%, European beech 35%; for plot no. 3: Norway spruce 65%, European beech 35%, for plot no. 4: Norway spruce 65% and European beech 35%. For all plots, it is recommended to have a minimum of 35% improving and stabilizing species.

The species representation was determined based on experimental circular plots, where the percentage of individual species was determined. In plots no. 1 and no. 4 (CHS 43), a slightly predominant species composition of Norway spruce (40%) was recorded, followed by European larch 38%, European white birch [*Betula pendula* (Roth)] 4%, European aspen [*Populus tremula* (L.)] 2% and others 15%: Scots pine [*Pinus sylvestris* (L.)], European beech, English oak [*Quercus robur* (L.)], durmast oak [*Quercus petraea* (Mattuschka) Liebl.], littleleaf linden [*Tilia cordata* (Mill.)], largeleaf linden, European hornbeam [*Carpinus betulus* (L.)], goat willow [*Salix caprea* (L.)]. Plots no. 2 and no. 3 (CHS 45) were dominated by Norway spruce 74%, European aspen 2%, European larch 2%, and others 23% Scots pine, European beech, English oak, durmast oak, littleleaf linden, largeleaf linden, European hornbeam, and goat willow. Most of the naturally regenerated trees were 1-year-old, with the exception of soliters (up to 1%) that remained after harvesting.

The most regenerated tree species in the plots is Norway spruce, a intermediately shade-intolerant species when young but becomes more shade-tolerant as it matures and it requires regular moisture, especially during its early years of growth (Lebourgeois et al., 2010; Lévesque et al., 2013; Yang et al., 2020). Adequate water availability is crucial for its establishment and initial development; later, it has a higher tolerance to summer drought stress (Battipaglia et al., 2009). Norway spruce competes well with other tree species in mixed forests but can also form pure stands under suitable conditions. It reproduces by seeds, which are typically dispersed by wind (Caudullo et al., 2016).

In plots 1 and 4, European larch is also represented on a larger scale, which is relatively shade-intolerant (Ellenberg, 2009; Fellner et al., 2016). It prefers full sunlight for optimal growth and development. European larch requires adequate moisture, it does well in areas with moderate to high precipitation but can also tolerate periods of drought once established. It can grow in mixed forests alongside other tree species or form pure stands. It is often found in association with other coniferous and broadleaf trees in mid-to-high altitudes (Lévesque et al., 2013). European larch reproduces by seeds, with cones that disperse the seeds (Da Ronch et al., 2016).

Detailed characterization of research plots is written in Table 1.

The mean annual temperature of the study area in 2021 was 8.7°C; the long-term average temperatures in the Central Bohemian Region and Prague is 9°C (Czech Hydrometeorological Institute, 2022). The maximum temperature, 19°C, was recorded in July, and the minimum

FIGURE 2
Individual plots shown after felling in 2021, harvesting took place at the end of 2020; data source: Czech Office for Surveying, Mapping, and Cadastre.

TABLE 1 Descriptive characteristics of individual plots (ÚHÚL, 2022).

Research area	Location	Mean elevation (m)	Area size	Species composition before felling	Type of soil (Půdní mapa, 2022)
Plot no. 1	49.9139 N, 14.9141 E	350	0.92 ha	Majority spruce, basic pine	Pseudoglue
Plot no. 2	49.9341 N, 14.9123 E	425	1.32 ha	Dominant spruce, admixture of larch and oak/elm/linden	Ilimerized
Plot no. 3	49.9219 N, 14.9095 E	440	0.92 ha	Pure spruce	Brown acidic soil
Plot no. 4	49.9221 N, 14.9193 E	430	0.74 ha	Pure spruce	Ilimerized

temperature, −0.3°C, was recorded in January and February. The mean annual precipitation in 2021 was 627 mm, whereas the long-term average in the region is 583 mm (Czech Hydrometeorological Institute, 2022).

The forest stands were harvested due to natural disturbance (bark beetle infestation) at the beginning of 2021; in the spring of 2021, the first data collection took place with a UAV to evaluate the state of the microrelief, determine the topographic wetness index and solar radiation. At the end of 2021, a second collection was carried out, during which the regenerated seedlings were evaluated, and the remaining predictors determined. After harvesting, all plots were subdivided for alternative treatments (refer to Figure 3). The plot was subdivided into halves by a narrow strip (D; 2 m) that was neither fenced nor treated in any manner. One half of the plot was fenced (E, F, G), while the other half (A, B, C) was left unfenced to evaluate the effects of ungulate browsing. For areas A and E, branches were cleared away and the soil was actively prepared with slow-moving single-disk soil cutters. For areas B and F, only larger branches were cleared with no soil treatments. For areas C and G, the soil was prepared with a plow. Plow (mostly plowing plate with 12 teeth) is used in interaction with the agricultural tractor and there is the possibility of adjusting the tilting of the plate from 20 to 45°. Slow-moving single-disk soil cutters are intended for strip soil preparation for reforestation with strong disturbance and calamity areas.

2.2 Data acquisition

To acquire natural regeneration data for each plot, we used a multirotor DJI Phantom 4 Pro (©2022 SZ DJI Technology Co., Ltd., Shenzhen, China) with an integrated 20 megapixel RGB camera with the following parameters: lens: FOV 84° 8.8/24 mm (35 mm format equivalent) f/2.8–f/11 auto focus at 1 m—∞, physical pixel size of 4,096 µm × 2,160 µm, focal length of 8.8/24 mm, and 1″ CMOS.

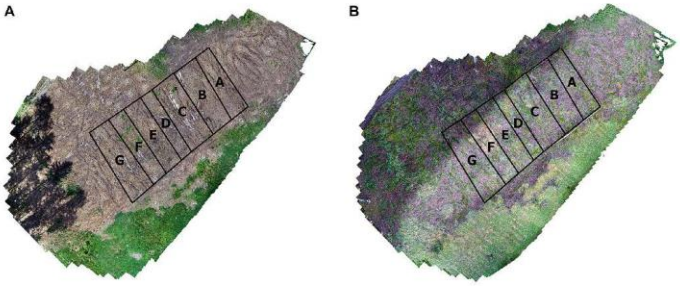

FIGURE 3
Schematic of the post-harvesting preparation of soil, left image spring 2021 **(A)**, right image spring 2022 **(B)**.

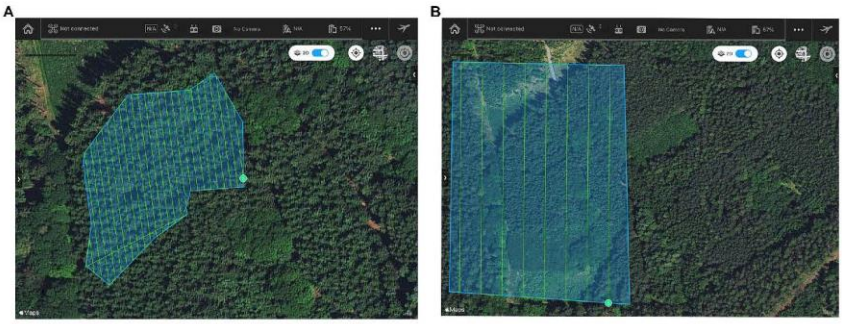

FIGURE 4
Flight mission in plot no. 3 at a height of 15 m **(A)** and a height of 110 m **(B)**.

The proposed method requires very high spatial resolution to evaluate the microrelief and natural regeneration of forest stands. We used a multirotor UAV for data collection because of its high maneuverability, although flight time was limited to about 30 min (Pajares, 2015; Burgués and Marco, 2020). Data were acquired in 2021, once in the spring and again during autumn. For each plot, two flights were conducted; one at 15 m above the ground using hovering and capture mode to collect data on the microrelief, and a second flight at 110 m above the ground for capturing a broader of the plot and the surrounding areas.

Flight missions were planned in the application DJI Ground Station Pro (©2022 SZ DJI Technology Co., Ltd.: Shenzhen, China) with the following parameters:

1. Low flight: Front Overlap Ratio: 85%, Side Overlap Ratio: 85%, Flight Speed: 5.0 m/s, Height above the ground: 15 m, Accuracy: 0.4 cm/pix, and Capture Mode: Hover and Capture at a Point (Figure 4A).
2. High flight: Front Overlap Ratio: 85%, Side Overlap Ratio: 85%, Flight Speed: 8.8 m/s, Height above the ground: 110 m, Accuracy: 0.4 cm/pix, and Capture Mode: Capture without hovering (Figure 4B).

2.3 Data processing and statistical analyses

The data were initially processed using structure-from-motion (SfM) in the Agisoft Metashape software (©2022 Agisoft, LLC, St. Petersburg, Russia) to create a point cloud, a dense cloud, 3D maps, and a digital surface model (DSM). Properties was set to alignment: medium, medium-quality dense cloud. Accuracy of align photos was medium, key points 40,000, tie points 4,000 with generic preselection, reference preselection, and reset current alignment chosen. Dense Cloud was built in medium quality with Mild Depth Filtering. The DSM was created in coordinate system WGS 84 (EPSG: 4326), and an orthomosaic was created from the DSM surface using the blending mode Mosaic. We then manually specified the position of the images using markers (8 on each plot) uniformly distributed throughout the area to increase the precision of the models to the order of centimeters (Figure 5).

FIGURE 5
Manually-created marker points with which we refined the positions of the images: left plate is spring 2021 **(A)**, right plate is spring 2022 **(B)**.

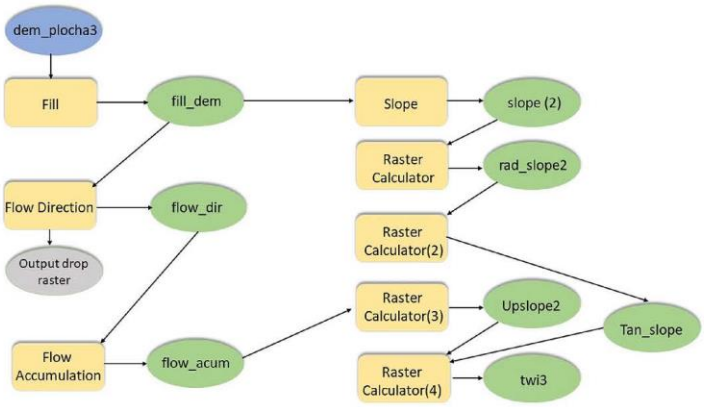

FIGURE 6
Schema for calculation of the topographic wetness index.

We then analyzed the data using the spatial and hydrology analytical tools in ArcGIS Pro 2.8.3 (©2022 ESRI Inc., Redlands, CA, United States). Water accumulation was determined at the level of microrelief, as represented by the calculated topographic wetness index (TWI; Figure 6).

The TWI metric was calculated using a multistep process based on a combination of the estimated slope angle and the raster map to evaluate upslope areas for calculating flow accumulation. Using ArcGIS Pro, the digital terrain model was initially modified with the Fill function. Subsequently, a raster of the water flow direction in the given area was calculated using Flow Direction. The calculated Flow Accumulation raster represented the number of cells through which water flows. The Slope was then determined from the digital model of the terrain with degrees were chosen as the unit of measure. TThe Slope was then expressed in radians by the following formula (Equation 1) in the Raster Calculator:

$$\text{Slope}_{\text{rad}} = \left(\text{Slope raster in degrees}^{*}\ 1.570796\right) / 90 \quad (1)$$

The slope tangent was then calculated by Equation 2:

$$\text{Slope}_{\text{tan}} = \text{Con}\left(\begin{matrix}\text{Slope raster in radians} > 0, \\ \tan\left(\text{Rad\_Slope\_1}\right), 0.01\end{matrix}\right) \quad (2)$$

Raster flow accumulation was rescaled according to the resolution of the raster and to avoid zeros values (Equation 3):

$$\begin{matrix}\text{Raster flow} \\ \text{accumulation}_{\text{scaled}}\end{matrix} = \left(\begin{matrix}\left(\text{Raster of Flow Accumulatio} + 1\right)^{*} \\ \text{spatial resolution of raster}\end{matrix}\right) \quad (3)$$

In the final step, TWI was calculated using the following formula (Equation 4) in the raster calculator:

$$\text{TWI} = \ln\left(\text{upslope contributing area} / \tan\left(\text{slope angle}\right)\right) \quad (4)$$

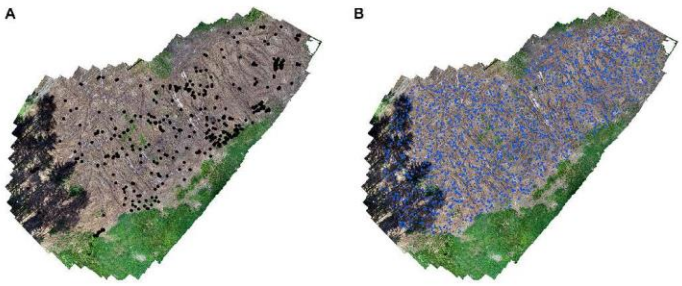

FIGURE 7
On left image **(A)** presence data and on right image **(B)** absence in plot no. 1.

TWI values typically range from 3 to 30. To avoid undefined areas due to zero values for flow accumulation or zero slope, Equation 5 was used:

$$\mathrm{TWI} = \mathrm{if}\left(\mathrm{Slope} > 0, \ln\left(\left(\left(\mathrm{Flow\ accumulation} + 1\right)^{*}\ \mathrm{pixel\ size}^{2}\right)/\left(\tan\left(\mathrm{PI}^{*}\mathrm{slope\ in\ degrees}/180\right)\right)\right), \ln\left(\left(\left(\mathrm{Flow\ accumulation} + 1\right)^{*}\ \mathrm{pixel\ size}^{2}\right)/\left(\text{“Small no”} + \tan\left(\mathrm{slope}/57.29\right)\right)\right)\right) \quad (5)$$

The resultant value (0.00565) corresponds to a plane and slope close to zero.

Solar radiation was calculated using the Area Solar Radiation function from the Spatial Analyst tool. The raster of potential exposure was used to determine suitability for various light-demanding or shade-bearing species. Plot No. 1 is on a gentle slope with southwest exposure, Plot No. 2 is on a level to steep slope with west exposure, Plot No. 3 is on a gentle to steep slope with southeast exposure, and Plot No. 4 is on a gentle slope with southeast exposure.

Presence data of naturally-regenerated seedlings were determined manually based on orthomosaics. Automatic classification was not an effective approach in this case because the presence data (i.e., number of seedlings) was rather sparse and insufficient to create training sets for the classification model. We created a vector polygon layer delineating the various treatment areas based on accurate orthomosaics. Furthermore, a vector point layer was created in which records of the presence of recovered seedlings were stored. We generated absence points (2,000 per plot) using the randomPoints function of the dismo (Hijmans et al., 2023) package in R Studio software (Figure 7).

We then used the extract function (raster package, software R Studio) to obtain for each presence-absence point a value from the topographic wetness index raster and from the solar radiance raster. Based on the spatial location of each point (function Extract Values to Points, ArcGIS Pro), we were able to assign fencing (Fence; binary) and soil treatments (Soil; single-disk, none, plow) and the distance to the nearest forest edge (Dist_m; linear measure in meters).

We used the R Studio and ArcGIS Pro software's for all data analysis. We fit a generalized linear mixed-effects model with binomial errors and a logit link function using the "glmer" function from the lme4 package (Bates et al., 2023). We included random intercepts for each of the four study plots to account for predictors that may have different ranges of values across different plots (Zuur et al., 2009; Harrison et al., 2018).

We used the following model formula (Equation 6):

$$\mathrm{Y} \sim \mathrm{Dist\_m} + \mathrm{Fence} + \mathrm{Soil} + \mathrm{scale\_twi} + \mathrm{scale\_solar} + \mathrm{scale\_twi2} + \left(1|\mathrm{Plot}\right) \quad (6)$$

The presence/absence of seedlings, Y, is a function of the relative effects of the various predictors. In addition to the treatment factors (Dist_m, Fence, Soil), we also included water accumulation and potential sunlight exposure; normalizing these values transforms their means to 0 and all values within 1 SD of the mean. Raster values of potential water accumulation (TWI) were represented in the model in their scaled forms of TWI (scale_twi) and it squared value (TWI^2; scale_twi2). Scaled raster values of potential sunlight exposure (scale_solar) for all plots were also included. Fixed effects in this model are Dist_m, Fence, Soil, scale_twi, scale_solar, and scale_twi2 and the random effect in this model is (1|Plot).

3 Results

We determined that a UAV equipped with an RGB camera can acquire very high-resolution terrain information, which can be incorporated into a species distribution model to determine the suitability of the local environment with a higher probability of survival for various tree species. The most important predictors in our model included a topographic wetness index, solar radiation, and fencing. Soil treatments and distance to the forest edges were less important to the establishment of naturally-regenerated seedlings. The GLMM was based on 9,508 observations of seedlings across the four plots. The strongest effects variables from the model were fencing, topographic wetness index, and solar radiation. The estimates of the model fixed effects are included in Table 2.

The scaled residuals indicate how well the model fit the data. The values ranged from −0.9662 to 3.9978. Residuals close to zero suggest

TABLE 2 Output data from the glmer model used for data evaluation.

Predictor	Estimate	Std. Error	z-value	Pr(>|z|)
(Intercept)	−1.791183	0.272808	−6.566	$5.18e^{-11}$***
Dist_m	−0.001746	0.004534	−0.385	0.700217
Fence	0.983035	0.083654	11.751	$< 2e^{-16}$***
Soil2	0.017208	0.097514	0.176	0.859931
Soil3	−0.263379	0.116543	−2.260	0.023826*
scale_twi	0.319827	0.133707	2.392	0.016757*
scale_solar	−0.465018	0.106108	−4.382	$1.17e^{-05}$***
scale_twi2	0.489607	0.133558	3.666	0.000246***

The number of stars represents the significance of the correlation, and more stars mean a more significant correlation.

a good fit, while extreme values may indicate model inadequacy or influential outliers. The estimated variance of the random intercept for Plot was 0.2524, and the corresponding standard deviation was 0.5024.

The presence of fencing had a positive effect on the probability of the occurrence of naturally-regenerated seedlings with a coefficient of 0.983, as it protects against unwanted browsing from forest animals or driving by heavy machinery. Fencing serves as a barrier against external degrading factors. The presence of water is directly an essential component for the growth of all vegetation, the topographic wetness index (0.489) had a positive impact on the probability of occurrence of seedlings. So, the more water the microrelief captured, the better it was for regenerated seedlings; no places with excess water were found in the research plots, which negatively affected the growth. In our research, soil treatment after felling had no significant effect, specifically, Soil2 (type no. 2; larger branches were cleared and no soil treatment) only marginally increased the odds of occurrence (0.017), and Soil3 (type no. 3; larger branches were cleared and treatment by a plow) had a negative impact on the seedling establishment (−0.263).

The size of the deforested areas was small (< 2 ha), but even so, we verified the influence of the edge effect and the ability of seedlings to spread, the distance of the point from the edge of the forest stand had a slightly negative impact (−0.002). Sunlight had a strong negative effect on the presence of regenerated seedlings; this result will be justified by the excessive impact of light radiation on the plots, and for the seedlings were more suited to locations in the shade (−0.465). The most statistically significant predictors were fencing, solar radiation, and topographic wetness index. The graphically represented predicted probabilities of individual variables are presented in Appendix 1.

Figure 8 presents a prediction map for each of the four plot areas. Points with higher values have a higher predicted probability of the presence of seedlings at that location. Furthermore, the model suggests a higher degree of confidence that the location is more suitable for the presence of seedlings. In contrast, points with lower values have a lower predicted probability of the presence of seedlings, and the model has less confidence that seedlings would be present at that location. Prediction maps showed that the most suitable areas/areas with higher probability of survival were inside the fence and also closer to the edge of the study area where shading by mature surrounding trees and lower levels of solar radiation occurred, solar was noted as a significant predictor of the model. Figure shows all investigated points of presence-absence of naturally regenerated trees, each point on the map identifying the suitability of the location. It can be seen from the individual sub-maps that the more suitable locations are located inside the fences (points with a higher probability of survival are shown in yellow; these areas have a rectangular character that reflects the areas built by the fences). Solar radiation and topographic wetness index cannot be visually derived well from raster data because these input raster variables contain high spatial resolution pixel information.

4 Discussion

Conducting data collection at two different times of the year, spring and autumn, enabled us to monitor vegetation development in deforested areas. Our results suggest the practical applicability of this approach for further use. Using the data collection and analysis as outlined in this work, it is possible to accurately identify areas suitable for regeneration. This approach can be particularly helpful for managers across large areas that have experienced intensive disturbances. This methodology could be used as an important basis for foresters when deciding on a restoration plan for several reasons. First, it is possible to predict how sufficient natural regeneration will be on a given site, thus avoiding unnecessary economic costs of artificial planting (seed, human capacity) on areas where it is not needed. If, based on the analysis, it is found that natural regeneration will not be sufficient and artificial regeneration is needed in some places, it would be advisable to again follow this methodology and direct artificial planting to places where water will accumulate. It would be appropriate to follow up this study with more extended monitoring and to evaluate the regeneration over a longer time horizon. In the future, it would be appreciated to focus on automatically detecting regenerated trees, including determining the height of individual trees and deriving their volume using Structure from Motion metrics.

4.1 Protection of fencing from browsing

The negative effects of browsing by deer on seedlings has been demonstrated in several studies (Castleberry et al., 2000; Rooney, 2009), and fencing has proven to have a positive effect on tree seedling survival and growth (Vercauteren et al., 2006; Vacek et al., 2014). However, the effects of fencing are not consistent across all settings, and positive changes may only become apparent over longer time horizons (Bernard et al., 2017).

Our results show that fencing had a positive effect on regenerated seedlings. However, a longer period of observation would be appropriate to confirm this statement. In some cases, deer populations reduce the effects of one species and, conversely, they influence the success of other species; for example, Bernard et al. (2017) observed the decline of silver

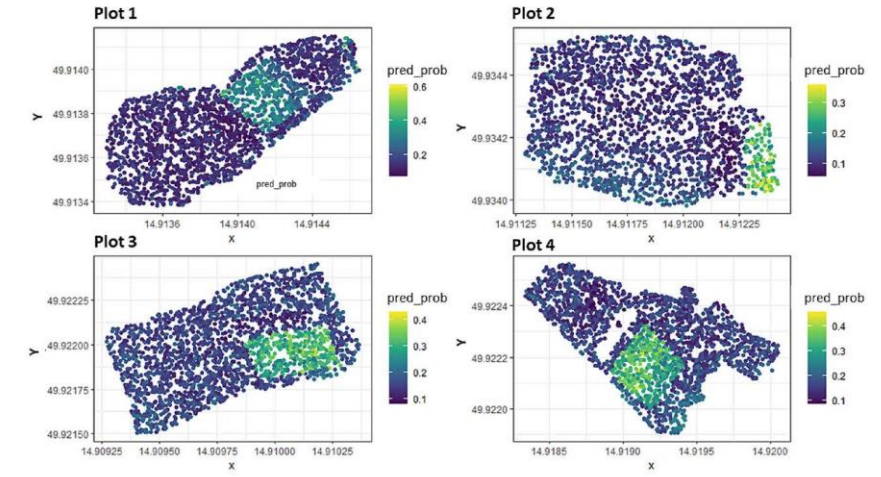

FIGURE 8
Prediction maps of the probability of occurrence for plots.

fir (*Abies alba* Mill.) and, conversely, the increase of Norway spruce [*Picea abies* (L.) Karst.] was recorded. In a study by Vacek et al. (2014), they studied the natural regeneration of a mixed-species forest, including fir (*Abies*), maple (*Acer*), hornbeam (*Carpinus betulus* L.), rowan (*Sorbus*), beech (*Fagus sylvatica* L.), and Norway spruce, on plots with and without fencing; areas with fencing were found to have sufficient natural regeneration, but in areas with no fencing, they observed significant deaths or damage to seedlings, with the most significant damage to *Abies* and *Acer* species.

A long-term experiment by Rooney (2009) followed the effects of fencing for a 16-year period, and they observed 83% relative coverage of grass and sedge species (*Poaceae* and *Cyperaceae* spp.) in areas without fencing; in contrast, areas with fencing had relative coverage of the same species at less than 10%. According to Parker et al. (2020), the density of seedlings was not affected in the first 10 years of their study, but the height of the seedlings was reduced, and the horizontal and vertical structure of the forest was changed due to the effects of the browsing. Parker et al. (2020) recorded a higher coverage of forbs, ferns, huckleberry, and blueberry in unfenced areas.

4.2 Solar radiation

Our results suggested that sunlight exposure had a negative effect on the establishment of seedlings; areas with high exposure to sunlight do not appear to be suitable habitats for restoration. In a study by Strand et al. (2006), they investigated the influence of sunlight and the competition between pine (*Pinus*) trees. No correlation was found between the height of the trees and the amount of light, but a negative correlation was recorded between tree height and its nearest shelter tree. The soil was sandy with low nitrogen content. Therefore, it will be the rationale of results for the competitive struggle of the roots for minerals. Reduced solar radiation (shade/semi-shade) minimizes moisture loss from the soil and thus may influence competing vegetation.

Promis et al. (2010) investigated the growth of *Nothofagus betuloides* (Mirb.) Oerst. seedlings in small-scale deforested areas under different intensities of solar radiation, and they found that shading by mature vegetation did not affect seedling growth compared to seedlings grown under open conditions. The seedlings were tolerant of long-term shading and thus they could be sustainably managed in the southern Chilean old-growth *Nothofagus* forests using a selective harvesting system. However, in Patagonian forests, Rago et al. (2021) demonstrated the negative, linear relationship between diffuse radiation and forest canopy cover and basal area; some seedling groups exhibited a significant response to the amount of diffuse radiation, thus pine plantations affected the vegetation in the understories.

In the study (Örlander, 1993) increased mortality of 2-year-old cuttings of Norway spruce was demonstrated at high solar irradiation of surfaces in interaction with low temperatures below the freezing point; half-shade habitats appear to be the most suitable for restoration. On the contrary, a higher density of oak seedlings (*Quercus petraea* [Mattuschka] Liebl.) was correlated with higher solar radiation (Kuehne et al., 2020). The ideal solar conditions for the natural regeneration of oak have not been unequivocally researched and therefore depend on several other factors—soil pH, presence of iron in the soil, basal area, and species composition of the overstory (Březina and Dobrovolný, 2011; Annighöfer et al., 2015; Kuehne et al., 2020).

4.3 Soil moisture

In studying surface moisture and understanding its distribution, it is necessary to explore various explanatory variables, collect relevant data, and determine the influence of the most important factors. The

intensity and extent of dry areas have increased over the past few decades (McCarthy and Intergovernmental Panel on Climate Change, 2001; Dai et al., 2004; Amani et al., 2017). For sufficient soil moisture, precipitation is the main factor (Tromp-van Meerveld and McDonnell, 2006; Molina-Moral et al., 2022), however, microrelief across sites and amount of vegetation on the sites also have a large impact on soil moisture. Soil moisture can be used as a direct indicator to determine the degree of soil drying, or it can be predicted using indirect indicators. Our study focused on the analysis of microrelief, which was used to create a topographic wetness index in a GIS environment; the index allows users to identify places with a higher probability of water accumulation based on the relief of the terrain.

In a study by Amani et al. (2017), they used a new indicator to assess the landscape, namely the Temperature-Vegetation-Soil Moisture Dryness Index; which combines the values of land surface temperature, perpendicular vegetation index and soil moisture, this index correlated very well with the values measured in the field. The issue of drought is a complex problem and the use of indices combining several critical input factors will be desirable for its understanding and prediction.

4.4 Preparation of soil

In our research, the mechanical soil preparation treatments did not significantly improve the establishment of tree seedlings. More pronounced differences could be observed in the longer term with the increasing number of weeds that could compete more with seedlings. Mechanical preparation can be useful to remove weeds and provide sufficient space for seedlings to grow, but intensive preparation can reduce the quality of the soil and deteriorate its properties for seedling growth. This predictor was insignificant, so we do not elaborate on the discussion further.

4.5 Distance to the edge

The distance of the seedling to the edge may have potentially improved seedling establishment near mature forest edges. In our study, this predictor has a low impact on the presence of seedlings, perhaps because of the relatively small size of the areas (< 2 ha), which would suggest that the dispersal of the seeds from the surrounding mature trees was sufficient. Seed dispersal is limited to a maximal distance of one or two times the height of the mature forest stands of Norway spruces (Hanssen, 2003).

5 Conclusion

In this study, we focused on evaluating the presence of seedlings. Based on the research questions, we find out that a passive camera with R, G, and B spectral resolution can provide terrain models in a very high spatial resolution if the data collection is taken at a low height level and with the Hover and Capture Mode. Using GIS analyses and a species distribution model, seeding areas were identified as the most significant predictors: fencing, topographic wetness index, and solar radiation. Fencing and a higher probability of water accumulation positively influenced the presence of seedlings, while solar radiation had a negative effect on the establishment of new seedlings. Given the dynamic changes many ecosystems are experiencing related to changing climates, forest managers will need efficient and effective tools to address the demand for reforestation and restoration, and our proposed methodology offers a means to quickly and efficiently identify areas favorable for tree seedling establishment.

The presented methodology offers a quick and efficient assessment of natural regeneration in deforested areas; this prediction could serve as a basis for determining the rate of natural regeneration and for reducing the economic intensity of artificial afforestation.

Data availability statement

The raw data supporting the conclusions of this article will be made available by the authors, without undue reservation.

Author contributions

TH: Data curation, Funding acquisition, Investigation, Methodology, Project administration, Writing – original draft, Formal Analysis, Resources, Software, Visualization. RM: Conceptualization, Software, Writing – review & editing. PS: Conceptualization, Supervision, Writing – review & editing, Methodology.

Funding

The author(s) declare financial support was received for the research, authorship, and/or publication of this article. This research was funded by Czech University of Life Sciences, Faculty of Forestry and Wood Sciences IGA/A_21_18 and by "Ministry of Agriculture of the Czech Republic, grant number QK21010435."

Conflict of interest

The authors declare that the research was conducted in the absence of any commercial or financial relationships that could be construed as a potential conflict of interest.

Publisher's note

All claims expressed in this article are solely those of the authors and do not necessarily represent those of their affiliated organizations, or those of the publisher, the editors and the reviewers. Any product that may be evaluated in this article, or claim that may be made by its manufacturer, is not guaranteed or endorsed by the publisher.

Supplementary material

The Supplementary material for this article can be found online at: https://www.frontiersin.org/articles/10.3389/ffgc.2023.1329675/full#supplementary-material

References

Amani, M., Salehi, B., Mahdavi, S., Masjedi, A., and Dehnavi, S. (2017). Temperature-vegetation-soil moisture dryness index (TVMDI). *Remote Sens. Environ.* 197, 1–14. doi: 10.1016/j.rse.2017.05.026

Annighöfer, P., Beckschäfer, P., Vor, T., and Ammer, C. (2015). Regeneration patterns of European oak species (*Quercus petraea* (Matt.) Liebl., *Quercus robur* L.) in dependence of environment and neighborhood. *PLoS One* 10:e0134935. doi: 10.1371/journal.pone.0134935

Bates, D., Maechler, M., Bolker, B., Walker, S., Christensen, R. H. B., Singmann, H, et al. (2023). lme4: Linear mixed-effects models using "Eigen" and S4. Available at: https://cran.r-project.org/web/packages/lme4/index.html (Accessed October 21, 2023).

Battipaglia, G., Saurer, M., Cherubini, P., Siegwolf, R. T. W., and Cotrufo, M. F. (2009). Tree rings indicate different drought resistance of a native (*Abies alba* mill.) and a nonnative (*Picea abies* (L.) karst.) species co-occurring at a dry site in southern Italy. *For. Ecol. Manag.* 257, 820–828. doi: 10.1016/j.foreco.2008.10.015

Bernard, M., Boulanger, V., Dupouey, J.-L., Laurent, L., Montpied, P., Morin, X., et al. (2017). Deer browsing promotes Norway spruce at the expense of silver fir in the forest regeneration phase. *For. Ecol. Manag.* 400, 269–277. doi: 10.1016/j.foreco.2017.05.040

Brang, P., von Felten, S., and Wagner, S. (2005). Morning, noon, or afternoon: does timing of direct radiation influence the growth of Picea abies seedlings in mountain forests? *Ann. For. Sci.* 62, 697–705. doi: 10.1051/forest:2005058

Brede, B., Lau, A., Bartholomeus, H., and Kooistra, L. (2017). Comparing RIEGL RiCOPTER UAV LiDAR derived canopy height and DBH with terrestrial LiDAR. *Sensors* 17:2371. doi: 10.3390/s171023711

Březina, I., and Dobrovolný, L. (2011). Natural regeneration of sessile oak under different light conditions. *J. For. Sci.* 57, 359–368. doi: 10.17221/12/2011-JFS

Burgués, J., and Marco, S. (2020). Environmental chemical sensing using small drones: a review. *Sci. Total Environ.* 748:141172. doi: 10.1016/j.scitotenv.2020.141172

Çalışkan, A., Güney, H. S., and Çalışkan, S. (2014). Effects of different soil preparation techniques on the Anatolian black pine (Pinus nigra Arnold subsp. pallasiana (lamb.) Holmboe) regeneration. *J. Fac. Istanbul* 64:56. doi: 10.17099/jffiu.74421

Castleberry, S. B., Ford, W. M., Miller, K. V., and Smith, W. P. (2000). Influences of herbivory and canopy opening size on forest regeneration in a southern bottomland hardwood forest. *For. Ecol. Manag.* 131, 57–64. doi: 10.1016/S0378-1127(99)00200-5

Caudullo, G., Tinner, W., and de Rigo, D. (2016). *Picea abies* in Europe: Distribution, habitat, usage and threats. Publication Office of the European Union 2016, Luxembourg.

Czech Hydrometeorological Institute (2022). Historical data: weather: maps of climate characteristics. Czech Hydrometeorological institute. Available at: https://www.chmi.cz/historicka-data/pocasi/mapy-charakteristik-klimatu (Accessed November 18, 2022).

Da Ronch, F., Caudullo, G., Tinner, W., and de Rigo, D. (2016). Larix decidua and other larches in Europe: Distribution, habitat, usage and threats. Publication Office of the European Union 2016, Luxembourg.

Dai, A., Trenberth, K. E., and Qian, T. (2004). A global dataset of palmer drought severity index for 1870–2002: relationship with soil moisture and effects of surface warming. *J. Hydrometeorol.* 5, 1117–1130. doi: 10.1175/JHM-386.1

Elith, J., Phillips, S. J., Hastie, T., Dudík, M., Chee, Y. E., and Yates, C. J. (2011). A statistical explanation of MaxEnt for ecologists: statistical explanation of MaxEnt. *Divers. Distrib.* 17, 43–57. doi: 10.1111/j.1472-4642.2010.00725.x

Ellenberg, H. (2009). *Vegetation Ecology of Central Europe. 4 Edn.* Cambridge: Cambridge Univ. Press

European Commission and Joint Research Centre (2020). Vulnerability of European forests to natural disturbances: JRC PESETA IV project: Task 12. LU: Publications Office Available at: https://data.europa.eu/doi/10.2760/736558 (Accessed January 31, 2023).

Falk, W., and Mellert, K. H. (2011). Species distribution models as a tool for forest management planning under climate change: risk evaluation of *Abies alba* in Bavaria: species distribution models as a tool for forest management planning. *J. Veg. Sci.* 22, 621–634. doi: 10.1111/j.1654-1103.2011.01294.x

Fellner, H., Dirnberger, G. F., and Sterba, H. (2016). Specific leaf area of European larch (Larix decidua mill.). *Trees* 30, 1237–1244. doi: 10.1007/s00468-016-1361-1

Franklin, J. (2010). Moving beyond static species distribution models in support of conservation biogeography: moving beyond static species distribution models. *Divers. Distrib.* 16, 321–330. doi: 10.1111/j.1472-4642.2010.00641.x

Franklin, J., and Miller, J. A. (2009). *Mapping Species Distributions: Spatial Inference and Prediction.* Cambridge; New York: Cambridge University Press

Fu, P., and Rich, P. M. (2002). A geometric solar radiation model with applications in agriculture and forestry. *Comput. Electron. Agric.* 37, 25–35. doi: 10.1016/S0168-1699(02)00115-1

Guisan, A., and Zimmermann, N. E. (2000). Predictive habitat distribution models in ecology. *Ecol. Model.* 135, 147–186. doi: 10.1016/S0304-3800(00)00354-9

Hanssen, K. H. (2003). Natural regeneration of Picea abies on small clear-cuts in SE Norway. *For. Ecol. Manag.* 180, 199–213. doi: 10.1016/S0378-1127(02)00610-2

Harrison, X. A., Donaldson, L., Correa-Cano, M. E., Evans, J., Fisher, D. N., Goodwin, C. E. D., et al. (2018). A brief introduction to mixed effects modelling and multi-model inference in ecology. *PeerJ* 6:e4794. doi: 10.7717/peerj.4794

Hijmans, R. J., Phillips, S., and Elith, J. L. and (2023). Dismo: Species distribution modeling. Available at: https://cran.r-project.org/web/packages/dismo/index.html (Accessed October 21, 2023).

Huo, L., Persson, H. J., and Lindberg, E. (2021). Early detection of forest stress from European spruce bark beetle attack, and a new vegetation index: normalized distance red & SWIR (NDRS). *Remote Sens. Environ.* 255:112240. doi: 10.1016/j.rse.2020.112240

Hycza, T., Stereńczak, K., and Bałazy, R. (2018). Potential use of hyperspectral data to classify forest tree species. *N.Z. J. For. Sci.* 48, 1–13. doi: 10.1186/s40490-018-0123-9

Junttila, S., Näsi, R., Koivumäki, N., Imangholiloo, M., Saarinen, N., Raisio, J., et al. (2022). Multispectral imagery provides benefits for mapping spruce tree decline due to bark beetle infestation when acquired late in the season. *Remote Sens.* 14:909. doi: 10.3390/rs14040909

Klouček, T., Komárek, J., Surový, P., Hrach, K., Janata, P., and Vašíček, B. (2019). The use of UAV mounted sensors for precise detection of bark beetle infestation. *Remote Sens.* 11:1561. doi: 10.3390/rs11131561

Kuehne, C., Pyttel, P., Modrow, T., Kohnle, U., and Bauhus, J. (2020). Seedling development and regeneration success after 10 years following group selection harvesting in a sessile oak (Quercus petraea [Mattuschka] Liebl.) stand. *Ann. For. Sci.* 77:71. doi: 10.1007/s13595-020-00972-y

Lebourgeois, F. (2007). Climatic signal in annual growth variation of silver fir (*Abies alba* mill.) and spruce (*Picea abies* karst.) from the French permanent plot network (RENECOFOR). *Ann. For. Sci.* 64, 333–343. doi: 10.1051/forest:2007010

Lebourgeois, F., Rathgeber, C. B. K., and Ulrich, E. (2010). Sensitivity of French temperate coniferous forests to climate variability and extreme events (*Abies alba*, *Picea abies* and *Pinus sylvestris*). *J. Veg. Sci.* 21, 364–376. doi: 10.1111/j.1654-1103.2009.01148.x

Lévesque, M., Saurer, M., Siegwolf, R., Eilmann, B., Brang, P., Bugmann, H., et al. (2013). Drought response of five conifer species under contrasting water availability suggests high vulnerability of Norway spruce and European larch. *Glob. Chang. Biol.* 19, 3184–3199. doi: 10.1111/gcb.12268

McCarthy, J. J., and Intergovernmental Panel on Climate Change (eds.) (2001). Climate change 2001: Impacts, adaptation, and vulnerability: Contribution of working group II to the third assessment report of the intergovernmental panel on climate change. Cambridge, UK; New York: Cambridge University Press.

Meentemeyer, R. K., Moody, A., and Franklin, J. (2001). Landscape-scale patterns of shrub-species abundance in California chaparral. *Plant Ecol.* 156, 19–41. doi: 10.1023/A:1011944805738

Molina-Moral, J. C., Moriana-Elvira, A., and Pérez-Latorre, F. J. (2022). Estimation of the water Reserve in the Soil Using GIS and its application in irrigated olive groves in Jaen, (Spain). *Agronomy* 12:2188. doi: 10.3390/agronomy12092188

Örlander, G. (1993). Shading reduces both visible and invisible frost damage to Norway spruce seedlings in the field. *Forestry* 66, 27–36. doi: 10.1093/forestry/66.1.27

Pajares, G. (2015). Overview and current status of remote sensing applications based on unmanned aerial vehicles (UAVs). *Photogram. Engng. Rem. Sens.* 81, 281–330. doi: 10.14358/PERS.81.4.281

Parker, H. A., Larkin, J. T., Heggenstaller, D., Duchamp, J., Tyree, M. C., Rushing, C. S., et al. (2020). Evaluating the impacts of white-tailed deer (Odocoileus virginianus) browsing on vegetation in fenced and unfenced timber harvests. *For. Ecol. Manag.* 473:118326. doi: 10.1016/j.foreco.2020.118326

Piedallu, C., and Gégout, J.-C. (2007). Multiscale computation of solar radiation for predictive vegetation modelling. *Ann. For. Sci.* 64, 899–909. doi: 10.1051/forest:2007072

Promis, A., Gärtner, S., Reif, A., and Cruz, G. (2010). Effects of natural small-scale disturbances on below-canopy solar radiation and regeneration patterns in an old-growth Nothofagus betuloides forest in Tierra del Fuego, Chile. *Allgem. Forst Jagdzeit.* 181, 53–64.

Půdní mapa (2022). Půdní mapa 1: 50 000. Available at: https://mapy.geology.cz/pudy/# (Accessed November 18, 2022).

Rago, M. M., Urretavizcaya, M. F., and Defossé, G. E. (2021). Relationships among forest structure, solar radiation, and plant community in ponderosa pine plantations in the Patagonian steppe. *For. Ecol. Manag.* 502:119749. doi: 10.1016/j.foreco.2021.119749

Rooney, T. P. (2009). High white-tailed deer densities benefit graminoids and contribute to biotic homogenization of forest ground-layer vegetation. *Plant Ecol.* 202, 103–111. doi: 10.1007/s11258-008-9489-8

Seidl, R., Schelhaas, M.-J., Rammer, W., and Verkerk, P. J. (2014). Increasing forest disturbances in Europe and their impact on carbon storage. *Nat. Clim. Chang.* 4, 806–810. doi: 10.1038/nclimate2318

Sequens, J. (2007). Hospodářská úprava lesů Souhrn. Available at: https://katedry.czu.cz/storage/3844_Souhrn_HUL.pdf.

Strand, M., Löfvenius, M. O., Bergsten, U., Lundmark, T., and Rosvall, O. (2006). Height growth of planted conifer seedlings in relation to solar radiation and position in scots pine shelterwood. *For. Ecol. Manag.* 224, 258–265. doi: 10.1016/j.foreco.2005.12.038

Thornton, P. E., Hasenauer, H., and White, M. A. (2000). Simultaneous estimation of daily solar radiation and humidity from observed temperature and precipitation: an application over complex terrain in Austria. *Agric. For. Meteorol.* 104, 255–271. doi: 10.1016/S0168-1923(00)00170-2

Tromp-van Meerveld, H. J., and McDonnell, J. J. (2006). On the interrelations between topography, soil depth, soil moisture, transpiration rates and species distribution at the hillslope scale. *Adv. Water Resour.* 29, 293–310. doi: 10.1016/j.advwatres.2005.02.016

Tusa, E., Laybros, A., Monnet, J.-M., Dalla Mura, M., Barré, J.-B., Vincent, G., et al. (2019). "Fusion of hyperspectral imaging and LiDAR for forest monitoring" in *Data Handling in Science and Technology* (Amsterdam, The Netherlands: Elsevier), 281–303.

ÚHÚL (2022). Informace o lesním hospodářství. Available at: https://geoportal.uhul.cz/mapy/mapyIlpovyst.html (Accessed November 18, 2022).

Vacek, Z., Vacek, S., Bílek, L., Král, J., Remeš, J., Bulušek, D., et al. (2014). Ungulate impact on natural regeneration in spruce-beech-fir stands in Černý důl nature Reserve in the Orlické Hory Mountains, case study from central Sudetes. *Forests* 5, 2929–2946. doi: 10.3390/f5112929

Vercauteren, K. C., Lavelle, M. J., and Hygnstrom, S. (2006). Fences and deer-damage management: a review of designs and efficacy. *Wildl. Soc. Bull.* 34, 191–200. doi: 10.2193/0091-7648(2006)34[191:FADMAR]2.0.CO;2

Wieser, M., Mandlburger, G., Hollaus, M., Otepka, J., Glira, P., and Pfeifer, N. (2017). A case study of UAS borne laser scanning for measurement of tree stem diameter. *Remote Sens.* 9:1154. doi: 10.3390/rs9111154

Wollan, A. K., Bakkestuen, V., Kauserud, H., Gulden, G., Halvorsen, R., and Svenning, J.-C. (2008). Modelling and predicting fungal distribution patterns using herbarium data. *J. Biogeogr.* 35, 2298–2310. doi: 10.1111/j.1365-2699.2008.01965.x

Yang, Q., Blanco, N. E., Hermida-Carrera, C., Lehotai, N., Hurry, V., and Strand, Å. (2020). Two dominant boreal conifers use contrasting mechanisms to reactivate photosynthesis in the spring. *Nat. Commun.* 11:128. doi: 10.1038/s41467-019-13954-0

Zhu, X. (2016). *GIS for Environmental Applications: A Practical Approach*. London; New York, NY: Routledge

Zuur, A. F., Ieno, E. N., Walker, N., Saveliev, A. A., and Smith, G. M. (2009). *Mixed Effects Models and Extensions in Ecology With R*. New York, NY: Springer New York

Discussion

Deteriorated health status and stress associated with a higher risk of mortality of forest stands has been a severe issue in recent years. Degradation of the forest and the subsequent premature harvesting of damaged trees, on the one hand, negatively affects the local ecosystem and thus has a very significant secondary impact on climate change and carbon sequestration. The best strategy for maintaining forest ecosystems in good vitality is to prevent or minimize natural disturbances and their accompanying adverse effects. Therefore, this thesis focused on the possibilities of cutting-edge methods for natural disturbances using modern mapping techniques. Accurate map data can be crucial for further mathematical modeling of strategic interventions (Yoshimoto et al., 2017). The idea is to search for alternative, innovative methods for data analysis and thus get more timely or extensive information about natural disturbances and related processes. The stress can stem from many causes, in the next part the discussion focuses mostly on bark beetle, fire and mortality of regeneration.

In the case of a bark beetle attack, the damage to the forest stand can be estimated based on an assessment of the health of the stand and a prediction of its spread. Accurate and proven remote sensing imaging methods are now available to detect bark beetle infestation. The changes resulting from these stress conditions normally appear after 6 - 10 weeks and only in approximately 40% of attacked trees (Kautz et al., 2023). Although methods working with changes in spectral expression are ideal for mapping dead trees, they are not appropriate for early detection (Matejčíková et al., 2024).

Early detection has been described many times, and it is a viable method but usually works only partially (Brovkina et al., 2018). That is why this thesis aims to earlier identification, even before the spectral reflectance of the canopy changes. Much earlier manifestations are non-optical changes, consisting of chemical communication between bark beetles (aggregation pheromone), defense reactions of stressed trees (a group of volatile organic substances), and changes in local microclimate. Changes in the local microclimate are promising; several studies have shown the effect of forest cover on the local microclimate, with significant differences between temperatures and humidity in the forest cover and open space (Aussenac, 2000; Kašpar et al., 2021).

Kopáček et al. (2020) devoted to investigating the change of the temperature and humidity profile in the attacked stand over a longer time horizon. This thesis worked with the hypothesis that in case of stress and damage to trees, there will be reduced ability of transpiration and thus bring measurable non-optical changes in the manifestations of the local microclimate. Our measurements show that changes could occur much earlier, in the first weeks of an attack (Hüttnerová and Surový, 2024). The prediction of a potential infestation can be derived already at the beginning of the growing season based on the analysis of individual spectral bands of multispectral data of the Planet. The subsequent infestation depends, of course, on the presence of bark beetle (Trubin et al., 2023).

In the case of forest fires, the damage and extent of the fire is easily identifiable visually but escaped emissions can have a much more significant and severe impact. Satellite imaging is used for abiotic disturbances, mapping the intensity of fires, including emissions (Van Der Velde et al., 2021b; Byrne et al., 2024). Nechita-Banda et al. (2018) examined fires in Indonesia in 2015, recorded significant increase in concentrations of carbon monoxide, and estimated the total amount of carbon monoxide at 0.35–0.60 Pg. In our study (Hüttnerová and Surový, submitted), we recorded a 36.7% increase in carbon monoxide emissions in the first three days of the fire. Increased concentrations during forest fires have been mapped in several studies, including characterizing changes by type of biomass burned (Ross et al., 2013; Nechita-Banda et al., 2018; Van Der Velde et al., 2021a; Byrne et al., 2024).

After the dieback of adult forest stands, or in managed forests after the harvest (either planned either salvage), another stress factors may endanger the forest cycle continuation and increase its vulnerability. It is the mortality of regeneration caused by various biotic and abiotic factors. Deforested areas bring risks associated with reduced stability, erosion, and habitat loss, so timely forest restoration is essential (Veldkamp et al., 2020; Khodadadi et al., 2021). Restoration of forest stands is a time-consuming and financially expensive process. Some areas may have the potential for natural restoration and only minimal human intervention (Jonášová and Prach, 2004). Therefore, we focused on finding a methodology for evaluating the influence of terrain on natural regeneration. Our study used microrelief analysis to create a topographic wetness index in a Geographic Information System (GIS) environment, which allows for identifying places with a higher probability of water

accumulation based on terrain relief. Topographic wetness index had a significant positive effect, which indicates the importance of soil moisture (Hüttnerová et al., 2024).

The main aim of this thesis is to evaluate modern remote sensing sensors and their capability to "map" and numerically quantify the stresses in the forests. For all the above-mentioned stresses, mapping techniques were evaluated and tested and in next part of discussion will be described on various levels from ground to satellite.

Mapping methods for stress assessment

The appropriate mapping technique depends on the goals of the mapping research, the required resolution, and the details of the output processing. Ground data collection techniques obtain the greatest detail at the expense of time-consuming data collection in scale of large areas. At the same time, some forests are impossible to map in this way due to their inaccessibility. On the other hand, satellite chemical data products cover a much larger area, but stress mapping at the level of one tree is unrealistic, given the resolution of 5.5 km x 3.5 km, but they are very suitable for global analyses or emission leakage from entire forest stands.

Mapping – ground level

First, we focused on ground data collection and using conventional analytic chemical methods for stress mapping. SPME and cartridge noted differences in the concentrations of VOC. The output from the field measurement was a 3D cloud of alpha-pinene in details on a single tree (Stříbrská et al., 2023b). Conventional chemical analytical methods accurately quantify given compounds, including their amounts. The sampling is time-consuming, and collecting data on an SPME fiber or a sampling cartridge takes 30-60 minutes in the field; all samples must be kept in the cold immediately. Subsequent analysis is performed on a gas chromatograph; the time required for one sample is approx. 30 minutes. The stress of spruce trees caused by natural disturbances (bark beetle, drought) was monitored by chemical analytical methods in several studies (Santos et al., 2006; Amin et al., 2013; Stříbrská et al., 2023a; Basile et al., 2024) . However, the small number of samples is insufficient for global upscaling; there is potential for use as a validation dataset. More extensive collection can be carried out using electronic noses or satellite data.

This thesis demonstrated the detection ability of electronic noses to map stress and thus identify changes that bring natural disturbances together. The most accurate Bosch sensor tested achieved a detection capability of 95% in differentiating between healthy and infested parts of forest stands. Bosch is a low-cost sensor, and there is potential for its wide use, for example, within a large-scale observation mapping network. Bosch does not have an integrated GNSS module and is not equipped with recognition software; the data cannot be displayed immediately during the measurement.

These limitations are overcome by the SDEA, a technically advanced device with 89% in detection capability testing; this electronic nose offers immediate viewing of measured data within individual graphs (each chemical sensor has its graphical output live) and it has GNSS. Promising results were achieved by Paczkowski et al. (2021), who tested the GGS1330, GGS2330, and GGS5330 sensor series for chemical changes in forest ecosystems due to bark beetle infestation.

The proof that these substances are detectable and located near the attacked trees is the research of specially trained dogs (sniffer dogs), trained to search for synthetic semiochemicals (substances very similar to the aggregation pheromone). Sniffer dogs are much faster than Fieldworkers and can sense attacks up to 150 meters away (Johansson et al., 2019; Vošvrdová et al., 2023). The practical use of this technique in forestry is limited by the potential upscaling, mostly due to the easy distraction of the dog after several successes and lack of quantification of the exact smell the dog feels (in other words what it is sensitive to). On the other hand, chemical quantification of inventory stands would require only minimum effort and can bring significant information when used in modeled data (eliminating the influence of time and annual period).

Mapping technique – close-range UAV level

Ground measurements with electronic noses are still not fast and efficient enough for large-scale analyses. Therefore, we focused on the interaction of the electronic nose with the UAV platform. We studied the possible height comparison between ground-based and UAV data collection above tree canopy. We achieved the highest correlation between sensor value and distance from infested trees for ground collection. We did not observe an increased correlation above canopy during UAV data collection (Hüttnerová et al., 2023). Paczkowski et al (2021) also did not confirm

in his research the sensor's ability to record changes due to stress above the canopy. This could be due to more significant wind divergence, lower chemical concentrations, etc. Here, we see the possibility of validating UAV data collection under the tree canopy, where such substantial wind divergence might not be recorded.

As a result of natural disturbances, increased logging and deforested areas are recorded in European forests. Deforested areas can cause soil erosion and associated drought. In recent years, the extent of the dry regions has increased (Dai et al., 2004; Amani et al., 2017). In study Hüttnerová et al. (2024) is potential for water accumulation based on the analysis of microrelief. However, due to lower precipitation and other factors, these potential "accumulation sites" may not be fulfilled, and the area identified as potentially suitable for water accumulation may suffer from drought. Therefore, we suggest using electronic noses that can measure air humidity for future testing. An interesting finding could be a study investigating the correlation between the potential for microrelief for accumulation and measured air humidity values in deforested areas.

Solar radiation had a negative coefficient in our natural regeneration research, meaning that overly illuminated areas were unsuitable for regeneration, and increased mortality could have been recorded there (Hüttnerová et al., 2024). Örlander (1993) found increased mortality of spruces exposed to high sunlight combined with frost, with partial shade proving more suitable. Kuehne et al. (2020) identified a positive effect of sunlight on seedling density of oak seedlings (*Quercus petraea* [Mattuschka] Liebl.) It would be appropriate to supplement the solar radiation potential based on the terrain model with temperature measurements using electronic noses for a more detailed examination of variations.

Mapping technique – satellite level

Hüttnerová and Surový (submitted) demonstrated the ability of carbon monoxide data products from TROPOMI to map emissions from forest fires in Czechia and model the distribution. In this article, we were able to map the extent of the affected area as a result of the forest fire and the beginning and end of the spread of the carbon monoxide cloud. However, determining the total emissions in the thesis is still very speculative. For a correct estimate it will be necessary to estimate gas dynamics from snapshot satellite images. Another variable that will affect the total amount

of emissions will be the type of biomass burned. Van Der Velde et al. (2021a) characterizing changes by type of biomass burned, with boreal forests recording 3x to 6x higher emissions during forest fires than tropical forests and savannas. For this purpose, it will be important to determine the tree biomass burned by the fire. In the fire inventory, we recorded various degrees of burning intensity, where even in case of fire with highest severity, trees remained almost intact in terms of their dimensions.

For the severity estimates, it would be appropriate to use accurate difference canopy height models from Light Detection and Ranging (LiDAR) technology as shown in Berdych (2024) where aerial lidars were used. UAV lidar scans can cover the territory of individual forest units with even higher accuracy with a point density of 200 and more points/m^2 (Slavík et al., 2020; Da Costa et al., 2021). For larger extents it would be more appropriate to use a satellite platform. The LiDAR satellite Global Ecosystem Dynamics Investigation (GEDI) or the Radio Detection and Ranging (RADAR) satellite TerraSAR-X Add-on for Digital Elevation Measurement (TanDEM-X) can be used to estimate tree canopy extent and height and calculate the volumes (Schlund et al., 2019; Turubanova et al., 2023; Lei et al., 2024; Moudrý et al., 2024). Such data coupled with detail emission can lead in future to more precise information about the carbon emissions from forest fires (Van Der Velde et al., 2021b) where the application of this research can be continued.

All the mentioned mapping techniques are nowadays capable to quantify the stress and provide reliable maps. On the other hand, it is important to mention that many of these tools were unavailable just a few years ago. In the next few years, technological advances may bring more advanced and easy-to-use sensors, and this work can hopefully work as a base for future research and studies.

6.1. Conclusion

Non-optical mapping of forest ecosystems is a new chapter that opens the possibilities of advanced forest mapping, focusing on early identification of stress and associated processes. With the advanced development and miniaturization of sensors, high-tech chemical detectors and electronic noses are available nowadays and are conventionally used in industry and agriculture. The object of mapping was both biotic natural disturbance (bark beetle attack) and non-biotic natural disturbance (forest fire); conventional analytical chemical methods, electronic noses, and TROPOMI satellite sensors were used.

This thesis presented individual data collection and analysis methods, presenting the acquired knowledge and results in scientific articles with an emphasis on practical use for the innovation of forest management to minimize ecological losses and more effective planning. The methodology presented is very experimental; the procedures described are an entry point for non-optical mapping in forestry and show high potential for practical uses in forest protection and management.

6.2. Further research

During this work, the author came across several exciting points worth more extensive research and further investigation. Unfortunately, the time for theses and the research itself is limited, but I hope that this scientific activity will not end, and I will be able to participate in the discovery of further knowledge about this new topic. Below are summarized interesting findings that would be worth considering and possibly more extensive research.

A more detailed investigation of microclimate changes using non-optical mapping would be appropriate as part of further research. Focus on more extensive research about determining when changes occur, what effect seasonality has on temperature buffering, and how temperature and humidity manifestations change with height - possible measurements with UAV. More extensive mapping of emissions from forest fires with a focus on the issue of deriving total emissions based on snapshot images.

A more permanent network for long-term monitoring in real-time with data logging into the cloud - a method that could serve as a screening of the forests for initial records of changes in stress. The system would serve on the principle of, for example, smoke detectors; it would issue a warning report about a risky situation, based on which a field worker would go to the site and verify the problem, for example, by mapping with an electronic nose on a UAV.

More extensive verification of the UAV platform should be focused on collecting under the treetops, finding a suitable trajectory for a safe flight, and, at the same time, a more extensive and faster survey of forests, including those that are difficult to access. The use of artificial intelligence methods to teach electronic noses to recognize specific groups of chemical substances and, for example, the extent of changes in the microclimate, which could more effectively identify stress.

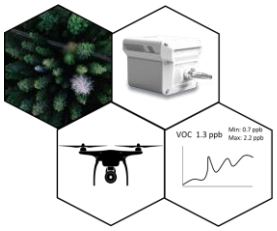

References

Abdullah, H., Darvishzadeh, R., Skidmore, A. K., and Heurich, M. (2019a). Sensitivity of Landsat-8 OLI and TIRS Data to Foliar Properties of Early Stage Bark Beetle (Ips typographus, L.) Infestation. *Remote Sensing* 11, 398. doi: 10.3390/rs11040398

Abdullah, H., Skidmore, A. K., Darvishzadeh, R., and Heurich, M. (2019b). Timing of red-edge and shortwave infrared reflectance critical for early stress detection induced by bark beetle (Ips typographus, L.) attack. *International Journal of Applied Earth Observation and Geoinformation* 82, 101900. doi: 10.1016/j.jag.2019.101900

Alfieri, G., Modesti, M., Riggi, R., and Bellincontro, A. (2024). Recent Advances and Future Perspectives in the E-Nose Technologies Addressed to the Wine Industry. *Sensors* 24, 2293. doi: 10.3390/s24072293

Amani, M., Salehi, B., Mahdavi, S., Masjedi, A., and Dehnavi, S. (2017). Temperature-Vegetation-soil Moisture Dryness Index (TVMDI). *Remote Sensing of Environment* 197, 1–14. doi: 10.1016/j.rse.2017.05.026

Amin, H. S., Russo, R. S., Sive, B., Richard Hoebeke, E., Dodson, C., McCubbin, I. B., et al. (2013). Monoterpene emissions from bark beetle infested Engelmann spruce trees. *Atmospheric Environment* 72, 130–133. doi: 10.1016/j.atmosenv.2013.02.025

Andersen, P. C., Williford, C. J., and Birks, J. W. (2010). Miniature Personal Ozone Monitor Based on UV Absorbance. *Anal. Chem.* 82, 7924–7928. doi: 10.1021/ac1013578

Aussenac, G. (2000). Interactions between forest stands and microclimate: Ecophysiological aspects and consequences for silviculture. *Ann. For. Sci.* 57, 287–301. doi: 10.1051/forest:2000119

Baier, P., Führer, E., Kirisits, T., and Rosner, S. (2002). Defence reactions of Norway spruce against bark beetles and the associated fungus Ceratocystis polonica in secondary pure and mixed species stands. *Forest Ecology and Management* 159, 73–86. doi: 10.1016/S0378-1127(01)00711-3

Baron, R., and Saffell, J. (2017). Amperometric Gas Sensors as a Low Cost Emerging Technology Platform for Air Quality Monitoring Applications: A Review. *ACS Sens.* 2, 1553–1566. doi: 10.1021/acssensors.7b00620

Bárta, V., Hanuš, J., Dobrovolný, L., and Homolová, L. (2022). Comparison of field survey and remote sensing techniques for detection of bark beetle-infested trees. *Forest Ecology and Management* 506, 119984. doi: 10.1016/j.foreco.2021.119984

Bárta, V., Lukeš, P., and Homolová, L. (2021). Early detection of bark beetle infestation in Norway spruce forests of Central Europe using Sentinel-2.

International Journal of Applied Earth Observation and Geoinformation 100, 102335. doi: 10.1016/j.jag.2021.102335

Basile, S., Stříbrská, B., Kalyniukova, A., Hradecký, J., Synek, J., Gershenzon, J., et al. (2024). Physiological and biochemical changes of Picea abies (L.) during acute drought stress and their correlation with susceptibility to Ips typographus (L.) and I. duplicatus (Sahlberg). *Front. For. Glob. Change* 7, 1436110. doi: 10.3389/ffgc.2024.1436110

Bax, C., Sironi, S., and Capelli, L. (2020). How Can Odors Be Measured? An Overview of Methods and Their Applications. *Atmosphere* 11, 92. doi: 10.3390/atmos11010092

Berdych, M. (2024). Analýza materiálů DPZ pro hodnocení intenzity lesního požáru v NP České Švýcarsko 2022. Prague: CZU Prague.

Birgersson, G., Schlyter, F., Löfqvist, J., and Bergström, G. (1984). Quantitative variation of pheromone components in the spruce bark beetleIps typographus from different attack phases. *J Chem Ecol* 10, 1029–1055. doi: 10.1007/BF00987511

Borg-Karlson, A.-K., Lindström, M., Norin, T., Persson, M., Valterová, I., Chanon, M., et al. (1993). Enantiomeric Composition of Monoterpene Hydrocarbons in Different Tissues of Norway Spruce, Picea abies (L.) Karst. A Multi-dimensional Gas Chromatography Study. *Acta Chem. Scand.* 47, 138–144. doi: 10.3891/acta.chem.scand.47-0138

Bozzini, A., Brugnaro, S., Morgante, G., Santoiemma, G., Deganutti, L., Finozzi, V., et al. (2024). Drone-based early detection of bark beetle infested spruce trees differs in endemic and epidemic populations. *Front. For. Glob. Change* 7, 1385687. doi: 10.3389/ffgc.2024.1385687

Brovkina, O., Cienciala, E., Surový, P., and Janata, P. (2018). Unmanned aerial vehicles (UAV) for assessment of qualitative classification of Norway spruce in temperate forest stands. *Geo-spatial Information Science* 21, 12–20. doi: 10.1080/10095020.2017.1416994

Buchelt, A., Adrowitzer, A., Kieseberg, P., Gollob, C., Nothdurft, A., Eresheim, S., et al. (2024). Exploring artificial intelligence for applications of drones in forest ecology and management. *Forest Ecology and Management* 551, 121530. doi: 10.1016/j.foreco.2023.121530

Burgués, J., and Marco, S. (2018). Low Power Operation of Temperature-Modulated Metal Oxide Semiconductor Gas Sensors. *Sensors* 18, 339. doi: 10.3390/s18020339

Burgués, J., and Marco, S. (2020). Environmental chemical sensing using small drones: A review. *Science of The Total Environment* 748, 141172. doi: 10.1016/j.scitotenv.2020.141172

Byrne, B., Liu, J., Bowman, K. W., Pascolini-Campbell, M., Chatterjee, A., Pandey, S., et al. (2024). Carbon emissions from the 2023 Canadian wildfires. *Nature* 633, 835–839. doi: 10.1038/s41586-024-07878-z

CABI (2022). Ips typographus (eight-toothed bark beetle). 28843. doi: 10.1079/cabicompendium.28843

Carrozzo, M., De Vito, S., Esposito, E., Salvato, M., Formisano, F., Massera, E., et al. (2018). UAV Intelligent Chemical Multisensor Payload for Networked and Impromptu Gas Monitoring Tasks., in *2018 5th IEEE International Workshop on Metrology for AeroSpace (MetroAeroSpace)*, (Rome: IEEE), 112–116. doi: 10.1109/MetroAeroSpace.2018.8453543

Chen, Z., and Lu, C. (2005). Humidity Sensors: A Review of Materials and Mechanisms. *Sen Lett* 3, 274–295. doi: 10.1166/sl.2005.045

Christiansen, E., Waring, R. H., and Berryman, A. A. (1987). Resistance of conifers to bark beetle attack: Searching for general relationships. *Forest Ecology and Management* 22, 89–106. doi: 10.1016/0378-1127(87)90098-3

Da Costa, M. B. T., Silva, C. A., Broadbent, E. N., Leite, R. V., Mohan, M., Liesenberg, V., et al. (2021). Beyond trees: Mapping total aboveground biomass density in the Brazilian savanna using high-density UAV-lidar data. *Forest Ecology and Management* 491, 119155. doi: 10.1016/j.foreco.2021.119155

Dai, A., Trenberth, K. E., and Qian, T. (2004). A Global Dataset of Palmer Drought Severity Index for 1870–2002: Relationship with Soil Moisture and Effects of Surface Warming. *Journal of Hydrometeorology* 5, 1117–1130. doi: 10.1175/JHM-386.1

Dainelli, R., Toscano, P., Di Gennaro, S. F., and Matese, A. (2021). Recent Advances in Unmanned Aerial Vehicles Forest Remote Sensing—A Systematic Review. Part II: Research Applications. *Forests* 12, 397. doi: 10.3390/f12040397

Dalponte, M., Solano-Correa, Y. T., Frizzera, L., and Gianelle, D. (2022). Mapping a European Spruce Bark Beetle Outbreak Using Sentinel-2 Remote Sensing Data. *Remote Sensing* 14, 3135. doi: 10.3390/rs14133135

Dinh, T.-V., Choi, I.-Y., Son, Y.-S., and Kim, J.-C. (2016). A review on non-dispersive infrared gas sensors: Improvement of sensor detection limit and interference correction. *Sensors and Actuators B: Chemical* 231, 529–538. doi: 10.1016/j.snb.2016.03.040

Fahse, L., and Heurich, M. (2011). Simulation and analysis of outbreaks of bark beetle infestations and their management at the stand level. *Ecological Modelling* 222, 1833–1846. doi: 10.1016/j.ecolmodel.2011.03.014

Fearnside, P. M. (2015). Deforestation soars in the Amazon. *Nature* 521, 423–423. doi: 10.1038/521423b

Fine, G. F., Cavanagh, L. M., Afonja, A., and Binions, R. (2010). Metal Oxide Semi-Conductor Gas Sensors in Environmental Monitoring. *Sensors* 10, 5469–5502. doi: 10.3390/s100605469

Forest Europe (2020). State of Europe's Forests 2020 Report. *Bonn, Germany*.

Fuentes, S., Tongson, E., Unnithan, R. R., and Gonzalez Viejo, C. (2021). Early Detection of Aphid Infestation and Insect-Plant Interaction Assessment in Wheat Using a Low-Cost Electronic Nose (E-Nose), Near-Infrared Spectroscopy and Machine Learning Modeling. *Sensors* 21, 5948. doi: 10.3390/s21175948

Gardner, J. W., and Bartlett, P. N. (1999). *Electronic Noses: Principles and Applications*. Oxford University PressOxford. doi: 10.1093/oso/9780198559559.001.0001

Ghasempour, F., Sekertekin, A., and Kutoglu, S. H. (2021). Google Earth Engine based spatio-temporal analysis of air pollutants before and during the first wave COVID-19 outbreak over Turkey via remote sensing. *Journal of Cleaner Production* 319, 128599. doi: 10.1016/j.jclepro.2021.128599

Ghimire, R. P., Kivimäenpää, M., Blomqvist, M., Holopainen, T., Lyytikäinen-Saarenmaa, P., and Holopainen, J. K. (2016). Effect of bark beetle (Ips typographus L.) attack on bark VOC emissions of Norway spruce (Picea abies Karst.) trees. *Atmospheric Environment* 126, 145–152. doi: 10.1016/j.atmosenv.2015.11.049

Gitelson, A. A., and Merzlyak, M. N. (1997). Remote estimation of chlorophyll content in higher plant leaves. *International Journal of Remote Sensing* 18, 2691–2697. doi: 10.1080/014311697217558

Gorelick, N., Hancher, M., Dixon, M., Ilyushchenko, S., Thau, D., and Moore, R. (2017). Google Earth Engine: Planetary-scale geospatial analysis for everyone. *Remote Sensing of Environment* 202, 18–27. doi: 10.1016/j.rse.2017.06.031

Götz, L., Psomas, A., and Bugmann, H. (2020). Früherkennung von Buchdruckerbefall dank Fern erkundung: Was ist schon möglich? *Schweizerische Zeitschrift fur Forstwesen* 171, 36–43. doi: 10.3188/szf.2020.0036

Hakola, H., Taipale, D., Praplan, A., Schallhart, S., Thomas, S., Tykkä, T., et al. (2023). Emissions of volatile organic compounds from Norway spruce and potential atmospheric impacts. *Front. For. Glob. Change* 6, 1116414. doi: 10.3389/ffgc.2023.1116414

Hantson, S., Padilla, M., Corti, D., and Chuvieco, E. (2013). Strengths and weaknesses of MODIS hotspots to characterize global fire occurrence. *Remote Sensing of Environment* 131, 152–159. doi: 10.1016/j.rse.2012.12.004

Hodgkinson, J., and Tatam, R. P. (2013). Optical gas sensing: a review. *Meas. Sci. Technol.* 24, 012004. doi: 10.1088/0957-0233/24/1/012004

Honkavaara, E., Näsi, R., Oliveira, R., Viljanen, N., Suomalainen, J., Khoramshahi, E., et al. (2020). USING MULTITEMPORAL HYPER- AND MULTISPECTRAL UAV IMAGING FOR DETECTING BARK BEETLE INFESTATION ON NORWAY SPRUCE. *Int. Arch. Photogramm. Remote Sens. Spatial Inf. Sci.* XLIII-B3-2020, 429–434. doi: 10.5194/isprs-archives-XLIII-B3-2020-429-2020

Hunter, G. W., Akbar, S., Bhansali, S., Daniele, M., Erb, P. D., Johnson, K., et al. (2020). Editors' Choice—Critical Review—A Critical Review of Solid State Gas Sensors. *J. Electrochem. Soc.* 167, 037570. doi: 10.1149/1945-7111/ab729c

Huo, L., Lindberg, E., Fransson, J. E. S., and Persson, H. J. (2022). Comparing Spectral Differences Between Healthy and Early Infested Spruce Forests Caused by Bark Beetle Attacks using Satellite Images., in *IGARSS 2022 - 2022 IEEE International Geoscience and Remote Sensing Symposium*, (Kuala Lumpur, Malaysia: IEEE), 7709–7712. doi: 10.1109/IGARSS46834.2022.9883420

Hüttnerová, T., Muscarella, R., and Surový, P. (2024). Drone microrelief analysis to predict the presence of naturally regenerated seedlings. *Front. For. Glob. Change* 6, 1329675. doi: 10.3389/ffgc.2023.1329675

Hüttnerová, T., Paczkowski, S., Neubert, T., Jirošová, A., and Surový, P. (2023). Comparison of Individual Sensors in the Electronic Nose for Stress Detection in Forest Stands. *Sensors* 23, 2001. doi: 10.3390/s23042001

Hüttnerová, T., and Surový, P. (2024). Bark beetle detection method using electronic nose sensors. A possible improvement of early forest disturbance detection? *Front. For. Glob. Change* 7, 1445094. doi: 10.3389/ffgc.2024.1445094

Immitzer, M., and Atzberger, C. (2014). Frühzeitige Erkennung von Borkenkäferbefall an Fichten mittels WorldView-2 Satellitendaten. *pfg* 2014, 351–367. doi: 10.1127/1432-8364/2014/0229

Jaakkola, E., Gärtner, A., Jönsson, A. M., Ljung, K., Olsson, P.-O., and Holst, T. (2022). Spruce bark beetle (Ips typographus) infestation cause up to 700 times higher bark BVOC emission rates from Norway spruce (Picea abies). Biodiversity and Ecosystem Function: Terrestrial. doi: 10.5194/bg-2022-125

Johansson, A., Birgersson, G., and Schlyter, F. (2019). Using synthetic semiochemicals to train canines to detect bark beetle–infested trees. *Annals of Forest Science* 76, 58. doi: 10.1007/s13595-019-0841-z

Jonášová, M., and Prach, K. (2004). Central-European mountain spruce (Picea abies (L.) Karst.) forests: regeneration of tree species after a bark beetle outbreak. *Ecological Engineering* 23, 15–27. doi: 10.1016/j.ecoleng.2004.06.010

Kandasamy, D., Gershenzon, J., Andersson, M. N., and Hammerbacher, A. (2019). Volatile organic compounds influence the interaction of the Eurasian spruce bark beetle (*Ips typographus*) with its fungal symbionts. *The ISME Journal* 13, 1788–1800. doi: 10.1038/s41396-019-0390-3

Kašpar, V., Hederová, L., Macek, M., Müllerová, J., Prošek, J., Surový, P., et al. (2021). Temperature buffering in temperate forests: Comparing microclimate models based on ground measurements with active and passive remote sensing. *Remote Sensing of Environment* 263, 112522. doi: 10.1016/j.rse.2021.112522

Kautz, M., Feurer, J., and Adler, P. (2024). Early detection of bark beetle (Ips typographus) infestations by remote sensing – A critical review of recent research. *Forest Ecology and Management* 556, 121595. doi: 10.1016/j.foreco.2023.121595

Kautz, M., Meddens, A. J. H., Hall, R. J., and Arneth, A. (2017). Biotic disturbances in Northern Hemisphere forests - a synthesis of recent data, uncertainties and implications for forest monitoring and modelling: Biotic disturbances in Northern Hemisphere forests. *Global Ecol. Biogeogr.* 26, 533–552. doi: 10.1111/geb.12558

Kautz, M., Peter, F. J., Harms, L., Kammen, S., and Delb, H. (2023). Patterns, drivers and detectability of infestation symptoms following attacks by the European spruce bark beetle. *J Pest Sci* 96, 403–414. doi: 10.1007/s10340-022-01490-8

Khodadadi, M., Alewell, C., Mirzaei, M., Ehssan-Malahat, E., Asadzadeh, F., Strauss, P., et al. (2021). Deforestation effects on soil erosion rates and soil physicochemicalproperties in Iran: a case study of using fallout radionuclides ina Chernobyl contaminated area. doi: 10.5194/soil-2021-2

Khorramifar, A., Karami, H., Lvova, L., Kolouri, A., Łazuka, E., Piłat-Rożek, M., et al. (2023). Environmental Engineering Applications of Electronic Nose Systems Based on MOX Gas Sensors. *Sensors* 23, 5716. doi: 10.3390/s23125716

Klouček, T., Komárek, J., Surový, P., Hrach, K., Janata, P., and Vašíček, B. (2019). The Use of UAV Mounted Sensors for Precise Detection of Bark Beetle Infestation. *Remote Sensing* 11, 1561. doi: 10.3390/rs11131561

Kopáček, J., Bače, R., Hejzlar, J., Kaňa, J., Kučera, T., Matějka, K., et al. (2020). Changes in microclimate and hydrology in an unmanaged mountain forest catchment after insect-induced tree dieback. *Science of The Total Environment* 720, 137518. doi: 10.1016/j.scitotenv.2020.137518

Korotcenkov, G., and Cho, B. K. (2013). Engineering approaches for the improvement of conductometric gas sensor parameters. *Sensors and Actuators B: Chemical* 188, 709–728. doi: 10.1016/j.snb.2013.07.101

Krofta, J. (n.d.). *Návody pro laboratorní cvičení z analytické chemie II*., 6th Edn. Praha: VŠCHT.

Kuehne, C., Pyttel, P., Modrow, T., Kohnle, U., and Bauhus, J. (2020). Seedling development and regeneration success after 10 years following group selection harvesting in a sessile oak (Quercus petraea [Mattuschka] Liebl.) stand. *Annals of Forest Science* 77, 71. doi: 10.1007/s13595-020-00972-y

Latifi, H., Dahms, T., Beudert, B., Heurich, M., Kübert, C., and Dech, S. (2018). Synthetic RapidEye data used for the detection of area-based spruce tree mortality induced by bark beetles. *GIScience & Remote Sensing* 55, 839–859. doi: 10.1080/15481603.2018.1458463

Le Maire, G., François, C., and Dufrêne, E. (2004). Towards universal broad leaf chlorophyll indices using PROSPECT simulated database and hyperspectral reflectance measurements. *Remote Sensing of Environment* 89, 1–28. doi: 10.1016/j.rse.2003.09.004

Lei, Y., Wang, Y., Wang, G., Song, C., Cao, H., and Xiao, W. (2024). Estimating Forest Canopy Height based on GEDI Lidar Data and Multi-source Remote Sensing Images. *Int. Arch. Photogramm. Remote Sens. Spatial Inf. Sci.* XLVIII-1–2024, 297–303. doi: 10.5194/isprs-archives-XLVIII-1-2024-297-2024

Licen, S., Di Gilio, A., Palmisani, J., Petraccone, S., De Gennaro, G., and Barbieri, P. (2020). Pattern Recognition and Anomaly Detection by Self-Organizing Maps in a Multi Month E-nose Survey at an Industrial Site. *Sensors* 20, 1887. doi: 10.3390/s20071887

Loutfi, A., Coradeschi, S., Mani, G. K., Shankar, P., and Rayappan, J. B. B. (2015a). Electronic noses for food quality: A review. *Journal of Food Engineering* 144, 103–111. doi: 10.1016/j.jfoodeng.2014.07.019

Loutfi, A., Coradeschi, S., Mani, G. K., Shankar, P., and Rayappan, J. B. B. (2015b). Electronic noses for food quality: A review. *Journal of Food Engineering* 144, 103–111. doi: 10.1016/j.jfoodeng.2014.07.019

Marković, D., Vujičić, D., Tanasković, S., Đorđević, B., Ranđić, S., and Stamenković, Z. (2021). Prediction of Pest Insect Appearance Using Sensors and Machine Learning. *Sensors* 21, 4846. doi: 10.3390/s21144846

Martin, C. R., Zeng, N., Karion, A., Dickerson, R. R., Ren, X., Turpie, B. N., et al. (2017). Evaluation and environmental correction of ambient CO2 measurements from a low-cost NDIR sensor. *Atmos. Meas. Tech.* 10, 2383–2395. doi: 10.5194/amt-10-2383-2017

Matejčíková, J., Vébrová, D., and Surový, P. (2024). Comparative Analysis of Machine Learning Techniques and Data Sources for Dead Tree Detection: What Is the Best Way to Go? *Remote Sensing* 16, 3086. doi: 10.3390/rs16163086

Mathews, L. E. H., and Kinoshita, A. M. (2020). Urban Fire Severity and Vegetation Dynamics in Southern California. *Remote Sensing* 13, 19. doi: 10.3390/rs13010019

McRae, T. G., and Kulp, T. J. (1993). Backscatter absorption gas imaging: a new technique for gas visualization. *Appl. Opt.* 32, 4037. doi: 10.1364/AO.32.004037

Minařík, R., Langhammer, J., and Lendzioch, T. (2021). Detection of Bark Beetle Disturbance at Tree Level Using UAS Multispectral Imagery and Deep Learning. *Remote Sensing* 13, 4768. doi: 10.3390/rs13234768

Ministerstvo zemědělství (2023). Zpráva o stavu lesa a lesního hospodářství 2022. Available at: www.eagri.cz

Moliterno, A. A. C., Jakuš, R., Modlinger, R., Unelius, C. R., Schlyter, F., and Jirošová, A. (2023). Field effects of oxygenated monoterpenes and estragole combined with pheromone on attraction of Ips typographus and its natural enemies. *Front. For. Glob. Change* 6, 1292581. doi: 10.3389/ffgc.2023.1292581

Moudrý, V., Gábor, L., Marselis, S., Pracná, P., Barták, V., Prošek, J., et al. (2024). Comparison of three global canopy height maps and their applicability to biodiversity modeling: Accuracy issues revealed. *Ecosphere* 15, e70026. doi: 10.1002/ecs2.70026

Nechita-Banda, N., Krol, M., Van Der Werf, G. R., Kaiser, J. W., Pandey, S., Huijnen, V., et al. (2018). Monitoring emissions from the 2015 Indonesian fires using CO satellite data. *Phil. Trans. R. Soc. B* 373, 20170307. doi: 10.1098/rstb.2017.0307

Netherer, S., Kandasamy, D., Jirosová, A., Kalinová, B., Schebeck, M., and Schlyter, F. (2021). Interactions among Norway spruce, the bark beetle Ips typographus and its fungal symbionts in times of drought. *J Pest Sci* 94, 591–614. doi: 10.1007/s10340-021-01341-y

Netherer, S., Lehmanski, L., Bachlehner, A., Rosner, S., Savi, T., Schmidt, A., et al. (2024). Drought increases Norway spruce susceptibility to the Eurasian spruce bark beetle and its associated fungi. *New Phytologist* 242, 1000–1017. doi: 10.1111/nph.19635

Örlander, G. (1993). Shading Reduces both Visible and Invisible Frost Damage to Norway Spruce Seedlings in the Field. *Forestry* 66, 27–36. doi: 10.1093/forestry/66.1.27

Paczkowski, S., Datta, P., Irion, H., Paczkowska, M., Habert, T., Pelz, S., et al. (2021). Evaluation of Early Bark Beetle Infestation Localization by Drone-Based Monoterpene Detection. *Forests* 12, 228. doi: 10.3390/f12020228

Parks, S., Dillon, G., and Miller, C. (2014). A New Metric for Quantifying Burn Severity: The Relativized Burn Ratio. *Remote Sensing* 6, 1827–1844. doi: 10.3390/rs6031827

Patacca, M., Lindner, M., Lucas-Borja, M. E., Cordonnier, T., Fidej, G., Gardiner, B., et al. (2023). Significant increase in natural disturbance impacts on European forests since 1950. *Global Change Biology* 29, 1359–1376. doi: 10.1111/gcb.16531

Popa, D., and Udrea, F. (2019). Towards Integrated Mid-Infrared Gas Sensors. *Sensors* 19, 2076. doi: 10.3390/s19092076

Puliti, S., Ene, L. T., Gobakken, T., and Næsset, E. (2017). Use of partial-coverage UAV data in sampling for large scale forest inventories. *Remote Sensing of Environment* 194, 115–126. doi: 10.1016/j.rse.2017.03.019

Puliti, S., Talbot, B., and Astrup, R. (2018). Tree-Stump Detection, Segmentation, Classification, and Measurement Using Unmanned Aerial Vehicle (UAV) Imagery. *Forests* 9, 102. doi: 10.3390/f9030102

Ravikumar, A. P., Wang, J., and Brandt, A. R. (2017). Are Optical Gas Imaging Technologies Effective For Methane Leak Detection? *Environ. Sci. Technol.* 51, 718–724. doi: 10.1021/acs.est.6b03906

Romain, A. C., and Nicolas, J. (2010). Long term stability of metal oxide-based gas sensors for e-nose environmental applications: An overview. *Sensors and Actuators B: Chemical* 146, 502–506. doi: 10.1016/j.snb.2009.12.027

Ross, A. N., Wooster, M. J., Boesch, H., and Parker, R. (2013). First satellite measurements of carbon dioxide and methane emission ratios in wildfire plumes. *Geophysical Research Letters* 40, 4098–4102. doi: 10.1002/grl.50733

Santos, A. M., Vasconcelos, T., Mateus, E., Farrall, M. H., Gomes Da Silva, M. D. R., Paiva, M. R., et al. (2006). Characterization of the volatile fraction emitted by phloems of four pinus species by solid-phase microextraction and gas chromatography–mass spectrometry. *Journal of Chromatography A* 1105, 191–198. doi: 10.1016/j.chroma.2005.10.049

Schlund, M., Magdon, P., Eaton, B., Aumann, C., and Erasmi, S. (2019). Canopy height estimation with TanDEM-X in temperate and boreal forests. *International Journal of Applied Earth Observation and Geoinformation* 82, 101904. doi: 10.1016/j.jag.2019.101904

Schneising, O., Buchwitz, M., Reuter, M., Bovensmann, H., Burrows, J. P., Borsdorff, T., et al. (2019). A scientific algorithm to simultaneously retrieve carbon monoxide and methane from TROPOMI onboard Sentinel-5 Precursor. *Atmos. Meas. Tech.* 12, 6771–6802. doi: 10.5194/amt-12-6771-2019

Seidl, R., Schelhaas, M.-J., Rammer, W., and Verkerk, P. J. (2014). Increasing forest disturbances in Europe and their impact on carbon storage. *Nature Clim Change* 4, 806–810. doi: 10.1038/nclimate2318

Seidl, R., Thom, D., Kautz, M., Martin-Benito, D., Peltoniemi, M., Vacchiano, G., et al. (2017). Forest disturbances under climate change. *Nature Clim Change* 7, 395–402. doi: 10.1038/nclimate3303

Silvestrini, E., Michelozzi, M., Skroppa, T., Brancaleoni, E., and Ciccioli, P. (2004). Characterisation of different clones of Picea abies (L.) Karst using head-space sampling of cortical tissues combined with enantioselective capillary gas chromatography for the separation of chiral and non-chiral monoterpenes. *Journal of Chromatography A* 1034, 183–189. doi: 10.1016/j.chroma.2004.02.001

Slavík, M., Kuželka, K., Modlinger, R., Tomášková, I., and Surový, P. (2020). UAV Laser Scans Allow Detection of Morphological Changes in Tree Canopy. *Remote Sensing* 12, 3829. doi: 10.3390/rs12223829

Smith, B. J., John, G., Christensen, L. E., and Chen, Y. (2017). Fugitive methane leak detection using sUAS and miniature laser spectrometer payload: System, application and groundtruthing tests., in *2017 International Conference on Unmanned Aircraft Systems (ICUAS)*, (Miami, FL, USA: IEEE), 369–374. doi: 10.1109/ICUAS.2017.7991403

Stetter, J. R., and Li, J. (2008). Amperometric Gas SensorsA Review. *Chem. Rev.* 108, 352–366. doi: 10.1021/cr0681039

Stříbrská, B., Hradecký, J., Čepl, J., Modlinger, R., Tomášková, I., and Jirošová, A. (2023a). Physiological and biochemical indicators in Norway spruces freshly infested by Ips typographus: potential for early detection methods. *Front. For. Glob. Change* 6, 1197229. doi: 10.3389/ffgc.2023.1197229

Stříbrská, B., Moliterno, A. A. C., Hüttnerová, T., Leiner, M., Surový, P., and Jirošová, A. (2023b). Pilot Study of 3D Spatial Distribution of α-Pinene Emitted by Norway Spruce (L.) Karst Recently Infested by Ips typographus (L. 1758) (Coleoptera: Scolytinae). *Forests* 15, 10. doi: 10.3390/f15010010

Teodoro, A., and Amaral, A. (2019). A Statistical and Spatial Analysis of Portuguese Forest Fires in Summer 2016 Considering Landsat 8 and Sentinel 2A Data. *Environments* 6, 36. doi: 10.3390/environments6030036

Trubin, A., Kozhoridze, G., Zabihi, K., Modlinger, R., Singh, V. V., Surový, P., et al. (2023). Detection of susceptible Norway spruce to bark beetle attack using PlanetScope multispectral imagery. *Front. For. Glob. Change* 6, 1130721. doi: 10.3389/ffgc.2023.1130721

Turner, M. G. (2010). Disturbance and landscape dynamics in a changing world. *Ecology* 91, 2833–2849. doi: 10.1890/10-0097.1

Turubanova, S., Potapov, P., Hansen, M. C., Li, X., Tyukavina, A., Pickens, A. H., et al. (2023). Tree canopy extent and height change in Europe, 2001–2021, quantified using Landsat data archive. *Remote Sensing of Environment* 298, 113797. doi: 10.1016/j.rse.2023.113797

USDA Forest Service (1935). Bark beetle enemies of California forests. *USDA Bureau of Entomology and Plant Quarantine, Project 3F-2–302 and the Emergency Educational Program.*

Van Der Velde, I. R., Van Der Werf, G. R., Houweling, S., Eskes, H. J., Veefkind, J. P., Borsdorff, T., et al. (2021a). Biomass burning combustion efficiency observed from space using measurements of CO and NO₂ by the TROPOspheric Monitoring Instrument (TROPOMI). *Atmos. Chem. Phys.* 21, 597–616. doi: 10.5194/acp-21-597-2021

Van Der Velde, I. R., Van Der Werf, G. R., Houweling, S., Maasakkers, J. D., Borsdorff, T., Landgraf, J., et al. (2021b). Vast CO2 release from Australian

fires in 2019–2020 constrained by satellite. *Nature* 597, 366–369. doi: 10.1038/s41586-021-03712-y

Veefkind, J. P., Aben, I., McMullan, K., Förster, H., De Vries, J., Otter, G., et al. (2012). TROPOMI on the ESA Sentinel-5 Precursor: A GMES mission for global observations of the atmospheric composition for climate, air quality and ozone layer applications. *Remote Sensing of Environment* 120, 70–83. doi: 10.1016/j.rse.2011.09.027

Veldkamp, E., Schmidt, M., Powers, J. S., and Corre, M. D. (2020). Deforestation and reforestation impacts on soils in the tropics. *Nat Rev Earth Environ* 1, 590–605. doi: 10.1038/s43017-020-0091-5

Vošvrdová, N., Johansson, A., Turčáni, M., Jakuš, R., Tyšer, D., Schlyter, F., et al. (2023). Dogs trained to recognise a bark beetle pheromone locate recently attacked spruces better than human experts. *Forest Ecology and Management* 528, 120626. doi: 10.1016/j.foreco.2022.120626

Wang, C., Yin, L., Zhang, L., Xiang, D., and Gao, R. (2010). Metal Oxide Gas Sensors: Sensitivity and Influencing Factors. *Sensors* 10, 2088–2106. doi: 10.3390/s100302088

Wang, M., and Chen, Y. (2024). Electronic nose and its application in the food industry: a review. *Eur Food Res Technol* 250, 21–67. doi: 10.1007/s00217-023-04381-z

Wermelinger, B. (2004). Ecology and management of the spruce bark beetle Ips typographus—a review of recent research. *Forest Ecology and Management* 202, 67–82. doi: 10.1016/j.foreco.2004.07.018

White, P. S., and Pickett, S. T. A. (1985). "Natural Disturbance and Patch Dynamics: An Introduction," in *The Ecology of Natural Disturbance and Patch Dynamics*, (Elsevier), 3–13. doi: 10.1016/B978-0-12-554520-4.50006-X

Wojnowski, W., Dymerski, T., Gębicki, J., and Namieśnik, J. (2019). Electronic Noses in Medical Diagnostics. *CMC* 26, 197–215. doi: 10.2174/0929867324666171004164636

Wulder, M. A., Dymond, C. C., White, J. C., Leckie, D. G., and Carroll, A. L. (2006). Surveying mountain pine beetle damage of forests: A review of remote sensing opportunities. *Forest Ecology and Management* 221, 27–41. doi: 10.1016/j.foreco.2005.09.021

Xulu, S., Mbatha, N., and Peerbhay, K. (2021). Burned Area Mapping over the Southern Cape Forestry Region, South Africa Using Sentinel Data within GEE Cloud Platform. *IJGI* 10, 511. doi: 10.3390/ijgi10080511

Yang, S., Talbot, R. W., Frish, M. B., Golston, L. M., Aubut, N. F., Zondlo, M. A., et al. (2018). Natural Gas Fugitive Leak Detection Using an Unmanned Aerial Vehicle: Measurement System Description and Mass Balance Approach. *Atmosphere* 9, 383. doi: 10.3390/atmos9100383

Yoshimoto, A., Asante, P., Konoshima, M., and Surový, P. (2017). INTEGER PROGRAMMING APPROACH TO CONTROL INVASIVE SPECIES SPREAD BASED ON CELLULAR AUTOMATON MODEL. *Natural Resource Modeling* 30, nrm.12101. doi: 10.1111/nrm.12101

Yuan, K., Zhu, Q., Zheng, S., Zhao, L., Chen, M., Riley, W. J., et al. (2021). Deforestation reshapes land-surface energy-flux partitioning. *Environ. Res. Lett.* 16, 024014. doi: 10.1088/1748-9326/abd8f9

Zakrzewska, A., and Kopeć, D. (2022). Remote sensing of bark beetle damage in Norway spruce individual tree canopies using thermal infrared and airborne laser scanning data fusion. *Forest Ecosystems* 9, 100068. doi: 10.1016/j.fecs.2022.100068

Zarco-Tejada, P. J., Miller, J. R., Noland, T. L., Mohammed, G. H., and Sampson, P. H. (2001). Scaling-up and model inversion methods with narrowband optical indices for chlorophyll content estimation in closed forest canopies with hyperspectral data. *IEEE Trans. Geosci. Remote Sensing* 39, 1491–1507. doi: 10.1109/36.934080

Zhan, Y., Chen, P., Xu, W., Chen, S., Han, Y., Lan, Y., et al. (2022). Influence of the downwash airflow distribution characteristics of a plant protection UAV on spray deposit distribution. *Biosystems Engineering* 216, 32–45. doi: 10.1016/j.biosystemseng.2022.01.016

Zhang, N., Zhang, X., Yang, G., Zhu, C., Huo, L., and Feng, H. (2018). Assessment of defoliation during the Dendrolimus tabulaeformis Tsai et Liu disaster outbreak using UAV-based hyperspectral images. *Remote Sensing of Environment* 217, 323–339. doi: 10.1016/j.rse.2018.08.024

Zifarelli, A., De Palo, R., Patimisco, P., Giglio, M., Sampaolo, A., Blaser, S., et al. (2022). Multi-gas quartz-enhanced photoacoustic sensor for environmental monitoring exploiting a Vernier effect-based quantum cascade laser. *Photoacoustics* 28, 100401. doi: 10.1016/j.pacs.2022.100401